Topologische Eigenschaften von Tiles

Dissertation[1]

Benoît Loridant

Betreuer:
Ao.Univ.-Prof. Dipl.-Ing. Dr.techn. Jörg Thuswaldner

Lehrstuhl für Mathematik und Statistik
Department Mathematik und Informationstechnologie
Montanuniversität Leoben

November 2007

[1]Diese Arbeit wurde durch die FWF Projekte S9604, S9610 und S9612 unterstützt.

Contents

List of Figures

List of Tables

Chapter 1

Introduction

The term "fractal" was introduced by Mandelbrot in 1975 in his book *Les Objets fractals: forme, hasard et dimension* [49]. However, the space-filling curves described by Peano and Hilbert (see [25, 56]) in the late XIX-th century may be considered as the first fractals constructed by mathematicians. The purpose was to find a curve which fills in the unit square. Since such curves exist, this indicates that the intuitive notion of dimension (curve = 1, plane = 2) is not always the right one. These curves have an infinite length and are in some sense everywhere irregular, which is part of the notion of fractal. The word fractal has in fact no exact definition, it has even no well-defined gender when used as a noun in French, but it usually refers to objects that present similarities at every level of magnification, like coastlines, snow flakes, clouds, Romanesco broccoli.

A "tessellation" or "tiling" is a collection of patterns that fill the space without overlaps or gaps. Tessellations inspired many artists and decorate lots of places. The patterns (or "tiles") may be all different, but most of the time there is a finite number of shapes, that fit well together. Maurits Cornelis Escher drew for example a tiling of the plane by horses, putting the horses alternatively standing and upside down such that the legs imbricate. Escher also figurated a tessellation of the circle by black bats and white angels (see Figure 1.1). The painting is called *Circle limit IV*: the shapes get smaller and smaller when approaching the boundary of the circle.

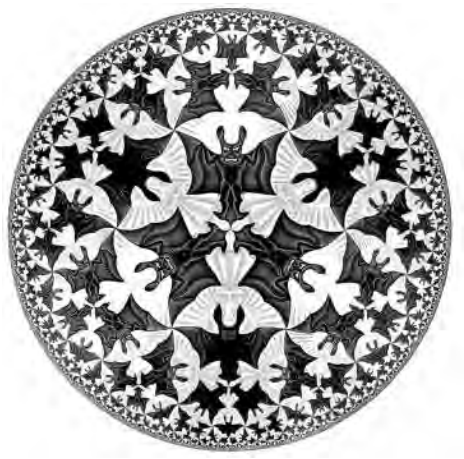

Figure 1.1: *Circle Limit IV*, M.C. Escher.

Both notions of fractal and tessellation can be combined by considering tessellations of the space by fractal patterns. The "miracle" here is that despite their fractal boundary, the tiles still

fit together to provide a tessellation.

The purpose of this thesis is the investigation of the topology of fractal tiles giving rise to a tessellation. Although tiles in n-dimensional spaces will be defined, the topological study will mainly concern plane tiles. By topological study of a tile we then mainly mean: is the tile connected? Is it homeomorphic to a closed disk? If not, what can be said about its fundamental group? Can we describe the connected components of its interior? The tilings will be generated by a single shape. We will consider the general class of crystallographic tiles, where the tilings can involve not only translations but other isometric transformations, like rotations or reflections of the tiles. The research in this general setting started quite recently, thus we will only deal with the question of homeomorphy to a closed disk. Afterwards, we will concentrate on lattice tilings, which allow only translations of the tiles. This more rigid case has already been much more investigated, we will push forward the study of a special class of lattice tilings related to number systems.

Part of the results of this thesis were presented in the Fractal Workshop of Hangzhou in September 2006 and at the Journées de numération in Graz in April 2007. All results are either accepted for publication in international journals and reviews (*cf.* [41, 43, 44, 45]) or under submission (*cf.* [42]).

Acknowledgements

I am mainly grateful to Jörg Thuswaldner for his supervision. This includes the careful reading of this thesis, his enthusiasm in discussions and the constant suggestions of new problems. I also thank Jun Luo for the cooperation work, last year in Guangzhou and this year in Leoben. I eventually thank Michael Drmota for introducing me to Jörg and keeping an eye on me during these two years.

For financial support, I thank the Austrian Science Foundation (FWF) and more particularly the National Research Network "Analytic Combinatorics and Probabilistic Number Theory", projects S9604 (Michael Drmota), S9610 (Jörg Thuswaldner) and S9612 (Reinhard Winkler). Part of this work was also supported by the Sun Yat Sen University of Guangzhou and by the cooperation project "Aktion Österreich-Ungarn" 67öu1 between the University of Leoben and the University of Debrecen.

Chapter 2

Basic notions

The fractal sets described in the present PhD thesis are attractors of certain iterated function systems. Moreover, isometric copies of these sets will tile the plane with no overlap or gap. In this chapter, we recall the basic facts on iterative constructions of fractal sets and introduce the particular kind of tilings of the space we are going to consider, the so-called crystallographic tilings.

2.1 Fractal sets

If not mentioned otherwise, the definitions and results below can be found in [17, 18].

2.1.1 Hausdorff metric

Let (X, d) be a metric space and $A, B \subset X$ non-empty subsets of X. We define a distance between A and B by:

$$d(A, B) = \inf\{d(x, y); x \in A, y \in B\},$$

and write $d(x, A)$ instead of $d(\{x\}, A)$ if $x \in X$. d is not a metric on $\Omega(X) \setminus \{\emptyset\}$ (for example, from $d(A, B) = 0$ it does not follow that $A = B$). To get around the problem, let

$$e(A, B) = \sup\{d(x, B); x \in A\}$$

be the *excess* of A over B. This supremum may be infinite for certain choices of A and B. One can then evaluate how far A and B are from each other by taking the maximum of both excesses $e(A, B)$ and $e(B, A)$, as stated in a more formal way in the following definition.

Definition 2.1.1 (Hausdorff distance)**.** If A, B are two non-empty subsets of a metric space (X, d), the *Hausdorff distance* between A and B is

$$h(A, B) = \max\{\sup\{\inf\{d(x, y); y \in B\}; x \in A\},\ \sup\{\inf\{d(x, y); y \in A\}; x \in B\}\}.$$

Now, from $h(A, B) = 0$ follows that $\overline{A} = \overline{B}$.

Notation 2.1.2. We denote by $\mathcal{K}(X)$ the set of non-empty compact subsets of X.

Proposition 2.1.3 (Hausdorff metric)**.** *$(\mathcal{K}(X), h)$ is a metric space, and h is called* Hausdorff metric associated to d. *Moreover, $(\mathcal{K}(X), h)$ is complete iff (X, d) is.*

An equivalent definition for the Hausdorff distance reads as follows.

Definition 2.1.4 (η-distance)**.** Let $A \subset X$ be non-empty and $\delta > 0$. The *δ-neighborhood* of A is the set

$$A_\delta = \{y \in X; \exists x \in A,\ d(x, y) \leq \delta\}.$$

The *η-distance* between A and B is

$$\eta(A, B) = \inf\{\delta > 0;\ A \subset B_\delta, B \subset A_\delta\}.$$

Proposition 2.1.5. *For all $A, B \subset X$ non-empty, we have:*

$$\eta(A, B) = h(A, B).$$

2.1.2 Iterated function systems

Let (X, d) be a metric space.

Definition 2.1.6 (Isometry, similarity, contraction)**.** A mapping $f : X \to X$ is

(i) a *similarity* on X iff there is a $r \geq 0$ such that for all $x, y \in X$, $d(f(x), f(y)) = r\ d(x, y)$. The number r is called the *similarity ratio* of f.

(ii) an *isometry* on X iff it is a similarity of ratio $r = 1$.

(iii) a *contraction* on X iff there is $r \in [0, 1)$ such that for all $x, y \in X$, $d(f(x), f(y)) \leq r\ d(x, y)$. The minimal r with this property is called the *contraction ratio* of f.

As an example, we recall the following result of Beckmann and Quarles (see [9]).

Proposition 2.1.7. *Let $X = \mathbb{R}^n$ and d be the Euclidean metric. Assume that $f : \mathbb{R}^n \to \mathbb{R}^n$ satisfies the following property.*

$$\exists\, c > 0,\ \forall\, x, y \in \mathbb{R}^n,\ d(x, y) = c \ \Rightarrow\ d(f(x), f(y)) = c.$$

Then there is an orthogonal $n \times n$-matrix A and a vector $b \in \mathbb{R}^n$, such that $f(x) = Ax + b$ for all $x \in \mathbb{R}^n$.

Consequently, the similarities on the Euclidean space are the mappings $f(x) = rAx + b$ where $r \in [0, 1)$, A is an orthogonal matrix and $b \in \mathbb{R}^n$.

An easy construction of fractals results from iterated application of contractions to a given compact set. It uses the Banach fixed point theorem, that appeared in Stefan Banach's PhD thesis in 1920. Let us write a version of this theorem with weakened hypotheses.

Proposition 2.1.8 (Weak contraction mapping theorem)**.** *Let (X, d) be a complete metric space and $f : X \to X$ be a mapping such that some iterate f^p is a contraction on X. Then f has a unique fixed point in X. For any $x_0 \in X$, the sequence of iterates $x_0,\ f(x_0),\ f(f(x_0)), \ldots$ converges to the fixed point of f.*

Thus for $p = 1$ the above proposition is the usual Banach fixed point theorem.

Definition 2.1.9 (IFS)**.** A finite collection $(f_i)_{1 \leq i \leq m}$ $(m \in \mathbb{N})$ of contractions on X is called *iterated function system (IFS) on X.*

Proposition 2.1.10. *Let $n \in \mathbb{N}$ and $(f_i)_{1 \leq i \leq m}$ an IFS, r_i the associated contraction ratios. Then the map*

$$\begin{array}{rcl} F : \mathcal{K}(X) & \to & \mathcal{K}(X) \\ M & \mapsto & \bigcup_{i=1}^m f_i(M) \end{array}$$

is a contraction on $\mathcal{K}(X)$, with contraction ratio $r = \max_{1 \leq i \leq m}\{r_i\}$ (with respect to h, the Hausdorff metric associated to d).

We deduce from Propositions 2.1.8 and 2.1.10 the following fixed point theorem.

Theorem 2.1.11. *Suppose (X, d) is complete. Let $(f_i)_{1 \leq i \leq m}$ be an IFS on X. Then there exists a unique non-empty compact set $E \subset X$ satisfying*

$$E = \bigcup_{i=1}^m f_i(E).$$

Moreover, let the map F be defined on $\mathcal{K}(X)$ by $F(M) = \bigcup_{i=1}^m f_i(M)$. Then for all non-empty compact set $A \subset X$, the sequence of iterates $(F^k(A))_{k \in \mathbb{N}}$ converges to E in the Hausdorff metric associated to d.

Definition 2.1.12 (Attractor of an IFS)**.** With the notations of the above theorem, the set E is called the *attractor* of the IFS $(f_i)_{1\leq i\leq m}$.

Theorem 2.1.11 thus gives an iterative construction of the attractor of an IFS. One can for example start from a set $\{x_0\}$ containing one point and iterate the IFS. If x_0 is chosen in the attractor E, then the constructed approximations are subsets of the attractor.

Remark 2.1.13. The weak version of the contraction mapping theorem (Proposition 2.1.8) allows to define the attractor of an "almost IFS". Indeed, if the $(f_i)_{1\leq i\leq m}$ are mappings from X into itself, it is sufficient for the existence and unicity of the fixed point that the associated function $F : \mathcal{K}(X) \to \mathcal{K}(X)$ with $F(M) = \bigcup_{i=1}^{m} f_i(M)$ has some contracting iterate F^p.

Definition 2.1.14 (Self-affine, self-similar set)**.** Let (X, d) be a complete metric space. A non-empty compact set $E \subset X$ is *self-affine* if it is the attractor of an IFS $(f_i)_{1\leq i\leq m}$ of affine transformations. It is *self-similar* if it is the attractor of an IFS $(f_i)_{1\leq i\leq m}$ of similarities.

Eventually, we mention the open set condition and its consequence.

Definition 2.1.15 (Open set condition)**.** Let $(f_i)_{1\leq i\leq m}$ be mappings on (X,d). Then $(f_i)_{1\leq i\leq m}$ satisfy the *open set condition (OSC)* if there is an open set V such that the sets $f_i(V)$ $(1 \leq i \leq m)$ are pairwise disjoint subsets of V.

Proposition 2.1.16. *If an IFS $(f_i)_{1\leq i\leq m}$ on a complete metric space satisfies the open set condition, the subpieces $f_i(E)$ $(1 \leq i \leq m)$ of its attractor E are pairwise non-overlapping.*

2.1.3 Systems of graph directed sets

Graph directed sets generalize the preceding notion of attractor.

Definition 2.1.17 (Graph directed IFS)**.** A *geometric graph directed construction* of $\mathbb{R}^n$ consists of

(1) finitely many compact subsets $J_1, \ldots, J_q$ of $\mathbb{R}^n$ such that each J_i has nonempty interior;

(2) a directed graph $G(V, E)$ with set of vertices $V = \{1, \ldots, q\}$ and to each edge $e \in E$ a contraction T_e having the following properties:

   a) Each vertex has outgoing edges.

   b) Let E_{ij} be the set of edges leading from i to j. Then $\bigcup_j \{T_e(J_j); e \in E_{ij}\}$ is a non-overlapping family and

$$J_i \supset \bigcup_j \{T_e(J_j); e \in E_{ij}\} \quad (i \in \{1, \ldots, q\}). \tag{2.1.1}$$

A very similar definition can be found in Mauldin and Williams [50] (see also [8] and [18]). Despite the definition of geometric graph directed construction in [50] is more restrictive in some regards the following result is still valid with the same proof.

Proposition 2.1.18 ([50, Theorem 1])**.** *Given a geometric graph directed construction of $\mathbb{R}^n$ as in the preceding definition, there exists a unique vector $(K_1, \ldots, K_q)$ of compact subsets of $\mathbb{R}^n$ such that for each $i \in \{1, \ldots, q\}$*

$$K_i = \bigcup_j \{T_e(K_j); e \in E_{ij}\} \tag{2.1.2}$$

holds.

Definition 2.1.19 (Self-similar, self-affine systems of graph directed sets)**.** With the notations of Proposition 2.1.18, $(K_1, \ldots K_q)$ is called a *system of graph directed sets*. If the T_e are affinities the system is called *self-affine GIFS*, if they are similarities, it is called *self-similar GIFS*.

2.2 Crystallographic tilings

2.2.1 Tilings

The definitions and facts of this subsection may be found in Grünbaum and Shephard' book *Tilings and patterns* [22]. We adopt the following notation.

Notation 2.2.1. For a set M in a topological space, the interior of M will be denoted by $\mathrm{int}(M)$ (or sometimes shortly by M^o).

Definition 2.2.2 (Tiling, tile)**.** A *tiling* of $\mathbb{R}^n$ is a family $\{T_i; i \in I\}$ such that:

(i) $T_i = \overline{\mathrm{int}(T_i)}$ for all $i \in I$,

(ii) $\mathbb{R}^n = \bigcup_{i\in I} T_i$,

(iii) $\mathrm{int}(T_i) \cap \mathrm{int}(T_j) = \emptyset$ for $i \neq j$ with $i, j \in I$.

A non-empty compact set which coincides with the closure of its interior, as in (i), is called a *tile*.

Hence, a tile is a regular-closed subset of $\mathbb{R}^n$, and a tiling is a family of tiles covering $\mathbb{R}^n$ without overlaps or gaps. By Item (iii) of the preceding definition, the pieces of a tiling can only intersect at their boundary.
In this general definition, the tiles may concentrate in small regions of the tiling. To avoid this, we deal with locally finite tilings.

Definition 2.2.3 (Locally finite tiling)**.** A tiling $\{T_i; i \in I\}$ is *locally finite* if each bounded set intersects only a finite number of sets T_i.

Definition 2.2.4 (Prototile)**.** If all the tiles of a tiling are congruent to a single tile T, then T is called a *prototile* of the tiling (congruent to T means that it is the image of T by some isometry).

In this thesis, we will be concerned by locally finite tilings using a single prototile T. In this case, there is a discrete family Γ of isometries such that $\{\gamma(T); \gamma \in \Gamma\}$ is a tiling of $\mathbb{R}^n$, and we say that T *tiles* $\mathbb{R}^n$ *by* Γ.

2.2.2 Crystallographic groups

Definition 2.2.5 (Cocompact subgroup, fundamental domain)**.** A discrete subgroup Γ of the group of isometries $\mathrm{Isom}(\mathbb{R}^n)$ on $\mathbb{R}^n$ is *cocompact* if there is a compact set K, such that $\{\gamma(K); \gamma \in \Gamma\}$ is a tiling of $\mathbb{R}^n$. Such a K is then called a *fundamental domain* of Γ.

Notation 2.2.6. We denote by $\mathrm{Isom}(\mathbb{R}^n)$ the group of all isometries on $\mathbb{R}^n$ with respect to a metric d, and by id the identity mapping of $\mathbb{R}^n$.

Definition 2.2.7 (Crystallographic group)**.** A *crystallographic group in dimension n* is a discrete cocompact subgroup Γ of $\mathrm{Isom}(\mathbb{R}^n)$.

A crystallographic group is nothing else but the symmetry group of a crystal.

Theorem 2.2.8 (Theorem of Bieberbach [11])**.** *A subgroup* Γ *of* $\mathrm{Isom}(\mathbb{R}^n)$ *is a crystallographic group in dimension n if and only if there is a normal subgroup* $\Lambda \subset \Gamma$ *with finite index, which is isomorphic to* $\mathbb{Z}^n$*, and which is a maximal abelian subgroup in* Γ*.*

Definition 2.2.9 (Lattice, point group)**.** With the notations of Theorem 2.2.8, the group Λ is called the *lattice* of Γ, and the quotient Γ/Λ of the crystallographic group by its lattice is called the *point group* of Γ.

$p2$-pavement.

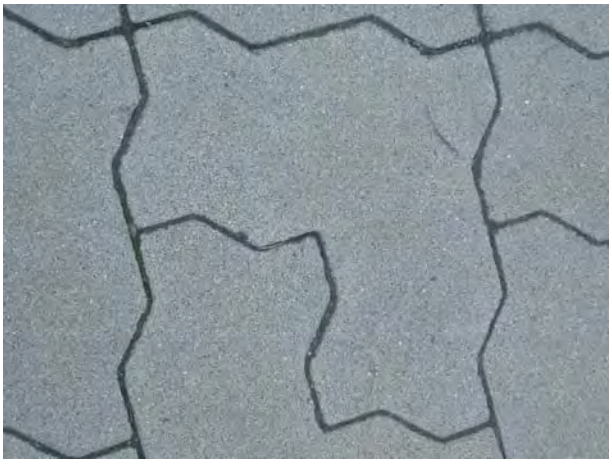

$p2$-prototile.

Figure 2.1: The pavement of Leoben's main train station: a $p2$-tiling.

In the plane, there are seventeen isomorphy classes of crystallographic groups. For example, a $p2$-group is a group generated by two independent translations and one π-rotation (thus its point group has one non trivial element).

Definition 2.2.10 ($p2$-group)**.** Let $u(x,y) = (x+1, y),\ v(x,y) = (x, y+1),\ r(x,y) = (-x,-y)$. Then a *$p2$-group* is a group of isometries of $\mathbb{R}^2$ isomorphic to the subgroup of $\mathrm{Isom}(\mathbb{R}^2)$ generated by the translations u, v and the π-rotation r.

Similarly, a *$p3$-group* is a group generated by two independent translations and a $2\pi/3-$rotation: the point group has two non-trivial elements. A *pm-group* is generated by two perpendicular translations and a reflection along one of the translation vectors.

2.2.3 Crystallographic tilings

Definition 2.2.11 (Crystallographic tiling, crystallographic tile, central tile)**.** If Γ is a crystallographic group, T a tile and $\{\gamma(T); \gamma \in \Gamma\}$ a tiling of $\mathbb{R}^n$, then $\{\gamma(T); \gamma \in \Gamma\}$ is called a *crystallographic tiling* of $\mathbb{R}^n$. A *crystallographic tile* is any tile belonging to a crystallographic tiling. T is called the *central tile* of the tiling. We call the corresponding tilings *Γ-tilings*, and the tiles in the tiling are *Γ-tiles*.

In fact, by a slight abuse of notation, if for example Γ is a $p2$-group, we will call the tiling a $p2$-tiling, and similarly for the tiles. An example of $p2$-tiling can be seen in Figure 2.1. We also mention that another term for crystallographic tiling is isohedral tiling (see [22]).

The crystallographic groups offer the minimal requirement for the study of reasonable tiles. Indeed, the discreteness of the group is a necessary condition for the tiling to be locally finite, and its cocompactness for the tiles to be compact.

Remark 2.2.12. In the special case where Γ is isomorphic to $\mathbb{Z}^n$, or in other words, where Γ has trivial point group, the collection $\{\gamma(T); \gamma \in \Gamma\}$ is a said to be a *lattice tiling* of $\mathbb{R}^n$. One then often says that T *tiles* the space *by* "its translates": there are n independent translation vectors $t_1, \ldots, t_n \in \mathbb{R}^n$ such that the family $\{T + k_1 t_1 + \ldots + k_n t_n; k_1, \ldots, k_n \in \mathbb{Z}\}$ is a tiling of $\mathbb{R}^n$.

Definition 2.2.13 (Neighbors)**.** Let T' be a tile of a crystallographic tiling $\{\gamma(T), \gamma \in \Gamma\}$, where Γ is a crystallographic group and T the central tile. The *set of neighbors* of T' is defined by

$$\mathcal{S}(T') := \{\gamma \in \Gamma \setminus \{\mathrm{id}\}; T' \cap \gamma(T') \neq \emptyset\}. \tag{2.2.1}$$

Hence, a *neighbor* of the tile T' is in fact an isometry $\gamma \in \Gamma \setminus \{\mathrm{id}\}$ such that $\gamma(T')$ intersects T'.

Lemma 2.2.14. *$\mathcal{S}(T')$ defined above is a finite set.*

Proof. This is because the tiling is locally finite (recall that Γ is discrete and T' is compact). □

Among the possible neighbors of a tile, we mark out the following ones.

Definition 2.2.15 (Vertex and adjacent neighbors)**.** Let T' be a tile of a crystallographic tiling $\{\gamma(T), \gamma \in \Gamma\}$, where Γ is a crystallographic group and T the central tile. An element $\gamma \in \mathcal{S}(T')$ is called

- *vertex neighbor* of T' if $T' \cap \gamma(T') = \{x\}$ for some $x \in \mathbb{R}^n$;
- *adjacent neighbor* of T' if $T' \cap \gamma(T')$ contains a point of $\mathrm{int}(T' \cup \gamma(T'))$.

The set of adjacent neighbors of T' is denoted by $\mathcal{A}(T')$.

For the composition of mappings, we adopt the following notations.

Notation 2.2.16. If m_1, m_2 are two mappings, we write $m_1 \circ m_2$ or shortly $m_1 m_2$ for the mapping $x \mapsto m_1(m_2(x))$. For iterative compositions

$$\underbrace{m_1 m_1 \cdots m_1}_{p \text{ times}},$$

we rather write m_1^p. If M_1 and M_2 are sets of mappings, then $M_1 M_2$ stands for $\{m_1 m_2; m_1 \in M_1, m_2 \in M_2\}$. M_1^p means

$$\underbrace{M_1 M_1 \cdots M_1}_{p \text{ times}}.$$

If M_1 happens to contain only one mapping m_1, we will write $m_1 M_2$ for $\{m_1\} M_2$. An analogous notation is used if M_2 contains one element. Eventually, if the elements of M_1 are invertible, M_1^{-1} stands for $\{m_1^{-1}; m_1 \in M_1\}$.

Remark 2.2.17. We have the simple relations, writing $T' = \gamma'(T)$ for some $\gamma' \in \Gamma$:

$$\mathcal{S}(\gamma'(T)) = \gamma' \mathcal{S}(T),$$
$$\mathcal{A}(\gamma'(T)) = \gamma' \mathcal{A}(T).$$

Notation 2.2.18. The above remark invites us to write simply $\mathcal{S}$ for the set of neighbors of the central tile T, and $\mathcal{A}$ for the set of its adjacent neighbors.

The configuration of the tiles in the tiling can be visualized with the help of graphs. We recall some notions and definitions related to non-directed and non-labelled graphs. We refer to [15] for more precisions.

Definition 2.2.19 (Graph; vertex or state, edge; incident and end vertices; subgraph and induced subgraph)**.** A *graph* is a pair $G = (V, E)$ of sets such that E is a set of 2-subsets of V, with V and E finite or infinite; thus, the elements of E are of the form $\{x, y\}$ with $x, y \in V$. The elements of V are called *vertices* or *states* of the graph G, the elements of E are called *edges*. Two vertices are *incident* if they constitute an edge. The two vertices incident with an edge are its *end vertices* or *ends*, and an edge *joins* its ends. An edge $\{x, y\}$ is usually written as xy (or yx). A *subgraph* of G is a graph (V', E') with $V' \subset V$ and $E' \subset E$. Eventually, if $V' \subset V$, the *subgraph of G induced by* V' is the graph $G' = (V', E')$ with vertex set V' and edges the elements of V that are 2-subsets of V'.

The usual way to draw a graph is by drawing a dot for each vertex and joining two of these dots by a line if the corresponding two vertices form an edge.

Definition 2.2.20 (Planar graph)**.** If one can draw a graph G in the plane in a way that no two edges meet in a point other than a common end, G is *planar*.

Notation 2.2.21. Let $\{\gamma(T);\ \gamma \in \Gamma\}$ be a crystallographic tiling, where Γ is a crystallographic group, T the central tile and $\mathcal{S}$ the set of neighbors of the central tile. For $\gamma \in \mathcal{S}$, we write

$$B_\gamma = T \cap \gamma(T).$$

Definition 2.2.22 (Neighbor graph, adjacency graph and double neighboring graph)**.** For a finite symmetric set $M \subset \Gamma$, we define $G(M)$ as the graph with vertex set Γ and for which a 2-element set $\{\gamma_1, \gamma_2\} \subset \Gamma$ is an edge whenever $\gamma_1^{-1}\gamma_2 \in M$. For the particular choice $M = \mathcal{S}$, $G_N := G(\mathcal{S})$ is the *neighbor graph*, and for $M = \mathcal{A}$, $G_A := G(\mathcal{A})$ is the *adjacency graph* of the tiling. If $\mathcal{A}' \subset \mathcal{A}$, we will write $G_A(\mathcal{A}') := G(\mathcal{A}')$ the corresponding subgraph of G_A.
The *double neighboring graph* G_2 is the one having $\{\gamma\,(B_{\gamma'})\,;\gamma \in \Gamma, \gamma' \in \mathcal{A}\}$ as set of states and in which two distinct elements $\gamma_1\left(B_{\gamma_1'}\right)$ and $\gamma_2\left(B_{\gamma_2'}\right)$ are incident whenever they intersect each other.

Note that the neighbor graph and the adjacency graph are variants of Cayley graphs (see for example [24]).

Definition 2.2.23 (Regular graph, degree of a graph)**.** A graph G is *regular* if each vertex is incident with the same number of edges, called the *degree* of the graph.

A consequence of Remark 2.2.17 is the following lemma.

Lemma 2.2.24. *G_N and G_A as in Definition 2.2.22 are regular graphs by the group property of Γ.*

The tiling property of Definition 2.2.11 leads to the following remark.

Remark 2.2.25.

1. The neighbor graph G_N is always connected; otherwise, choose a component of G_N with vertex set $\mathcal{V}_0$, then $\bigcup_{\gamma\in\mathcal{V}_0}\gamma(T)$ would be a subset of $\mathbb{R}^n$ which is both closed and open, contradicting the connectivity of $\mathbb{R}^n$.

2. The neighbor set $\mathcal{S}$ of T is a symmetric generating set of Γ (*i.e.*, $\Gamma = \langle\mathcal{S}\rangle$) and $\gamma \in \mathcal{S}$ if and only if $\gamma^{-1} \in \mathcal{S}$. If Γ is a lattice, then $\#\mathcal{S}$, the cardinality of $\mathcal{S}$, is an even number, at least $2n$.

Chapter 3

Crystallographic tiles

The present chapter is devoted to the study of self-affine tiles providing a crystallographic tiling of $\mathbb{R}^n$ (see Definitions 2.1.14 and 2.2.11). The self-affinity of such a tile occurs in the following way: there is an affine expansion that blows up the tile onto k of its isometric copies for some $k \in \mathbb{N}$. Hence, it is called crystallographic replicating tile, or crystallographic reptile for short, even *crystile* for very short. Gelbrich [19] introduced these tiles in 1994. He proved that for each k there are only finitely many isomorphy classes of plane crystiles which are homeomorphic to a closed disk (*disk-like*). He gave all candidates of disk-like crystiles for $k = 3$ in the case that the crystallographic group is $p2$ but could not decide whether these are really disk-like or not.

We will first give the exact definition of a crystile and present some general properties. Since it turns out that the topology of a crystile is closely related to the configuration of its neighboring tiles in the tiling, we will give an algorithm to compute the set of neighbors. Several criteria of homeomorphy to a closed disk will then be proved. The first one will be stated for crystallographic tiles in general. The next two criteria will concern crystallographic reptiles. The last criterion will handle two special classes of crystiles: the lattice and the $p2$-crystiles. Throughout this chapter, a norm $||\cdot||$ on $\mathbb{R}^n$ and its associated metric d are fixed. We refer to Appendix A for the definitions and facts of plane topology.

3.1 Crystiles: definitions and example

Crystiles are compact sets mapped onto a finite union of their isometric copies by an expanding mapping. In this section, we give some definitions and an example of these fractal sets.

Definition 3.1.1 (Expanding affine mapping)**.** A mapping $g : \mathbb{R}^n \to \mathbb{R}^n$ is *expanding affine* if $g(x) = Ax + t$ for all $x \in \mathbb{R}^n$, where $t \in \mathbb{R}^n$ and A is an $n \times n$ *expanding matrix* with real entries, *i.e.*, its eigenvalues all have modulus greater than 1. Hence, the vector t is the *translation part*, the matrix A the *linear part* of g.

Let Γ be a crystallographic group.

Notation 3.1.2. Let γ be an isometry in Γ. We denote by A_γ its linear part and by t_γ its translation part. Hence for all $x \in \mathbb{R}^n$, $\gamma(x) = A_\gamma x + t_\gamma$.

Definition 3.1.3 (Crystallographic reptile, cf. [19])**.** A *crystallographic reptile with respect to* Γ is a set $\mathcal{T} \subset \mathbb{R}^n$ with the following properties.

- The family $\{\gamma(\mathcal{T}); \gamma \in \Gamma\}$ is a tiling of $\mathbb{R}^n$.
- There is an expanding affine mapping $g : \mathbb{R}^n \to \mathbb{R}^n$ that conjugates Γ onto a subgroup, *i.e.*, $g\Gamma g^{-1} \leq \Gamma$, and a finite collection $\mathcal{D} \subset \Gamma$, called set of digits, such that

$$g(\mathcal{T}) = \bigcup_{\delta \in \mathcal{D}} \delta(\mathcal{T}). \tag{3.1.1}$$

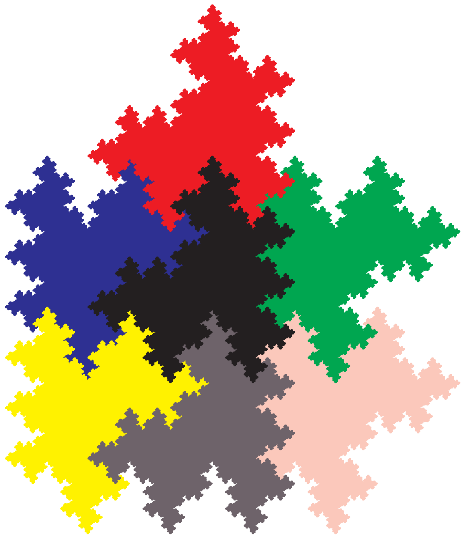

Figure 3.1: $p2$-crystile with its neighboring tiles.

$\mathcal{T}$ is the crystallographic reptile with respect to $(\Gamma, \mathcal{D}, g)$.

We will call a crystallographic reptile also simply a *crystile*, and the tiles associated to the digits $(\delta(\mathcal{T}),\ \delta \in \mathcal{D})$ in the above definition, *digit tiles*.

From the replicating property (3.1.1), we deduce some compatibility relations between the expansion g and the digit set $\mathcal{D}$. Since $g(\mathcal{T})$ is the union of non-overlapping copies of $\mathcal{T}$, its volume is exactly $|\mathcal{D}|$ times the volume of $\mathcal{T}$, hence $|\mathcal{D}| = |\det A|$. However, this is not the only restriction. Indeed, the tiling property and the replicating property iterated once imply that

$$\bigcup_{\gamma\in\Gamma} \gamma(\mathcal{T}) = \mathbb{R}^n = g(\mathbb{R}^n) = \bigcup_{\gamma\in\Gamma} g\gamma g^{-1} \bigcup_{\delta\in\mathcal{D}} \delta(\mathcal{T}),$$

hence $\Gamma = g\Gamma g^{-1}\Gamma$ $\mathcal{D}$ and $\mathcal{D}$ must be a complete set of right coset representatives of $\Gamma/g\Gamma g^{-1}$ (see [19]).

Example 3.1.4. We give an example of a plane $p2$-crystile, which will be studied in Subsection 3.3.4.

Take the map g defined by

$$g(x, y) = \left(y, -3x - \frac{1}{2}\right)$$

and the digit set

$$\mathcal{D} = \{\mathrm{id}, b, c\},$$

where $b(x, y) = (x, y + 1)$ and $c(x, y) = (-x, -y)$. The set $\mathcal{T}$ fulfilling

$$g(\mathcal{T}) \ = \ \mathcal{T} \cup b(\mathcal{T}) \cup c(\mathcal{T})$$

is then a crystile. The requirement $g\Gamma g^{-1} \subset \Gamma$ (see Definition 3.1.3) is fulfilled because

$$gag^{-1} = b^{-3},\ gbg^{-1} = a,\ gcg^{-1} = b^{-1}c.$$

$\mathcal{T}$ induces a tiling, as can be seen on Figure 3.1.

Remark 3.1.5.

1. Without loss of generality, one can assume that the digit set $\mathcal{D}$ contains id (see [19]).
2. By definition, the expanded shape $g(\mathcal{T})$ is the union of $\delta(\mathcal{T})$ with δ running through the set $\mathcal{D}$. Thus for each $\gamma \in \Gamma$, there is a uniquely determined collection $\mathcal{D}_\gamma \subset \Gamma$ such that $g\gamma(\mathcal{T})$ is the union of all the tiles $\delta(\mathcal{T})$ with δ running through $\mathcal{D}_\gamma$; more precisely, we have $\mathcal{D}_\gamma = g\gamma g^{-1}\mathcal{D}$.

Equivalent to the replicating property is the subdivision principle

$$\mathcal{T} = \bigcup_{\delta\in\mathcal{D}} g^{-1}\delta(\mathcal{T}). \tag{3.1.2}$$

Remark 3.1.6. Iterating the subdivision principle, one gets that, for each m, a crystile $\mathcal{T}$ is the union of its (non-overlapping) subpieces $\left\{g^{-1}\delta_1 \dots g^{-1}\delta_m(\mathcal{T}); \delta_1, \dots, \delta_m \in \mathcal{D}\right\}$.

Definition 3.1.7 (Subpiece of level m)**.** For a crystile $\mathcal{T}$ with respect to $(\Gamma, \mathcal{D}, g)$ and an integer m, a *subpiece of level m* is any

$$g^{-1}\delta_1 \dots g^{-1}\delta_m(\mathcal{T}),$$

where $\delta_1, \dots, \delta_m \in \mathcal{D}$.

The functions $g^{-1}\delta$ are affine mappings. Nevertheless, crystiles need not be self-affine in the sense of Definition 2.1.14. The $g^{-1}\delta$ contract the volumes, because the eigenvalues of their linear part are smaller than 1, but they may not contract the distances. However, even if the mapping $F(M) = \bigcup_{\delta\in\mathcal{D}} g^{-1}\delta(M)$ is not a contraction, one of its iterates will be. Hence, a crystile is a self-affine attractor in the sense of Remark 2.1.13.

Proposition 3.1.8. *With the notations of Definition 3.1.3, the mapping $F(M) = \bigcup_{\delta\in\mathcal{D}} g^{-1}\delta(M)$ becomes contracting after finitely many iterations: there is an $m \geq 1$ such that F^m is a contraction on $\mathcal{K}(\mathbb{R}^n)$.*

Proof. It suffices to show that there is an m for which $g^{-1}\delta_1 \dots g^{-1}\delta_m$ is a contraction on $\mathbb{R}^n$ for every family $(\delta_i)_{1\leq i\leq m}$ of digits. Then F^m will be a contraction on the $\mathcal{K}(\mathbb{R}^n)$. Thus let $p \in \mathbb{N}$ and $(\delta_i)_{1\leq i\leq p}$ any family of digits. Since $g\Gamma g^{-1} \subset \Gamma$, there are some isometries $\gamma_1, \dots, \gamma_p$ of Γ such that

$$g^{-1}\delta_1 \dots g^{-1}\delta_p = g^{-p}\gamma_1 \dots \gamma_p.$$

Since $g(x) = Ax + t$, we have for all $x, y \in \mathbb{R}^n$ that

$$g^{-p}(x) - g^{-p}(y) = A^{-p}(x - y).$$

Denoting by $|||\cdot|||$ the matrix norm associated to the norm $||\cdot||$, and remembering that the γ_i are isometries, we have for all $x, y \in \mathbb{R}^n$:

$$||g^{-1}\delta_1 \dots g^{-1}\delta_p(x) - g^{-1}\delta_1 \dots g^{-1}\delta_p(y)|| \ \leq \ |||A^{-p}||| \ ||x - y||.$$

We now just choose p such that $|||A^{-p}||| \ < \ 1$ (which is possible, since A is an expanding matrix) and set $m = p$. □

Notation 3.1.9. If K is a compact set, we denote by $\mathrm{diam}(K)$ the maximal distance between two points of K.

Remark 3.1.10. It follows from the above computation that for every sequence $(\delta_i)_{i\in\mathbb{N}}$ of digits and every $x, y \in \mathbb{R}^n$,

$$\lim_{p\to\infty} ||g^{-1}\delta_1 \dots g^{-1}\delta_p(x) - g^{-1}\delta_1 \dots g^{-1}\delta_p(y)|| = 0. \tag{3.1.3}$$

We can even say that, if K is a compact set and $\varepsilon > 0$ is given, then there is $p \in \mathbb{N}$ such that

$$\mathrm{diam}(g^{-1}\delta_1 \dots g^{-1}\delta_p(K)) < \varepsilon \tag{3.1.4}$$

for any sequence of digits $(\delta_i)_{1\leq i\leq p}$.

We thus have the following topological property, stated in Hata [23] for self-similar sets.

Proposition 3.1.11 (Hata [23])**.** *Let $\mathcal{T}$ be a connected crystile. Then $\mathcal{T}$ has property (S) and is therefore locally connected and arcwise connected.*

The above considerations lead to the following representation of a crystile.

Proposition 3.1.12. *Let $\mathcal{T}$ be a crystile with respect to $(\Gamma, \mathcal{D}, g)$. Let $a \in \mathbb{R}^n$. Then*

$$\mathcal{T} = \left\{ \lim_{m\to\infty} g^{-1}\delta_1 \dots g^{-1}\delta_m(a); (\delta_i)_{i\in\mathbb{N}} \in \mathcal{D}^{\mathbb{N}} \right\}. \tag{3.1.5}$$

Proof. Proposition 3.1.8 together with Proposition 2.1.8 indicate that $(g, \mathcal{D})$ gives rise to a unique compact set $\mathcal{T}$ satisfying the subdivision principle (3.1.2) (see also Remark 2.1.13). Let K be the set on the right side of Equation (3.1.5). Then K is a compact set that also satisfies (3.1.2), hence $K = \mathcal{T}$ by the uniqueness of the attractor. □

Definition 3.1.13 (Isomorphic crystiles, *cf.* [19])**.** Let $\mathcal{T}, \mathcal{T}'$ be two crystiles with respect to crystallographic groups Γ, Γ', with expansions g, g' and digit sets $\{\delta_1, \dots, \delta_q\}, \{\delta'_1, \dots, \delta'_q\}$, respectively. An affine bijection $\phi : \mathcal{T} \to \mathcal{T}'$ is said to *preserve pieces of level* $m \in \mathbb{N}$ if for each sequence of indices $i_1, \dots, i_m$ there is a sequence $j_1, \dots, j_m$ such that ϕ is a bijection from $g^{-1}\delta_{i_1} \dots g^{-1}\delta_{i_m}(\mathcal{T})$ onto $g'^{-1}\delta'_{j_1} \dots g'^{-1}\delta'_{j_m}(\mathcal{T})$. We say that two crystiles $\mathcal{T}$ and $\mathcal{T}'$ are *isomorphic* iff there is an affine bijection $\phi : \mathcal{T} \to \mathcal{T}'$ preserving the pieces of all levels.

3.2 Neighbors of a crystile

The results of this section will be published in the joint article [44] with Jun Luo and Jörg Thuswaldner. For a crystallographic tiling, we already defined the neighbor graph, the adjacency graph and the double neighboring graph in Definition 2.2.22. These graphs describe the geometrical configuration of the tiles in the tiling. In addition to these, for a crystile, we introduce graphs that take the fractal structure into account. They are useful in order to compute algorithmically the set of neighbors of a crystile.

In the sequel we consider a crystile $\mathcal{T}$ with respect to a crystallographic group Γ; g is the corresponding expanding mapping and $\mathcal{D} \subset \Gamma$ the set of digits, which is supposed to contain id, the identity map of Γ. The set of neighbors of $\mathcal{T}$ is denoted by $\mathcal{S}$, the set of its adjacent neighbors by $\mathcal{A}$, and B_γ stands for $\mathcal{T} \cap \gamma(\mathcal{T})$, as in Subsection 2.2.3.

We first introduce the neighborhood graph and the contact graph associated to the crystile $\mathcal{T}$. We then show how the neighborhood graph can be used to characterize the boundary of the crystile. We also give properties of the contact graph, and eventually give an algorithm which allows to compute the neighborhood graph from this graph.

3.2.1 Definition of graphs

As we will show in the next subsection, the set of neighbors $\mathcal{S}$ can be computed algorithmically from the data $(\Gamma, g, \mathcal{D})$. The construction of the set $\mathcal{S}$ will require a set $\mathcal{R}$ which is related to the neighbors of certain approximations of $\mathcal{T}$. It is defined as follows.

Let Q be an n-dimensional polyhedron that is the closure of a fundamental domain of Γ. The boundary of Q consists of a union of $(n-1)$-dimensional faces (parts of hyperplanes of $\mathbb{R}^n$).
We can define $\mathcal{R}_0$ as the set of adjacent neighbors of the fundamental domain together with the identity, *i.e.*,

$$\begin{aligned} \mathcal{R}_0 &:= \{\mathrm{id}\} \cup \{\gamma \in \Gamma; \gamma(Q) \cap Q \text{ is an } (n-1)\text{-dimensional face}\} \\ &= \{\mathrm{id}\} \cup \{\gamma \in \Gamma; \gamma(Q) \cap Q \text{ contains an inner point of } \gamma(Q) \cup Q\}\ . \end{aligned}$$

Starting from this set, we define a sequence $(\mathcal{R}_p)_{p\geq 1}$ recursively by

$$\mathcal{R}_p := \mathcal{R}_{p-1} \cup \{\gamma \in \Gamma; g\gamma g^{-1}\, \mathcal{D} \,\cap\, \mathcal{D}\, \mathcal{R}_{p-1} \,\neq \emptyset\}. \tag{3.2.1}$$

Definition 3.2.1 (Contact set)**.** The *contact set* of the crystile $\mathcal{T}$ is

$$\mathcal{R} = \bigcup_{p\geq 0} \mathcal{R}_p.$$

Lemma 3.2.2. *The contact set $\mathcal{R}$ is finite: $\mathcal{R}_p$ eventually stabilizes,* i.e.*, there is a $p_0 \in \mathbb{N}$ such that $\mathcal{R}_p = \mathcal{R}_{p_0}$ for $p \geq p_0$.*

Remark 3.2.3. Lemma 3.2.2 follows from the facts that g is an expanding mapping and that Γ is a discrete group. An estimate for p_0 will be obtained in Remark 3.2.30, at the end of this section.

Definition 3.2.4 (Neighborhood graph, contact graph)**.** For $M \subseteq \Gamma$ we define the graph $\mathbf{G}(M)$ as follows. The states of $\mathbf{G}(M)$ are the elements of M. Moreover, there is an edge

$$\gamma \xrightarrow{\delta|\delta'} \gamma' \in \mathbf{G}(M)$$

iff

$$\delta^{-1}\, g\gamma g^{-1}\, \delta' \;=\; \gamma' \text{ with } \gamma, \gamma' \in M \text{ and } \delta, \delta' \in \mathcal{D}.$$

The following special cases are of particular importance:

- The *neighborhood graph* $\mathbf{G}(\mathcal{S})$.
- The *contact graph* $\mathbf{G}(\mathcal{R})$.

3.2.2 Properties of the neighborhood graph

The non-overlapping property yields for the boundary of $\mathcal{T}$ that $\partial\mathcal{T} = \bigcup_{\gamma\in\mathcal{S}} B_\gamma$. The following holds for every $\gamma \in \mathcal{S}$.

$$\begin{array}{rcl} g(B_\gamma) & = & g(\mathcal{T} \cap \gamma(\mathcal{T})) \;=\; g(\mathcal{T}) \cap g\gamma(\mathcal{T}) \\ & = & \bigcup_{\delta\in\mathcal{D}} \delta(\mathcal{T}) \,\cap\, \bigcup_{\delta'\in\mathcal{D}} g\gamma g^{-1}\, \delta'(\mathcal{T}) \\ & = & \displaystyle\bigcup_{\delta,\delta'\in\mathcal{D}} \delta(\underbrace{\mathcal{T} \,\cap\, \delta^{-1} g\gamma g^{-1}\, \delta'(\mathcal{T})}_{B_{\delta^{-1}\, g\gamma g^{-1}\, \delta'}}). \end{array}$$

Consequently, we obtain the following set equation for B_γ:

$$B_\gamma \;=\; \bigcup_{\delta,\delta'\in\mathcal{D}} g^{-1}\delta(\, B_{\delta^{-1}\, g\gamma g^{-1}\, \delta'}\,)\,. \tag{3.2.2}$$

Using the neighborhood graph defined in Definition 3.2.4 and the fact that $B_{\gamma'} \neq \emptyset$ iff $\gamma' \in \mathcal{S}$, the set equation above reduces to

$$\partial\mathcal{T} \;=\; \bigcup_{\gamma\in\mathcal{S}} B_\gamma \qquad \text{where} \qquad B_\gamma \;=\; \bigcup_{\substack{\delta\in\mathcal{D},\gamma'\in\mathcal{S},\\ \exists\, \delta'\in\mathcal{D},\; \gamma\xrightarrow{\delta|\delta'}\gamma' \,\in\mathbf{G}(\mathcal{S})}} g^{-1}\delta(B_{\gamma'})\,. \tag{3.2.3}$$

Remark 3.2.5. $(B_\gamma)_{\gamma\in\mathcal{S}}$ is not always a system of graph directed sets in the strict sense of Definition 2.1.19, since the mappings $g^{-1}\delta$ may not be strict contractions.

Remark 3.2.6. The graph $\mathbf{G}(\mathcal{S})$ has the following properties.

- To given $\gamma, \gamma' \in \mathcal{S}, \delta \in \mathcal{D}$, there is at most one $\delta' \in \mathcal{D}$ with $\gamma \xrightarrow{\delta|\delta'} \gamma'$ in $\mathbf{G}(\mathcal{S})$.
- The graph $\mathbf{G}(\mathcal{S})$ is *left-resolving, i.e.*,

$$\forall\, (\gamma', \delta') \in \mathcal{S} \times \mathcal{D},\ \exists!\, (\gamma, \delta) \in \mathcal{S} \times \mathcal{D} :\ \gamma \xrightarrow{\delta|\delta'} \gamma'\ \in \mathbf{G}(\mathcal{S}).$$

  Indeed, if $(\gamma', \delta') \in \mathcal{S} \times \mathcal{D}$ then there exists exactly one $(\gamma, \delta) \in \Gamma \times \mathcal{D}$ such that the equality $\gamma' \delta'^{-1} = \delta^{-1} g \gamma g^{-1}$ holds. This is true because $\mathcal{D}$ is a complete set of right coset representatives of $g\Gamma g^{-1}$. Moreover,

$$\begin{array}{ll} & \mathcal{T} \cap \gamma'(\mathcal{T}) \neq \emptyset \\ \Rightarrow & \mathcal{T} \cap \delta^{-1} g \gamma g^{-1} \delta'(\mathcal{T}) \neq \emptyset \\ \Rightarrow & \underbrace{g^{-1}\delta(\mathcal{T})}_{\subset \mathcal{T}} \cap \underbrace{\gamma g^{-1} \delta'(\mathcal{T})}_{\subset \gamma(\mathcal{T})} \neq \emptyset \\ \Rightarrow & \mathcal{T} \cap \gamma(\mathcal{T}) \neq \emptyset\,. \end{array}$$

  This implies that $\gamma \in \mathcal{S}$, and by the definition of $\mathbf{G}(\mathcal{S})$ we conclude that $\gamma \xrightarrow{\delta|\delta'} \gamma'\ \in \mathbf{G}(\mathcal{S})$.

One can wonder how many tiles of the tiling meet the tile $\mathcal{T}$ at a point of the boundary of $\mathcal{T}$.

Definition 3.2.7 (L-vertices)**.** For $\gamma_1, \ldots, \gamma_L\ \in \mathcal{S}$ pairwise different, we call

$$V_L(\gamma_1, \ldots, \gamma_L) = \{x \in \mathbb{R}^n; x \in \mathcal{T} \cap \gamma_1(\mathcal{T}) \cap \ldots \cap \gamma_L(\mathcal{T})\}$$

the set of points (so-called *L-vertices*) that are common to $\gamma_1(\mathcal{T}), \ldots, \gamma_L(\mathcal{T})$ and $\mathcal{T}$, and

$$V_L = \bigcup_{\{\gamma_1, \ldots, \gamma_L\} \subseteq \mathcal{S}} V_L(\gamma_1, \ldots, \gamma_L)$$

the set of L-vertices of $\mathcal{T}$.

Note that $V_1(\gamma) = B_\gamma$ holds.

There are characterizations of these sets using the neighborhood graph. Let us first characterize a point belonging to two tiles (say w.l.o.g. to the central tile $\mathcal{T}$ and one of its neighbors). To this matter, we recall the following definitions.

Definition 3.2.8 (Walk, length of a walk)**.** A *walk* in a directed graph G *starting from* a state γ of this graph is a sequence of edges

$$\gamma \xrightarrow{\delta|\delta'} \gamma_1 \xrightarrow{\delta_1|\delta_1'} \gamma_2 \xrightarrow{\delta_2|\delta_2'} \ldots.$$

The number of edges in the walk is called the *length* of the walk (this can be infinite).

Characterization 3.2.9. *Let $a \in \mathbb{R}^n$, $(\delta_j)_{j \in \mathbb{N}} \in \mathcal{D}^{\mathbb{N}}$ a sequence of digits and $\gamma \in \mathcal{S}$. Then the following assertions are equivalent.*

- $x = \lim_{m \to \infty} g^{-1}\delta_1 \ldots g^{-1}\delta_m(a)\ \in B_\gamma$.
- *There is an infinite walk in $\mathbf{G}(\mathcal{S})$ of the shape*

$$\gamma \xrightarrow{\delta_1|\delta_1'} \gamma_1 \xrightarrow{\delta_2|\delta_2'} \gamma_2 \xrightarrow{\delta_3|\delta_3'} \ldots \tag{3.2.4}$$

  for some $\gamma_j \in \mathcal{S}$ and $\delta_j' \in \mathcal{D}$.

Proof. Suppose that $x = \lim_{m\to\infty} g^{-1}\delta_1 \dots g^{-1}\delta_m(a) \in B_\gamma$, then x has also a representation of the shape

$$x \;=\; \lim_{m\to\infty} \gamma g^{-1}\delta'_1 \dots g^{-1}\delta'_m(a)$$

for some $\delta'_j \in \mathcal{D}$.
The elements $\gamma_1 = {\delta_1}^{-1} g\gamma g^{-1}\delta'_1$, $\gamma_2 = {\delta_2}^{-1} g\gamma_1 g^{-1}\delta'_2, \dots$ can then successively be shown to belong to $\mathcal{S}$. Indeed, if $\gamma_1 = {\delta_1}^{-1} g\gamma g^{-1}\delta'_1$ then

$$\delta_1^{-1} g\,(x) \;=\; \underbrace{\lim_{m\to\infty} g^{-1}\delta_2 \dots g^{-1}\delta_m(a)}_{\in\,\mathcal{T}} \;=\; \underbrace{\lim_{m\to\infty} \gamma_1 g^{-1}\delta'_2 \dots g^{-1}\delta'_m(a)}_{\in\,\gamma_1(\mathcal{T})},$$

and similarly for $\gamma_2, \gamma_3, \dots$ The elements $\gamma_1, \gamma_2, \dots$ now yield the required infinite walk in $\mathbf{G}(\mathcal{S})$, by the definition of the edges in this graph.

Conversely, if the infinite walk (3.2.4) in $\mathbf{G}(\mathcal{S})$ is given, by the definition of the edges of this graph the equation

$$g^{-1}\delta_1 \dots g^{-1}\delta_m\gamma_m(a) \;=\; \gamma g^{-1}\delta'_1 \dots g^{-1}\delta'_m(a)$$

holds for every m and thus for $m \to \infty$. Similarly to the proof of Proposition 3.1.8, and using that $\mathcal{S}$ is a finite set, one can write

$$\forall m \in \mathbb{N},\ ||g^{-1}\delta_1 \dots g^{-1}\delta_m\gamma_m\,(a) \;-\; g^{-1}\delta_1 \dots g^{-1}\delta_m\,(a)|| \;\le\; |||A^{-m}||| \max_{\gamma\in\mathcal{S}}\{||a-\gamma(a)||\},$$

where A is the linear part of g. A being expanding, $|||A^{-m}||| \to 0$ for $m \to \infty$, thus

$$\underbrace{\lim_{n\to\infty} \gamma g^{-1}\delta'_1 \dots g^{-1}\delta'_m\,(a)}_{\in\,\gamma(\mathcal{T})} \;=\; \lim_{m\to\infty} g^{-1}\delta_1 \dots g^{-1}\delta_m\gamma_m\,(a) \;=\; \underbrace{\lim_{n\to\infty} g^{-1}\delta_1 \dots g^{-1}\delta_m\,(a)}_{\in\,\mathcal{T}}$$

and we are done. □

In a similar way we obtain the following generalization.

Characterization 3.2.10. *Let $a \in \mathbb{R}^n$ and $\gamma_{01}, \dots, \gamma_{0L} \in \mathcal{S}$ pairwise different. Furthermore let be $(\delta_j)_{j\in\mathbb{N}} \in \mathcal{D}^{\mathbb{N}}$ a sequence of digits. Then the following assertions are equivalent.*

- $x = \lim_{m\to\infty} g^{-1}\delta_1 \dots g^{-1}\delta_m(a) \;\in V_L(\gamma_{01}, \dots, \gamma_{0L})$.
- *There are L infinite walks in $\mathbf{G}(\mathcal{S})$ of the shape*

  $$\gamma_{0i} \xrightarrow{\delta_1|\delta_{1i}} \gamma_{1i} \xrightarrow{\delta_2|\delta_{2i}} \gamma_{2i} \xrightarrow{\delta_3|\delta_{3i}} \dots \quad (1 \le i \le L)$$

  for some $\gamma_{1i}, \gamma_{2i} \dots \in \mathcal{S}$ and $\delta_{1i}, \delta_{2i} \dots \in \mathcal{D}$.

Characterization 3.2.11. *Let be $\gamma \in \Gamma$. Then the following assertions hold.*

- *γ is a vertex neighbor iff every sequence $(\delta_j)_{j\in\mathbb{N}}$ of digits associated to an infinite walk in the graph $\mathbf{G}(\mathcal{S})$, $\gamma \xrightarrow{\delta_1|\delta'_1} \gamma_1 \xrightarrow{\delta_2|\delta'_2} \dots$ with $\gamma_1, \dots \in \mathcal{S}$ and $\delta'_1, \delta'_2, \dots \in \mathcal{D}$, leads to the same point $x = \lim_{m\to\infty} g^{-1}\delta_1 \dots g^{-1}\delta_m(a)$.*
- *γ is an adjacent neighbor (i.e., $\gamma \in \mathcal{A}$) iff the set $B_\gamma \setminus V_2$ is nonempty iff there is a sequence $(\delta_j)_{j\in\mathbb{N}}$ of digits such that for each infinite walk in $\mathbf{G}(\mathcal{S})$ of the form*

  $$\gamma_1 \xrightarrow{\delta_1|\delta'_1} \gamma_2 \xrightarrow{\delta_2|\delta'_2} \dots$$

  where $\gamma_1, \gamma_2, \dots \in \mathcal{S}$ and $\delta'_1, \delta'_2, \dots \in \mathcal{D}$, we have $\gamma_1 = \gamma$.

3.2.3 Properties of the contact graph

Let Q be the closure of a fundamental domain of Γ. Q is a non-empty compact set of $\mathbb{R}^n$, so an iterative construction of $\mathcal{T}$ reads

$$\begin{cases} \mathcal{T}_0 & := & Q, \\ \mathcal{T}_p & := & \bigcup_{\delta\in\mathcal{D}} g^{-1}\delta(\mathcal{T}_{p-1}). \end{cases}$$

In the Hausdorff metric, we have $\mathcal{T}_p \to \mathcal{T}$ for $p \to \infty$, *cf.* [27]).

By induction on p, one can readily prove the following result.

Proposition 3.2.12. *For every $p \geq 0$, $\{\gamma(\mathcal{T}_p); \gamma \in \Gamma\}$ is a tiling of $\mathbb{R}^n$.*

Notation 3.2.13. For each approximation $\mathcal{T}_p$, we denote by $B_{\gamma,p}$ the set $\mathcal{T}_p \cap \gamma(\mathcal{T}_p)$.

Using Proposition 3.2.12 we have

$$\partial\mathcal{T}_p = \bigcup_{\gamma\in\Gamma\setminus\{\mathrm{id}\}} B_{\gamma,p}\,. \tag{3.2.5}$$

This is in fact a finite union because the tiling is locally finite.

Remark 3.2.14. For every $p \geq 0$, $g^p(\mathcal{T}_p)$ is a union of n-dimensional non-overlapping polyhedrons, *i.e.*,

$$g^p(\mathcal{T}_p) = \bigcup_{\delta_0,\ldots,\delta_{p-1}\in\mathcal{D}} g^{p-1}\delta_{p-1}g^{-(p-1)}g^{p-2}\delta_{p-2}g^{-(p-2)}\ldots g\delta_1 g^{-1}\ \delta_0\ (Q)$$

where each $g^k\delta_k g^{-k}$ is an isometry of Γ. Thus for every $\gamma \in \Gamma$, $g^p\gamma(\mathcal{T}_p) = g^p\gamma g^{-p}\ g^p(\mathcal{T}_p)$ is also a union of n-dimensional non-overlapping polyhedrons and $g^p(B_{\gamma,p})$ is the intersection of two unions of polyhedrons that do not overlap. This also holds for $B_{\gamma,p}$, and, hence, this set is the union of $(n-1)$-dimensional faces.

The following result shows the correspondence between the boundary of $\mathcal{T}_p$ and the set $\mathcal{R}_p$ defined in (3.2.1).

Proposition 3.2.15. *If $B_{\gamma,p}$ contains an $(n-1)$-dimensional face then $\gamma \in \mathcal{R}_p$.*

Proof. We proceed by induction on p. First note that the result is obviously true for $p = 0$. We assume the result is true for a $p-1 \in \mathbb{N}$. The number of faces of $B_{\gamma,p}$ is also the number of faces of $g(B_{\gamma,p})$. We have

$$\begin{array}{rcl} g(B_{\gamma,p}) & = & \bigcup_{\delta,\delta'\in\mathcal{D}} \delta(\mathcal{T}_{p-1}) \ \cap\ g\gamma g^{-1}\delta'(\mathcal{T}_{p-1}) \\ & = & \bigcup_{\delta,\delta'\in\mathcal{D}} \delta(B_{\delta^{-1}g\gamma g^{-1}\delta',p-1}) \end{array}$$

and by (3.2.1) this last union contains an $(n-1)$-dimensional face only if $\gamma \in \mathcal{R}_p$. □

Consequently, as $\partial\mathcal{T}_p$ is the union of its $(n-1)$-dimensional faces, from (3.2.5) follows that

$$\partial\mathcal{T}_p = \bigcup_{\gamma\in\mathcal{R}_p\setminus\{\mathrm{id}\}} B_{\gamma,p}$$

with

$$B_{\gamma,p} = \bigcup_{\substack{\delta\in\mathcal{D},\gamma'\in\mathcal{R}_{p-1}\setminus\{\mathrm{id}\} \\ \exists\delta'\in\mathcal{D},\ \gamma\xrightarrow{\delta|\delta'}\gamma'\ \in\mathbf{G}(\mathcal{R})}} g^{-1}\delta(B_{\gamma',p-1}).$$

Note that if $B_{\gamma,p}$ is not an $(n-1)$-dimensional face, then it must be already contained in other $(n-1)$-dimensional faces of other sets $B_{\gamma',p}$ with $\gamma' \neq \gamma$. This also holds for the sets $g^{-1}\delta(B_{\gamma',p-1})$

in the union above. Thus, remembering that $\mathcal{R}_p \subset \mathcal{R}$ for every p and using Proposition 3.2.15, we get for the boundary of the approximations

$$\partial\mathcal{T}_p = \bigcup_{\gamma\in\mathcal{R}\setminus\{\mathrm{id}\}} B_{\gamma,p}$$

with

$$B_{\gamma,p} = \bigcup_{\substack{\delta\in\mathcal{D},\gamma'\in\mathcal{R}\setminus\{\mathrm{id}\}\\ \exists\delta'\in\mathcal{D},\ \gamma\xrightarrow{\delta|\delta'}\gamma'\ \in\mathbf{G}(\mathcal{R})}} g^{-1}\delta(B_{\gamma',p-1}). \tag{3.2.6}$$

There is a relation between the structure of the graph $\mathbf{G}(\mathcal{R})$ and the geometry of the sets $B_{\gamma,p}$ as follows.

Proposition 3.2.16. *Let $\gamma \in \mathcal{R}$. If all the walks in $\mathbf{G}(\mathcal{R})$ starting from γ are at most of length ℓ, then $B_{\gamma,p}$ has no $(n-1)$-dimensional face for $p > \ell$.*

Proof. Let us take $p > \ell$. Starting from the set equation (3.2.6) above and writing it for the sets $B_{\gamma',p-1}, B_{\gamma'',p-2}, \ldots$ that appear at each iteration, one comes after ℓ steps to

$$B_{\gamma,p} \ = \bigcup_{\gamma\xrightarrow{\delta}\gamma'\ \in\mathbf{G}(\mathcal{R})} \ \cdots \bigcup_{\gamma^{(\ell)}\xrightarrow{\delta^{(\ell)}}\gamma^{(\ell+1)}\ \in\mathbf{G}(\mathcal{R})} g^{-1}\delta\ldots g^{-1}\delta^{(\ell)}\ (B_{\gamma^{(\ell+1)},p-(\ell+1)})\ ,$$

but by assumption there is no edge $\gamma^{(\ell)} \to \gamma^{(\ell+1)}$ in $\mathbf{G}(\mathcal{R})$, so no $B_{\gamma^{(\ell+1)},p-(\ell+1)}$ and hence $B_{\gamma,p}$ can not have an $(n-1)$-dimensional face. □

3.2.4 Neighbor finding algorithm

Scheicher and Thuswaldner [59] gave an algorithm starting from $\mathbf{G}(\mathcal{R})$ to get the neighborhood graph $\mathbf{G}(\mathcal{S})$ in the case of lattice reptiles. In this section, we write this algorithm in a "crystallographic way". Examples of contact and neighborhood graphs obtained by this algorithm will be computed in Subsection 3.3.4.

Definition 3.2.17 (Reduced graph)**.** If G is a directed graph, we denote by $\mathrm{Red}(G)$ the graph emerging from G if all states of G that are not the starting point of a walk of infinite length are removed. Such a graph is called a *reduced graph*.

Definition 3.2.18 (Product graph)**.** For two subgraphs $\mathbf{G}_1$ and $\mathbf{G}'_1$ of $\mathbf{G}(\Gamma)$ we define the *product graph* $\mathbf{G}_2 = \mathbf{G}_1 \otimes \mathbf{G}'_1$ as follows.

- A state r_2 belongs to $\mathbf{G}_2$ iff $r_2 = r_1 r'_1$ or $r_2 = r'_1 r_1$ for some $r_1 \in \mathbf{G}_1,\ r'_1 \in \mathbf{G}'_1$.
- For $r_2,\ s_2$ states of $\mathbf{G}_2$, and $\delta_1,\ \delta_2$ digits of $\mathcal{D}$, then there is an edge $r_2 \xrightarrow{\delta_1|\delta_2} s_2\ \in \mathbf{G}_2$

$$\begin{array}{rl} \text{iff} & \text{there are edges } r_1 \xrightarrow{\delta_1|\delta'_1} s_1\ \in \mathbf{G}_1 \text{ and } r'_1 \xrightarrow{\delta'_1|\delta_2} s'_1\ \in \mathbf{G}'_1 \\ & \text{with } r_2 = r_1 r'_1,\ s_2 = s_1 s'_1 \text{ and } \delta'_1 \in \mathcal{D} \\ \text{or} & \text{there are edges } r'_1 \xrightarrow{\delta_1|\delta'_1} s'_1\ \in \mathbf{G}'_1 \text{ and } r_1 \xrightarrow{\delta'_1|\delta_2} s_1\ \in \mathbf{G}_1 \\ & \text{with } r_2 = r'_1 r_1,\ s_2 = s'_1 s_1 \text{ and } \delta'_1 \in \mathcal{D}\ . \end{array}$$

The conditions of the second item both lead to the same set of edges if $\mathbf{G}_1 = \mathbf{G}'_1$.
We write $\otimes_{i=1}^{m}\mathbf{G}_1 = \underbrace{\mathbf{G}_1 \otimes \ldots \otimes \mathbf{G}_1}_{m \text{ times}}$.

Definition 3.2.19 (Property (C))**.** A subgraph $\mathbf{G}(M)$ of $\mathbf{G}(\Gamma)$ is said to have *property (C)* if for each pair $(\gamma', \delta) \in M \times \mathcal{D}$ there exists a unique pair $(\gamma, \delta') \in M \times \mathcal{D}$ such that $\gamma \xrightarrow{\delta|\delta'} \gamma'\ \in \mathbf{G}(M)$.

From the last three definitions and the fact that $\mathcal{D}$ is a complete set of right coset representatives of $g\Gamma g^{-1}$, we derive the following proposition.

Proposition 3.2.20. *If $\mathbf{G}_1$ and $\mathbf{G}'_1$ are subgraphs of $\mathbf{G}(\Gamma)$ having property (C), then for r_2, s_2 states of $\mathbf{G}_1 \otimes \mathbf{G}'_1$ and $\delta_1, \delta_2 \in \mathcal{D}$,*

$$\text{there exists an edge } r_2 \xrightarrow{\delta_1|\delta_2} s_2 \ \in \mathbf{G}_1 \otimes \mathbf{G}'_1 \quad \text{iff} \quad gr_2g^{-1}\delta_2 = \delta_1 s_2.$$

Furthermore, $\mathbf{G}_1 \otimes \mathbf{G}'_1$ and hence $\mathrm{Red}(\mathbf{G}_1 \otimes \mathbf{G}'_1)$ have property (C).

The proof of this result runs along the same lines as in the case of lattice tilings (cf. [59]) and we omit it.

This means that the product graph of two subgraphs satisfying property (C) is again a subgraph of $\mathbf{G}(\Gamma)$ and it has property (C), as well as its reduced graph.

Algorithm 3.2.21. *We denote by $\mathbf{G}(S)$ the graph obtained from $\mathbf{G}(\mathcal{R})$ by the following algorithm.*

$p := 1$
$A[1] := \mathrm{Red}(\mathbf{G}(\mathcal{R}))$
repeat
$p := p + 1,\ A[p] := \mathrm{Red}(A[p-1] \otimes A[1])$
until $A[p] = A[p-1]$
$\mathbf{G}(S) := A[p] \setminus \{\mathrm{id}\}$

Proposition 3.2.22. *Algorithm 3.2.21 ends after finitely many steps and yields the neighborhood graph (i.e., $\mathbf{G}(S) = \mathbf{G}(\mathcal{S})$).*

In order to show this result we have to adapt the proof of the corresponding result in the case of lattice tilings of Scheicher and Thuswaldner [59]. First we need the following lemmata to get bounding sets for $\mathcal{S}$ (with respect to the inclusion) from below and above.

Lemma 3.2.23. *Each state of $\mathbf{G}(\mathcal{R}') := \mathrm{Red}(\mathbf{G}(\mathcal{R}))$ has infinitely many predecessors and infinitely many successors. Thus $\mathbf{G}(\mathcal{R}')$ is a union of cycles of $\mathbf{G}(\Gamma)$ and of walks connecting these cycles. Furthermore, $\mathbf{G}(\mathcal{R}')$ has property (C).*

This can be proved in the same way as in the lattice tiling case (cf. [59]).

Lemma 3.2.24. *The graph $\mathbf{G}(\mathcal{S} \cup \{\mathrm{id}\})$ is the union of all cycles of $\mathbf{G}(\Gamma)$ and all walks connecting two of these cycles.*

Proof. Let γ be a state contained in a cycle of $\mathbf{G}(\Gamma)$, *i.e.*, there exists

$$\gamma \xrightarrow{\delta_1|\delta'_1} \gamma_1 \xrightarrow{\delta_2|\delta'_2} \dots \xrightarrow{\delta_{l-1}|\delta'_{l-1}} \gamma_l \xrightarrow{\delta_l|\delta'_l} \gamma$$

a cycle in $\mathbf{G}(\Gamma)$. Then for all $p \in \mathbb{N}$ we have

$$\gamma\ \left(g^{-1}\delta'_1 \dots g^{-1}\delta'_l\right)^p\ =\ \left(g^{-1}\delta_1 \dots g^{-1}\delta_l\right)^p\ \gamma.$$

If we take $a \in \mathbb{R}^n$ and set $\delta_{j+pl} := \delta_j,\ \delta'_{j+pl} = \delta'_j$ for every $p \in \mathbb{N},\ j \in \{1, \dots, l\}$, then we can write

$$\gamma\left(\lim_{m\to\infty} g^{-1}\delta'_1 \dots g^{-1}\delta'_m(a)\right)\ =\ \lim_{m\to\infty} g^{-1}\delta_1 \dots g^{-1}\delta_m(\gamma(a))\ =\ \lim_{m\to\infty} g^{-1}\delta_1 \dots g^{-1}\delta_m(a)$$

(the last equality follows from Equation (3.1.3) of Remark 3.1.10). This means that $\gamma \in \mathcal{S} \cup \{\mathrm{id}\}$. All walks connecting two cycles of $\mathbf{G}(\Gamma)$ are also contained in $\mathbf{G}(\mathcal{S} \cup \{\mathrm{id}\})$. This follows inductively, starting from the last state of the walk, that belongs to $\mathcal{S} \cup \{\mathrm{id}\}$ as we just saw, and going the walk backwards: the existence of an edge $\gamma_1 \xrightarrow{\delta|\delta'} \gamma_2$ in $\mathbf{G}(\Gamma)$ with $\gamma_2 \in \mathcal{S} \cup \{\mathrm{id}\}$ implies $\gamma_1 \in \mathcal{S} \cup \{\mathrm{id}\}$ (see Remark 3.2.6).
No other state is contained in $\mathbf{G}(\mathcal{S} \cup \{\mathrm{id}\})$, because $\mathcal{S}$ is finite and each state of $\mathbf{G}(\mathcal{S} \cup \{\mathrm{id}\})$ must have infinitely many predecessors and infinitely many successors. These states must be in a cycle or in a walk connecting two cycles. □

Corollary 3.2.25. $\mathrm{Red}(\mathbf{G}(\mathcal{R})) \subseteq \mathbf{G}(\mathcal{S} \cup \{\mathrm{id}\})$.

This lower bound follows from Lemma 3.2.23 and 3.2.24. For the upper bound, we need one more lemma.

Lemma 3.2.26. *Let* $\mathbf{G}(\mathcal{R}') := \mathrm{Red}(\mathbf{G}(\mathcal{R}))$. *Then* $\mathcal{R}'$ *contains a generator set* $B := \{\gamma_1, \dots, \gamma_q\}$ *of* Γ. *By symmetry and because* $\mathrm{id} \to \mathrm{id}$ *is a cycle in* $\mathbf{G}(\mathcal{R})$, $\mathcal{R}'$ *even contains the set* $\{\mathrm{id}\} \cup B \cup B^{-1}$.

Proof. $\mathcal{R}$ being a finite set, let $\ell := |\mathcal{R}|$. Then for $p > \ell$, the fact that $B_{\gamma,p}$ contains an $(n-1)$-dimensional face implies that γ belongs to $\mathcal{R}'$. Indeed, because of Proposition 3.2.16, there must be a walk of length $p > \ell$ in $\mathbf{G}(\mathcal{R})$ starting from γ. In this walk, a state $\gamma' \in \mathcal{R}$ has to appear at least twice (because $p > |\mathcal{R}|$). This provides a cycle in the walk which can be repeated to get an infinite walk starting from γ. Thus $\gamma \in \mathcal{R}'$. This allows the following description of the boundary of $\mathcal{T}_p$ for $p > \ell$:

$$\partial \mathcal{T}_p = \bigcup_{\gamma \in \mathcal{R}' \setminus \{\mathrm{id}\}} B_{\gamma,p}.$$

Now we show that $\mathcal{R}'$ generates Γ. Let $\alpha \in \Gamma$. Remember (Proposition 3.2.12) that $\{\gamma(\mathcal{T}_p), \gamma \in \Gamma\}$ is a tiling of $\mathbb{R}^n$; let $x \in \mathcal{T}_p$ and $y \in \alpha(\mathcal{T}_p)$ (but x, y not vertices of these tiles), one can draw a line from x to y avoiding the vertices of the tiles. $\mathcal{T}_p$ is compact, so this line passes through a finite number of tiles $\mathcal{T}_p, \alpha_1(\mathcal{T}_p), \dots, \alpha_q(\mathcal{T}_p)$ in this order. Two consecutive tiles have an $(n-1)$-dimensional face in common, so $\alpha_1, \alpha_1^{-1}\alpha_2, \dots, \alpha_q^{-1}\alpha$ are elements of $\mathcal{R}'$, thus α is a product of elements of $\mathcal{R}'$. □

Corollary 3.2.27. *The inclusion*

$$\mathrm{Red}(\mathbf{G}(\mathcal{R})^{p_0}) \supseteq \mathbf{G}(\mathcal{S} \cup \{\mathrm{id}\})$$

holds for some positive integer p_0. *Furthermore,* $\mathrm{Red}(\mathbf{G}(\mathcal{R})^{p_0})$ *has property (C).*

Proof. If B is a generator set of Γ contained in $\mathcal{R}'$ (hence in $\mathcal{R}$ too), then the set of states of $\mathbf{G}(\mathcal{R})^p$ contains all elements of $(\{\mathrm{id}\} \cup B \cup B^{-1})^p$ (see Lemma 3.2.26). As $\mathcal{S}$ is finite, there is a p_0 with $\mathbf{G}(\mathcal{R})^{p_0} \supset \mathbf{G}(\mathcal{S} \cup \{\mathrm{id}\})$, and each state of $\mathbf{G}(\mathcal{S}) \cup \{\mathrm{id}\}$ having infinitely many successors, the required inclusion holds. The second claim follows from Proposition 3.2.20. □

The following lemma will be useful in the conclusion of the proof of Proposition 3.2.22. It can be obtained in a similar way as in the case of lattice tilings, we refer the reader to [59, Section 5] for more details.

Lemma 3.2.28. *If* $\mathbf{G}(\mathcal{R}')$ *denotes* $\mathrm{Red}(\mathbf{G}(\mathcal{R}))$, *then the identity*

$$\mathrm{Red}(\mathbf{G}(\mathcal{R}')^p) \;=\; \underbrace{\mathrm{Red}(\dots \mathrm{Red}(\mathrm{Red}(\mathbf{G}(\mathcal{R}')) \otimes \mathbf{G}(\mathcal{R}')) \otimes \mathbf{G}(\mathcal{R}')) \dots \otimes \mathbf{G}(\mathcal{R}'))}_{p \text{ times}}$$

holds for every $p \in \mathbb{N}$.

Proof of Proposition 3.2.22. The proof of Proposition 3.2.22 is then similar as in [59]. Firstly, the algorithm terminates: choosing p_0 as in Corollary 3.2.27, we have by Lemma 3.2.28 that $A[p_0] = \mathrm{Red}(\mathbf{G}(\mathcal{R})^{p_0})$, thus $A[p_0] \supseteq \mathbf{G}(\mathcal{S} \cup \{\mathrm{id}\})$. This implies in view of Lemma 3.2.24 that $A[p_0]$ contains each reduced finite subgraph of $\mathbf{G}(\Gamma)$ with the property that each of its states has a predecessor. Thus $A[p_0 + 1] \subseteq A[p_0]$, and the opposite inclusion being trivial we even have $A[p_0 + 1] = A[p_0]$. Hence the algorithm terminates for a $p_1 \leq p_0 + 1$, and we have $\mathbf{G}(S) = A[p_1] \setminus \{\mathrm{id}\}$.
Secondly, $\mathbf{G}(S)$ is the neighborhood graph: note that by the definition of p_1 and of the algorithm, $A[p_1] = A[p_1 + 1] = \dots = A[p_0 + 1] = A[p_0]$ holds. Moreover, Lemma 3.2.24 indicates that $\mathbf{G}(\mathcal{S} \cup \{\mathrm{id}\})$ contains all reduced finite subgraphs $\mathbf{G}(\Gamma)$ for which each state has a predecessor, and Proposition 3.2.20 states that $A[p_0]$ has property (C), so that each state of $A[p_0]$ has a predecessor. Hence $A[p_0] \subseteq \mathbf{G}(\mathcal{S} \cup \{\mathrm{id}\}) = A[p_1] = A[p_0]$, showing that $\mathbf{G}(S) = \mathbf{G}(\mathcal{S})$. □

We end up this subsection by giving an upper bound for the number of steps required by Algorithm 3.2.21 to compute the neighbor graph from the contact graph. We first give a bound for the number of neighbors, *i.e.*, for the cardinality of $\mathcal{S}$. Let $||\cdot||$ be the Euclidean norm on $\mathbb{R}^n$, with respect to which the elements of Γ are isometries. We denote also by $||\cdot||$ the induced matrix norm. Remember that we write $g(x) = Ax + t$, where A is the expanding matrix and t the translation vector associated to g. Similarly, for an isometry $\gamma \in \Gamma$: $\gamma(x) = A_\gamma x + t_\gamma$, where A_γ is an isometry matrix (in particular, $||A_\gamma|| = 1$), and t_γ is the translation vector of γ.

Proposition 3.2.29. *We have the upper bound*

$$|\mathcal{S}| \leq |\Gamma/\Lambda| \cdot \left(4 \cdot \max_{\delta \in \mathcal{D}} \{||t - t_\delta||\} \cdot \sum_{j=1}^{\infty} ||A^{-j}|| \right)^n$$

for the number of neighbors of the crystile $\mathcal{T}$.

Proof. We compute a bound M for the norms of the possible translational parts t_γ of the elements $\gamma \in \mathcal{S}$. Then, the volume of the hypercube of side size $2M$ will bound the number of these allowed translation parts. Multipliying this volume by the cardinality of the point group, we get the desired upper bound.
Let $\gamma \in \mathcal{S}$, then some point belongs to $\mathcal{T}$ and $\gamma(\mathcal{T})$. Thus there are sequences of digits (δ_j), (δ'_j), such that

$$\lim_{m\to\infty} g^{-1}\delta_1 \dots g^{-1}\delta_m(0) = \lim_{m\to\infty} \gamma g^{-1}\delta'_1 \dots g^{-1}\delta'_m(0).$$

This means for the translation part of γ that

$$t_\gamma = \lim_{m\to\infty} A_\gamma \sum_{j=0}^{m-1} A_{\delta'_0}A^{-1}A_{\delta'_1}A^{-1}\dots A_{\delta'_j}A^{-1}(t_{\delta'_{j+1}} - t) \; - \; \sum_{j=0}^{m-1} A_{\delta_0}A^{-1}A_{\delta_1}A^{-1}\dots A_{\delta_j}A^{-1}(t_{\delta_{j+1}} - t),$$

where by convention $A_{\delta_0} = A_{\delta'_0} = \mathrm{id}$.
We recall now that, by Definition 3.1.3, $g\Gamma g^{-1} \subset \Gamma$, hence if an isometry $\gamma \in \Gamma$ is given, there is another isometry $\gamma' \in \Gamma$ such that $\gamma g^{-1} = g^{-1}\gamma'$. This property also holds for the linear parts: given A_γ, there is $A_{\gamma'}$ such that $A_\gamma A^{-1} = A^{-1}A_{\gamma'}$. Using this fact, one can rewrite the products of matrices in the first sum above in the following way: for each j, there are matrices $A_{\gamma_0^{(j)}}, A_{\gamma_1^{(j)}}, \dots, A_{\gamma_j^{(j)}}$ such that

$$A_{\delta'_0}A^{-1}A_{\delta'_1}A^{-1}\dots A_{\delta'_j}A^{-1} \;=\; A^{-(j+1)}A_{\gamma_0^{(j)}}A_{\gamma_1^{(j)}}\dots A_{\gamma_j^{(j)}},$$

and similarly for the other sum. Taking the norm and using the triangle inequality and the fact that isometries have norm 1, we obtain the majoration

$$||t_\gamma|| \leq 2 \cdot \sum_{j=1}^{\infty} ||A^{-j}|| \cdot \max_{\delta\in\mathcal{D}}\{||t_\delta - t||\} \;=: M.$$

□

Remark 3.2.30. The bound in Proposition 3.2.29 often applies to the number of elements in the contact set $\mathcal{R}$. Indeed, in practical applications, looking at a picture of the tiling, it is possible to guess an appropriate set $\mathcal{R}_0$ to start with, corresponding to a good first approximating polyedron of the central tile. In this case, we eventually obtain $\mathcal{R} \setminus \{\mathrm{id}\} \subset \mathcal{S}$. Often, we even have that $\mathcal{R}$ is much smaller than $\mathcal{S}$. A better general upper bound can not be given, the cardinality of the contact set and the number of neighbors really depend on the geometry of the particular example (crystiles with arbitrarily large number of neighbors can be produced, see [5]).

Proposition 3.2.31. *Let $q := |\Gamma/\Lambda|$ be the cardinality of the point group. Then there is a basis $\mathcal{B}_L$ of the lattice Λ such that $\mathcal{B}_L \cup \mathcal{B}_L^{-1}$ are states of $\mathbf{G}(\mathcal{R}')^q$. Consider the translational parts of the elements of $\mathcal{S}$. If N is the maximal Euclidean norm of these translational parts, then $\mathcal{S}$ is contained in the set of states of $\mathbf{G}(\mathcal{R}')^{Nq}$. Hence Algorithm 3.2.21 terminates after at most Nq steps.*

Proof. First note that by Lemma 3.2.28, the graph $\mathrm{Red}(\mathbf{G}(\mathcal{R}')^{Nq})$ will be exactly equal to the graph obtained when reduction happens after each step, like in Algorithm 3.2.21. This graph is moreover a subgraph of $\mathbf{G}(\mathcal{R}')^{Nq}$. Since q is the order of the point group and by Lemma 3.2.26 the set $\mathcal{R}'$ contains a generator for Γ, the product $\mathcal{R}'^{\,q} = \{r_1 \dots r_q; r_i \in \mathcal{R}'\}$ contains a basis for the lattice Λ and is equal to the set of states of $\mathbf{G}(\mathcal{R}')^q$. It even contains all the elements of Γ whose translation vector has norm less than 1. Then, the set of states of $\mathbf{G}(\mathcal{R}')^{2q}$ contains all the elements of Γ whose translation vector has norm less than $1+1=2$. Consequently, the neighbor(s) with maximal translation vector will be reached after iterating at most N times this operation, as well as all the neighbors with smaller translation vector. □

3.3 Criteria for disk-likeness

The results and examples of this section appear in the joint articles [43, 44] with Jun Luo and Jörg Thuswaldner as well as in the joint article [42] with Jun Luo. We will establish several criteria for the disk-likeness of plane crystallographic tiles and plane crystiles. The first criterion concerns crystallographic tiles in general. One gets easier conditions when the fractal structure is involved. This is the purpose of the second criterion. The third criterion can be easily visualized on the neighbor graph of a given crystile. The last criterion is dedicated to lattice and $p2$-crystiles and mainly states that disk-likeness occurs when the neighbor set has the right shape and the right configuration, and when the digit set has some connectedness property.

We use the sets and graphs defined in Subsection 3.2.1.
We recall the following fundamental facts, easily seen from the definition of the set of neighbors $\mathcal{S}$ and the set of adjacent neighbors $\mathcal{A}$. Let T be a tile of a crystallographic tiling with respect to the group Γ.

- In $\mathcal{A}$, there is a set of generators for Γ, and $\mathcal{A} \subseteq \mathcal{S}$.
- The boundary of T satisfies $\partial T = \cup_{\gamma\in\mathcal{S}} B_\gamma = \cup_{\gamma\in\mathcal{A}} B_\gamma$, where $B_\gamma = T \cap \gamma(T)$.
- For each $\mathcal{A}' \subseteq \mathcal{S}$ with $\partial T = \cup_{\gamma\in\mathcal{A}'} B_\gamma$, we have $\mathcal{A}' \supseteq \mathcal{A}$.

3.3.1 A criterion for a crystallographic tile

The following criterion is stated for general crystallographic tilings of the plane.

Theorem 3.3.1. *Suppose that $\{\gamma(T); \gamma \in \Gamma\}$ is a crystallographic tiling of $\mathbb{R}^2$. Then, T is disk-like if and only if the following three conditions all hold.*

(1) The triple intersection $V_2(\gamma_1, \gamma_2) = T \cap \gamma_1(T) \cap \gamma_2(T)$ is either empty or a single point set for any distinct $\gamma_1, \gamma_2 \in \mathcal{S}$.

(2) For each $\gamma \in \mathcal{S}$, the double edge B_γ is either a single point or a simple arc.

(3) The subgraph of the double neighboring graph G_2 (see Definition 2.2.22) with set of vertices $\{B_\gamma; \gamma \in \mathcal{A}\}$ consists of a simple loop.

We first need a lemma, deduced from the results of plane topology presented in Appendix A.

Notation 3.3.2. If C is a simple closed curve in the plane, the complement of C has two components. We denote by $\mathrm{Interior}(C)$ the bounded one and by $\mathrm{Exterior}(C)$ the unbounded one.

Lemma 3.3.3. *Let $\{\gamma(T), \gamma \in \Gamma\}$ be a crystallographic tiling with disk-like tiles, and γ, γ' two elements of Γ. Then $(\gamma(T) \cup \gamma'(T))^c$ has no bounded component. In other words, no pair of tiles can surround a third one.*

Proof.

(*i*) For each $\gamma, \gamma' \in \Gamma$, $(\gamma(T) \cup \gamma'(T))^c$ has finitely many bounded connected components. Indeed, because of the tiling property, every component of $(\gamma(T) \cup \gamma'(T))^c$ being open, it is intersected by the interior of at least one tile $\gamma''(T)$ with $\gamma'' \neq \gamma, \gamma'$, thus it contains the whole tile $\gamma''(T)$, since this tile is disk-like. For this reason, disjoint components contain distinct tiles, and all of these tiles have the same Lebesgue-measure. But note that there is a bounded domain containing all the bounded components of $(\gamma(T) \cup \gamma'(T))^c$. Hence $(\gamma(T) \cup \gamma'(T))^c$ can have only finitely many bounded components.

(*ii*) For each $\gamma \in \Gamma$, there are at most finitely many $\gamma' \in \Gamma$ such that $(\gamma(T) \cup \gamma'(T))^c$ has a bounded component. Indeed, because the tiles are disk-like, if $\gamma' \notin \gamma\mathcal{S}$, then $(\gamma(T) \cup \gamma'(T))^c$ is connected and unbounded.

(*iii*) If Z is a bounded component of $(\gamma(T) \cup \gamma'(T))^c$, we denote by $N(\gamma, \gamma', Z)$ the number of tiles whose interior intersects Z. Note again that $\gamma''(T^o) \subset Z$ as soon as $\gamma''(T) \cap Z \neq \emptyset$, because of the disk-likeness of the tiles, thus this number is finite. Moreover, we have $N(\gamma', \gamma'\gamma, \gamma' Z) = N(\mathrm{id}, \gamma, Z)$ for every $\gamma, \gamma' \in \Gamma$, and every component Z' of $(\gamma'(T) \cup \gamma'\gamma(\mathcal{T}))^c$ is obtained in this way (*i.e.*, $Z' = \gamma' Z$ with Z bounded component of $(\mathcal{T} \cup \gamma(\mathcal{T}))^c$).

(*iv*) Let

$$N := \begin{cases} \cdot \max\{N(\mathrm{id}, \gamma, Z); \gamma \in \Gamma, Z \text{ bounded component of } (T \cup \gamma(T))^c\} \\ \text{ if } (T \cup \gamma(T))^c \text{ has a bounded component for some } \gamma \in \Gamma, \\ \cdot 0 \text{ otherwise.} \end{cases}$$

Suppose that $N > 0$. Let γ, Z with $N = N(\mathrm{id}, \gamma, Z)$. By Lemma A.0.20, there exist disjoint points a, b in $T \cap \gamma(T)$ and simple open arcs $C_{\mathrm{id}}, C_\gamma$ contained in $T^o, \gamma(T^o)$ respectively, such that $Z \subset \mathrm{Interior}(C)$ with $C := C_{\mathrm{id}} \cup C_\gamma \cup \{a, b\}$ and such that for $\gamma' \notin \{\mathrm{id}, \gamma\}$ with $\gamma'(T) \cap \mathrm{Interior}(C) \neq \emptyset$, we have $\gamma'(T^o) \subset Z$. Let $\gamma' \notin \{\mathrm{id}, \gamma\}$ with $\gamma'(T) \cap \mathrm{Interior}(C) \neq \emptyset$. Then $\gamma'(T)$ lies entirely in $\mathrm{Interior}(C) \cup \{a, b\}$. Moreover, $\gamma'' := \gamma'\gamma$ and $Z' := \gamma' Z$ satisfy $N(\gamma', \gamma'', Z') = N$.

(*v*) We have $\gamma''(T) \cap Z = \emptyset$. Otherwise $\gamma''(T) \subset \mathrm{Interior}(C) \cup \{a, b\}$ and the bounded components of $(\gamma'(T) \cup \gamma''(T))^c$ have to lie in Z, but they are all different from Z since they do not contain $\gamma'(T^o)$ nor $\gamma''(T^o)$ that are both in Z; in particular for Z' we have $N = N(\gamma', \gamma'', Z') < N(\mathrm{id}, \gamma, Z) = N$, a contradiction.

(*vi*) We have $\gamma'' \notin \{\mathrm{id}, \gamma\}$. For sure, $\gamma'' = \gamma'\gamma \neq \gamma$, and if $\gamma'' = \mathrm{id}$ we obtain the same contradiction as in item (*v*): the bounded components of $(\gamma'(T) \cup \mathcal{T})^c$ lie in Z but do not contain $\gamma'(T^o)$, so $N = N(\gamma', \mathrm{id}, Z') < N(\mathrm{id}, \gamma, Z) = N$, a contradiction.

(*vii*) By Items (*v*) and (*vi*), $\gamma''(T) \subset \mathrm{Exterior}(C) \cup \{a, b\}$. Thus $\gamma'(T) \cap \gamma''(T) = \{a, b\}$, because these tiles intersect in at least two points but are contained in $\mathrm{Interior}(C) \cup \{a, b\}$ and $\mathrm{Exterior}(C) \cup \{a, b\}$, respectively.

(*viii*) Consider a simple open arc $C_{\gamma''}$ from a to b within $\gamma''(T)$. We may assume that $C_{\mathrm{id}} \subset \mathrm{Exterior}(C_{\gamma'} \cup \{a, b\} \cup C_{\gamma''})$.
We now have that $(T \cup \gamma''(T))^c$ has a bounded component Z'' containing Z and $\gamma(T^o)$. Indeed, each of these sets is in some bounded component of $(T \cup \gamma''(T))^c$. Moreover, by Lemma A.0.20, $\overline{Z} \cap \gamma(T)$ is a simple arc from a to b that does not intersect T except in a and b, and that lies in $\mathrm{Interior}(C) \cup \{a, b\}$, so it does not intersect $\gamma''(T)$ except in a and b either. Thus one can find at least one point $c \in \overline{Z} \cap \gamma(T) \cap (T \cup \gamma''(T))^c$, and this point connects the open disks Z and $\gamma(T^o)$ within $(T \cup \gamma''(T))^c$: indeed, $Z \cup \{c\} \cup \gamma(T^o)$ is connected and lies in $(T \cup \gamma''(T))^c$, thus the sets Z and $\gamma(T^o)$ lie in the same bounded component of $(T \cup \gamma''(T))^c$.

(*ix*) From Item (*viii*), $N(\mathrm{id}, \gamma'', Z'') > N(\mathrm{id}, \gamma, Z) = N$, contradicting the maximality of N.

This means that the assumption $N > 0$ in Item (*iv*) is false. Hence no union of two tiles has a complement which contains a bounded component. □

Proof of Theorem 3.3.1. We first suppose that the three items hold and prove that T is disk-like.

Items (1) and (3) indicate that the compact sets $\{B_\gamma; \gamma \in \mathcal{A}\}$ form a circular chain, and Item (2) implies that for each $\gamma \in \mathcal{A}$, B_γ and B_γ^c are both connected. This means that $\{B_\gamma; \gamma \in \mathcal{A}\}$ form a circular chain of continua, each of which does not separate the plane. By Corollary A.0.15, $\mathbb{R}^2 \setminus \left(\bigcup_{\gamma\in\mathcal{A}} B_\gamma\right) = \mathbb{R}^2 \setminus \partial T$ is then the union of two connected sets; the bounded one is T^o and the unbounded one is $\mathbb{R}^2 \setminus T$, since $T = \overline{T^o}$ and $T^o = \mathbb{R}^2 \setminus \left(\bigcup_{\gamma\neq \mathrm{id}} \gamma(T)\right)$. Moreover, because ∂T is the union of arcs forming a circular chain, it has no cut point and Lemma A.0.19 assures that T is disk-like.

Conversely, we assume that the tile T is disk-like and prove that the three items hold.

Proof of Item (1).

Let us assume that the triple intersection $T \cap \gamma_1(T) \cap \gamma_2(T)$ contains at least two distinct points, say a and b. Then, choosing a point p in T^o, one can find two disjoint simple open arcs A and A' in T^o leading from p to a and b, respectively. $C := A \cup \{p\} \cup A'$ is then a simple open arc leading from a to b with $C \subset T^o$. Similarly for the other tiles, one can find simple open arcs $C_1 \subset \gamma_1(T^o)$, $C_2 \subset \gamma_2(T^o)$, each of which joins a, b. Then $\theta := \{a, b\} \cup C \cup C_1 \cup C_2$ is a theta-curve whose complementary set consists of three regions. Assume with no loss of generality that C_1 does not intersect the unbounded component of $\mathbb{R}^2 \setminus \theta$. Then $\gamma_1(T^o)$ entirely lies in the interior of the simple closed curve $C' = \{a, b\} \cup C \cup C_2$, indicating that $(T \cup \gamma_2(T))^c$ has a bounded component there, a contradiction to Lemma 3.3.3.

Proof of Item (2).

Suppose that $B_\gamma \neq \emptyset$. In view of Lemma A.0.11 and Lemma 3.3.3, B_γ must be connected. Thus B_γ is a connected subset of the simple closed curve ∂T. If $B_\gamma = \partial T$ this would imply that T is surrounded by $\gamma(T)$ which is impossible. Thus B_γ is homeomorphic to a (possibly degenerated) interval and the proof is done.

Item (3) now follows from the disk-likeness of T together with Items (1) and (2). □

3.3.2 Disk-likeness of a crystile

The following result gives informations on the topology of a connected attractor.

Proposition 3.3.4 (see [47, Theorem 1.1])**.** *Let $f_1, \ldots, f_m$ be an IFS of injective contractions on $\mathbb{R}^2$ satisfying the open set condition (see Definition 2.1.15) and E its attractor. If E is connected, then the following statements hold.*

(*i*) *The interior E^o of E either is empty or has no hole.*

(*ii*) *The boundary ∂E of E is connected.*

(*iii*) *Whenever E^o is connected, ∂E is a simple closed curve, thus E is homeomorphic to a closed disk.*

Let $\mathcal{T}$ be a crystile with respect to $(\Gamma, \mathcal{D}, g)$. By Remark 3.1.10, even if $(g^{-1}\delta)_{\delta\in\mathcal{D}}$ are not contractions, the pieces $g^{-1}\delta_1 \ldots g^{-1}\delta_p(\mathcal{T})$ can be made arbitrarily small for p large enough, independently of $(\delta_j)_{1\leq j\leq p} \in \mathcal{D}^p$. Moreover, $\mathcal{T}$ satisfies the open set condition with $V = \mathcal{T}^o$. Since these are the main facts needed in the proof of Proposition 3.3.4, one can state the following theorem.

Theorem 3.3.5. *Let $\mathcal{T}$ be a crystile as in Definition 3.1.3. Then the following statements hold.*

(*i*) *$\mathcal{T}^o$ either is empty or has no hole.*

(*ii*) *The boundary* $\partial\mathcal{T}$ *of* $\mathcal{T}$ *is connected.*

(*iii*) *If* $\mathcal{T}^o$ *is connected, then* $\mathcal{T}$ *is disk-like.*

Remark 3.3.6. In fact, (*i*) and (*ii*) already follow from the tiling property. Indeed, if $\mathcal{T}^o$ has a hole, by the tiling property and connectedness of the tiles, this should contain a whole tile $\gamma(\mathcal{T})$ for some $\gamma \in \Gamma$. Again, this new tile has a hole and surrounds another tile $\gamma'(\mathcal{T})$ for some $\gamma' \in \Gamma, \gamma' \neq \gamma$. Iteratively, one gets infinitely many tiles surrounded by $\mathcal{T}$, a contradiction to the local finiteness of the tiling. We refer to Lemma B.0.24 of the appendix for the connectedness of the boundary.

Theorem 3.3.5 will be the main tool in proving the disk-likeness of crystiles in the remaining criteria of this chapter.

3.3.3 A criterion for a crystile

Using the replicating property, we will now get an "easier " version of Theorem 3.3.1. Since a crystallographic reptile $\mathcal{T}$ with respect to Γ induces a crystallographic tiling $\{\gamma(\mathcal{T}); \gamma \in \Gamma\}$, the disk-like question for crystiles is solved if we can verify the three items of Theorem 3.3.1, or disprove a single one. In general, Items (1) and (3) can be checked by concrete algorithms, while we still need to deal with Item (2). The self-affine structure of T will provide an algorithm to solve the disk-like question of crystiles in $\mathbb{R}^2$, without verifying Item (2) of Theorem 3.3.1.

We will need the following subgraph of the double neighboring graph G_2 (see Definition 2.2.22). Its definition looks a bit awkward. We explain it in Remark 3.3.8.

Definition 3.3.7 (A subgraph of the double neighboring graph)**.** For each $\gamma \in \mathcal{A}$, denote by $\mathcal{V}_\gamma$ the set of states

$$\left\{\delta\left(B_{\delta^{-1}g\gamma g^{-1}\delta'}\right);\ \text{there is } \delta, \delta' \in \mathcal{D} \text{ with } \delta^{-1}g\gamma g^{-1}\delta' \in \mathcal{A}\right\}.$$

Then G_γ is the subgraph of the double neighboring graph G_2 with set of vertices $\mathcal{V}_\gamma$.

Remark 3.3.8. Equation (3.2.2) gives an explanation to the graph G_γ defined in Definition 3.3.7. Indeed, the union of its set of vertices is equal to $g(B_\gamma)$. Thus G_γ contains some information about the connectivity of $g(B_\gamma)$ and, hence, of B_γ. Indeed, we will use this graph to show that B_γ is connected under certain circumstances.

Theorem 3.3.9. *Let* $\mathcal{T} \subset \mathbb{R}^2$ *be a crystile with respect to* Γ *whose expanding map is* g *and whose digit set is* $\mathcal{D}$*. Then* $\mathcal{T}$ *is disk-like if and only if each of the following three conditions holds.*

(1) The triple intersection $V_2(\gamma_1, \gamma_2) = \mathcal{T} \cap \gamma_1(\mathcal{T}) \cap \gamma_2(\mathcal{T})$ *is either empty or a single point set for any disjoint pair* $\gamma_1, \gamma_2 \in \mathcal{S}$*.*

(2) For each $\gamma \in \mathcal{A}$*, the graph* G_γ *consists of a simple path.*

(3) The subgraph of the double neighboring graph G_2 *with set of vertices* $\{B_\gamma; \gamma \in \mathcal{A}\}$ *consists of a simple loop.*

Indeed, for a crystallographic reptile $\mathcal{T}$ with respect to Γ and the corresponding crystallographic tiling $\{\gamma(\mathcal{T}); \gamma \in \Gamma\}$, let g be the expanding map, and let the double neighboring graph $G_2(\Gamma)$, the sets $\mathcal{V}_\gamma$ and the graph G_γ be as in Definition 3.3.7. Then the union of all the elements of $\mathcal{V}_\gamma$ is exactly the image $g(B_\gamma)$ of B_γ under the expansion map g. If the complementary set $\mathbb{R}^2 \setminus B_\gamma$ has some bounded component U then the region will be "enlarged" as $g(U)$, which is a bounded component of $\mathbb{R}^2 \setminus g(B_\gamma)$. Under simple assumptions on the graph G_γ, we can exclude the existence of such a region U. This will eventually leads us to connectivity of $\mathcal{T}^o$ and hence disk-likeness of $\mathcal{T}$ (see Theorem 3.3.5).

Proof of Theorem 3.3.9. The necessity part is a direct corollary of Theorem 3.3.1, so we just need to show the sufficiency part. More precisely, we will assume the three conditions and infer that the interior $\mathcal{T}^o$ of $\mathcal{T}$ is connected. By Corollary A.0.15, we just need to show that B_γ does not separate the plane for each $\gamma \in \mathcal{A}$ and that $\{B_\gamma; \gamma \in \mathcal{A}\}$ is a collection of continua which form a circular chain.

Claim 1: B_γ^c is connected for every $\gamma \in \mathcal{A}$.
If it is not the case, consider the set

$$\mathcal{U} = \{U \subset \mathbb{R}^2; \exists \gamma \in \mathcal{A} \text{ such that } U \text{ is a bounded connected component of } B_\gamma^c\},$$

and choose $U \in \mathcal{U}$ with maximal area, associated to B_γ for some $\gamma \in \mathcal{A}$. Recall that

$$g(B_\gamma) = \bigcup_{\delta(B_{\delta^{-1}g\gamma g^{-1}\delta'}) \in \mathcal{V}_\gamma} \delta(B_{\delta^{-1}g\gamma g^{-1}\delta'}),$$

where the set $\mathcal{V}_\gamma$ has been defined in Definition 3.3.7. Then $g(U)$, a bounded component of $g(B_\gamma)^c$, lies in the complement of every $\delta(B_{\delta^{-1}g\gamma g^{-1}\delta'}) \in \mathcal{V}_\gamma$, thus, by maximality of U, it must entirely lie in the unbounded component of $\delta(B_{\delta^{-1}g\gamma g^{-1}\delta'})^c$ for every $\delta(B_{\delta^{-1}g\gamma g^{-1}\delta'}) \in \mathcal{V}_\gamma$. Let be $p \in g(U)$ and q in the unbounded component of $g(B_\gamma)^c$. Items (1) and (2) imply that the elements of $\mathcal{V}_\gamma$ form a chain. Thus we can apply Corollary A.0.14 to the sets of $\mathcal{V}_\gamma$ to obtain that the union of these sets, which is exactly $g(B_\gamma)$, does not cut between p and q, a contradiction to the choice of these points.

Claim 2: B_γ is connected for every $\gamma \in \mathcal{A}$.
Indeed, by Items (1) and (3), one can arrange the elements of $\mathcal{A}$ as $\gamma_1, \gamma_2, \ldots, \gamma_m$ such that the compact sets $B_{\gamma_1}, \ldots, B_{\gamma_m}$ form a circular chain. Note that their union is the continuum $\partial\mathcal{T}$. Without loss of generality, suppose that B_{γ_2} is disconnected. We denote by C_1 and C_3 the connected components of B_{γ_2} such that $\#C_1 \cap B_{\gamma_1} = 1 = \#C_3 \cap B_{\gamma_3}$. Then we have for each other component D of B_{γ_2} and for every $i \in \{1, 3, \ldots, m\}$ that $D \cap B_{\gamma_i} = \emptyset$.
If $C_1 = C_3 =: C$, then $C \neq B_{\gamma_2}$ and by Lemma A.0.8 there exists a clopen subset P of B_{γ_2} with $C \subseteq P \subsetneq B_{\gamma_2}$. Thus the boundary can be written as

$$\partial\mathcal{T} = (B_{\gamma_2} \setminus P) \cup \left(P \cup \bigcup_{i \in \{1,3,\ldots,m\}} B_{\gamma_i}\right),$$

which is a separation of ∂T into two disjoint closed subsets, a contradiction to the connectedness of $\partial\mathcal{T}$.
If $C_1 \neq C_3$, one can write

$$\partial\mathcal{T} = C_1 \cup C_3 \cup E \cup \bigcup_{i \in \{1,3,\ldots,m\}} B_{\gamma_i},$$

where E is the union of all connected components of B_{γ_2} different from C_1 and C_3. If $E = \emptyset$, note that the union $C_1 \cup C_3 \cup \bigcup_{i \in \{1,3,\ldots,m\}} B_{\gamma_i}$ is not a cut of the space (use Claim 1 and apply Corollary A.0.14 to the chain $C_3, B_{\gamma_3}, B_{\gamma_4}, \ldots, B_{\gamma_m}, B_{\gamma_1}, C_1$). But this union is exactly $\partial\mathcal{T}$. This contradicts the fact that $\mathcal{T}$ is a tile. If $E \neq \emptyset$, let C be a component of B_{γ_2} distinct from C_1 and C_3. Then using Lemma A.0.8 one can find clopen subsets P_1, P_3 of B_{γ_2} such that $C_1 \subseteq P_1, C_3 \subseteq P_3$ and $P_1 \cap C = P_3 \cap C = \emptyset$. Thus $P_1 \cup P_3 \subsetneq B_{\gamma_2}$ is a clopen subset of B_{γ_2}. This leads to the separation

$$\partial\mathcal{T} = (B_{\gamma_2} \setminus (P_1 \cup P_3)) \cup \left(P_1 \cup P_3 \cup \bigcup_{i \in \{1,3,\ldots,m\}} B_{\gamma_i}\right)$$

of the boundary of $\mathcal{T}$ into two disjoint closed subsets, contradicting the connectedness of $\partial\mathcal{T}$.

From Claims 1 and 2 and Items (1) and (3) we obtain that the $\{B_\gamma; \gamma \in \mathcal{A}\}$ form a circular chain of continua, each of which does not separate the plane. The disk-likeness of $\mathcal{T}$ then follows as in the first part of the proof of Theorem 3.3.1. □

3.3.4 Application to $p2$-crystiles

In this subsection, four examples of crystiles will be presented and we will answer the question of their disk-likeness using Theorem 3.3.9.

Let Γ be the following crystallographic group $p2$:

$$\Gamma = \{a^p b^q c^r; p, q \in \mathbb{Z}\ ,\ r \in \{0, 1\}\}$$

where the isometries a, b, c are defined by:

$$a(x, y) = (x + 1, y),\ \ b(x, y) = (x, y + 1),\ \ c(x, y) = (-x, -y).$$

The following examples are cases of 3-reptiles (*i.e.*, $|\mathcal{D}| = 3$) and correspond to disk-like candidates listed in Gelbrich [19].
For each example, we will proceed as follows.

(1) We compute the contact graph $\mathbf{G}(\mathcal{R})$, defined in Definition 3.2.4. Note that there are five types of fundamental domains of $p2$ given by Grünbaum and Shephard in [22, pp.288-290]. For each example, we have the possibility to choose one of these types for Q (hence for $\mathcal{R}_0$) to get the contact graph $\mathbf{G}(\mathcal{R})$.

(2) The neighborhood graph $\mathbf{G}(\mathcal{S})$ (Definition 3.2.4) is obtained by Algorithm 3.2.21.

(3) We use the neighborhood graph to give some informations concerning the crystile, about its sets of L-vertices (see Proposition 3.2.10), its vertex neighbors and its adjacent neighbors (set $\mathcal{A}$) (see Characterization 3.2.11).

The last part of the subsection is then devoted to the proof of the disk-likeness or non disk-likeness of the tiles presented in these examples by applying Theorem 3.3.9.

Example 3.3.10. This example corresponds to Gelbrich's picture [19, p.252, Fig.6 (i)]. It was presented as introductive example in Example 3.1.4. It is depicted again in Figure 3.2 together with the other digit tiles (images of the tile by the two other digits). This crystile will be shown to be disk-like.

The map g was defined by

$$g(x, y) = \left(y, -3x - \frac{1}{2}\right),\ \ \mathcal{D} = \{\mathrm{id}, b, c\},$$

and the tile fulfills

$$g(\mathcal{T}) \ = \ \mathcal{T} \cup b(\mathcal{T}) \cup c(\mathcal{T}).$$

(1) We choose $\mathcal{R}_0 = \{\mathrm{id}, b, b^{-1}, c, a^{-1}c\}$ (see the corresponding fundamental domain in Figure 3.6). This yields $\mathcal{R}_1 = \mathcal{R}_0 \cup \{a^{-1}b^{-1}c\}$, $\mathcal{R}_2 = \mathcal{R}_1 \cup \{b^{-1}c\} = \mathcal{R}_3$, so finally

$$\mathcal{R} = \{\mathrm{id}, b, b^{-1}, c, a^{-1}c, a^{-1}b^{-1}c, b^{-1}c\}.$$

(2) The application of Algorithm 3.2.21 leads to $\mathcal{S} = \mathcal{R} \setminus \{\mathrm{id}\}$, so the contact graph and the neighborhood graph are equal (up to the identity). They are depicted in Figure 3.7, and the edges are listed in Table 3.1.

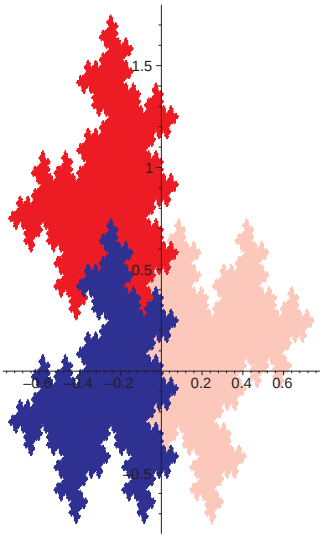

Figure 3.2: $p2$-crystile with its digit tiles (Example 3.3.10).

(3) *Sets of L-vertices.* Using Proposition 3.2.10, we read on the graph the sets of L-vertices and obtain the following results:

- $\#V_2(b,c) = \#V_2(b,a^{-1}c) = \#V_2(b^{-1},b^{-1}c) = \#V_2(b^{-1},a^{-1}b^{-1}c)$
  $= \#V_2(c,b^{-1}c) = \#V_2(a^{-1}b^{-1}c,a^{-1}c) \;=\; 1$. (The other sets of 2-vertices are empty.)
- $V_L = \emptyset$ for $L \geq 3$.

Vertex and adjacent neighbors. One can use the neighborhood graph together with Characterization 3.2.11 to get that there is no vertex neighbor and that the set of adjacent neighbors is the whole set $\mathcal{S}$. Another way to show this will be given in the last part of this section (Proposition 3.3.15).

Example 3.3.11. This example corresponds to Gelbrich's picture [19, p.252, Fig.6 (b)]. This crystile will be shown to be disk-like. It is depicted in Figure 3.3 together with its other digit tiles. We take

$$g(x,y) = (-y, 3x+1), \quad \mathcal{D} = \{\mathrm{id}, b, c\},$$

and the tile is defined by

$$g(\mathcal{T}) \;=\; \mathcal{T} \cup b(\mathcal{T}) \cup c(\mathcal{T}).$$

We have $g\Gamma g^{-1} \subset \Gamma$ because

$$gag^{-1} = b^3, \; gbg^{-1} = a^{-1}, \; gcg^{-1} = b^2c.$$

(1) We choose $\mathcal{R}_0 = \{\mathrm{id}, b, b^{-1}, c, bc, a^{-1}c\}$ (see Figure 3.6). This yields $\mathcal{R}_1 = \mathcal{R}_0$, so

$$\mathcal{R} = \{\mathrm{id}, b, b^{-1}, c, bc, a^{-1}c\}.$$

(2) The application of Algorithm 3.2.21 leads to $\mathcal{S} = \mathcal{R} \setminus \{\mathrm{id}\} \cup \{a^{-1}bc, a^{-1}b^{-1}c\}$. The graphs are depicted in Figure 3.7; the edges are listed in Tables 3.1 and 3.2.

(3) *Sets of L-vertices.* Using Proposition 3.2.10, we read off from the neighborhood graph the sets of L-vertices and obtain the following results:

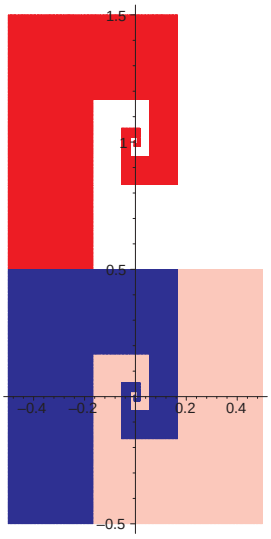

Figure 3.3: $p2$-crystile with its digit tiles (Example 3.3.11).

- $\#V_2(b, a^{-1}c) = \#V_2(b, a^{-1}bc) = \#V_2(b^{-1}, a^{-1}b^{-1}c) = \#V_2(b^{-1}, a^{-1}c)$
  $= \#V_2(a^{-1}c, a^{-1}bc) = \#V_2(a^{-1}c, a^{-1}b^{-1}c)$
  $= \#V_2(b, bc) = \#V_2(b^{-1}, c) = \#V_2(c, bc) = 1$. (The sets of 2-vertices that are not listed are empty.)
- $\#V_3(b, a^{-1}c, a^{-1}bc) = \#V_3(b^{-1}, a^{-1}b^{-1}c, a^{-1}c) = 1$. (The sets of of 3-vertices that are not listed are empty.)
- $V_L = \emptyset$ for $L \geq 4$.

Remark. For each of the first six sets $V(s, s')$ in the first item, using the neighborhood graph in Figure 3.7 one gets only one possible sequence of labels for a walk starting from s and s', but for the other sets, one finds exactly two possible walks. Let us just consider $V_2(b, bc)$. Then the infinite walks starting from b and bc are $(\mathrm{id}, \mathrm{id}, c, \mathrm{id}, c, \mathrm{id}, c, \ldots)$ and $(b, c, \mathrm{id}, c, \mathrm{id}, c, \mathrm{id}, \ldots)$. However, they represent the same point on the boundary of $\mathcal{T}$, because:

$$\lim_{m\to\infty} g^{-1}(g^{-1}g^{-1}c)^m(0,0) = \left(-\frac{1}{6}, \frac{1}{2}\right) = \lim_{m\to\infty} g^{-1}bg^{-1}c(g^{-}g^{-1}c)^m(0,0).$$

Vertex and adjacent neighbors. Looking at the graph in Figure 3.7, we see that there is exactly one infinite walk starting from the neighbors

$$\{a^{-1}bc, a^{-1}b^{-1}c\}.$$

This implies that these are vertex neighbors because of Characterization 3.2.11. One can also use Characterization 3.2.11 to obtain that the set of adjacent neighbors is

$$\mathcal{A} = \{\mathrm{id}, b, b^{-1}, c, bc, a^{-1}c\},$$

but another way will be given in Proposition 3.3.15.

Example 3.3.12. This example corresponds to Gelbrich's picture [19, p.253, Fig.8 (c)]. This crystile will be shown to be non disk-like. It is depicted in Figure 3.4 with the other digit tiles. We take

$$g(x, y) = (-y, -3x - y), \quad \mathcal{D} = \{\mathrm{id}, b, a^{-1}c\},$$

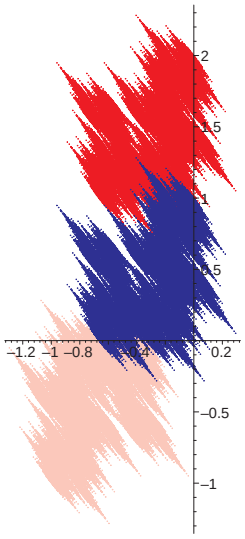

Figure 3.4: $p2$-crystile with its digit tiles (Example 3.3.12).

and the tile is defined by

$$g(\mathcal{T}) \;=\; \mathcal{T} \cup b(\mathcal{T}) \cup a^{-1}c(\mathcal{T}).$$

The property $g\Gamma g^{-1} \subset \Gamma$ holds because

$$ga^{-1}cg^{-1} = b^3c,\ gbg^{-1} = a^{-1}b^{-1},\ gcg^{-1} = c.$$

(1) We choose $\mathcal{R}_0 = \{\mathrm{id}, b, b^{-1}, a^{-1}c, c, bc\}$ (see Figure 3.6). This yields $\mathcal{R}_1 = \mathcal{R}_0 \cup \{a^{-1}bc\}$, $\mathcal{R}_2 = \mathcal{R}_1$, so finally

$$\mathcal{R} = \{\mathrm{id}, b, b^{-1}, a^{-1}c, c, bc, a^{-1}bc\}.$$

(2) The application of Algorithm 3.2.21 leads to

$$\mathcal{S} = \mathcal{R} \setminus \{\mathrm{id}\} \;\cup \{a, a^{-1}, a^{-1}b, ab^{-1}, a^{-1}b^2c, b^2c, a^{-2}b^2c\}.$$

The graphs are depicted in Figure 3.8, the edges listed in Tables 3.1 and 3.2.

Example 3.3.13. This example corresponds to Gelbrich's picture [19, p.254, Fig.7 (a)], one of the two "not as convincing" pictures listed by Gelbrich. We represented it in Figure 3.5. We take

$$g(x, y) = (x - y, 3x + 1),\ \mathcal{D} = \{\mathrm{id}, b, a^{-1}c\},$$

and the tile is defined by

$$g(\mathcal{T}) \;=\; \mathcal{T} \cup b(\mathcal{T}) \cup a^{-1}c(\mathcal{T}).$$

The property $g\Gamma g^{-1} \subset \Gamma$ holds because

$$ga^{-1}cg^{-1} = a^{-1}b^{-1}c,\ gbg^{-1} = a^{-1},\ gcg^{-1} = b^2c.$$

(1) We choose $\mathcal{R}_0 = \{\mathrm{id}, b, b^{-1}, c, a^{-1}c, bc, a^{-1}bc\}$ (see Figure 3.6). This yields $\mathcal{R}_1 = \mathcal{R}_0$, so

$$\mathcal{R} = \{\mathrm{id}, b, b^{-1}, a^{-1}c, c, bc, a^{-1}bc, a^{-1}bc\}.$$

(2) The application of Algorithm 3.2.21 leads to $\mathcal{S} = \mathcal{R} \setminus \{\mathrm{id}\}$. It is again a tile with six neighbors. The graphs are depicted in Figure 3.9.

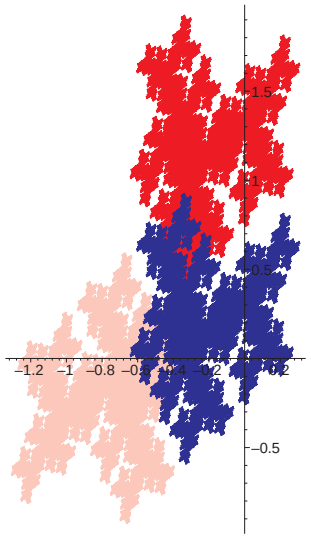

Figure 3.5: $p2$-crystile with its digit tiles (Example 3.3.13).

(3) *Sets of L-vertices.* Using Proposition 3.2.10, we read on the graph the sets of L-vertices and obtain following results:

- $\#V_2(b, bc) = \#V_2(b, a^{-1}bc) = \#V_2(b^{-1}, c) = \#V_2(b^{-1}, a^{-1}c)$ $= \#V_2(bc, c) = \#V_2(a^{-1}bc, a^{-1}c) = 1$. (The sets of 2-vertices that are not listed are empty.)
- $V_L = \emptyset$ for $L \geq 3$.

Vertex and adjacent neighbors. One can use the neighborhood graph together with Characterization 3.2.11 to get that there is no vertex neighbor and that the set of adjacent neighbors is exactly the whole set $\mathcal{S}$. Indeed, the infinite walks

$$(a^{-1}c, b, b, \ldots)\,, (\mathrm{id}, b, b, \ldots)\,, (b, b, b, \ldots), (a^{-1}c, a^{-1}c, \mathrm{id}, a^{-1}c, \mathrm{id}, \ldots)\,,$$
$$(\mathrm{id}, a^{-1}c, \mathrm{id}, a^{-1}c, \ldots)\,, (a^{-1}c, \mathrm{id}, a^{-1}c, \mathrm{id}, \ldots)$$

are in $\mathbf{G}_1(\mathcal{S})$ iff their starting points are respectively $b\,, b^{-1}\,, c\,, a^{-1}c\,, bc\,, a^{-1}bc\,.$ However, this result will also be obtained by Proposition 3.3.15.

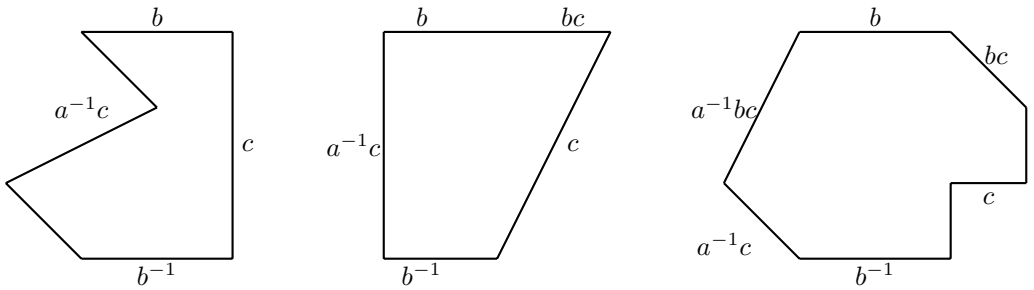

Example 3.3.10. Examples 3.3.11 and 3.3.12. Example 3.3.13.

Figure 3.6: Fundamental domain Q.

edges	labels	
id → id	id	id
	b	b
	c	c
id → b	id	b
id → b^{-1}	b	id
id → c	id	c
	c	id
id → $b^{-1}c$	b	c
	c	b
$b \to a^{-1}b^{-1}c$	c	b
$b \to a^{-1}c$	c	id
$b^{-1} \to a^{-1}b^{-1}c$	b	c
$b^{-1} \to a^{-1}c$	id	c
$c \to b^{-1}c$	id	id
$c \to b$	c	id
$c \to b^{-1}$	id	c
$a^{-1}c \to c$	b	b
$a^{-1}c \to b$	b	c
$a^{-1}c \to b^{-1}$	c	b
$a^{-1}b^{-1}c \to a^{-1}c$	b	b
$b^{-1}c \to a^{-1}b^{-1}c$	id	id

Example 3.3.10

edges	labels	
id → id	id	id
	b	b
	c	c
id → b	id	b
id → b^{-1}	b	id
id → c	id	c
	c	id
$b \to a^{-1}c$	id	c
$b^{-1} \to a^{-1}c$	c	id
$c \to c$	b	b
$c \to b$	b	c
$c \to b^{-1}$	c	b
$c \to bc$	id	b
	b	id
$bc \to a^{-1}c$	b	b
$a^{-1}c \to bc$	c	c
$a^{-1}c \to b$	c	id
$a^{-1}c \to b^{-1}$	id	c

Example 3.3.11

edges	labels	
id → id	id	id
	b	b
	$a^{-1}c$	$a^{-1}c$
id → b	id	b
id → b^{-1}	b	id
id → $a^{-1}c$	id	$a^{-1}c$
	$a^{-1}c$	id
$b \to bc$	$a^{-1}c$	id
$b \to c$	$a^{-1}c$	b
$b^{-1} \to bc$	id	$a^{-1}c$
$b^{-1} \to c$	b	$a^{-1}c$
$c \to c$	id	id
$bc \to b$	$a^{-1}c$	id
$bc \to b^{-1}$	id	$a^{-1}c$
$bc \to a^{-1}bc$	$a^{-1}c$	$a^{-1}c$
$a^{-1}bc \to a^{-1}bc$	id	b
	b	id
$a^{-1}bc \to b$	b	$a^{-1}c$
$a^{-1}bc \to b^{-1}$	$a^{-1}c$	b
$a^{-1}bc \to a^{-1}c$	b	b
$a^{-1}c \to bc$	b	b

Example 3.3.12

Table 3.1: Tables of edges for three examples of contact graphs.

edges	labels	
$b \to a^{-1}b^{-1}c$	b	c
$b^{-1} \to a^{-1}b^{-1}c$	c	b
$a^{-1}bc \to a^{-1}b^{-1}c$	id	id
$a^{-1}b^{-1}c \to a^{-1}bc$	c	c
$bc \to a^{-1}bc$	id	b
	b	id

Example 3.3.11

edges	labels	
$c \to a^{-1}b$	$a^{-1}c$	b
$c \to ab^{-1}$	b	$a^{-1}c$
$c \to a$	id	$a^{-1}c$
$c \to a^{-1}$	$a^{-1}c$	id
$b \to a^{-1}$	id	b
$b^{-1} \to a$	b	id
$a^{-1}bc \to a^{-1}b^2c$	id	id
$a^{-1}b^2c \to a$	$a^{-1}c$	b
$a^{-1}b^2c \to a^{-1}$	b	$a^{-1}c$
$a^{-1}b^2c \to a^{-1}b$	id	$a^{-1}c$
$a^{-1}b^2c \to ab^{-1}$	$a^{-1}c$	id
$a^{-1}b \to a^{-1}b$	b	id
$a^{-1}b \to a^{-2}b^2c$	id	$a^{-1}c$
$ab^{-1} \to ab^{-1}$	id	b
$ab^{-1} \to a^{-2}b^2c$	$a^{-1}c$	id
$a \to a^{-1}b^2c$	$a^{-1}c$	b
$a^{-1} \to a^{-1}b^2c$	b	$a^{-1}c$
$a^{-2}b^2c \to a^{-2}b^2c$	b	b
$a^{-1}c \to b^2c$	id	b
	b	id
$b^2c \to b^2c$	$a^{-1}c$	$a^{-1}c$

Example 3.3.12

Table 3.2: Additionnal edges for the neighborhood graphs.

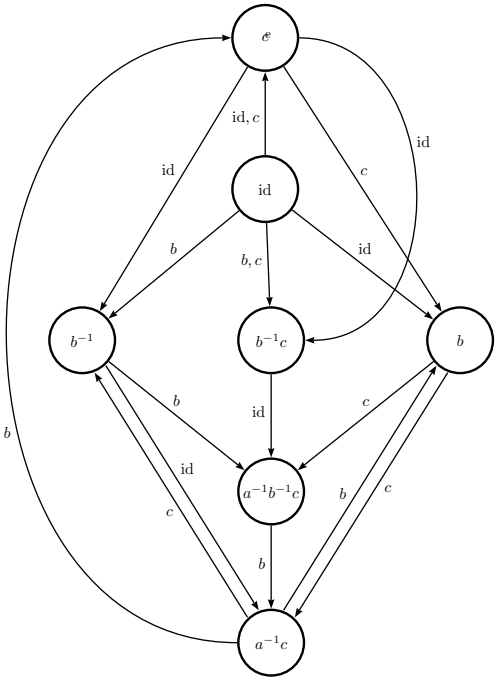

Example 3.3.10.

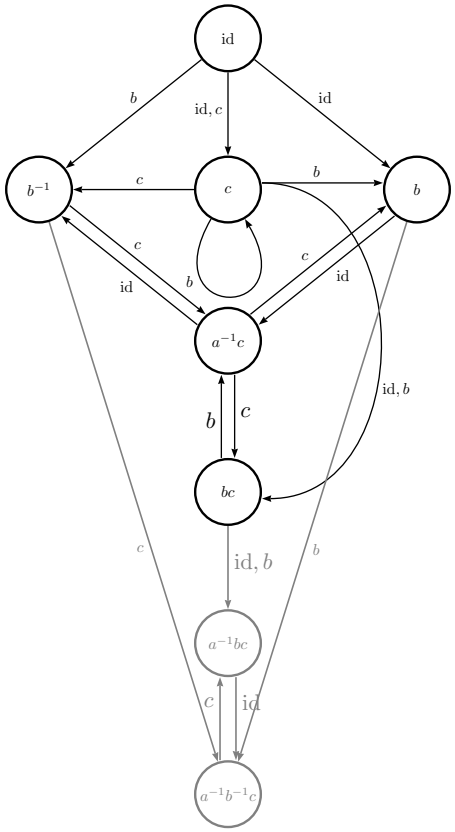

Example 3.3.11.

Figure 3.7: Examples 3.3.10 and 3.3.11: contact graphs $\mathbf{G}(\mathcal{R})$ (dark part) and neighborhood graphs $\mathbf{G}(\mathcal{S})$ (dark and dimmed parts).

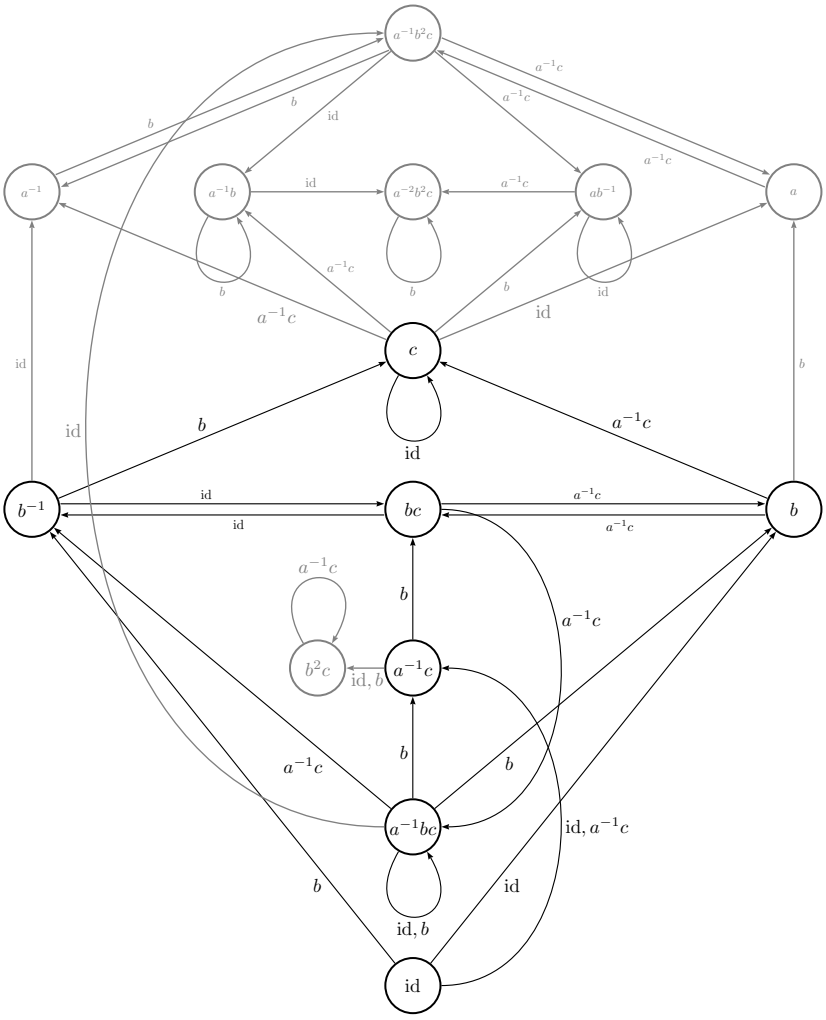

Figure 3.8: Example 3.3.12: contact graph $\mathbf{G}(\mathcal{R})$ (dark part) and neighborhood graph $\mathbf{G}(\mathcal{S})$ (dark and dimmed parts).

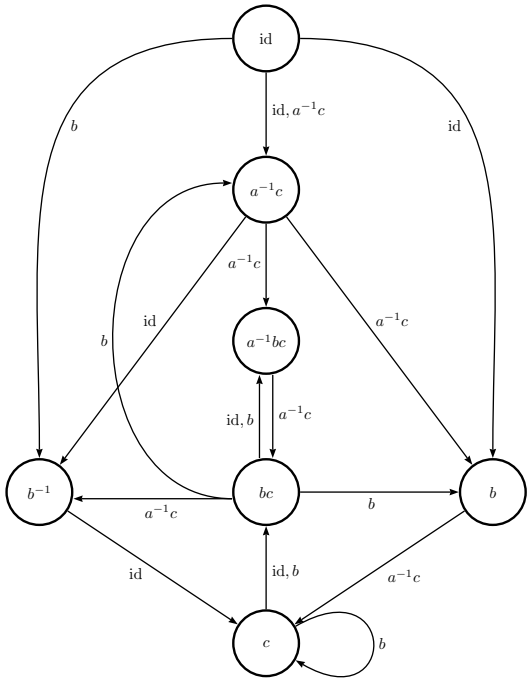

Figure 3.9: Example 3.3.13: contact graph $\mathbf{G}(\mathcal{R})$ and neighborhood graphs $\mathbf{G}(\mathcal{S})$.

We now answer the question of Gelbrich in these examples.

Proposition 3.3.14. *The following assertions hold.*

- *The tiles defined in Example 3.3.10, Example 3.3.11 and Example 3.3.13 are disk-like.*
- *The tile defined in Example 3.3.12 is not disk-like.*

To prove this, we will apply the criterion contained in Theorem 3.3.9 to the examples. To this matter, we want to identify the adjacent neighbors of the central tile $\mathcal{T}$ in another way than in Characterization 3.2.11.

Proposition 3.3.15. *Let $\mathcal{T}$ be a connected p2-tile. Let a, b be the translations of $\mathbb{R}^2$ defined by $a(x, y) = (x + 1, y)$ and $b(x, y) = (x, y + 1)$, c the π-rotation of the plane $c(x, y) = (-x, -y)$.*

(*i*) *If $\mathcal{T}$ has six neighbors*

$$\mathcal{S} = \{b^{\pm 1}, c, a^{-1}c, bc, a^{-1}bc\}$$
$$\textit{(or } \mathcal{S} = \{b^{\pm 1}, c, a^{-1}c, bc, a^{-1}b^{-1}c\} \textit{)}$$

then each element of $\mathcal{S}$ is an adjacent neighbor of id.

(*ii*) *If $\mathcal{T}$ has seven neighbors $\mathcal{S} = \{b^{\pm 1}, c, bc, a^{-1}c, a^{-1}bc, a^{-1}b^{-1}c\}$, then $\{b^{\pm 1}, c, bc, a^{-1}c\}$ are adjacent neighbors of* id.

(*iii*) *If $\mathcal{T}$ has eight neighbors $\mathcal{S} = \{b^{\pm 1}, c, a^{-1}c, bc, b^{-1}c, a^{-1}bc, a^{-1}b^{-1}c\}$*
(or $\mathcal{S} = \{c, bc, ac, ab^{-1}c, b^{\pm 1}, (a^{-1}b)^{\pm 1}\}$),
then $\{b^{\pm 1}, c, a^{-1}c\}$ (resp. $\{c, bc, ac, ab^{-1}c\}$) are adjacent neighbors of id.

(*iv*) *If* $\mathcal{T}$ *has twelve neighbors* $\{c, a^{-1}c, bc, abc, a^{-1}bc, a^{-1}b^{-1}c, a^{\pm 1}, b^{\pm 1}, (ab)^{\pm 1}\}$, *then* $\{c, a^{-1}c, bc\}$ *are adjacent neighbors of* id.

Proof. Let us consider the case of six neighbors. We will show that the rotation c is an adjacent neighbor. Let

$$T' := \mathcal{T} \cup a^{-1}b^{-1}c(\mathcal{T}) \ .$$

Then T' is a connected compact set that tiles $\mathbb{R}^2$ by $\mathbb{Z}^2$, *i.e.*, T' provides a lattice tiling of $\mathbb{R}^2$. We set

$$\begin{array}{rclcl} S_1 & = & \bigcup_{q\in\mathbb{Z}, r\in\{0,1\}} (ab)^q c^r(\mathcal{T}) & = & \bigcup_{q\in\mathbb{Z}} (ab)^q(T'), \\ \Omega_1 & = & \left(\bigcup_{q<q', r\in\{0,1\}} a^q b^{q'} c^r(\mathcal{T})\right) & = & \left(\bigcup_{q<q'} a^q b^{q'}(T')\right), \\ \Omega_2 & = & \left(\bigcup_{q>q', r\in\{0,1\}} a^q b^{q'} c^r(\mathcal{T})\right) & = & \left(\bigcup_{q>q'} a^q b^{q'}(T')\right). \end{array}$$

The identity $\mathbb{R}^2 \ = \ S_1 \cup \Omega_1 \cup \Omega_2$ holds, and because of the assumption on the set $\mathcal{S}$, we have $\Omega_1 \cap \Omega_2 = \emptyset$.
The tile T' being a connected compact set, Lemma B.0.24 assures that its boundary $\partial T'$ is connected. Let us suppose that $\partial T' \subseteq \Omega_1 \cup \Omega_2$, then we obtain

$$\partial T' \ = \ (\partial T' \cap \Omega_1) \ \cup \ (\partial T' \cap \Omega_2),$$

which is a partition of $\partial T'$ into two relative closed sets that have empty intersection, a contradiction to the connectedness of $\partial T'$.
Consequently, $\partial T' \cap (S_1 \setminus (\Omega_1 \cup \Omega_2)) \neq \emptyset$, thus there is an $s \in \{ab, a^{-1}b^{-1}\}$ such that

$$(T' \cap s(T')) \setminus \bigcup_{(q,q')\notin\{(0,0),\pm(1,1)\}} a^q b^{q'}(T') \ \neq \emptyset, \tag{3.3.1}$$

since $ab(T')$ and $a^{-1}b^{-1}(T')$ are the only lattice tiles in S_1 that are in contact with T' (this follows from the assumption on $\mathcal{S}$).
By the assumption on $\mathcal{S}$, we have

$$T' \cap ab(T') = \mathcal{T} \cap c(\mathcal{T}) \ \text{ and } \ T' \cap a^{-1}b^{-1}(T') = a^{-1}b^{-1}c(\mathcal{T}) \cap a^{-1}b^{-1}(\mathcal{T}), \tag{3.3.2}$$

hence, also by this assumption, $(T' \cap ab(T')) \cap \left(T' \cap a^{-1}b^{-1}(T')\right) = \emptyset$.
Thus, if $s = ab$, we get from (3.3.1) and (3.3.2) that

$$(\mathcal{T} \cap c(\mathcal{T})) \setminus \bigcup_{\gamma\in\Gamma\setminus\{\mathrm{id},c\}} \gamma(\mathcal{T}) \ \neq \emptyset.$$

This indicates that c is an adjacent neighbor.
If $s = a^{-1}b^{-1}$, we obtain similarly that $a^{-1}b^{-1}(\mathcal{T})$ and $a^{-1}b^{-1}c(\mathcal{T})$ are adjacent neighbors, hence after translation by ab we get again that c is an adjacent neighbor.
The other neighbors of the six-neighbor cases as well as the cases of seven, eight and twelve neighbors can be treated similarly. (Note that the case of translations, say b for instance, does not require the introduction of a substitution tile T': we can choose $S_1 = \bigcup_{q\in\mathbb{Z}} b^q(\mathcal{T})$ and use Lemma B.0.21 to obtain that $\partial\mathcal{T}$ intersects S_1.) □

We are now able to examine the disk-likeness of the tiles presented in Examples 3.3.10 to 3.3.13 by checking the three items of Theorem 3.3.9.
For each example, we will have to compute the graph G_γ for every $\gamma \in \mathcal{A}$. The set of states of G_γ is

$$\{\delta\,(B_{\gamma'})\,; \text{there is an edge } \gamma \xrightarrow{\delta|\delta'} \gamma' \text{ in } \mathbf{G}(\mathcal{A})\}.$$

There is an edge in G_γ between two states $\delta\,(B_{\gamma'})$ and $\delta'\,(B_{\gamma''})$ iff

$$\mathcal{T} \cap \gamma''(\mathcal{T}) \cap \delta'^{-1}\delta(\mathcal{T}) \cap \delta'^{-1}\delta\gamma'(\mathcal{T}) \ \neq \ \emptyset.$$

This can easily be checked by looking at the sets V_2 and V_3.
We will also need the subgraph of G_2 induced by the states $\{B_\gamma; \gamma \in \mathcal{A}\}$. Again, there is an edge between B_γ and $B_{\gamma'}$ in this graph iff

$$\mathcal{T} \cap \gamma(\mathcal{T}) \cap \gamma'(\mathcal{T}) \neq \emptyset,$$

which can be seen using the sets V_2.

Proof of Proposition 3.3.14.

- **Example 3.3.10**
  The first item of Theorem 3.3.9 is fulfilled as we checked in Example 3.3.10.
  From Proposition 3.3.15, we get

  $$\mathcal{A} = \{b, b^{-1}, c, a^{-1}c, a^{-1}b^{-1}c, b^{-1}c\}.$$

  We obtain the graphs G_γ for $\gamma \in \mathcal{A}$ in Figure 3.10. Each of them consists of a simple path. So the second item is fulfilled.
  The subgraph of G_2 induced by the states $\{B_\gamma; \gamma \in \mathcal{A}\}$ is represented on Figure 3.11: it is a simple loop.
  Thus the crystile of Example 3.3.10 is disk-like.

- **Example 3.3.11**
  The first item of Theorem 3.3.9 is fulfilled (see page 35).
  From Proposition 3.3.15, we get:

  $$\mathcal{A} = \{b, b^{-1}, c, a^{-1}c, a^{-1}b^{-1}c, b^{-1}c\}.$$

  We obtain the graphs G_γ in Figure 3.10. Each of them consists of a simple path. So the second item is fulfilled.
  The subgraph of G_2 induced by the states $\{B_\gamma; \gamma \in \mathcal{A}\}$ is represented on Figure 3.11: it is a simple loop.
  Thus the crystile of Example 3.3.11 is disk-like.

- **Example 3.3.12**
  We show that the first item of the criterion of Theorem 3.3.9 is not fulfilled, in particular we have

  $$\#V_2(a^{-1}bc, b^{-1}) \geq 2\,.$$

  Indeed, the infinite walks

  $$\begin{array}{ccccccccccc} a^{-1}bc & \xrightarrow{\mathrm{id}} & a^{-1}bc & \xrightarrow{b} & a^{-1}bc & \xrightarrow{b} & a^{-1}bc & \xrightarrow{b} & \dots \\ b^{-1} & \xrightarrow{\mathrm{id}} & a^{-1} & \xrightarrow{b} & a^{-1}b^2c & \xrightarrow{b} & a^{-1} & \xrightarrow{b} & \dots \end{array}$$

  labelled by (id, b, b, b, ...) and

  $$\begin{array}{ccccccccccc} a^{-1}bc & \xrightarrow{b} & a^{-1}c & \xrightarrow{\mathrm{id}} & b^2c & \xrightarrow{a^{-1}c} & b^2c & \xrightarrow{a^{-1}c} & b^2c & \xrightarrow{a^{-1}c} & \dots \\ b^{-1} & \xrightarrow{b} & c & \xrightarrow{\mathrm{id}} & a & \xrightarrow{a^{-1}c} & a^{-1}b^2c & \xrightarrow{a^{-1}c} & a & \xrightarrow{a^{-1}c} & \dots \end{array}$$

  labelled by (b, id, $a^{-1}c$, $a^{-1}c$, $a^{-1}c$, ...) are in $\mathbf{G}(\mathcal{S})$ (look at Figure 3.8). This means by Proposition 3.2.10 that the points

  $$x \;=\; \lim_{m\to\infty} g^{-1}(g^{-1}b)^m(0,0) \;=\; \left(-\frac{2}{3}, 1\right)$$

and

$$y \;=\; \lim_{m\to\infty} g^{-1}bg^{-1}(g^{-1}a^{-1}c)^m(0,0) \;=\; \left(-\frac{4}{9},\frac{1}{3}\right)$$

are two distinct points of $V_2(a^{-1}bc, b^{-1})$.
Thus the crystile of Example 3.3.12 is non disk-like.

- **Example 3.3.13**
  The first item of the criterion of Theorem 3.3.9 is fulfilled (see page 37).
  From Proposition 3.3.15 (replace b by b^{-1}) we have

$$\mathcal{A} = \{b, b^{-1}, c, a^{-1}c, a^{-1}bc, bc\}.$$

  We obtain the graphs G_γ in Figure 3.10. Each of them consists of a simple path. So the second item is fulfilled.
  The subgraph of G_2 induced by the states $\{B_\gamma; \gamma \in \mathcal{A}\}$ is represented in Figure 3.11: it is a simple loop.
  Thus the crystile of Example 3.3.13 is disk-like. □

γ	G_γ
b	$c(B_{a^{-1}b^{-1}c}) \;-\; c(B_{a^{-1}c})$
b^{-1}	$b(B_{a^{-1}b^{-1}c}) \;-\; B_{a^{-1}c}$
c	$B_{b^{-1}} \;-\; B_{b^{-1}c} \;-\; c(B_b)$
$a^{-1}c$	$c(B_{b^{-1}}) \;-\; b(B_c) \;-\; b(B_b)$
$a^{-1}b^{-1}c$	$b(B_{a^{-1}c})$
$b^{-1}c$	$B_{a^{-1}b^{-1}c}$

Example 3.3.10.

γ	G_γ
b	$B_{a^{-1}c}$
b^{-1}	$c(B_{a^{-1}c})$
c	$b(B_b) \;-\; b(B_{bc}) \;-\; b(B_c) \;-\; B_{bc} \;-\; c(B_{b^{-1}})$
bc	$b(B_{a^{-1}c})$
$a^{-1}c$	$B_{b^{-1}} \;-\; c(B_{bc}) \;-\; c(B_b)$

Example 3.3.11.

γ	G_γ
b	$a^{-1}c(B_c)$
b^{-1}	B_c
c	$b(B_{bc}) \;-\; b(B_c) \;-\; B_{bc}$
$a^{-1}c$	$B_{b^{-1}} \;-\; a^{-1}c(B_{a^{-1}bc}) \;-\; a^{-1}c(B_b)$
$a^{-1}bc$	$a^{-1}c(B_{bc})$
bc	$a^{-1}c(B_{b^{-1}}) \;-\; B_{a^{-1}bc} \;-\; b(B_{a^{-1}c}) \;-\; b(B_{a^{-1}bc}) \;-\; b(B_b)$

Example 3.3.13.

Figure 3.10: Subgraph G_γ of the double neighboring graph G_2.

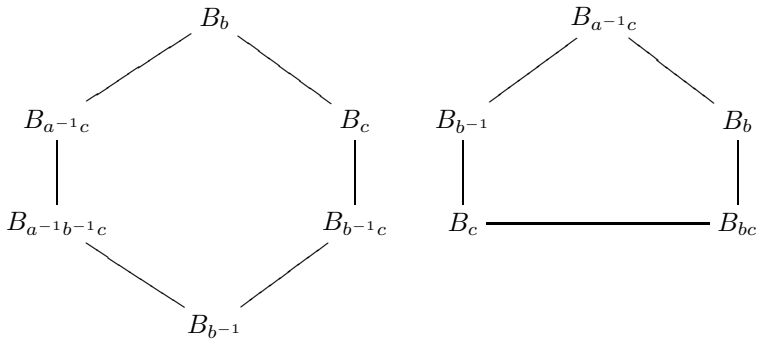

Example 3.3.10. Example 3.3.11.

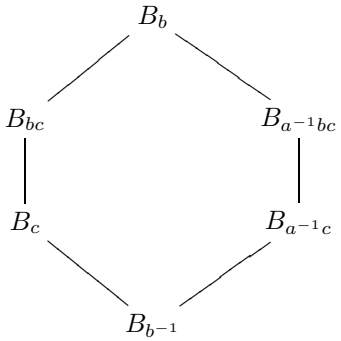

Example 3.3.13.

Figure 3.11: Restriction of G_2 to the set of states $\{B_\gamma; \gamma \in \mathcal{A}\}$.

3.3.5 A criterion for a crystile using the neighbor graph

We saw in Section 3.2 how to obtain the neighbors of a given crystile $\mathcal{T}$, *i.e.*, from the expansion map and the digit set defining the crystile. One thus easily gets the associated neighbor graph, whose vertices are the isometries γ and where two vertices γ, γ' are connected via an edge if $\gamma(T) \cap \gamma'(\mathcal{T}) \neq \emptyset$ (see Definition 2.2.22). In this subsection, we give a criterion for the disk-likeness of a crystile checkable on this neighbor graph. Remember Example 3.3.11, depicted again in Figure 3.12 with all of its neighbors. It produced a disk-like crystile $\mathcal{T}$ with seven neighbors, five of them being adjacent to $\mathcal{T}$. This leads to the adjacency and neighbor graphs seen on the same figure. We see that for this disk-like example, the whole neighbor graph is an extension of the adjacency graph obtained by adding the edges that join the vertices of the non-triangular faces of the adjacency graph. The theorem of the present subsection establishes the validity of this observation for crystiles in general and gives a reciprocal statement.

We will restrict the class of crystiles where the theorem applies, hence we give some definitions (*cf.* [15]) before stating and proving the criterion.

Definition 3.3.16 (Drawing of a graph; faces of a graph)**.** Let $G = (V, E)$ be a planar graph with set of vertices V and set of edges E. Then a *drawing* of G is a mapping $\pi : (V, E) \to \mathbb{R}^2$ such that $\pi(V)$ is a discrete set of the plane, $\pi(xy)$ is a simple arc joining $\pi(x)$ and $\pi(y)$, and

$$\pi(xy) \cap \pi(uv) = \{\pi(x), \pi(y)\} \cap \{\pi(u), \pi(v)\} \quad (xy, uv \in E \text{ disjoint}).$$

We also say that $\pi(G)$ is a drawing of G. For every planar graph G with a drawing π, the set $\mathbb{R}^2 \setminus \pi(G)$ is an open set; its components are the *faces* of $\pi(G)$.

Definition 3.3.17 (Derived graph, drawing extension and picture)**.** Given a planar graph $G = (V, E)$ and a drawing π of G, the *derived graph* of G is the graph $G_1 = (V, E_1)$ emerging from G

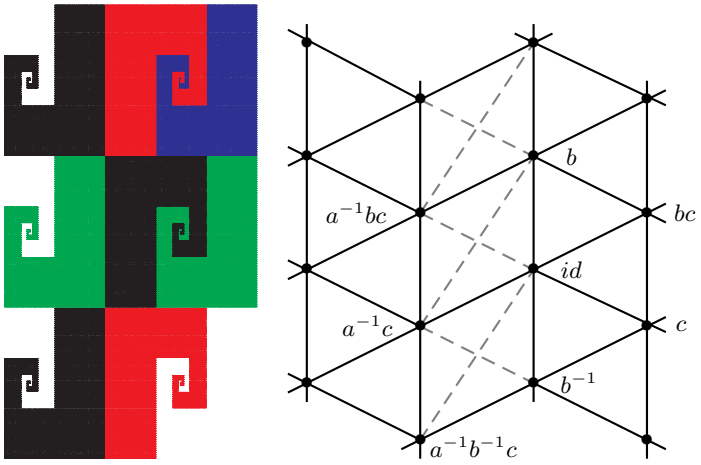

Figure 3.12: The adjacency graph (solid edges) and the neighbor graph (solid and dashed edges) for the $p2$-crystile of Example 3.3.11.

with the same set of vertices and where two vertices x, y are incident if their images $\pi(x), \pi(y)$ belong to the closure of the same face of G. E_1 contains E, and we extend π to a mapping π_1 on E_1 by joining the images of vertices corresponding to a new edge by a simple open arc inside one of their common faces. π_1 is called an *extension* of π. This extension gives rise to a *picture* of the graph G_1.

Remark 3.3.18. Such an extension π_1 is not unique. Also note that its picture does not to be a drawing in the above sense because the derived graph of a planar graph is not necessarily planar.

We need special drawings of the adjacency graph G_A. In the following definition as well as in the subsection we denote as follows a closed disk with radius r centered at x.

Notation 3.3.19. $B_r(x) = \{y \in \mathbb{R}^2; ||y - x|| \leq r\}$.

Definition 3.3.20 (Admissible drawing)**.** Let $G_A = (\Gamma, E)$ be the adjacency graph of a crystallographic tiling (see Definition 2.2.22), and let $G'_A = (\Gamma, E')$ be a subgraph of G_A (possibly $G'_A = G_A$). Assume that G'_A is planar. We say that a drawing π of G'_A is *admissible* if there is a $p \in \mathbb{R}^2$ with $\gamma_1(p) \neq \gamma_2(p)$ for all $\gamma_1, \gamma_2 \in \Gamma, \gamma_1 \neq \gamma_2$ such that:

- $\pi(\gamma) = \gamma(p) \quad (\gamma \in \Gamma)$.
- There is a constant $c \in \mathbb{R}$ such that for all $e \in E$ joining the vertices x and y, we have

$$\pi(e) \subset B_c(\pi(x)) \cap B_c(\pi(y)). \tag{3.3.3}$$

Definition 3.3.21 (Admissible extension drawing)**.** Let π_1 be an extension of π as defined above. We call π_1 *admissible* if it satisfies (3.3.3) for all $e \in E_1$ and the same constant c.

Theorem 3.3.22. *Assume that $\mathcal{T} \subset \mathbb{R}^2$ is a planar crystallographic reptile with respect to a crystallographic group Γ. Then $\mathcal{T}$ is disk-like, if and only if the following three conditions all hold.*

(i) The adjacency graph G_A is a connected planar graph.

(ii) The digit set $\mathcal{D}$ induces a connected subgraph in G_A.

(iii) G_A has an admissible drawing $\pi : G_A \to \mathbb{R}^2$ such that the derived graph of G_A is exactly the neighbor graph G_N.

Remark 3.3.23. Condition (iii) says that two tiles $\gamma_1(\mathcal{T}), \gamma_2(\mathcal{T})$ are neighbors if and only if the vertices $\pi(\gamma_1), \pi(\gamma_2)$ lie on the boundary of a single face of the drawing $\pi(G_A)$.

Proof of Theorem 3.3.22. Assume that $\mathcal{T} \subset \mathbb{R}^2$ is a planar crystallographic reptile with respect to a crystallographic group Γ, an expanding affine map g and a digit set $\mathcal{D}$. We split the proof of the theorem in two parts.

Sufficiency [1]. Assume that Conditions (i), (ii) and (iii) of Theorem 3.3.22 hold. In view of Proposition 3.3.5, it suffices to show that the interior of $\mathcal{T}$ is connected. We fix an admissible drawing π for G_A, which gives an associated constant c and a point p defined in Definition 3.3.20 (w.l.o.g., $p \in \mathcal{T}$). G_N is by assumption the derived graph of G_A and we call π_1 an admissible extension of the drawing π.

For each $k \in \mathbb{N}$, we define the set $\mathcal{D}^k$ of elements in Γ such that

$$g^k(\mathcal{T}) = \bigcup_{\gamma \in \mathcal{D}^k} \gamma(\mathcal{T}).$$

Thus we have $\mathcal{D}^1 = \mathcal{D}$, and using Condition (ii), it can be shown recursively that the subgraph G_A^k of G_A induced by $\mathcal{D}^k$ is connected for every $k \in \mathbb{N}$.

Our aim is to prove the result by contradiction. Indeed, assuming that $\mathrm{int}(\mathcal{T})$ is disconnected, we will find a curve in $\pi(G_A^k)$ intersecting a curve in $\pi_1(G_N \setminus G_A^k)$ and derive a contradiction ($G_N \setminus G_A^k$ is the subgraph of G_N induced by the set of vertices $\Gamma \setminus \mathcal{D}^k$).

We denote by D the diameter of the tiles $\gamma(\mathcal{T})$ (*i.e.*, the maximal distance between two points of a tile $\gamma(\mathcal{T})$, which does not depend on the isometry γ) and by L the minimal distance between two disjoint tiles. We set $M := \max\{D, L, c\}$.

Suppose that $\mathrm{int}(\mathcal{T})$ is disconnected, and let z_1 and z_2 be two points in different components of $\mathrm{int}(\mathcal{T})$. Let $k \in \mathbb{N}$ be large enough such that $B_{6M}(g^k(z_i)) \subset g^k(\mathrm{int}(\mathcal{T}))$ $(i \in \{1, 2\})$. For $i = 1, 2$, we denote by $\gamma^{(i)}$ an element of $\mathcal{D}^k$ such that the tile $\gamma^{(i)}(\mathcal{T})$ contains $g^k(z_i)$ and by Ω_i the component of $g^k(\mathrm{int}(\mathcal{T}))$ containing $g^k(z_i)$. In the following, A_p $(1 \leq p \leq 6)$ will stand for the unbounded connected region $\mathbb{R}^2 \setminus \big(B_{pM}(g^k(z_1)) \cup B_{pM}(g^k(z_2))\big)$.

Then the boundary $\partial\Omega_1$ of the component Ω_1 is contained in A_6 and separates between $\mathcal{B}_1 := B_{2M}(g^k(z_1))$ and $\mathcal{B}_2 := B_{2M}(g^k(z_2))$. Consider the the finite collection

$$\mathcal{U} := \{\gamma \in \Gamma \setminus \mathcal{D}^k; \gamma(\mathcal{T}) \cap \partial\Omega_1 \neq \emptyset\}.$$

This definition implies that $\bigcup_{\gamma \in \mathcal{U}} \gamma(\mathcal{T})$ is contained in A_5 and separates between $\mathcal{B}_1$ and $\mathcal{B}_2$. By Lemma A.0.18, there is a simple closed curve C in $\bigcup_{\gamma \in \mathcal{U}} \gamma(\mathcal{T})$ which separates between $\mathcal{B}_1$ and $\mathcal{B}_2$ too. We suppose that $\mathcal{B}_1$ lies in the bounded component of $\mathbb{R}^2 \setminus C$.

We denote by $(C(t), t \in [0, 1])$ a parametrization of C with $C(0) = C(1)$.

As C is uniformly continuous, we may find a constant $\delta > 0$ such that $d(C(t), C(t')) < L$ as soon as $|t - t'| < \delta$. Let $m \geq 2$ and $(t_j)_{0 \leq j \leq m}$ be a subdivision of $[0, 1]$ with $0 = t_0 < t_1 < \ldots < t_{m-1} < t_m = 1$ and $t_{j+1} - t_j < \delta$. Then, setting $C_j := C(t_j)$, we have $d(C_j, C_{j+1}) < L$ for all $0 \leq j \leq m - 1$. Choose now for each $j \in \{0, \ldots, m\}$ an element $\alpha_j \in \mathcal{U}$ with $\alpha_0 = \alpha_m$ and such that $C_j \in \alpha_j(\mathcal{T})$. Then for all $0 \leq j \leq m - 1$, $d(\alpha_j(\mathcal{T}), \alpha_{j+1}(\mathcal{T})) < L$. Thus, by the definition of L, two consecutive tiles are neighbors, *i.e.*, $\alpha_j^{-1}\alpha_{j+1} \in \mathcal{S} \cup \{\mathrm{id}\}$.

[1] Some parts of this proof are inspired by the proof of a theorem of Bandt and Wang in [7].

We now construct a closed curve that is homotopic to C in A_2 and is made by pieces $\pi(e)$ for some edges $e \in G_N \setminus G_A^k$. By Lemma A.0.17, this closed curve will also separate between $\mathcal{B}_1$ and $\mathcal{B}_2$.

Let $j \in \{0, \dots, m-1\}$. Consider the union R_j of the intersecting balls $B_{2M}(\alpha_j(p))$ and $B_{2M}(\alpha_{j+1}(p))$. Then $R_j \subset A_2$. Moreover, the line segments $\overline{\alpha_j(p)C_j}$ and $\overline{C_{j+1}\alpha_{j+1}(p)}$, the arc

$$E_j := \pi_1(\alpha_j(p)\alpha_{j+1}(p))$$

as well as the piece

$$C^j := \{C(t); t \in [t_j, t_{j+1}]\}$$

of the curve C are all contained in the simply connected set R_j. Thus the arc E_j can be obtained from the union of $\overline{\alpha_j(p)C_j}$, C^j and $\overline{C_{j+1}\alpha_{j+1}(p)}$ by a deformation in R_j.

Consequently, the union

$$\mathcal{E} := \bigcup_{0 \le j \le m-1} E_j$$

of the arcs is obtained from the union

$$\mathcal{F} := \bigcup_{0 \le j \le m-1} \left(\overline{\alpha_j(p)C_j} \cup C^j \cup \overline{C_{j+1}\alpha_{j+1}(p)} \right)$$

by a deformation in $\bigcup_{0 \le j \le m-1} R_j \subset A_2$.

Note that $\mathcal{F}$ separates between $\mathcal{B}_1$ and $\mathcal{B}_2$. By Lemma A.0.17, so does $\mathcal{E}$. Thus every curve from $\gamma^{(1)}(p) \in \mathcal{B}_1$ to $\gamma^{(2)}(p) \in \mathcal{B}_2$ intersects $\mathcal{E}$. Since the subgraph G_A^k of G_A induced by $\mathcal{D}^k$ is connected and $\gamma^{(1)}, \gamma^{(2)} \in \mathcal{D}_k$, there is a connected path $\gamma_1 := \gamma^{(1)}, \gamma_2, \dots, \gamma_{q-1}, \gamma_q := \gamma^{(2)}$ in G_A with $\gamma_i \in \mathcal{D}^k, i = 1, \dots, q$. The image by π of this path is a curve in $\pi(G_A^k)$ joining $\gamma^{(1)}(p)$ and $\gamma^{(2)}(p)$. It is intersected by $\mathcal{E}$, which is a closed curve in $\pi_1(G_N \setminus G_A^k)$. Thus, an arc $\pi_1(\alpha_j(p)\alpha_{j+1}(p))$ (possibly degenerated in the sense that $\alpha_i = \alpha_{j+1}$) must intersect an arc $\pi(\gamma_i(p)\gamma_{i+1}(p))$. But by the assumption on the drawing, either $\pi_1(\alpha_j(p)\alpha_{j+1}(p))$ is in $\pi(G_A)$ or

$$\pi_1(\alpha_j(p)\alpha_{j+1}(p)) \setminus \{\alpha_j(p), \alpha_{j+1}(p)\}$$

is contained in a face of the drawing. In both cases, these arcs must share a common end point to intersect, contradicting the disjointness of $\{\alpha_0, \dots, \alpha_m\}$ and $\{\gamma_1, \dots, \gamma_q\}$.

Necessity. Assume that $\mathcal{T}$ is disk-like. We have to check Conditions (i), (ii) and (iii) of Theorem 3.3.22. Condition (ii) can be directly inferred from the disk-likeness of $\mathcal{T}$. Thus we have to show that Conditions (i) and (iii) are also satisfied.

As $\gamma(\mathcal{T}) \cap \gamma'(\mathcal{T})$ is either empty or a connected set for all distinct elements $\gamma, \gamma' \in \Gamma$, the boundary $\partial\mathcal{T}$ consists of arcs $P_1, \dots, P_k$, where $3 \le k \le 6$ and $P_j = \mathcal{T} \cap \gamma_j(\mathcal{T})$ (*cf.* [19]). Here $\gamma_1, \dots, \gamma_k$ are the adjacent neighbors of id. The arcs $P_1, \dots, P_k$ can be arranged to a circular chain (see Definition A.0.13 in the appendix) in the sense that for all distinct $i, j \in \{1, 2, \dots, k\}$ the intersection $P_i \cap P_j$ is a singleton if $j \equiv i + 1 (\mathrm{mod}\, k)$, and is an empty set otherwise.

Choose an interior point x_1 of P_1 (in subspace topology), and let $\mathrm{Orb}(x_1) = \{\gamma(x_1); \gamma \in \Gamma\}$ be the Orbit of x_1 under the crystallographic group Γ. Clearly, the number of points in $\mathrm{Orb}(x_1) \cap \partial\mathcal{T}$ is between 1 and k. If it is not k, we can choose a least integer i_1 such that $\mathrm{Orb}(x_1) \cap P_{i_1} = \emptyset$. Let x_2 be an interior point of P_{i_1}, then $\mathrm{Orb}(x_1) \cap \mathrm{Orb}(x_2) = \emptyset$ and the number of points in $(\mathrm{Orb}(x_1) \cup \mathrm{Orb}(x_2)) \cap \partial\mathcal{T}$ is between 2 and k. Going on with this procedure for at most $k-1$ steps, we will find k' points $x_1, \dots, x_{k'}$ on $\partial\mathcal{T}$, where $k' \le k$, such that the number of points in

$$\left(\bigcup_{i=1}^{k'} \mathrm{Orb}(x_i) \right) \cap \partial\mathcal{T}$$

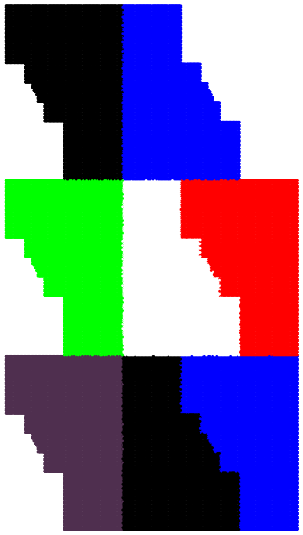

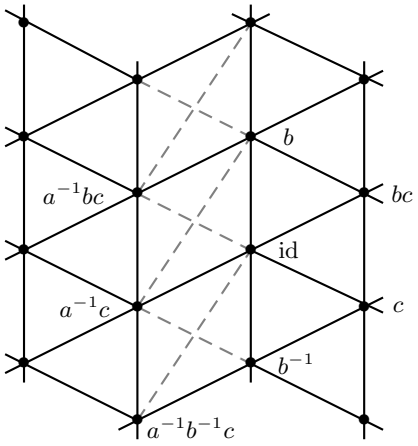

The graph G_A (solid)
and its derived graph (solid and dashed).

Figure 3.13: $p2$-crystile with seven neighbors, digit set $\{\mathrm{id}, b, c\}$.

is exactly k. Rename the k points of the above intersection as $y_1, \ldots, y_k$ with $y_l \in P_l$.

By the Schönflies Theorem [51], choose a homeomorphism $h : \mathcal{T} \to \{re^{\mathbf{i}t}; 0 \le t < 2\pi, 0 \le r \le 1\}$ such that $h(y_l) = e^{\frac{2\pi l}{k}\mathbf{i}}$. Let $R_l = \{re^{\frac{2\pi l}{k}\mathbf{i}}; 0 \le r \le 1\}$ be the radius joining the origin 0 and the point $h(y_l)$, for $1 \le l \le k$. Then $W = h^{-1}\left(\bigcup_{l=1}^{k} R_l\right)$ is a union of arcs in $\mathcal{T}$ which are disjoint except at their common endpoint $h^{-1}(0) \in \mathrm{int}(\mathcal{T})$.

Now we can see that $\bigcup_{\gamma\in\Gamma} \gamma(W)$ is an admissible drawing of G_A and that Condition (i) is satisfied. Clearly, each triple point of the tiling $\{\gamma(T); \gamma \in \Gamma\}$ must be enclosed in a face of the above drawing. Since an arc $\gamma \circ h^{-1}(R_l)$ is contained in the boundary of a face containing a triple point x if and only if $x \in \gamma(P_l)$, and since two tiles $\gamma(\mathcal{T}), \gamma'(\mathcal{T})$ are neighbors if and only if their intersection $\gamma(\mathcal{T}) \cap \gamma'(\mathcal{T})$ contains a triple point x, we see that Condition (iii) is satisfied. □

3.3.6 Applications

The examples of Subsection 3.3.4 could be treated with the third criterion (Theorem 3.3.22). We give here two new concrete examples, one of a $p2$-crystile with seven neighbors, and one of a $p3$-crystile, both with three digits. They correspond to disk-like candidates of Gelbrich's paper [19].

Example 3.3.24. (see [19, p. 252, (c)]) Let

$$\begin{aligned} a(x,y) &= (x+1, y), \\ b(x,y) &= (x, y+1), \\ c(x,y) &= (-x, -y). \end{aligned}$$

Then the $p2$ group Γ can be written as

$$\Gamma = \{a^i b^j c^k; i, j \in \mathbb{Z}, k \in \{0, 1\}\}.$$

The expanding mapping g is chosen as $g(x, y) = (y, 3x + 1)$, the digit set as $\mathcal{D} = \{\mathrm{id}, b, c\}$, thus the tile $\mathcal{T}$ is defined by the set equation

$$g(\mathcal{T}) = \mathcal{T} \cup b(\mathcal{T}) \cup c(\mathcal{T}).$$

It is depicted in Figure 3.13.

It can be shown with the tools developed in Section 3.2 that $\mathcal{T}$ has exactly the seven neighbors

$$\mathcal{S} = \{b, b^{-1}, c, b^{-1}c, a^{-1}c, a^{-1}bc, a^{-1}b^{-1}c\},$$

and that its adjacent neighbors are

$$\mathcal{A} = \{b, b^{-1}, c, b^{-1}c, a^{-1}c\}.$$

Thus the adjacency graph has a drawing as in Figure 3.13 (solid edges). Its neighbor graph G_N is exactly the derived graph of the drawing of G_A (see Figure 3.13 also, solid and dashed edges). In this case, $\mathcal{T}$ satisfies all the conditions in Theorem 3.3.22 because the digit set $\mathcal{D}$ is $\mathcal{A}$-connected. Hence it is disk-like.

Example 3.3.25. This example is devoted to a $p3$-crystile with ten neighbors which is called "terdragon". It also occurs in Gelbrich's paper (see [19, p. 255]). It is the only disk-like $p3$-reptile candidate with three digits found by Gelbrich. We show here that it is indeed disk-like.

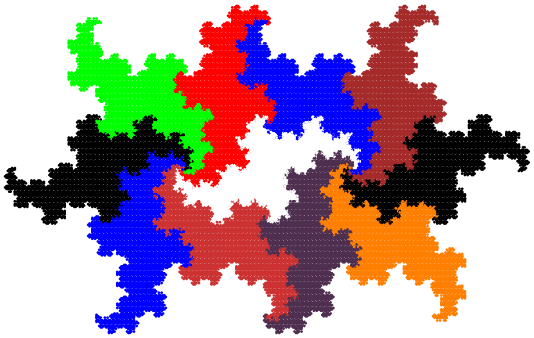

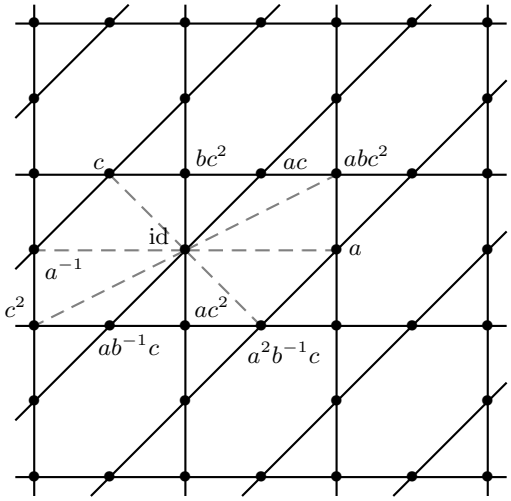

The graph G_A and part of its derived graph.

Figure 3.14: The "terdragon", a $p3$-crystile with ten neighbors, digit set $\{\mathrm{id}, ac^2, bc^2\}$.

Let

$$\begin{aligned} a(x,y) &= (x+1, y), \\ b(x,y) &= (x+1/2, y+\sqrt{3}/2), \\ c(x,y) &= \left((-x-\sqrt{3}y)/2, (\sqrt{3}x-y)/2\right). \end{aligned}$$

A $p3$-crystallographic group is then generated by a, b and c, *i.e.*,

$$\Gamma = \{a^i b^j c^k; i, j \in \mathbb{Z}, k \in \{0, 1, 2\}\}.$$

The expanding mapping g is chosen to be $g(x,y) = \sqrt{3}(y, -x)$, the digit set is $\mathcal{D} = \{\mathrm{id}, ac^2, bc^2\}$, thus the tile $\mathcal{T}$ is defined by the set equation

$$g(\mathcal{T}) = \mathcal{T} \cup ac^2(\mathcal{T}) \cup bc^2(\mathcal{T}).$$

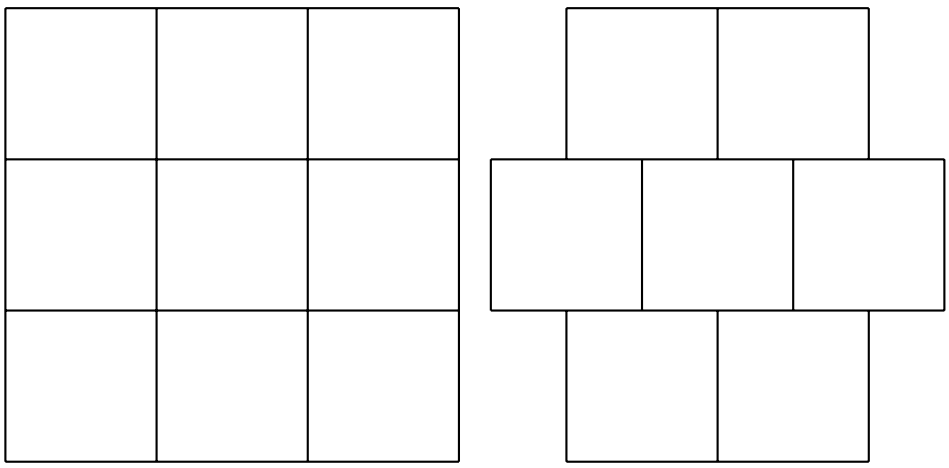

Figure 3.15: The two neighbor configurations of disk-like lattice tiles.

It is depicted in Figure 3.14. Using the tools developed in Section 3.2 it can be shown that $\mathcal{T}$ has exactly the ten neighbors

$$\mathcal{S} = \{a, a^{-1}, c, c^2, ac, ac^2, bc^2, ab^{-1}c, abc^2, a^2b^{-1}c\}$$

four of which are adjacent. These are given by

$$\mathcal{A} = \{ac, ac^2, bc^2, ab^{-1}c\}.$$

Thus the adjacency graph has a drawing as in Figure 3.14. The neighbor graph G_N is exactly its derived graph (see Figure 3.14 where the additional edges connected to id are dashed). In this case, $\mathcal{T}$ satisfies all the conditions in Theorem 3.3.22 because the digit set $\mathcal{D}$ is $\mathcal{A}$-connected. Hence it is disk-like.

3.3.7 A criterion for lattice and $p2$-crystiles

The last criterion will fully characterize the disk-like lattice and $p2$-reptiles. The preceding criterion is in a way inconvenient, because all the adjacent neighbors have to be determined, whereas simple techniques, as used in Proposition 3.3.15, only allow to identify some of them. In this subsection, we are interested in more specialized criteria, but easier to apply. In fact, Grünbaum and Shephard [22] listed all possible configurations of the neighbors of a disk-like crystallographic tile. There are two possibilities in the lattice case, corresponding to six and eight neighbors (see Figure 3.15), and six possibilities in the $p2$-case, corresponding to six, seven, eight and twelve neighbors. Hence we just need to concentrate on theses cases and get for them the sufficient conditions; this is what the general form of the preceding criterion will lead to.

The criterion of this subsection was already found in 2002 by Bandt and Wang in the lattice case (see [7]). In this case, as already told, disk-likeness happens only if $\mathcal{T}$ has six or eight neighbors; the criterion states that it eventually depends on the shape of the digit set $\mathcal{D}$. A new proof of this result is given here, as well as its extension to the $p2$-case. The technique of the proof makes use of the neighbor and adjacency neighbor graphs associated to the tilings. Moreover, on the way to the proof, we will see that lattice and $p2$-tiles (not necessarily with a replication property) always have at least six neighbors, whose configuration is fixed if the number of neighbors is exactly six.

The proof seems to give general ideas for other crystallographic groups but the details closely depend on the shape of the neighbor set of the crystile, that is why only the lattice and $p2$-cases

are treated here.

The condition on the digit set will use the following notion of set-connectedness.

Definition 3.3.26 (Set-connectedness)**.** If $\mathcal{D}$ and $\mathcal{F}$ are two sets of isometries in $\mathbb{R}^2$, we say that $\mathcal{D}$ is *$\mathcal{F}$-connected* iff for every disjoint pair (d, d') of elements in $\mathcal{D}$, there exist an $n \geq 1$ and elements $d =: d_0, d_1, \ldots, d_{n-1}, d_n := d'$ of $\mathcal{D}$ such that $d_i^{-1} d_{i+1} \in \mathcal{F}$ for $i = 0, \ldots, n-1$.

Remark 3.3.27. This notion of set-connectedness is related to the connectedness of tiles : it can be shown as in [23, 34] that a necessary and sufficient condition for a crystile as in Definition 3.1.3 to be connected is that the digit set is $\mathcal{S}$-connected, where $\mathcal{S}$ is the neighbor set of the crystile.

We will always assume that the groups Γ involved in the tilings below are the exact symmetry groups of the tilings (see [22]).

The main result in Bandt and Wang [7] was the following criterion of disk-likeness for plane crystiles defined as in Definition 3.1.3 in the case that Γ is a plane lattice.

Proposition 3.3.28 (see [7, Theorems 2.1 and 2.2])**.** *Let $\mathcal{T}$ be a self-affine lattice plane tile with digit set $\mathcal{D}$.*

(1) *Suppose that the neighbor set $\mathcal{S}$ of $\mathcal{T}$ has not more than six elements. Then $\mathcal{T}$ is disk-like iff $\mathcal{D}$ is $\mathcal{S}$-connected.*

(2) *Suppose that the neighbor set $\mathcal{S}$ of $\mathcal{T}$ has eight elements $\{a^{\pm 1}, b^{\pm 1}, (ab)^{\pm 1}, (ab^{-1})^{\pm 1}\}$, where a and b denote two independent translations. Then $\mathcal{T}$ is disk-like iff $\mathcal{D}$ is $\{a^{\pm 1}, b^{\pm 1}\}$-connected.*

We will give a new proof of this result and extend it to $p2$-groups as follows.

Theorem 3.3.29. *Let $\mathcal{T}$ be a crystile that tiles the plane by a $p2$-group. Let $\mathcal{D}$ be the corresponding digit set.*

(1) Suppose that the neighbor set $\mathcal{S}$ of $\mathcal{T}$ has six elements. Then $\mathcal{T}$ is disk-like iff $\mathcal{D}$ is $\mathcal{S}$-connected.

(2) Suppose that the neighbor set $\mathcal{S}$ of $\mathcal{T}$ has seven elements

$$\{b^{\pm 1}, c, bc, a^{-1}c, a^{-1}bc, a^{-1}b^{-1}c\},$$

where a, b are translations and c is a π-rotation.
Then $\mathcal{T}$ is disk-like iff $\mathcal{D}$ is $\{b^{\pm 1}, c, bc, a^{-1}c\}$-connected.

(3) Suppose that the neighbor set $\mathcal{S}$ of $\mathcal{T}$ has eight elements

$$\{b^{\pm 1}, c, a^{-1}c, bc, b^{-1}c, a^{-1}bc, a^{-1}b^{-1}c\}$$
$$\text{(or } \{c, bc, ac, ab^{-1}c, b^{\pm 1}, (a^{-1}b)^{\pm 1}\} \text{),}$$

where a, b are translations and c is a π-rotation.
Then $\mathcal{T}$ is disk-like iff $\mathcal{D}$ is $\{b^{\pm 1}, c, a^{-1}c\}$- (resp. $\{c, bc, ac, ab^{-1}c\}$-) connected.

(4) Suppose that the neighbor set $\mathcal{S}$ of $\mathcal{T}$ has twelve elements

$$\{c, a^{-1}c, bc, abc, a^{-1}bc, a^{-1}b^{-1}c, a^{\pm 1}, b^{\pm 1}, (ab)^{\pm 1}\},$$

where a, b are translations and c is a π-rotation.
Then $\mathcal{T}$ is disk-like iff $\mathcal{D}$ is $\{c, a^{-1}c, bc\}$-connected.

Remark 3.3.30 (To Proposition 3.3.28 and Theorem 3.3.29)**.**

1. According to Grünbaum and Shephard's classification of isohedral tilings (see [22, 6.2, p.285 ff]), the mentioned cases are the only ones for disk-like lattice and p2-tiles in the plane.

2. In each item of these statements, the set with respect to which the digit set is connected reveals to be exactly the set of adjacent neighbors of the central tile. Indeed, it corresponds to the set of adjacent neighbors of the involved disk-like tile in Grünbaum and Shephard's classification (see [22]).

3. Propositions 3.3.35 and 3.3.37 will give the exact shape of the neighbor set that appears in Proposition 3.3.28 (1) and Theorem 3.3.29 (1), *i.e.*, in the 6-neighbor cases.

An easy way to visualize these results is by considering the neighbor and adjacency graphs, whose definitions were given in the basics. They are depicted in Figures 3.16 to 3.19 (see Propositions 3.3.35 and 3.3.37 for the choice of the vertices in the six neighbor-cases). Disk-likeness happens iff $\mathcal{D}$ is connected along the solid edges; the remaining edges are dashed.

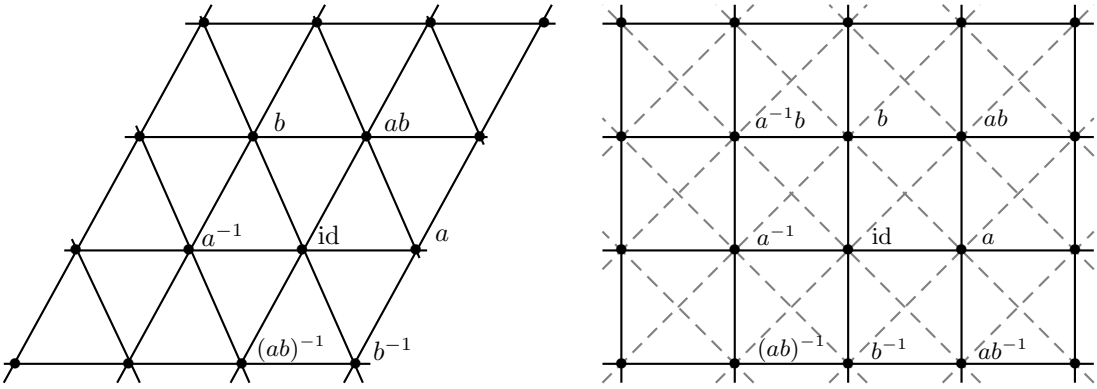

(1) 6 neighbor case (see also Proposition 3.3.35). (2) 8 neighbor case.

Figure 3.16: Proposition 3.3.28.

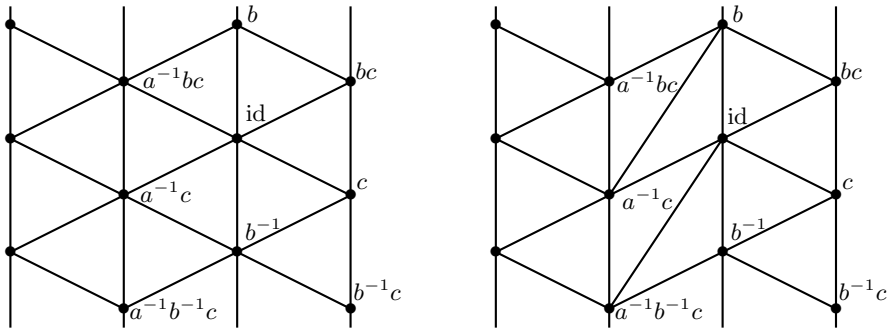

Shape 1. Shape 2.

Figure 3.17: Theorem 3.3.29 (1): 6 neighbor case (see also Proposition 3.3.37).

This remaining part of this subsection is organized as follows. We will first prove that 6 is the least number of neighbors for lattice and $p2$-tiles (with or without replication property). Then, we will see that for a lattice tile with six neighbors, the shape of its neighbor set is fixed. This will also hold for a $p2$-tile if it is supposed to be connected. Eventually, we use the neighbor and adjacency graphs to give a new proof of Bandt and Wang's result as well as the proof of its extension to $p2$-crystiles.

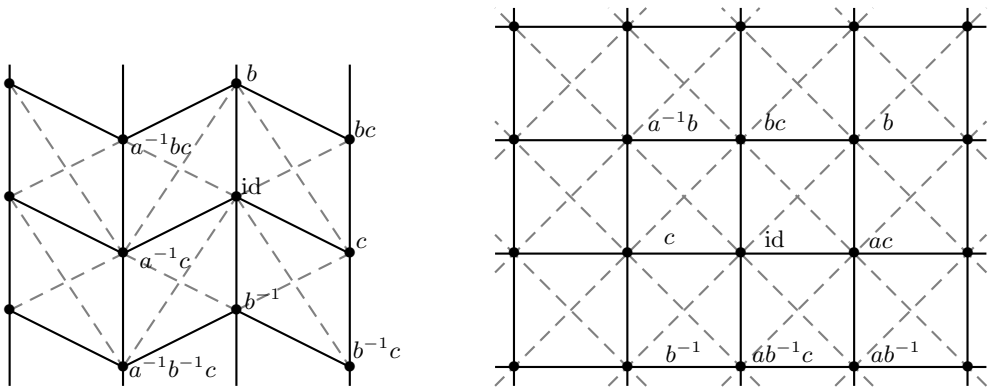

Shape 1. Shape 2.

Figure 3.18: Theorem 3.3.29 (3): 8 neighbor case.

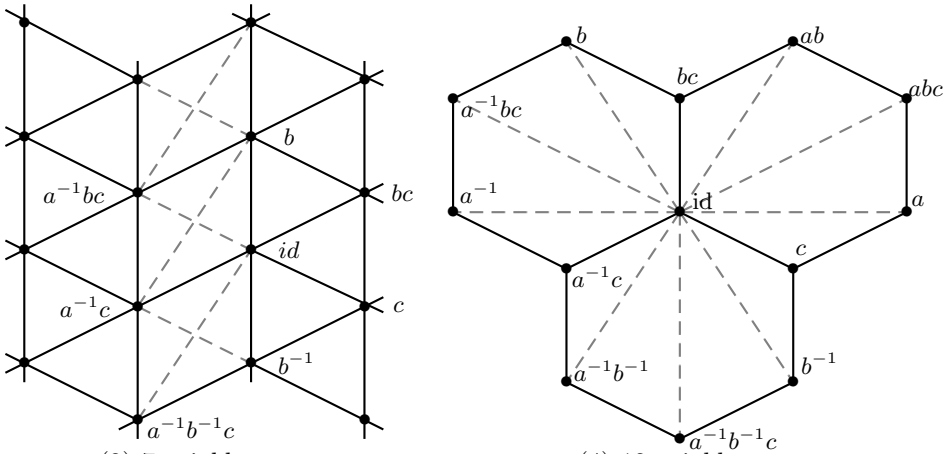

(2) 7 neighbor case. (4) 12 neighbor case.

Figure 3.19: Theorem 3.3.29 (2) and (4).

Least neighbor number

We are interested in the least number of neighbors a tile has in a lattice or a $p2$-tiling. We will show that for tilings using a single compact tile this number is six. The proof only uses the existence of triple points, defined as follows (compare with Definition 3.2.7).

Definition 3.3.31 (Double point, triple point)**.** Let $\{\gamma(T); \gamma \in \Gamma\}$ be a tiling of $\mathbb{R}^n$ which uses a single prototile T. A point $x \in T$ is a *double point* if there is $\gamma \in \Gamma \setminus \{\mathrm{id}\}$ such that $x \in \gamma(T)$; and $x \in T$ is called a *triple point* if there exist two distinct elements $\gamma_1, \gamma_2 \in \Gamma \setminus \{\mathrm{id}\}$ such that $x \in \gamma_1(T) \cap \gamma_2(T)$.

In Definition 3.2.7, we called V_L the set of $(L+1)$-folded points; V_1 is the boundary of the tile T. Note that sets of vertices have been recently studied, for example in [14] where the Hausdorff dimension of V_L was computed.

It is clear that a tiling of $\mathbb{R}$ by compact pieces has double points. Lebesgue's covering theorem [16, 26, p.78, Theorem 1.8.15] says that if $\mathcal{C}$ is a finite closed cover of the n-cube $[0,1]^n$ no member

of which meets two opposite faces of $[0,1]^n$ then $\mathcal{C}$ contains $n+1$ elements with a non-empty intersection. See also [1] for a recent sharpening of this result. As a corollary of this, we can infer the following proposition.

Proposition 3.3.32. *For each tiling $\{\gamma(T);\gamma\in\Gamma\}$ of $\mathbb{R}^n$ which uses a single compact prototile T, the set of $(n+1)$-vertices is nonempty.*

Proposition 3.3.33. *Let T be a compact tile providing a tiling of the plane by a lattice Γ. Then its set of neighbors $\mathcal{S}$ has at least six elements.*

Proof. Suppose $\mathcal{S}$ has less than six elements. Then $\mathcal{S}=\{a,a^{-1},b,b^{-1}\}$ for two independent translations $a,b\in\Gamma$ by Remark 3.1.5.3. By the existence of triple points, two intersections $T\cap a^i(T)$ and $T\cap b^j(T)$ (or $T\cap a^k(T)$) must intersect for some $i,j\in\{-1,1\}$ (or distinct $i,k\in\{-1,1\}$); but this leads to the existence of a new neighbor $a^ib^{-j}(T)$ (or $a^{i-k}(T)$). □

We now consider the case of $p2$-tiles.

Proposition 3.3.34. *Let T be a compact tile providing a tiling of the plane by a $p2$-group Γ. Then the set of neighbors $\mathcal{S}$ has at least six elements.*

Proof. Assume that Γ is generated by the two translations u,v and the rotation r of Definition 2.2.10. Then one can easily check the commutation rules $u^iv^j=v^ju^i$ and $u^iv^jr=ru^{-i}v^{-j}$ for all $i,j\in\mathbb{Z}$. Moreover, if both γ and γ' are π-rotations, $\gamma^{-1}\gamma'$ is a translation, and if exactly one of them is a translation, then $\gamma^{-1}\gamma'$ is a π-rotation. We will also often use the fact that $\gamma(T)\cap\gamma'(T)\neq\emptyset$ implies $\gamma^{-1}\gamma'\in\mathcal{S}$.

By Remark 3.1.5.3. the neighbor set $\mathcal{S}$ of T generates Γ; thus $\mathcal{S}$ contains an element $u^{i_0}v^{j_0}r=\eta r$, where $\eta=u^{i_0}v^{j_0}$ is a translation. Let $T'=T\cup\eta r(T)$, then $\{u^iv^j(T');i,j\in\mathbb{Z}\}$ is a lattice tiling of the plane.

Obviously, if T' has ten neighbors or more, then T has at least six neighbors.

If T' has eight neighbors, say $\{u^{i_k}v^{j_k}(T');1\le k\le 8\}=\{\gamma_k^{\pm1}(T');1\le k\le 4\}$, then

$$\begin{array}{c}[T\cup\eta r(T)]\cap[\gamma_k(T)\cup\gamma_k\eta r(T)]\neq\emptyset\\ \Rightarrow\quad \forall k\in\{1,\dots,4\},\ \{\gamma_k^{\pm1}\}\subset\mathcal{S}\text{ or }\gamma_k^{-1}\eta r\in\mathcal{S}\text{ or }\gamma_k\eta r\in\mathcal{S}.\end{array}$$

If $\gamma_k\in\mathcal{S}$ for some $k\in\{1,2,3,4\}$, then $\mathcal{S}$ has at least six elements. If $\gamma_k\notin\mathcal{S}$ for each $k\in\{1,2,3,4\}$, we have $\gamma_k^{i_k}\eta r\in\mathcal{S}$ for $i_1,i_2,i_3,i_4\in\{1,-1\}$. Then $\mathcal{S}$ has a sixth element. Otherwise, $\#\mathcal{S}=5$, and by the existence of triple points, $T\cap\gamma_j^{i_j}\eta r(T)$ must intersect $T\cap\gamma_k^{i_k}\eta r(T)$ for some $j,k\in\{1,2,3,4\}$ and $i_j\in\{-1,0,1\}$, $i_k\in\{-1,1\}$. This indicates that $\mathcal{S}$ has a sixth element $\gamma_j^{i_j}\gamma_k^{-i_k}$.

If T' has exactly six neighbors, there exist $\alpha,\beta\in\Gamma=\langle u,v\rangle$ such that $\alpha^{\pm1}(T'),\beta^{\pm1}(T'),\delta^{\pm1}(T')=(\alpha\beta)^{\pm1}(T')$ are the six neighbors of T' (see Proposition 3.3.35). Let $\mathcal{F}_1=\{\alpha^{\pm1},\beta^{\pm1},\delta^{\pm1}\}$. Then, T has at least four neighbors:

$$\eta r(T),\alpha^{i_1}(\eta r)^{k_1}(T),\beta^{i_2}(\eta r)^{k_2}(T),\delta^{i_3}(\eta r)^{k_3}(T)$$

for some $k_1,k_2,k_3\in\{0,1\}$ and $i_1,i_2,i_3\in\{-1,1\}$.

We claim that $\mathcal{S}$ contains at least one translation γ. Otherwise, the existence of triple points indicates that $T\cap tr(T)$ intersects $T\cap t'r(T)$ for some $tc\neq t'c\in\mathcal{S}$, where t,t' are translations. Then, $tr(T)\cap t'r(T)\neq\emptyset$ and $t^{-1}t'(T)\cap T\neq\emptyset$, thus $t^{-1}t'\in\mathcal{S}$.

By this claim, if $k_j\neq0$ for each $j\in\{1,2,3\}$, $\mathcal{S}$ contains a translation γ and thus

$$\{\eta r,\gamma^{\pm1},\alpha^{i_1}(\eta r)^{k_1},\beta^{i_2}(\eta r)^{k_2},\delta^{i_3}(\eta r)^{k_3}\}\subset\mathcal{S}.$$

If two of k_1, k_2, k_3 are 0, say $k_1 = k_2 = 0$, then $\mathcal{S}$ contains at least the six elements

$$\eta r, \alpha^{\pm 1}, \beta^{\pm 1}, \delta^{i_3}(\eta r)^{k_3}.$$

If now exactly one of k_1, k_2, k_3 is 0, say $k_1 = 0$, then $\mathcal{S}$ contains at least the five elements

$$\eta r, \alpha^{\pm 1}, \beta^{i_2}(\eta r), \delta^{i_3}(\eta r),$$

where $\delta = \alpha\beta$. If $\mathcal{S}$ has a sixth element, we are done. We suppose on the contrary that

$$\mathcal{S} = \{\eta r, \alpha^{\pm 1}, \beta^{i_2}(\eta r), \delta^{i_3}(\eta r)\}.$$

Consider $T'' = T \cup \beta^{i_2}\eta r(T)$, which tiles $\mathbb{R}^2$ under the action of the lattice $< \alpha, \beta >$. Then $\beta^{i_2}\eta r(T)$ has exactly five neighbors

$$\beta^{i_2}(T), \alpha^{\pm 1}\beta^{i_2}\eta r(T), T, \beta^{i_2}\delta^{-i_3}(T),$$

hence, T'' has exactly six neighbors

$$\beta^{\pm 1}(T''), \alpha^{\pm 1}(T''), \left(\delta^{i_3}\beta^{-i_2}\right)^{\pm 1}(T'').$$

We can infer from Proposition 3.3.35 that $\delta^{i_3}\beta^{-i_2} \in \{(\alpha\beta)^{\pm 1}, \left(\alpha\beta^{-1}\right)^{\pm 1}\}$. This is impossible, since $i_2, i_3 \in \{-1, 1\}$. □

Neighbor set

We now show that the shape of the neighbor set of a compact lattice tile or a compact connected $p2$-tile is already determined by the fact that it contains the least possible number of elements (*i.e.*, six elements).

Proposition 3.3.35. *Let T be a tile providing a tiling of the plane by a lattice. If the set $\mathcal{S}$ of neighbors of T has exactly six elements, then*

$$\mathcal{S} = \{a, a^{-1}, b, b^{-1}, ab, (ab)^{\pm 1}\}$$

for some $a, b \in \Gamma$ with $\Gamma = \langle a, b\rangle$.

Proof. By Remark 3.1.5.3. and Proposition 3.3.33 of the preceding subsection, we already know that there exist two elements $a, b \in \mathcal{S} \subset \Gamma$ such that $\Gamma = \langle a, b\rangle$ and $\mathcal{S} = \{a^{\pm 1}, b^{\pm 1}\} \cup \{\delta^{\pm 1}\}$ for some $\delta \in \Gamma$, we just need to assure that δ has the form $(ab)^{\pm 1}$ or $\left(ab^{-1}\right)^{\pm 1}$. This can be shown in the following four steps.

(*i*) $T \cap a(T)$ does not intersect $T \cap a^{-1}(T)$. Otherwise, $\delta = a^2$, and the union Q of all those compact sets $a^k(T \cap b(T))$ with $k \in \mathbb{Z}$ is a closed set such that $\mathbb{R}^2 \setminus Q$ has two unbounded components.
Let

$$Q_- = \bigcup_{k\leq 0} a^k(T \cap b(T)), \quad Q_+ = \bigcup_{k>0} a^k(T \cap b(T)).$$

Then, one can see that both $\mathbb{R}^2 \setminus Q_-$ and $\mathbb{R}^2 \setminus Q_+$ have exactly one unbounded component. That is two say, there are two points in the sphere separated by $\overline{Q} = Q \cup \{\infty\} = \overline{Q_-} \cup \overline{Q_+}$ which can not be separated by $\overline{Q_-} = Q_0 \cup \{\infty\}$ or $\overline{Q_+} = Q_+ \cup \{\infty\}$ alone. As the sphere is a Janizewski space (see [36, §61]), this implies that $Q_- = \bigcup_{k\leq 0} a^k(T \cap b(T))$ and $Q_+ = \bigcup_{k>0} a^k(T \cap b(T))$ must intersect each other.
Therefore, $a^i b(T) \cap a^j(T) \neq \emptyset$ for some $i \leq 0$ and $j > 0$, and thus $a^{j-i}b \in \mathcal{S}$ with $j - i \geq 1$, which would increase the number of neighbor.

(*ii*) Similar to item (*i*), $T \cap b(T)$ does not intersect $T \cap b^{-1}(T)$.

(*iii*) If $T \cap a^i(T)$ and $T \cap b^j(T)$ intersect for $i, j \in \{-1, 1\}$, then $ab \in \mathcal{S}$ or $ab^{-1} \in \mathcal{S}$, thus δ or δ^{-1} is equal to ab or ab^{-1}.

(*iv*) Suppose $\big(T \cap a^i(T)\big) \cap \big(T \cap b^j(T)\big) = \emptyset$ for every $i, j \in \{-1, 1\}$, then by items (i) and (ii) and the existence of triple points, $T \cap a^i(T)$ or $T \cap b^j(T)$ must intersect $[T \cap \delta(T)] \cup \big[T \cap \delta^{-1}(T)\big]$. We may assume without loss of generality that $T \cap a(T)$ intersects $T \cap \delta(T)$. Then, $a(T) \cap \delta(T) \neq \emptyset$ and $a^{-1}\delta \in \mathcal{S}$, while $\delta \notin \{a^{\pm 1}, b^{\pm 1}\}$. Thus we have $a^{-1}\delta \in \{b, b^{-1}\}$, that is to say, $\delta = ab$ or $\delta = ab^{-1}$ again.

□

In the case of $p2$-tiles, we require the tiles to be connected. Indeed, we will use Lemma B.0.24 of the appendix that tells that the boundary of connected tiles is connected.

Let us consider a tiling of the plane by a single tile T and a group of isometries Γ. Recall that $B_\gamma = T \cap \gamma(T)$ for $\gamma \in \mathcal{S}$.

Lemma 3.3.36. *Suppose that the neighbor set of T contains $m \geq 2$ elements $\gamma_1, \ldots, \gamma_m$ and that ∂T is connected. Then each B_{γ_i}, $i = 1, \ldots, m$ intersects at least one B_{γ_j}, $j \neq i$.*

Proof. Writing for the boundary $\partial T = \bigcup_{i=1}^m B_{\gamma_i}$, this follows from the connectivity of ∂T. □

Now Γ is supposed to be a $p2$-group.

Proposition 3.3.37. *If T is a compact connected set which is the central tile of a $p2$-tiling and if the neighbor set $\mathcal{S}$ of T contains exactly six elements, then $\mathcal{S}$ has one of the following shapes (where a, b are independent translations and c is a π-rotation):*

$$\mathcal{S} = \{b^{\pm 1}, c, a^{-1}c, bc, a^{-1}bc\} \quad \text{or} \quad \mathcal{S} = \{b^{\pm 1}, c, a^{-1}c, bc, a^{-1}b^{-1}c\}.$$

Remark 3.3.38. Since the inverse of tr is itself for t a translation and r a π-rotation, we have the symmetry property: $\mathcal{S} = \mathcal{S}^{-1}$.

Proof. We will freely make use of the following facts: if $\gamma, \gamma' \in \Gamma$, then from $B_\gamma \cap B_{\gamma'} \neq \emptyset$ it follows that $\gamma^{-1}\gamma' \in \mathcal{S}$. Moreover, if both γ and γ' are π-rotations, $\gamma^{-1}\gamma'$ is a translation, and if exactly one of them is a translation, then $\gamma^{-1}\gamma'$ is a π-rotation.

At least one translation $b \neq 1$ and a π-rotation c must belong to the neighbor set. Indeed, if $\mathcal{S}$ contains only translations, it can not generate a $p2$-group, which contradicts Remark 2.2.25.2. If it contains only rotations, then by the existence of triple points, two neighbors $\gamma(T), \gamma'(T)$ of T must intersect, thus the translation $\gamma^{-1}\gamma'$ should also be a neighbor.
Since if $\gamma(T)$ intersects T, then $\gamma^{-1}(T)$ also intersects T, and we obtain that $\{b, b^{-1}, c\} \subset \mathcal{S}$.

We now show that no other translation can be in $\mathcal{S}$. To this matter, we suppose on the contrary that

$$\mathcal{S} = \{b, b^{-1}, a, a^{-1}, c, c'\}$$

with $a \neq \mathrm{id}, b, b^{-1}$ a translation and c' a π-rotation. Two cases may occur.
If a and b are dependent, then the neighbor set contains four translations that are linearly dependent and two rotations. Using Lemma 3.3.36, one rotation can be written in terms of the translation b and of the other rotation. This contradicts the fact that $\mathcal{S}$ is a generating set for Γ.
If a and b are independent, then the set B_b can not intersect the sets $B_{b^{-1}}, B_a, B_{a^{-1}}$. Thus it intersects B_c or $B_{c'}$, thus $c' = b^{-1}c$ or $c = b^{-1}c'$. Doing the same with the set B_a, we obtain that also $c' = a^{-1}c$ or $c = a^{-1}c'$. This is a contradiction, since $a \neq b, b^{-1}$.

Consequently, we can write for the neighbor set:

$$\mathcal{S} = \{b, b^{-1}, c, c_1, c_2, c_3\},$$

where c_1, c_2, c_3 are the remaining π-rotations. If the set B_c intersects B_b or $B_{b^{-1}}$, then one of the remaining rotations must be $b^{\pm 1}c$; if it intersects one of the sets B_γ associated to the remaining rotations, say $\gamma = c_1$, then $cc_1 = b^{\pm 1}$, so $c_1 = b^{\pm 1}c$. Since by Lemma 3.3.36 one of these possibilities occurs, we can suppose w.l.o.g. (by exchanging b and b^{-1}) that bc belongs to the neighbor set, thus

$$\mathcal{S} = \{b, b^{-1}, c, bc, c_2, c_3\}.$$

To obtain a π-rotation that can be written in terms of a translation a independent of b, let us consider the tile $T' = T \cup c(T)$. This tile provides a lattice tiling of the plane: there are independent translations $a', b' \neq \mathrm{id}$ such that

$$\mathbb{R}^2 = \bigcup_{(i,j)\in\mathbb{Z}^2} a'^i b'^j (T').$$

By Remark 2.2.25.3. for a lattice tiling there must be a neighbor of the central tile that is not a translation by some powers of b, *i.e*, there is an $a \neq \mathrm{id}$ independent of b such that $a(T') \cap T' \neq \emptyset$. This leads, as $a \notin \mathcal{S}$, to $ac \in \mathcal{S}$ or $a^{-1}c \in \mathcal{S}$. W.l.o.g. (exchange a and a^{-1}), we suppose that $a^{-1}c \in \mathcal{S}$, such that

$$\mathcal{S} = \{b, b^{-1}, c, bc, a^{-1}c, c_3\}.$$

The rotation c_3 can be written with the help of a, b and c. Indeed, the set $B_{a^{-1}c}$ can not intersect the sets B_c and B_{bc} (this would introduce new translations in the set of neighbors), thus it must have nonempty intersection with $B_b, B_{b^{-1}}$ or B_{c_3}. In all these cases we obtain that $c_3 = a^{-1}b^{\pm 1}c$, thus $\mathcal{S}$ has one of the two shapes of our proposition. □

Proof of Bandt & Wang-like statements

This part is devoted to the proof of Proposition 3.3.28 and Theorem 3.3.29. We first recall a result of [7], which is a lattice tile analogue of Proposition 3.3.15 of Section 3.3.4, where adjacent neighbors of $p2$-tiles having a neighbor set of known shape could be identified. Then, we give a formulation of Theorem 3.3.22 with weaker assumptions. The proofs eventually follow.

If the shape of the neighbor set of the central tile is given, it is possible to identify all or some of the adjacent neighbors of this tile. This was already done for $p2$-tiles in Proposition 3.3.15, and the following is true for lattice tiles.

Proposition 3.3.39 (see [7, Lemma 3.3])**.** *Let T be a connected tile providing a lattice tiling. Let a, b be two independent translations.*

(*i*) *If T has six neighbors*

$$\mathcal{S} = \{a^{\pm 1}, b^{\pm 1}, (ab^{-1})^{\pm 1}\},$$

then $\mathcal{S}$ consists of adjacent neighbors of id*.*

(*ii*) *If $\mathcal{T}$ has eight neighbors*

$$\mathcal{S} = \{a^{\pm 1}, b^{\pm 1}, (ab^{-1})^{\pm 1}, (a^{-1}b)^{\pm 1}\},$$

then $\{a^{\pm 1}, b^{\pm 1}\}$ are adjacent neighbors of id*.*

Proof. This proposition was proved in [7] by an ε-argument, we give here a shorter proof using directly the connectedness of the boundary of ∂T as in Proposition 3.3.15]. The connectedness of ∂T is indeed assured by Lemma B.0.24 and the connectedness of T.
To Item (i) : consider the subsets of the plane:

$$\begin{array}{rcl} Q_+ : & = & \bigcup_{m,n\in\mathbb{Z},n>0} a^m b^n (T), \\ Q_- : & = & \bigcup_{m,n\in\mathbb{Z},n<0} a^m b^n (T). \end{array}$$

Then $Q_+ \cap Q_-$ is easily seen to be empty (a nonempty intersection would contradict the shape of $\mathcal{S}$). Assume that a is not an adjacent neighbor, hence a^{-1} is also not an adjacent neighbor, and the following equation for the boundary of T holds:

$$\partial T = \bigcup_{\gamma \in \{b^{\pm 1}, (ab^{-1})^{\pm 1}\}} T \cap \gamma(T),$$

hence, $\partial T = (\partial T \cap Q_+) \cup (\partial T \cap Q_-)$ induces a separation of ∂T.
The cases of b and a, b as well as Item (ii) are shown likewise. □

The criterion of disk-likeness as it is stated in Theorem 3.3.22 involves the knowledge of all adjacent neighbors of the central tile. Since Propositions 3.3.39 and 3.3.15 only identify some of them, we can not apply this criterion directly. We thus give the following criterion, derived from Theorem 3.3.22. We use the notations of Definition 2.2.22.

Proposition 3.3.40. *Assume that $\mathcal{T}$ is a plane crystallographic reptile with respect to a crystallographic group Γ, an expanding affine mapping g and a digit set $\mathcal{D}$. We write $\mathcal{D}^k$ for the set of isometries such that*

$$g^k(\mathcal{T}) = \bigcup_{\delta \in \mathcal{D}^k} \delta(\mathcal{T}).$$

Let $\mathcal{A}$ denote the set of adjacent neighbors of the central tile. Then $\mathcal{T}$ is disk-like, if and only if there is a subset $\mathcal{A}'$ of $\mathcal{A}$ with $\mathcal{A}'^{-1} = \mathcal{A}'$ such that the following three conditions all hold:

- (i) *The subgraph $G_A(\mathcal{A}')$ of the adjacent graph is a connected planar graph.*
- (ii) *For every $k \in \mathbb{N}$, the set $\mathcal{D}^k$ induces a connected subgraph in $G_A(\mathcal{A}')$.*
- (iii) *$G_A(\mathcal{A}')$ has an admissible draw $\pi : G_A(\mathcal{A}') \to \mathbb{R}^2$ such that the derived graph of $G_A(\mathcal{A}')$ is exactly the neighbor graph G_N.*

Remark 3.3.41. Condition (iii) says that two tiles $\gamma_1(\mathcal{T}), \gamma_2(\mathcal{T})$ are neighbors if and only if the vertices $\pi(\gamma_1), \pi(\gamma_2)$ lie on the boundary of a single face of the drawing $\pi(G_A(\mathcal{A}'))$.

The proof is omitted since it runs along the same lines as for Theorem 3.3.22 (note that the necessity part is simply proved by taking $\mathcal{A}' = \mathcal{A}$ and applying the quoted theorem).

We apply Proposition 3.3.40 in order to reprove Proposition 3.3.28 and to prove its extension to $p2$-crystiles, which is the content of Theorem 3.3.29. As we noticed in Remark 3.3.30, if $\mathcal{T}$ is disk-like, the sets $\mathcal{A}$ are given in Grünbaum and Shephard's classification. The main difficulty lies in the proof of Item (ii) of Proposition 3.3.40, *i.e.*, the $\mathcal{A}'$-connectivity of the iterates $\mathcal{D}^k$ when $\mathcal{D}$ is assumed to be $\mathcal{A}'$-connected. This part is the purpose of the two following lemmata.

We use the notations of Proposition 3.3.40.

Lemma 3.3.42. *Suppose that the collections $\mathcal{D} \cup \mathcal{D}_\gamma$ are $\mathcal{A}'$-connected for every $\gamma \in \mathcal{A}'$. Then so also is $\mathcal{D}^k$ for all $k \in \mathbb{N}$ (see Remark 3.1.5 for the definition of $\mathcal{D}_\gamma$).*

Proof. We prove that $\mathcal{D}^2$ is $\mathcal{A}'$-connected if $\mathcal{D} = \mathcal{D}^1$ is, the result then follows by induction on k.

First note that if a set $M \subset \Gamma$ is $\mathcal{A}'$-connected, then so is γM for all $\gamma \in \Gamma$. Let $d_1, d_2 \in \Gamma$ with $d_1^{-1} d_2 \in \mathcal{A}'$. Taking $M = \mathcal{D} \cup \mathcal{D}_{d_1^{-1} d_2}$ and $\gamma = g d_1 g^{-1}$, we see that $\mathcal{D}_{d_1} \cup \mathcal{D}_{d_2}$ is $\mathcal{A}'$-connected.
Write

$$\mathcal{D}^2 = \bigcup_{\gamma \in \mathcal{D}^1} \mathcal{D}_\gamma,$$

and choose $\gamma \in \mathcal{D}^1$ with $\gamma \neq \mathrm{id}$. By the $\mathcal{A}'$-connectedness of $\mathcal{D}^1$, there is a chain of elements $\gamma_1, \ldots, \gamma_n$ in $\mathcal{D}^1$ from $\gamma_1 = \mathrm{id}$ to $\gamma_n = \gamma$ such that $\gamma_i^{-1} \gamma_{i+1} \in \mathcal{A}'$. Thus $\mathcal{D}_{\gamma_1} \cup \ldots \cup \mathcal{D}_{\gamma_n} \subset \mathcal{D}^2$ is

$\mathcal{A}'$-connected. Doing this for each $\gamma \in \mathcal{D}^1 \setminus \{\mathrm{id}\}$, we obtain that $\mathcal{D}^2$ is $\mathcal{A}'$-connected.

Writing $\mathcal{D}^{k+1} = \bigcup_{\gamma \in \mathcal{D}^k} \mathcal{D}_\gamma$ and assuming that $\mathcal{D}^k$ is $\mathcal{A}'$-connected, one can show similarly that so is $\mathcal{D}^{k+1}$ too. □

Lemma 3.3.43. *Suppose the crystile $\mathcal{T}$ has the neighbor set $\mathcal{S}$ and that its set of digits $\mathcal{D}$ is $\mathcal{A}'$-connected, where the pairs $(\mathcal{S}, \mathcal{A}')$ are read off from the items Proposition 3.3.28 (2) and Theorem 3.3.29 (2)(3)(4). Then the collections $\mathcal{D} \cup \mathcal{D}_\gamma$ are $\mathcal{A}'$-connected for every $\gamma \in \mathcal{A}'$.*

Proof. We first state some properties valid for all the considered pairs $(\mathcal{S}, \mathcal{A}')$, and then give separate proofs.

Note that since $\mathcal{D}$ is a complete set of coset representatives of $\Gamma / g\Gamma g^{-1}$, we have

- $\mathcal{D}_\gamma \cap \mathcal{D}'_\gamma = \emptyset$ for $\gamma \neq \gamma'$, and
- $\forall \gamma \in \Gamma$, $\exists! \gamma' \in \Gamma$ such that $\gamma \in \mathcal{D}_{\gamma'}$.

For each constellation $(\mathcal{S}, \mathcal{A}')$, we consider a drawing π associated to $G_A(\mathcal{A}')$. In the sense of Definition 3.3.17, and by assumption on the neighbor set $\mathcal{S}$, a picture of the neighbor graph G_N is obtained by adding all the diagonal line segments in each of the non-gasket-like simple loops in Figures 3.20, 3.22, 3.23, 3.24 (in the figures, we write γ for $\pi(\gamma)$). This picture then corresponds to an extension π_1 of π and was already represented in Figures 3.16 to 3.19. Clearly, the degree of G_N is then $s := \#\mathcal{S}$. Moreover, for each connected subgraph of G_N with vertex set $\mathcal{D}'$, finite or infinite, the collection of vertices $\bigcup_{d \in \mathcal{D}'} \mathcal{D}_d$ induces a connected subgraph in G_N. We will use this fact at the end of the proof. Remember that "induces" means that we connect the vertices of $\mathcal{D}$ via all the available edges in G_N (so even if $\mathcal{D}$ is $\mathcal{A}'$-connected, crossing diagonals may appear in the picture of the subgraph of G_N induced by $\mathcal{D}$).

One can easily see that this picture has the following properties.

(*i*) Two lines $\pi_1(x_1x_2)$ and $\pi_1(y_1y_2)$ intersect if and only if they have a common vertex or they are the two diagonal line segments in the same face of $\pi(G_A)$.

(*ii*) G_N is s-connected, in the sense that for any $\mathcal{U} \subset \Gamma$ which has less than s elements, the subgraph induced by $\Gamma \setminus \mathcal{U}$ is connected.

(*iii*) Suppose $L = (V_1, E_1)$ is an arbitrary connected subgraph of $G_A(\mathcal{A}')$ with finite vertex set V_1. If each edge $xy \in E_1$ satisfies $x^{-1}y \in \mathcal{A}'$ and if $\mathbb{R}^2 \setminus \pi(L)$ has a bounded component intersecting $\pi(G_A(\mathcal{A}'))$ containing a point $\pi(\gamma)$ for some $\gamma \in \Gamma$, then $\Gamma \setminus V_1$ induces a disconnected subgraph in G_N, which has a component of finite vertex set containing γ. We can see that the image $\pi(L)$ of L must contain a loop, so we will in the sequel refer to this as *Loop Property*.

We now distinguish the constellations.

Lattice-8 neighbor-case. Let us consider first the pair $(\mathcal{S}, \mathcal{A}')$ of Proposition 3.3.28 (2) and suppose that $\mathcal{D} \cup \mathcal{D}_a$ is not $\{a^{\pm 1}, b^{\pm 1}\}$-connected. Since $g(T) = \bigcup_{d \in \mathcal{D}} d(T)$ and $ga(T) = \bigcup_{d' \in \mathcal{D}_a} d'(T)$ intersect each other, we can choose some $\delta \in \mathcal{D}$ and $\delta' \in \mathcal{D}_a$ with $\delta(T) \cap \delta'(T) \neq \emptyset$. Then, we must have $\delta^{-1}\delta' \in \{(ab)^{\pm 1}, \left(ab^{-1}\right)^{\pm 1}\} = \mathcal{S} \setminus \mathcal{A}'$. We may assume that $\delta = \mathrm{id}, \delta' = ab$. See Figure 3.20 for relative positions of id and ab. Let $\alpha, \beta \in \Gamma$ be the uniquely determined elements with $a \in \mathcal{D}_\alpha$, $b \in \mathcal{D}_\beta$. Because $\mathcal{D} \cup \mathcal{D}_a$ is not $\{a^{\pm 1}, b^{\pm 1}\}$-connected, α and β are both distinct from id and a.

Then, we can find a vertex $c \in \Gamma \setminus \{\mathrm{id}, a, \alpha, \beta\}$ such that $c(T) \cap T \neq \emptyset$ and $c(T) \cap a(T) \neq \emptyset$. We can see on Figure 3.20 that c must belong to $\{b, ab, b^{-1}, ab^{-1}\}$.

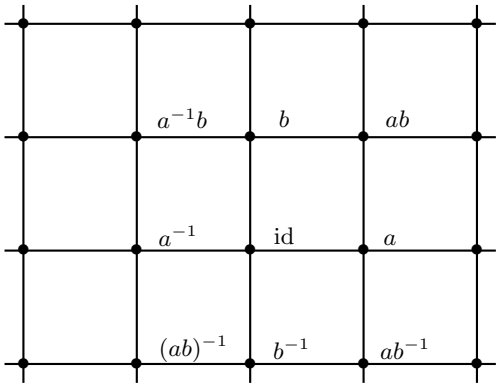

Figure 3.20: The graph $G_A(\mathcal{A}')$ in the lattice-8 neighbor-case.

Now, we can choose

$$d \in \mathcal{D},\ d_1, d_2 \in \mathcal{D}_c,\ d_3 \in \mathcal{D}_a$$

such that

$$d(T) \cap d_1(T) \neq \emptyset,\ d_2(T) \cap d_3(T) \neq \emptyset.$$

Then, $\{d^{-1}d_1, d_2^{-1}d_3\} \subset \{a^{\pm 1}, b^{\pm 1}, (ab)^{\pm 1}, \left(ab^{-1}\right)^{\pm 1}\}$. By $\{a^{\pm 1}, b^{\pm 1}\}$-connectivity of $\mathcal{D}_\gamma$ for every $\gamma \in \Gamma$, consider the three connected pieces $H_{\mathrm{id}}, H_a, H_c$ in the picture of G_N joining all the vertices $\mathcal{D}, \mathcal{D}_a, \mathcal{D}_c$ respectively and whose lines $\pi(xy)$ are defined for vertices $x, y \in \mathcal{D}$ (or $\mathcal{D}_a$, or $\mathcal{D}_c$) whenever $xy^{-1} \in \{a^{\pm 1}, b^{\pm 1}\}$. We can find three disjoint simple paths $P \subset H_{\mathrm{id}}$, $P_a \subset H_a$, and $P_c \subset H_c$ such that

- the two end points of P are $\pi(d)$ and $\pi(\mathrm{id})$,
- the two end points of P_c are $\pi(d_1)$ and $\pi(d_2)$,
- the two end points of P_a are $\pi(d_3)$ and $\pi(ab)$.

Note that $\pi(a)$ and $\pi(b)$ do not lie on these paths.

Therefore, the union J of $P \cup P_a \cup P_c$ with the three line segments $\pi_1(dd_1), \pi_1(d_2d_3), \pi_1(\mathrm{id}(ab))$ is a simple closed curve. Since the diagonal line segments $\pi_1(ab)$ and $\pi_1(\mathrm{id}(ab))$ intersect each other at a single point, the two points $\pi(a), \pi(b)$ are separated by J.

Since $\pi(a)$ and $\pi(b)$ (or equivalently, $\pi(\mathcal{D}_\alpha)$ and $\pi(\mathcal{D}_\beta)$) are separated by the loop J, we may assume that $\pi(a)$ is in the interior of J, thus the picture of the subgraph induced by $\mathcal{D}_\alpha$ is enclosed in the interior of J, according to the picture of G_N.

Note that $\pi_1(dd_1), \pi_1(d_2d_3)$ could be either diagonal, vertical or horizontal line segments (see Figure 3.21).

We discuss the possible three cases separately as follows.

Case 1 Suppose that $\pi_1(dd_1), \pi_1(d_2d_3)$ are both vertical or horizontal, *i.e.*, $\mathcal{D} \cup \mathcal{D}_c$ and $\mathcal{D}_c \cup \mathcal{D}_a$ are $\mathcal{A}'$-connected. Then the union J_1 of $P \cup P_a \cup P_c$ with the vertical or horizontal line segments $\pi_1(dd_1), \pi_1(d_2d_3), \pi_1(b(\mathrm{id})), \pi_1(b(ab))$ satisfies the condition in the "Loop Property". Then we can claim that $\Gamma \backslash (\mathcal{D} \cup \mathcal{D}_a \cup \mathcal{D}_c \cup \mathcal{D}_\beta)$ induces a disconnected subgraph in G_N. Otherwise, there would be a simple path P disjoint from all the π_1-images of the vertices of $\mathcal{V} = \mathcal{D} \cup \mathcal{D}_a \cup \mathcal{D}_c \cup \mathcal{D}_\beta$ which connects the vertex $\pi_1(a)$ to a vertex $\pi_1(\eta)$ in the exterior of J. We may assume without loss of generality that all the vertices $\pi_1(u)$ on the path P other than

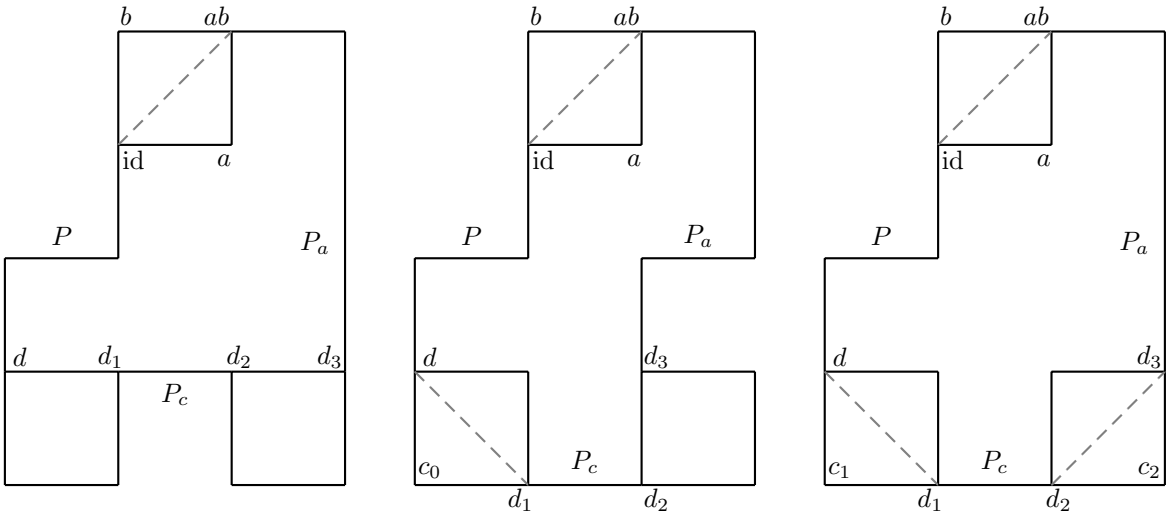

Case 1. Case 2. Case 3.

Figure 3.21: Lemma 3.3.43. Lattice-8 neighbor-case.

$\pi_1(\eta)$ belong to the interior of J. Then $\gamma(T) \cap \eta(T) \neq \emptyset$ for some $\pi_1(\gamma) \neq \pi_1(\eta)$ on the path P, where $\pi_1(\gamma)$ lies in the interior of J. This is a contradiction to the "Loop Property".

Case 2 Suppose that one of $\pi_1(dd_1), \pi_1(d_2d_3)$ is diagonal and the other is vertical or horizontal, say

$$dd_1^{-1} \in \left\{(ab)^{\pm 1}, \left(ab^{-1}\right)^{\pm 1}\right\}.$$

This means $\mathcal{D} \cup \mathcal{D}_c$ is not $\mathcal{A}'$-connected but $\mathcal{D}_c \cup \mathcal{D}_a$ is. We can choose $\pi_1(c_0)$ on J or in the exterior of J such that $d^{-1}c_0, c_0^{-1}d_1 \in \{a^{\pm 1}, b^{\pm 1}\}$. Then, the union J_2 of $P \cup P_a \cup P_c$ with the vertical or horizontal line segments $\pi_1(dc_0), \pi_1(c_0d_1), \pi_1(d_2d_3), \pi_1(b(\mathrm{id})), \pi_1(b(ab))$ satisfies the condition in the "Loop Property". By the same argument used in Case 1, we can infer that

$$\Gamma \setminus (\mathcal{D} \cup \mathcal{D}_\gamma \cup \mathcal{D}_a \cup \mathcal{D}_c \cup \mathcal{D}_\beta)$$

induces a disconnected subgraph in G_N, where $\gamma \in \Gamma$ is the unique element with $c_0 \in \mathcal{D}_\gamma$.

Case 3 Suppose that $\pi_1(dd_1), \pi_1(d_2d_3)$ are both diagonal line segments, *i.e.*, $\mathcal{D} \cup \mathcal{D}_c$ and $\mathcal{D}_c \cup \mathcal{D}_a$ are not $\mathcal{A}'$-connected. Then we can find $\pi_1(c_1), \pi_1(c_2)$ in the exterior of J according to the drawing of G_N such that

$$\{d^{-1}c_1, c_1^{-1}d_1\} \subset \{a^{\pm 1}, b^{\pm 1}\},\ \{d_2^{-1}c_2, c_2^{-1}d_3\} \subset \{a^{\pm 1}, b^{\pm 1}\}.$$

Then, the union J_3 of $P \cup P_a \cup P_c$ with the vertical or horizontal line segments

$$\pi_1(dc_1), \pi_1(c_1d_1), \pi_1(d_2c_2), \pi_1(c_2d_3), \pi_1(b(\mathrm{id})), \pi_1(b(ab))$$

satisfies the condition in the "Loop Property". Let γ_1, γ_2 be the two uniquely determined elements of Γ with

$$c_1 \in \mathcal{D}_{\gamma_1},\ c_2 \in \mathcal{D}_{\gamma_2}.$$

Put

$$\mathcal{V} := \mathcal{D} \cup \mathcal{D}_a \cup \mathcal{D}_c \cup \mathcal{D}_\beta \cup \mathcal{D}_{\gamma_1} \cup \mathcal{D}_{\gamma_2}.$$

Then $\Gamma \setminus \mathcal{V}$ induces a disconnected subgraph in G_N. By the same argument as the one used in Case 1, we can infer that $\Gamma \setminus (\mathcal{D} \cup \mathcal{D}_a \cup \mathcal{D}_c \cup \mathcal{D}_\beta)$ induces a disconnected subgraph in G_N.

In each of the above three cases, we have some $\mathcal{V}$, union of sets $\mathcal{D}_\gamma$ with γ running through a collection of at most six elements of Γ, such that the infinite collection $\Gamma \setminus \mathcal{V}$ induces a disconnected subgraph in G_N. This contradicts the 8-connectivity of G_N, as mentioned at the beginning of the proof.

Hence $\mathcal{D} \cup \mathcal{D}_a$ is $\{a^{\pm 1}, b^{\pm 1}\}$-connected. The cases of $\mathcal{D} \cup \mathcal{D}_{a^{-1}}, \mathcal{D} \cup \mathcal{D}_b, \mathcal{D} \cup \mathcal{D}_{b^{-1}}$ are treated similarly.

p2-7 neighbor-case. Secondly we deal with the constellation $(\mathcal{S}, \mathcal{A}')$ of Theorem 3.3.29 (2).

We want to show that $\mathcal{D} \cup \mathcal{D}_\gamma$ induces a connected subgraph in $G_A(\mathcal{A}')$ for each $\gamma \in \mathcal{A}' = \{b, b^{-1}, c, bc, a^{-1}c\}$ (see Figure 3.22).

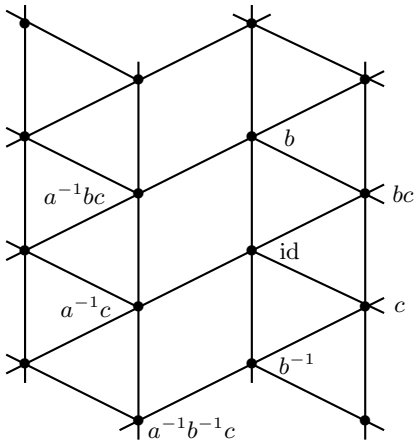

Figure 3.22: The graph $G_A(\mathcal{A}')$ in the p2-7 neighbor-case.

If $\gamma = b^{\pm 1}$ or $\gamma = a^{-1}c$, this can be obtained in a similar way as for the preceding lattice 8-neighbor case; this is due to the fact that id and γ have "enough" common neighbors for these values of γ, namely three. Let $\gamma = c$, which has only two common neighbors with id (the same kind of argument holds for $\gamma = bc$), and suppose that $\mathcal{D} \cup \mathcal{D}_c$ is not $\mathcal{A}'$-connected. Since $T \cap c(T) \neq \emptyset$, we have $g(T) \cap gc(T) \neq \emptyset$, thus there exist $d \in \mathcal{D}$ and $d' \in \mathcal{D}_c$ such that $d(T) \cap d'(T) \neq \emptyset$. In our assumption, $d^{-1}d' \in \mathcal{S} \setminus \mathcal{A}'$. W.l.o.g., either $\{d, d_1\} = \{\mathrm{id}, a^{-1}bc\}$ or $\{d, d_1\} = \{\mathrm{id}, a^{-1}b^{-1}c\}$.

We assume that $d = \mathrm{id},\ d_1 = a^{-1}bc$ (the treatment of $d_1 = a^{-1}b^{-1}c$ runs likewise). Let $\eta \in \Gamma$ be the uniquely determined element with $b \in \mathcal{D}_\eta$. Then $\eta \notin \{\mathrm{id}, c\}$, otherwise $\mathcal{D} \cup \mathcal{D}_c$ would be $\mathcal{A}'$-connected in G_A. Since $b \in \mathcal{D}_\eta$, both intersections $g\eta(T) \cap g(T)$ and $g\eta(T) \cap gc(T)$ are nonempty, thus taking their images by g^{-1}, we see that η must be a common neighbor of id and c, *i.e.*, $\eta \in \{bc, b^{-1}\}$. Similarly, let η' with $a^{-1}c \in \mathcal{D}_\eta$, then $\eta' \in \{bc, b^{-1}\}$.

We claim that $\eta = \eta'$. Indeed, if $\eta \neq \eta'$, by assumption on $\mathcal{S}$ the intersection $\eta(T) \cap \eta'(T)$ must be empty, thus so has to be its blow-up by g. But this is not the case, because $b \in \mathcal{D}_\eta$, $a^{-1}c \in \mathcal{D}_{\eta'}$, and $b(T) \cap a^{-1}c(T) \neq \emptyset$. Consequently, $\eta = \eta'$.

$\mathcal{D}_\eta$ being $\mathcal{A}'$-connected, there is a simple path P in $G_A(\mathcal{A}')$ from $\pi(b)$ to $\pi(a^{-1}c)$ such that all vertices in P belong to $\pi(\mathcal{D}_\eta)$. Since id, $a^{-1}bc \notin \mathcal{D}_\eta$, either P', the union of P with the broken line from $\pi(b)$ to $\pi(a^{-1}c)$ via $\pi(\mathrm{id})$, encloses $\pi(a^{-1}bc)$, or P'', the union of P with the broken line from $\pi(b)$ to $\pi(a^{-1}c)$ via $\pi(a^{-1}bc)$, encloses $\pi(\mathrm{id})$. Thus, by the "Loop Property", either $\Gamma \setminus (\mathcal{D}_\eta \cup \mathcal{D})$ or $\Gamma \setminus (\mathcal{D}_\eta \cup \mathcal{D}_c)$ is disconnected in G_N. This contradicts the 7-connectivity of G_N. Hence $\mathcal{D} \cup \mathcal{D}_c$ is also $\mathcal{A}'$-connected for every $\gamma \in \mathcal{A}'$.

p2-8 neighbor-case. The constellation of Theorem 3.3.29 (3) is treated as in the lattice case (see Figure 3.23).

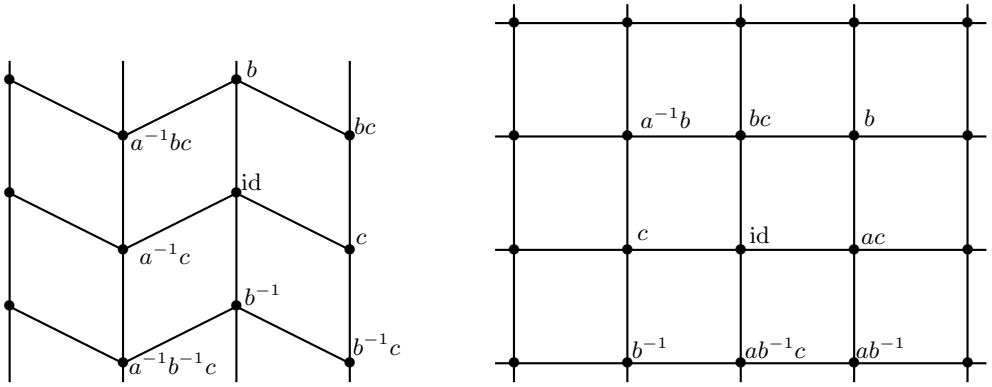

Figure 3.23: The graph $G_A(\mathcal{A}')$ in the $p2$-8 neighbor-case.

p2-12 neighbor-case. We eventually deal with the constellation $(S, \mathcal{A}')$ of Theorem 3.3.29 (4).

Assume that $\mathcal{D} \cup \mathcal{D}_\alpha$ is not $\mathcal{A}'$-connected for some $\alpha \in \mathcal{A}'$. As $\mathcal{D}$ is $\mathcal{S}$-connected, $\mathcal{D} \cup \mathcal{D}_\alpha$ must be $\mathcal{S}$-connected. Thus, there exist some $d_1 \in \mathcal{D}$ and $a_2 \in \mathcal{D}_\alpha$ with $d_1^{-1}a_2 \in (\mathcal{S} \setminus \mathcal{A}')$. That is to say, in the drawing π of $G_A(\mathcal{A}')$, $\pi(d_1)$ and $\pi(a_2)$ lie on the boundary of the same face F_1, but not on a single side of F_1. See Figure 3.25 for the three possible relative positions of d_1 and a_2. Moreover, if $d' \in \mathcal{D}$ and $a' \in \mathcal{D}_\alpha$ are neighbors, we must have $d'^{-1}a' \in (\mathcal{S} \setminus \mathcal{A}')$, thus $\pi(d')$ and $\pi(a')$ lie on boundary of the same face of $\pi\left(G_A(\mathcal{A}')\right)$ and not on a single side.

Clearly, $\partial F_1 \setminus \{\pi(d_1), \pi(a_2)\}$ is the union of two open polygonal arcs, each of which contains at least one element of $\pi(G)$.

Since $\#\left(\partial F_1 \cap \pi(G)\right) = 6$, while α and the identity id have exactly 8 common neighbors, we can choose a common neighbor β of α and id with $\mathcal{D}_\beta \cap \pi^{-1}\left(F_1\right) = \emptyset$.

Now, we can choose $d_2 \in \mathcal{D}$, $b_1, b_2 \in \mathcal{D}_\beta$, and $a_1 \in \mathcal{D}_\alpha$ with $\{b_1^{-1}d_2, a_1^{-1}b_2\} \subset \mathcal{S}$. Moreover let F_2, F_3 be the faces of $\pi\left(G_A(\mathcal{A}')\right)$ containing $\{\pi(b_1), \pi(d_2)\}$ and $\{\pi(b_2), \pi(a_1)\}$, respectively. As $\mathcal{D}_\beta \cap \pi^{-1}\left(F_1\right) = \emptyset$, $F_1 \notin \{F_2, F_3\}$.

By $\mathcal{A}'$-connectedness of $\mathcal{D}$, we can find three simple paths P, P_α, P_β in drawings of the subgraphs of $G_A(\mathcal{A}')$ respectively generated by $\mathcal{D}, \mathcal{D}_\alpha, \mathcal{D}_\beta$ such that

- $\pi(d_1), \pi(d_2)$ are the two ends of P,
- $\pi(a_1), \pi(a_2)$ are the two ends of P_α, and
- $\pi(b_1), \pi(b_2)$ are the two ends of P_β.

Note that the above three paths could be degenerate ones, like the case $d_1 = d_2$ thus $P = \{\pi(d_1)\}$.

Claim 1. $F_2 \neq F_3$. Otherwise, we would have $a_1^{-1}d_2 \in \mathcal{S} \setminus \mathcal{A}'$, and $\partial F_2 \setminus \{a_1, d_2\}$ consists of two open polygonal arcs each of which contains at least one element of $\pi(G) \cap \partial F_2$. (Similar to the case of F_1.) Then the union J_0 of $P \cup P_\alpha$ with the two line segments $\pi_1(a_2 d_1) \subset F_1$ and $\pi_1(d_2 a_1) \subset F_2$ is a polygonal simple closed curve in the plane, whose interior $\mathrm{Interior}(J_0)$ contains

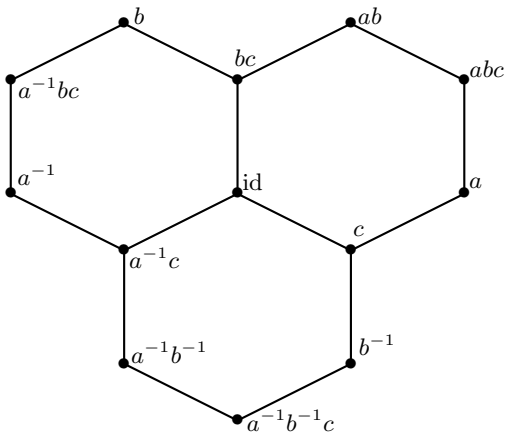

Figure 3.24: The graph $G_A(\mathcal{A}')$ in the p2-12 neighbor-case.

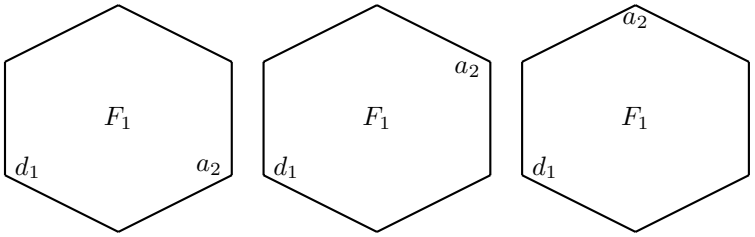

Figure 3.25: Lemma 3.3.43. p2-12 neighbor-case. Relative positions of d_1 and a_2 on F_1.

at least two elements, $\pi(\gamma_1) \in \pi(G) \cap F_1$ and $\pi(\gamma_2) \in \pi(G) \cap F_2$.

As $\left(F_i \setminus \overline{\text{Interior}(J_0)}\right) \cap \pi(G)$ has at most three elements for $i = 1, 2$, we may denote by $e_1, e_2, \ldots, e_k$ ($k \leq 6$) the elements of G with $\pi(e_i) \in (F_1 \cup F_2) \setminus \overline{\text{Interior}(J_0)}$, and choose ε_i ($1 \leq i \leq k$) of G with $e_i \in \mathcal{D}_{\varepsilon_i}$.

For $i = 1, 2$, let $P_i \subset \partial F_i$ be the open subarc which is contained in J_0's exterior $\text{Exterior}(J_0) = \mathbb{R}^2 \setminus \overline{\text{Interior}(J_0)}$. Now

$$P \cup P_\alpha \cup P_1 \cup P_2$$

satisfies the conditions of the "Loop Property". This means that

$$G \setminus (\{\text{id}, \alpha\} \cup \{\varepsilon_1, \varepsilon_2, \ldots, \varepsilon_k\})$$

induces a disconnected subgraph in G_N, a contradiction to the 12-connectivity of G_N. This proves Claim 1.

Let J be the union of $P \cup P_\alpha \cup P_\beta$ with the line segments $\pi_1(a_2 d_1)$, $\pi_1(d_2 b_1)$ and $\pi_1(b_2 a_1)$. Then, J is a polygonal simple closed curve in the plane with $\pi(\gamma_1) \in \text{Interior}(J)$.

Claim 2. $\left\{b_1^{-1} d_2, a_1^{-1} b_2\right\} \subset \mathcal{S} \setminus \mathcal{A}'$. Otherwise, say, $b_1^{-1} d_2 \in \mathcal{A}'$. Similar as for Claim 1, there are $k \leq 6$ elements $e_1, e_2, \ldots, e_k \in G$ with $\pi(e_i)$ lying in $(F_1 \cup F_3) \setminus \overline{\text{Interior}(J)}$. We can see that

$$G \setminus (\{\text{id}, \alpha, \beta\} \cup \{\varepsilon_1, \varepsilon_2, \ldots, \varepsilon_k\})$$

induces a disconnected subgraph in G_N, which has a component with finite vertex set containing γ_1. This again contradicts the 12-connectivity of G_N.

Claim 2 immediately indicates that $\text{Interior}(J) \cap F_i \cap \pi(G)$ contains at least one element for each $1 \leq i \leq 3$. Actually, we may further show that $\text{Interior}(J) \cap F_i \cap \pi(G)$ contains exactly one element for each $1 \leq i \leq 3$. Otherwise, there would be $k \leq 8$ elements $e_1, e_2, \ldots, e_k$ with $\pi(e_i)$ lying in $(F_1 \cup F_2 \cup F_3) \setminus \overline{\text{Interior}(J)}$. If ε_i $(1 \leq i \leq k)$ are elements of G with $e_i \in \mathcal{D}_{\varepsilon_i}$, where $\varepsilon_i = \varepsilon_j$ is possible, the subgraph of G_N induced by

$$G \setminus (\{\text{id}, \alpha, \beta\} \cup \{\varepsilon_1, \varepsilon_2, \ldots, \varepsilon_k\})$$

has a component with finite vertex set containing γ_1. This is impossible by the 12-connectivity of G_N.

Recall that $\{\pi(\gamma_1)\} = \text{Interior}(J) \cap F_1 \cap \pi(G)$, we denote by γ_i $(i = 2, 3)$ the unique element of G with $\pi(\gamma_i)$ lying in $\text{Interior}(J) \cap F_i \cap \pi(G)$. Here, $\gamma_i = \gamma_j$ is possible.

Let $e_1, e_2, \ldots, e_9$ be the nine elements of G with $\pi(e_i)$ belonging to $(F_1 \cup F_2 \cup F_3) \setminus \overline{\text{Interior}(J)}$, and $\varepsilon_1, \varepsilon_2, \ldots, \varepsilon_9$ the corresponding elements of G with $e_i \in \mathcal{D}_{\varepsilon_i}$. Also, $\varepsilon_i = \varepsilon_j$ is possible here. W.l.o.g., we may assume that

$$\{\pi(e_1), \pi(e_2), \pi(e_3)\} \subset F_1, \quad \{\pi(e4), \pi(e_5), \pi(e_6)\} \subset F_2, \quad \{\pi(e_7), \pi(e_8), \pi(e_9)\} \subset F_3.$$

See Figure 3.26 for a graphical explanation of the relative positions of F_1, F_2, F_3.

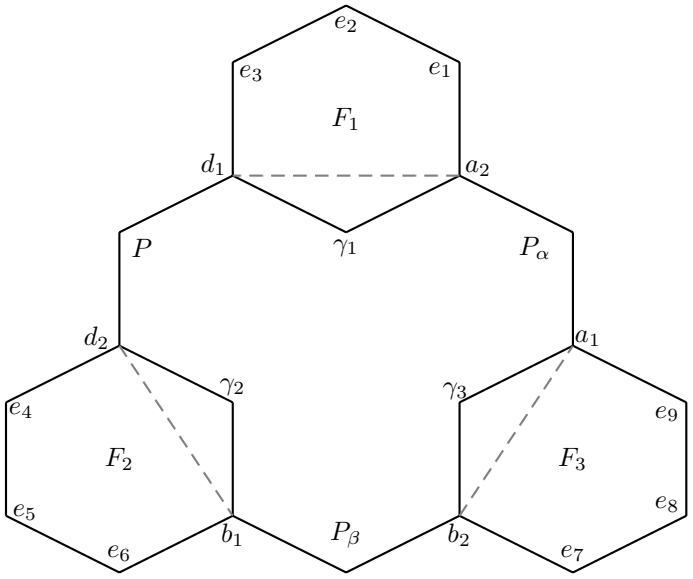

Figure 3.26: Lemma 3.3.43. p2-12 neighbor-case.

Claim 3. $\{\gamma_1, \gamma_2, \gamma_3\} \subset \mathcal{D}_\delta$ for a single $\delta \in \Gamma$. Otherwise, we may assume that $\gamma_2 \in \mathcal{D}_{\delta'}$ for some $\delta' \neq \delta$. Thus

$$G \setminus (\{\text{id}, \alpha, \beta, \delta'\} \cup \{\varepsilon_1, \varepsilon_2, \varepsilon_3, \varepsilon_7, \varepsilon_8, \varepsilon_9\})$$

would induce a disconnected subgraph in G_N, contradicting its 12-connectivity.

Claim 4. $\varepsilon_i \neq \varepsilon_j$ for $i \neq j$. Otherwise, assume for instance $\varepsilon_1 = \varepsilon_2$. Then $G \setminus \{\text{id}, \alpha, \beta, \varepsilon_2, \varepsilon_3, \ldots, \varepsilon_9\}$ would induce a disconnected subgraph G_N, which is again impossible by 12-connectivity of G_N.

Claim 5. $\{\delta, \alpha^{-1}\delta, \beta^{-1}\delta\} = \mathcal{A}'$. Otherwise, say, $\alpha^{-1}\delta \notin \mathcal{A}'$; then, α and δ would not belong to a single edge of $G_A(\mathcal{A}')$, thus α and δ would have exactly four common neighbors, see the Figure 3.26. This contradicts Claim 3 and Claim 4, which imply that α and δ have eight distinct common neighbors $\mathrm{id}, \beta, \varepsilon_1, \varepsilon_2, \varepsilon_3, \varepsilon_7, \varepsilon_8, \varepsilon_9$.

Conclusion. Claim 5 is impossible. Indeed, $\alpha \in \mathcal{A}'$ by the beginning assumption, and $\delta \in \mathcal{A}'$ by Claim 5. But $\mathcal{A}' = \{c, a^{-1}c, bc\}$, hence α and δ are π-rotations. Thus $\alpha^{-1}\delta$ is a translation and can not belong to $\mathcal{A}'$, a contradiction to Claim 5. This ends our proof. □

We are now ready to prove Proposition 3.3.28 and Theorem 3.3.29, using Proposition 3.3.40.

The lattice case.

Proof of Proposition 3.3.28.

(**1**) **6 neighbor-case.** Assume that $\mathcal{T}$ has exactly six neighbors. By Propositions 3.3.35 and 3.3.39, the neighbor set is $\mathcal{S} = \{b, b^{-1}, a, a^{-1}, a^{-1}b, ab^{-1}\}$ for independent translations a, b and only consists of adjacent neighbors, *i.e.*, $\mathcal{S} = \mathcal{A}$. The graph G_A has a drawing like in Figure 3.27. The equivalence now follows from Proposition 3.3.40 by taking $\mathcal{A}' = \mathcal{A}$ (in this case, Condition (ii) of Proposition 3.3.40 reduces to (ii'): $\mathcal{D}$ is $\mathcal{S}$-connected).

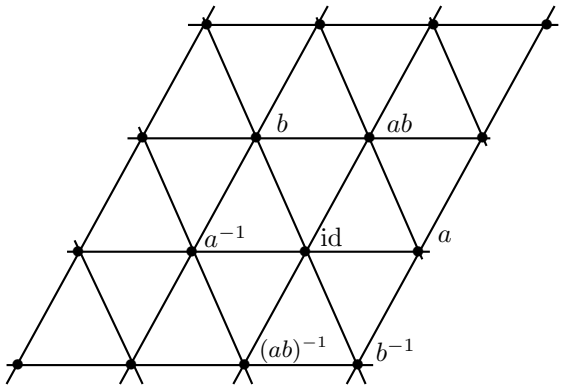

Figure 3.27: The graph G_A in the lattice-6 neighbor-case.

(**2**) **8 neighbor-case.** Assume that $\mathcal{T}$ has exactly the neighbor set

$$\mathcal{S} = \{a^{\pm 1}, b^{\pm 1}, (ab)^{\pm 1}, (b^{-1}a)^{\pm 1}\}.$$

By Proposition 3.3.39, $\mathcal{S}$ contains $\mathcal{A}' := \{a^{\pm 1}, b^{\pm 1}\}$ as adjacent neighbors. The corresponding graph $G_A(\mathcal{A}')$ has the drawing depicted in Figure 3.20.
If $\mathcal{T}$ is disk-like, we have $\mathcal{A}' = \mathcal{A}$ and the result follows from Condition (ii) of Proposition 3.3.40 ($\mathcal{D}^1 = \mathcal{D}$). On the other side, suppose that $\mathcal{D}$ is $\mathcal{A}'$-connected. Then the drawing of $G_A(\mathcal{A}')$ in Figure 3.20 satisfies Conditions (i) and (iii) of Proposition 3.3.40. The verification of Condition (ii) is the content of Lemmata 3.3.42 and 3.3.43. By Proposition 3.3.40, $\mathcal{T}$ is disk-like. □

The $p2$-case.

Proof of Theorem 3.3.29.

We note that if $\mathcal{T}$ is disk-like or if $\mathcal{D}$ is $\mathcal{F}$-connected (for some $\mathcal{F} \subset \mathcal{S}$, and hence for $\mathcal{F} = \mathcal{S}$), then $\mathcal{T}$ is itself connected (see Remark 3.3.27). Thus we can assume in this proof that the tile $\mathcal{T}$ is connected.

(**1**) **6 neighbor-case.** Assume that $\mathcal{T}$ has exactly six neighbors. By Propositions 3.3.37 and 3.3.15, the neighbor set $\mathcal{S}$ only consists of adjacent neighbors, *i.e.*, $\mathcal{S} = \mathcal{A}$. The graph G_A has a drawing like in Figure 3.28. The equivalence now follows from Proposition 3.3.40 by taking $\mathcal{A}' = \mathcal{A}$ (in this case, Condition (ii) of Proposition 3.3.40 again reduces to (ii'): $\mathcal{D}$ is $\mathcal{S}$-connected).

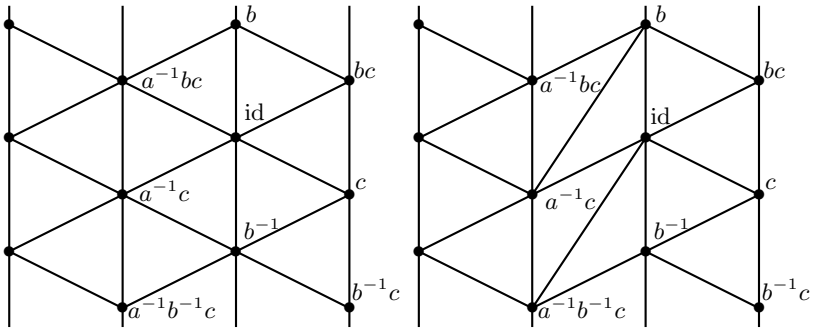

Figure 3.28: The graph G_A in the $p2$-6 neighbor-case.

(**2**) **7 neighbor-case.** Assume that $\mathcal{T}$ has exactly the neighbor set

$$\mathcal{S} = \{b^{\pm 1}, c, bc, a^{-1}c, a^{-1}bc, a^{-1}b^{-1}c\}.$$

By Proposition 3.3.15, $\mathcal{S}$ contains $\mathcal{A}' := \{b^{\pm 1}, c, bc, a^{-1}c\}$ as adjacent neighbors. The corresponding graph $G_A(\mathcal{A}')$ has the drawing depicted in Figure 3.22. If $\mathcal{T}$ is disk-like, we have $\mathcal{A}' = \mathcal{A}$ and the result follows from Condition (ii) of Proposition 3.3.40 ($\mathcal{D}^1 = \mathcal{D}$). On the other side, suppose that $\mathcal{D}$ is $\mathcal{A}'$-connected. Then the drawing of $G_A(\mathcal{A}')$ in Figure 3.22 satisfies Conditions (i) and (iii) of Proposition 3.3.40. Condition (ii) is the direct corollary of Lemmata 3.3.42 and 3.3.43. By Proposition 3.3.40, $\mathcal{T}$ is disk-like.

(**3**) **8 neighbor-case.** Assume that $\mathcal{T}$ has a neighbor set of the shape

$$\mathcal{S} = \{b^{\pm 1}, c, a^{-1}c, bc, b^{-1}c, a^{-1}bc, a^{-1}b^{-1}c\} \quad (\text{ resp. } \mathcal{S} = \{c, bc, ac, a^{-1}bc, b^{\pm 1}, (a^{-1}b)^{\pm 1}\}\ ).$$

By Proposition 3.3.15, the set $\mathcal{A}' := \{b^{\pm 1}, c, a^{-1}c\}$ (resp. $\mathcal{A}' := \{c, bc, ac, a^{-1}bc\}$) is a subset of the adjacent neighbor set $\mathcal{A}$. The corresponding graph $G_A(\mathcal{A}')$ has the drawing depicted in Figure 3.23. If $\mathcal{T}$ is disk-like, we have $\mathcal{A}' = \mathcal{A}$ and the result follows from Condition (ii) of Proposition 3.3.40 ($\mathcal{D}^1 = \mathcal{D}$). On the other side, suppose that $\mathcal{D}$ is $\mathcal{A}'$-connected. Then the drawing of $G_A(\mathcal{A}')$ in Figure 3.23 satisfies Conditions (i) and (iii) of Proposition 3.3.40. Condition (ii) is contained in Lemmata 3.3.42 and 3.3.43. By Proposition 3.3.40, $\mathcal{T}$ is disk-like.

(**4**) **12 neighbor-case.** Assume that $\mathcal{T}$ has twelve neighbors of the shape

$$\mathcal{S} = \{c, a^{-1}c, bc, abc, a^{-1}bc, a^{-1}b^{-1}c, a^{\pm 1}, b^{\pm 1}, (ab)^{\pm 1}\}.$$

Then $\mathcal{A}' := \{c, a^{-1}c, bc\}$ is a subset of the adjacent neighbor set $\mathcal{A}$ (Proposition 3.3.15). The corresponding graph $G_A(\mathcal{A}')$ has the drawing depicted in Figure 3.24. If $\mathcal{T}$ is disk-like, we have $\mathcal{A}' = \mathcal{A}$ and the result follows from Condition (ii) of Proposition 3.3.40 ($\mathcal{D}^1 = \mathcal{D}$). On the other side, suppose that $\mathcal{D}$ is $\mathcal{A}'$-connected. Then the drawing of $G_A(\mathcal{A}')$ in Figure 3.24 satisfies Conditions (i) and (iii) of Proposition 3.3.40. Condition (ii) follows from Lemmata 3.3.42 and 3.3.43. By Proposition 3.3.40, $\mathcal{T}$ is disk-like. □

3.3.8 Examples and counterexamples

The assumptions of Proposition 3.3.28 were shown in [7] to be minimal. This is also the case for our Theorem 3.3.29. As noticed in Remark 3.3.30.1, we listed all possible disk-like cases of $p2$-tiles. We illustrate the counterpart by considering examples of disk-like and non disk-like crystiles having from six to twelve neighbors.

In this section, the maps u, v, r are defined by $u(x, y) = (x + 1, y)$, $v(x, y) = (x, y + 1)$ and $r(x, y) = (-x, -y)$, as in Definition 2.2.10.

Examples of disk-like $p2$-crystiles

We are first interested in examples of disk-like $p2$-crystiles.

6 neighbor case. We consider the $p2$-crystile defined by the expanding mapping

$$g(x, y) = (x - 2y, x + 2y - 1)$$

and the digit set $\mathcal{D} = \{\mathrm{id}, r, ur, vr\}$. The crystile $\mathcal{T}$ is solution of the set equation

$$g(\mathcal{T}) = \mathcal{T} \cup r(\mathcal{T}) \cup ur(\mathcal{T}) \cup vr(\mathcal{T}).$$

With the methods developped in Section 3.2, we compute that the set of neighbors is

$$\mathcal{S} = \{u^{\pm 1}, r, ur, vr, uvr\}.$$

It has the first shape given in Proposition 3.3.37 (take $a = v^{-1}, b = u, c = r$). The tile $\mathcal{T}$ together with its neighbors is depicted in Figure 3.29. The digit set is $\mathcal{S}$-connected, as can be checked on the graph of the same figure. Thus by Theorem 3.3.29 (1), $\mathcal{T}$ is disk-like.

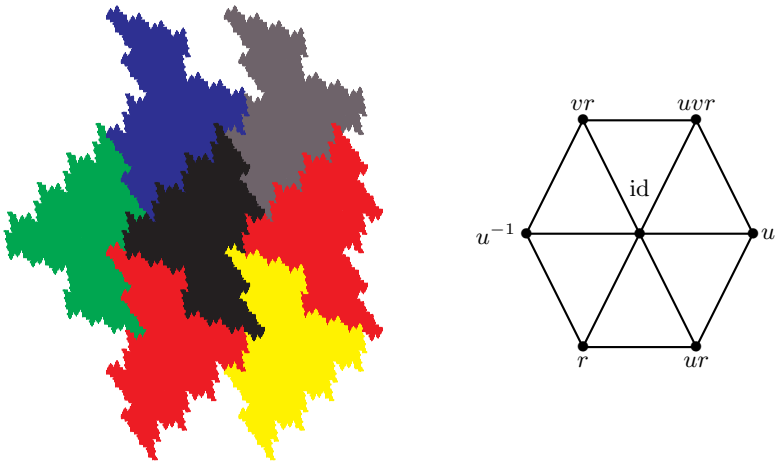

Figure 3.29: Disk-like $p2$-crystile with six neighbors (shape 1).

Taking now the expansion

$$g(x, y) = (x - y, 2x + 2y - \frac{1}{2}),$$

and the same digit set $\mathcal{D}$, we obtain another crystile $\mathcal{T}$ whose neighbor set is

$$\mathcal{S} = \{v^{\pm 1}, r, ur, vr, uv^{-1}r\}.$$

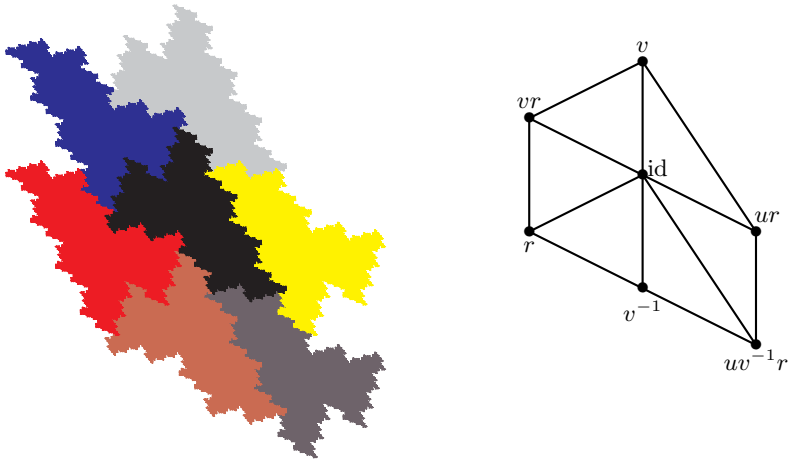

Figure 3.30: Disk-like $p2$-crystile with six neighbors (shape 2).

It has the second shape given in Proposition 3.3.37 (take $a = u, b = v^{-1}, c = ur$). The tile $\mathcal{T}$ together with its neighbors is depicted in Figure 3.30 and is disk-like by Theorem 3.3.29 (1).

7 neighbor case. We consider an example that Gelbrich [19] listed as "not convincing", since he could not decide from the figure if it is disk-like or not. The expansion g reads

$$g(x, y) = \left(-x + y - \frac{1}{2}, -2x - y\right),$$

the digit set is $\mathcal{D} = \{\mathrm{id}, v, r\}$, hence the crystile $\mathcal{T}$ is solution of the set equation

$$g(\mathcal{T}) = \mathcal{T} \cup v(\mathcal{T}) \cup r(\mathcal{T}).$$

With the methods developped in Section 3.2 we compute that the set of neighbors is

$$\mathcal{S} = \{v, v^{-1}, r, vr, u^{-1}r, u^{-1}vr, u^{-1}v^{-1}r\}.$$

The tile $\mathcal{T}$ and its neighbors are depicted in Figure 3.31. By Theorem 3.3.29 (2) (identify u, v, r with a, b, c respectively), $\mathcal{T}$ is disk-like.

8 neighbor case. A disk-like $p2$-crystile with eight neighbors of the first shape is obtained by considering the union of gray squares given in Figure 3.32. The expansion map reads $g(x, y) = (4x, 4y)$ and the sixteen digits are easily read off from the picture. Indeed, let $\mathcal{T}$ denote the union of gray squares of side length $1/4$ as in this picture. Then $g^{-1}(\mathcal{T}) = 1/4\,\mathcal{T}$ is a smaller copy of $\mathcal{T}$ entirely contained in the lower left square of side length $1/4$. One then recovers the whole tile $\mathcal{T}$ by rotating and translating this smaller copy in an obvious way; each of these transformations corresponds to a digit. Exactly $8 \times 2 = 16$ digits are needed.

Consider now the expansion $g(x, y) = (2x + 1/2, -x - 2y - \frac{1}{2})$, and the digit set $\mathcal{D} = \{\mathrm{id}, r, ur, vr\}$. The corresponding crystile $\mathcal{T}$ has the neighbor set

$$\mathcal{S} = \{r, ur, vr, uvr, u^{\pm 1}, v^{\pm 1}\}.$$

It has the second shape given in Theorem 3.3.29 (3) (take $a = uv, b = v, c = r$). The tile $\mathcal{T}$ together with its neighbors are depicted in Figure 3.33 and is disk-like by Theorem 3.3.29 (3).

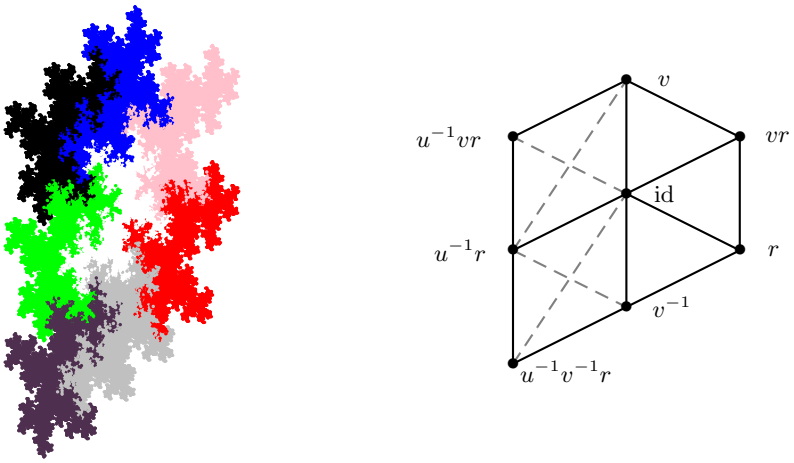

Figure 3.31: Disk-like $p2$-crystile with seven neighbors.

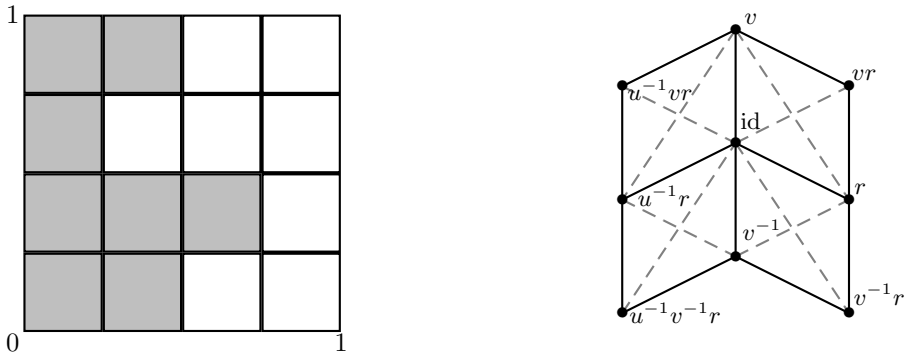

Figure 3.32: Disk-like $p2$-crystile (gray) with eight neighbors (shape 1).

12 neighbor case. Like a right angled isoceles triangle, the "stair case" crystile on Figure 3.34 gives rise to a $p2$-tiling where each tile has twelve neighbors.

Here, the expansion map is $g(x, y) = (3x, 2y)$ and the digit set $\mathcal{D} = \{\mathrm{id}, a_1, a_1^2, b_1, a_1b_1c_1, a_1^2b_1^2\}$, with $a_1(x, y) = (x - 2, y)$, $b_1(x, y) = (x, y + 1)$ and $c_1(x, y) = (-x, -y)$. This crystile is disk-like by Theorem 3.3.29 (4) (take $a = b_1^{-1}$, $b = a_1^{-1}b_1$, $c = a_1c_1$).

Examples of non disk-like p2-crystiles.

We are now moving to the non disk-like examples, varying the number of neighbors. Since we are interested in connected tiles, the case of six neighbors can be excluded (see the later comments in Section 3.4). Thus we start with a seven neighbor example.

7 neighbor case. Each tile $\mathcal{T}$ is the union of nine squares of side length 1/3 (gray on Figure 3.35). Using the expansion $g(x, y) = (6x, 6y)$, one sees that $g(\mathcal{T})$ is the union of 36 isometric copies of $\mathcal{T}$. It is Grünbaum's 36-$p2$-reptile. The tile has the seven neighbors indicated in Theorem 3.3.29 (2), but the digit set is not connected in the drawing of its adjacency graph.

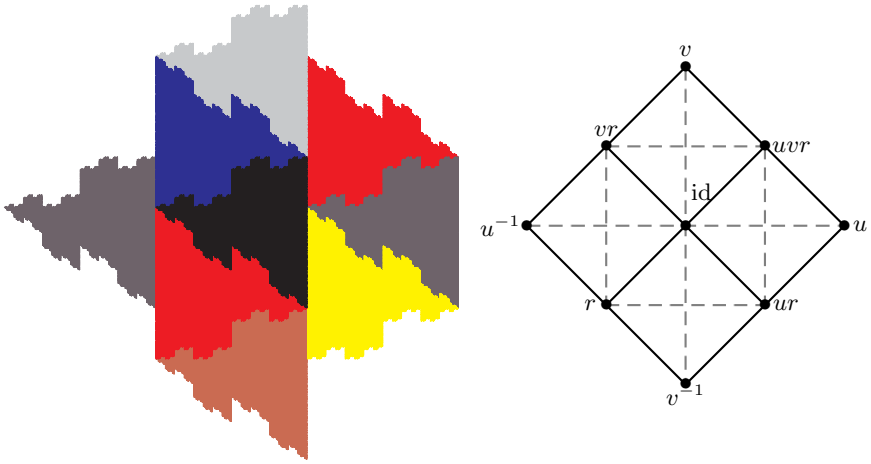

Figure 3.33: Disk-like $p2$-crystile with eight neighbors (shape 2).

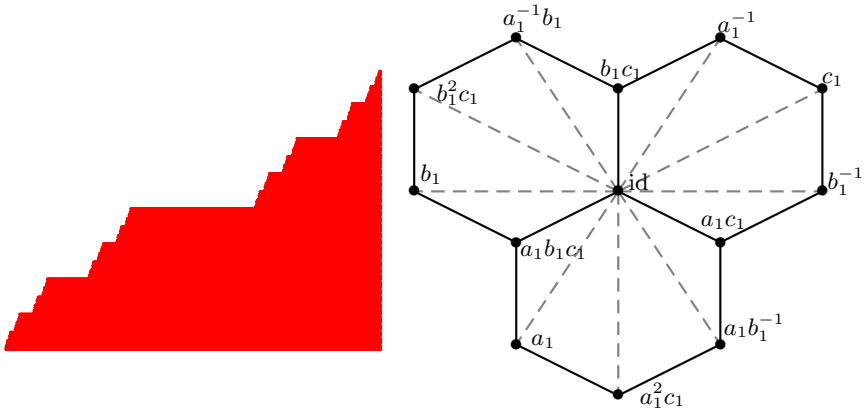

Figure 3.34: Disk-like $p2$-crystiles with twelve neighbors.

8 neighbor case. This example is depicted in Figure 3.36. It is a $p2$-crystile with 16 digits. It is obtained after an obvious modification of the digit set of the disk-like example of Figure 3.32; it has the same neighbor set.

9 neighbor case. Again, this tile is constructed from squares (see Figure 3.37). It has nine neighbors, among which seven are adjacent.

10 neighbor case. Let $g(x, y) = (-2x - 1/2, -x + 2y)$ be the expansion and the digit set $\mathcal{D} = \{\mathrm{id}, u, v, r\}$. The crystile $\mathcal{T}$ defined by

$$g(\mathcal{T}) = \mathcal{T} \cup u(\mathcal{T}) \cup v(\mathcal{T}) \cup r(\mathcal{T})$$

has the neighbor set

$$\mathcal{S} = \{u^{\pm 1}, v^{\pm 1}, (uv)^{\pm 1}, r, vr, u^{-1}r, u^{-1}v^{-1}r\}$$

(see Figure 3.38).

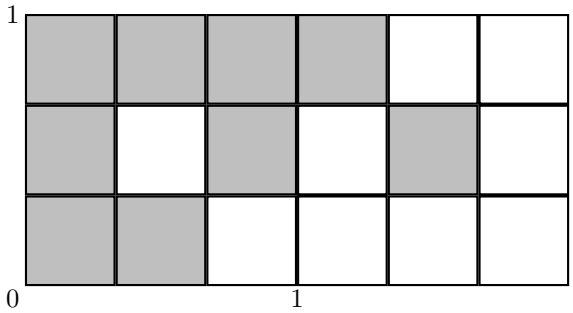

Figure 3.35: Non disk-like 36-$p2$-reptile (gray) with seven neighbors.

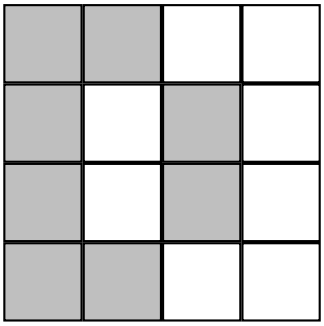

Figure 3.36: Non disk-like $p2$-16-reptile with eight neighbors.

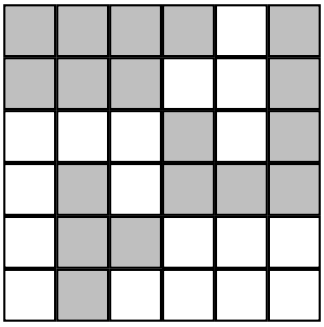

Figure 3.37: Non disk-like $p2$-36-reptile (gray) with nine neighbors.

11 neighbor case. The crystile of Figure 3.39 is trivially non disk-like and is again a 36-reptile constructed from squares. It has eleven neighbors, seven of them are adjacent.

12 neighbor case. Our last example is a perturbation of the stair case disk-like example.

It still has twelve neighbors in the induced tiling and is depicted on Figure 3.40. It is obtained by taking the expansion $g(x, y) = (3x, 3y)$ and the digit set $\mathcal{D} = \{\mathrm{id}, a, a^2, b, b^2, c, ac, bc, abc\}$,

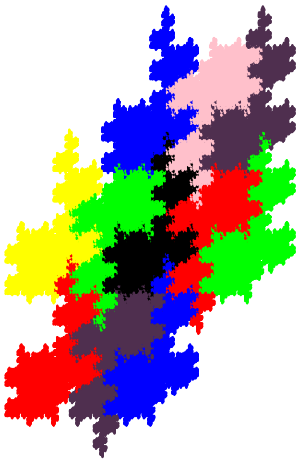

Figure 3.38: Non disk-like $p2$-crystile with ten neighbors.

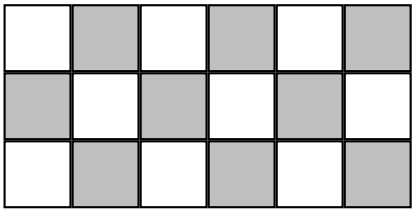

Figure 3.39: Non disk-like $p2$-36-reptile (gray) with eleven neighbors.

Figure 3.40: Non disk-like $p2$-crystile with twelve neighbors.

where $a(x, y) = (x - 2, y)$, $b(x, y) = (x, y + 1)$, $c(x, y) = (-x, -y)$.

3.4 Comments and questions

We were mainly interested in the neighbor relations in a tiling by crystallographic tiles and reptiles. For Γ being a lattice or a $p2$ group, the *minimal neighbor number* of a Γ-tile was shown to be 6. In both cases, all neighbors turned out to be adjacent. Since a crystile with neighbor set $\mathcal{S}$ is connected if and only if the digit set is $\mathcal{S}$-connected (see Remark 3.3.27), we conclude from Proposition 3.3.28 and Theorem 3.3.29 that a lattice or $p2$-crystile with minimal number of neighbors is connected if and only if it is disk-like. We conjecture that this remains true for the other crystallographic groups for which the least neighbor number is 6. Note that not all crystallographic groups have this number as minimal neighbor number, since it is 8 for the *pm*-group (generated by two perpendicular translations and a reflection along one of the translation vectors).

After dealing with the minimal neighbor number, we may now wonder how many neighbors and adjacent neighbors a crystile can have. Indeed, we found in the last section $p2$-crystiles with six to twelve neighbors, is then every number greater than 6 admissible? If not, which numbers are forbidden? How are they related to the crystallographic group? Even the lattice case is still open: is every even number greater than 6 admissible? Some partial results are known, for lower number of neighbors and it is also known that lattice reptiles can be constructed with $6 + 4k$ neighbors for every $k \in \mathbb{N}$: these are tiles associated to canonical number systems (see the next chapter). Concerning the adjacent neighbors, Grünbaum and Shephard's results on normal tilings (see [22]) indicate that 4 and 6 are the only possible numbers of adjacent neighbors for disk-like lattice tiles, and $3, 4, 5$ and 6 for disk-like $p2$-tiles, hence these restrictions remain valid for disk-like lattice and $p2$-crystiles. What about non disk-like crystiles? We already gave in this study two examples of $p2$-crystiles with seven adjacent neighbors. Can there be more? Or is this number limited by some rigidity of the crystallographic group?

Chapter 4

Lattice tiles: the class associated to canonical number systems

Lattice tiles are a particular case of the crystallographic tiles described in the previous chapter when the crystallographic group has a trivial point group (see Definition 2.2.7 and Remark 2.2.12). Lattice reptiles were studied long before the crystallographic reptiles. More is known about their topology (see for instance [21, 37, 38, 39, 48]), and many classes arise from the consideration of number representations (see *e.g.* [4, 20, 30, 31, 32, 58]). We concentrate on one of these classes, the class of self-affine tiles associated to canonical number systems.

Dealing only with translations, we will use vector sums instead of mapping compositions. Indeed, let w.l.o.g. $g(x) = \mathbf{A}x$ be expanding on the Euclidean space $\mathbb{R}^n$, Γ isomorphic to $\mathbb{Z}^n$ a lattice group, and $\mathcal{D}$ a complete set of right coset representatives of $\Gamma/g\Gamma g^{-1}$. In this case, this is equivalent to $\mathcal{D}$ being a complete set of coset representatives of $\mathbb{Z}^n/\mathbf{A}\mathbb{Z}^n$. Writing $\delta(x) = x + d$ for the digits, we have for $a \in \mathbb{R}^n$ and $m \in \mathbb{N}$ that

$$g^{-1}\delta_1 g^{-1}\delta_2 \dots g^{-1}\delta_m(a) = \mathbf{A}^{-m}a + \sum_{i=1}^{m} \mathbf{A}^{-i}d_i.$$

Redefining $\mathcal{D}$ as the set of translational parts d of the digits δ, the crystile $\mathcal{T}$ with respect to $(\Gamma, g, \mathcal{D})$ has the form

$$\mathcal{T} = \left\{ \sum_{i=1}^{\infty} \mathbf{A}^{-i}d_i; (d_i)_{i\in\mathbb{N}} \in \mathcal{D}^{\mathbb{N}} \right\} \tag{4.0.1}$$

(compare with (3.1.5)). We write $f_d(x) = \mathbf{A}^{-1}(x + d)$ for $d \in \mathcal{D}$, and we rather use the notation $\{\mathcal{T} + u, u \in \mathbb{Z}^n\}$ for the tiling induced by $\mathcal{T}$.

Unlike crystiles in general, lattice crystiles are self-affine in the strict sense of Definition 2.1.14. More precisely, a norm can be defined on $\mathbb{R}^n$ that makes all the functions f_d be contractions. The following definition uses the same notations as above.

Definition 4.0.1 (Lind Norm, *cf.* [40])**.** Let λ_j, $j = 1, \dots, n$ be the eigenvalues of $\mathbf{A}$ and r any number satisfying $1 < r < \min_{1\le j\le n} |\lambda_i|$. If $||\cdot||$ denotes the Euclidean norm, the formula

$$||x||' = \sum_{k=0}^{\infty} r^k ||\mathbf{A}^{-k}x||$$

defines a norm on $\mathbb{R}^n$, the so-called *Lind Norm*.

Proposition 4.0.2 (see [38])**.** *All the maps $f_d(x) = \mathbf{A}^{-1}(x + d)$ are contractions with respect to the Lind Norm.*

In this chapter, we are interested in a generalization of a class of self-affine plane lattice tiles connected to real complex number representations in a given basis. The tiles are presented in the first section, most of the facts can be found in the extensive study of Shigeki Akiyama and Jörg Thuswaldner [5] and their survey [4]. The characterization of disk-like tiles was fully treated there, hence we concentrate on the topological properties of non-disk like tiles. The second section is dedicated to the fundamental goup of these tiles. It turns out that, as soon as such a tile is not disk-like, then its fundamental group is uncountable. In the third section, the closure of a connected component of the interior of a tile is computed. We prove that the adresses of its points, *i.e.*, the sequences (d_i) of digits such the point $\sum_{i=1}^{\infty} \mathbf{A}^{-i} d_i$ belongs to that component closure, can be read off from a finite graph.

4.1 Canonical number systems : basic and known facts

We will deal with a class of self-affine tiles associated to canonical number systems (*cf.* [57]).

Definition 4.1.1 (Canonical number system (CNS))**.** For $n \geq 1$, let

$$P = x^n + b_{n-1}x^{n-1} + ... + b_0 \ \in \mathbb{Z}[x],$$

$\mathcal{N} = \{0, 1, ...|b_0| - 1\}$ and $\mathcal{Q} = \mathbb{Z}[x] \ / \ P\,\mathbb{Z}[x]$. Let us denote the projection of x into $\mathcal{Q}$ by $[x]$. Then the pair $(P, \mathcal{N})$ is called a *canonical number system* (or *CNS*) with *digit set* $\mathcal{N}$ if each element γ of $\mathcal{Q}$ can be written in the form

$$\gamma \ = \ a_0 \ + \ a_1[x] \ + \ \ldots \ + a_{l(\gamma)}[x]^{l(\gamma)}$$

with $a_i \in \mathcal{N}$ and $l(\gamma) \in \mathbb{N}$.

Note that, in this definition, if P is irreducible and α is a root of P then $\mathcal{Q}$ is isomorphic to $\mathbb{Z}[\alpha]$, thus $[x]$ can be replaced by α in the above expansion. Characterizations of CNS have been studied for example by Scheicher and Thuswaldner [60], Akiyama and Rao [3] and Brunotte [10]. Also, Knuth ([35]) pointed out in 1981 important applications in computer science of the fact that for each integer $b \geq 1$, $-b$ forms a CNS. For larger values of n, the quadratic case ($n = 2$) is the only one where a characterization of all CNS is known. For the other cases there are only partial characterizations, involving conditions on the coefficients of the polynomial.

Notation 4.1.2. In the case of quadratic CNS, we write $P = x^2 + Ax + B \in \mathbb{Z}[x]$.

Then it was established (*cf.* [10, 20, 31, 32]) that

$$(P, \mathcal{N}) \ \text{ is a CNS} \quad \text{iff} \quad B \geq 2 \ \text{ and } \ -1 \leq A \leq B. \tag{4.1.1}$$

To each quadratic CNS, a tile $\mathcal{T}$ is attached in the following way (see the work of Lagarias and Wang [38] for more details, as well as [28, 30]).

Definition 4.1.3 (Quadratic CNS-tile)**.** Let $(P, \mathcal{N})$ be a quadratic CNS. Let

$$\mathbf{A} \ = \ \begin{pmatrix} 0 & -B \\ 1 & -A \end{pmatrix} \ \text{ and } \ \mathcal{D} = \left\{ \begin{pmatrix} 0 \\ 0 \end{pmatrix}, \ldots, \begin{pmatrix} B-1 \\ 0 \end{pmatrix} \right\},$$

then the set $\mathcal{T}$ defined by

$$\mathbf{A}\mathcal{T} \ = \ \bigcup_{d \in \mathcal{D}} (\mathcal{T} + d)$$

is a self-similar plane tile of $\mathbb{R}^2$ satisfying

$$\mathcal{T} \ = \ \left\{ \sum_{i \geq 1} \mathbf{A}^{-i} d_i ; d_i \in \mathcal{D} \right\}$$

(see the introduction of this chapter). $\mathcal{T}$ tiles the plane by $\mathbb{Z}^2$. It is called the *quadratic CNS-tile* with expansion matrix $\mathbf{A}$ and digit set $\mathcal{D}$ or also often the *fundamental domain* of the canonical number system $(P, \mathcal{N})$.

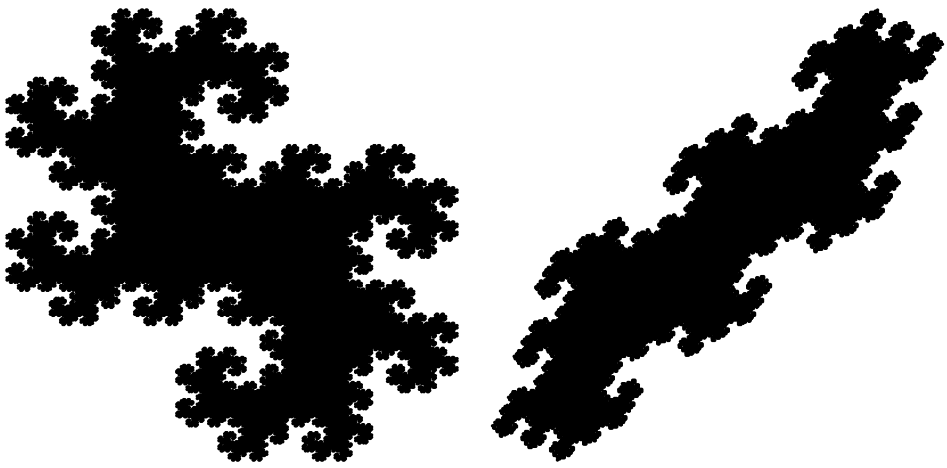

Figure 4.1: Disk-like CNS-tiles (on the left, the Knuth dragon).

The tiles are defined in the same way for $n > 2$ (see [5]). An example of (disk-like) quadratic CNS-tile is depicted on the left hand side of Figure 4.1. It is called the Knuth twin dragon (see [35]) and is associated to the polynomial $P = x^2 + 2x + 2$ (so $A = 2$ and $B = 2$). A root of P is $\alpha = -1 + \sqrt{-1}$ and, sloppily spoken, $\mathcal{T}$ represents the complex numbers whose representation in the basis α has integer part zero. For the picture, we used the similar matrix

$$\mathbf{A} \;=\; \begin{pmatrix} -1 & 1 \\ -1 & -1 \end{pmatrix}.$$

The example on the right hand side of Figure 4.1 is also disk-like and is associated to the the root $\alpha = -1 + \sqrt{-2}$ of $P = x^2 + 2x + 3$.

The following quantity is of great importance for the topology of the tiles. It is related to the number of neighbors the tile has in the induced tiling.

Notation 4.1.4. We define

$$J \;=\; \max\left\{1, \left\lfloor \frac{B-1}{B-A+1} \right\rfloor \right\}.$$

Note that

$$J > 1 \quad \text{iff} \quad 2A \geq B + 3.$$

In Section 3.2 of the preceding chapter, we defined the neighborhood graph of a crystile $\mathcal{T}$ and showed how this rather abstract graph can be used to identify boundary points of $\mathcal{T}$. This graph will also be an important tool in the next two sections. We will make use of the additive notation, thus we will redefine it for CNS-tiles and list some of its properties partially given in Subsection 3.2.2. It will be even more interesting to introduce the transposed graph of the neighborhood graph of Definition 3.2.4, since it reveals to be an adding machine.

Definition 4.1.5. If G is a graph, the *transposed graph* G^T is the graph with the same vertices as G obtained by changing the direction of every edge of G: $s \xrightarrow{d|d'} s' \in G^T$ iff $s' \xrightarrow{d|d'} s \in G$.

In the remaining part of this subsection, $\mathcal{T}$ is a quadratic CNS-tile with expansion matrix $\mathbf{A}$ and digit set $\mathcal{D}$. Let $\mathcal{S}$ be the neighbor set of $\mathcal{T}$ in the induced lattice tiling, *i.e.*,

$$\mathcal{S} \;=\; \left\{ s \in \mathbb{Z}^2; s \neq 0, \mathcal{T} \cap (\mathcal{T} + s) \;\neq \emptyset \right\}.$$

As will be seen soon, the neighborhood graph $\mathbf{G}(\mathcal{S})$ will be replaced by its transposed $\mathbf{G}^T(\mathcal{S})$, which we will call graph of neighbors and denote by $\mathcal{G}_1(\mathcal{S})$ to avoid confusion.

Definition 4.1.6 (Adding graph of a CNS; input and output; string)**.** We define in $\mathbb{Z}^2$ the directed labelled graph $\mathcal{G}_1(\mathbb{Z}^2)$ as follows:

- each $s \in \mathbb{Z}^2$ is a state of $\mathcal{G}_1(\mathbb{Z}^2)$.
- for $s, s' \in \mathcal{G}_1(\mathbb{Z}^2)$ and $d, d' \in \mathcal{D}$, there exists an edge $s \xrightarrow{d|d'} s'$ from s to s' labelled by $d|d'$ if and only if $s + d = \mathbf{A}s' + d'$. It is the *adding graph* of the quadratic CNS-tile with expansion matrix $\mathbf{A}$ and digit set $\mathcal{D}$. As $\mathcal{D}$ is a complete set of coset representatives of $\mathbb{Z}^2/\mathbf{A}\mathbb{Z}^2$, s' and the *output digit* d' are uniquely determined by s and the *input digit* d, and this addition is well-defined for all $s \in \mathbb{Z}^2$ and all $d \in \mathcal{D}$. Thus $\mathcal{G}_1(\mathbb{Z}^2)$ is a so-called *adding machine* or *adding graph*.
  If $d_0, \ldots, d_n$ are digits, then $w = (d_0, \ldots, d_n)$ is called a *string*. If n is the maximal i for which d_i is non zero, the *length* of the string, written $|w|$, is said to be equal to $n + 1$.
  For $s \in \mathcal{G}_1(\mathbb{Z}^2)$, one can associate an *output string* $c = (d'_0, \ldots, d'_n)$ to an *input string* by "feeding" the graph with the input string from left to right as input digits, starting at the sate s and collecting the corresponding output digits (see also [48]).

Definition 4.1.7 (Graph of neighbors)**.** The *graph of neighbors* $\mathcal{G}_1(\mathcal{S})$ is the restriction of $\mathcal{G}_1(\mathbb{Z}^2)$ to the subset $\mathcal{S}$ of $\mathbb{Z}^2$.

It is shown that the graph $\mathcal{G}_1(\mathcal{S} \cup \{0\})$ is stable by addition of any digit to any state.

Remark 4.1.8. This graph is called $\mathcal{G}_1(S)$ in [5] and $G^T(S)$ in [48].

The graph of neighbors for quadratic CNS has been found in [5]: defining the points

$$P_n = \begin{pmatrix} n - (n-1)A \\ -(n-1) \end{pmatrix}, \quad Q_n = \begin{pmatrix} -n + nA \\ n \end{pmatrix}, \quad R = \begin{pmatrix} -A \\ -1 \end{pmatrix}, \quad n \geq 1,$$

then the set of neighbors consists of the $2 + 4J$ elements

$$\pm P_1, \ldots, \pm P_J, \pm Q_1, \ldots, \pm Q_J, \pm R.$$

Definition 4.1.9 (State level)**.** The states $\pm P_1, \pm Q_1, \pm R$ defined above are said to be of *first level*, the states $\pm P_n, \pm Q_n$ of *level* n for $2 \leq n \leq J$.

The edges are given in [5, p.1471] and are reproduced in Table 4.1.
We obtain the graph of Figure 4.2, explicitely depicted there until $J = 2$, and where we also wrote the point $(0, 0)$ as an empty state and the corresponding edges. Moreover, if τ stands for the label $d|d'$, then $-\tau$ stands for $d'|d$. For the special case $J = 1$ we have the graph of Figure 4.3, which is a subgraph of the general graph.

Since we are working with the transposed graph, we complete Definition 3.2.8 with the following one.

Definition 4.1.10 (Walk)**.** A *walk* in a graph G ending in a state s_0 of this graph is a sequence of edges (finite or infinite)

$$s_0 \xleftarrow{d_0|d'_0} s_1 \xleftarrow{d_1|d'_1} s_2 \xleftarrow{d_2|d'_2} \ldots.$$

Considering the graph in Figure 4.2, we get the following result (see [5]).

Proposition 4.1.11. *Let W be an infinite walk ending in a state s_0 of the graph of neighbors $\mathcal{G}_1(\mathcal{S})$, then one of the following possibilities occurs.*

edge	labels		name
$0 \to 0$	0 $\vdots$ $B-1$	0 $\vdots$ $B-1$	
$P_1 \to 0$	0 $\vdots$ $B-2$	1 $\vdots$ $B-1$	β
$P_1 \to R$	$B-1$	0	γ
$R \to Q_1$	0 $\vdots$ $A-1$	$B-A$ $\vdots$ $B-1$	δ
$R \to -P_1$	A $\vdots$ $B-1$	0 $\vdots$ $B-A-1$	ϵ
$P_{n+1} \to Q_n$ $(1 \le n < J)$	0 $\vdots$ $A-3-(n-1)(B-A+1)$	$1+n(B-A+1)$ $\vdots$ $B-1$	κ_n
$P_{n+1} \to -P_n$ $(1 \le n < J)$	$A-2-(n-1)(B-A+1)$ $\vdots$ $B-1$	0 $\vdots$ $n(B-A+1)$	λ_n
$Q_n \to P_n$ $(1 \le n \le J)$	0 $\vdots$ $n(B-A+1)-1$	$A-1-(n-1)(B-A+1)$ $\vdots$ $B-1$	μ_n
$Q_n \to -Q_n$ $(1 \le n \le J)$	$n(B-A+1)$ $\vdots$ $B-1$	0 $\vdots$ $A-2-(n-1)(B-A+1)$	ν_n

Table 4.1: Edges of the general graph of neighbors $\mathcal{G}_1(\mathcal{S})$.

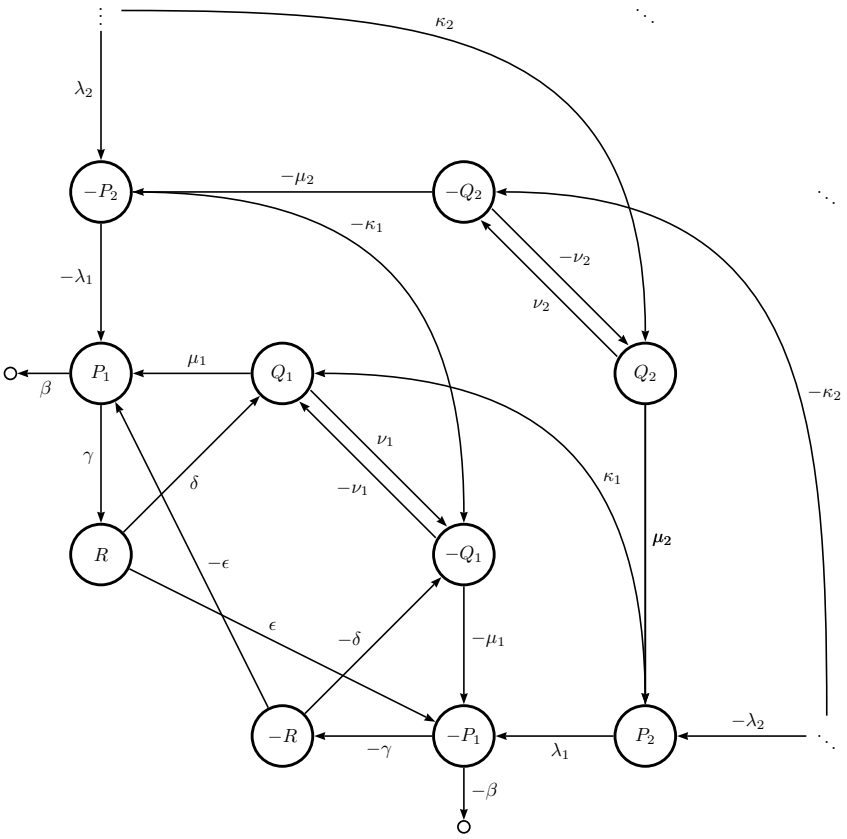

Figure 4.2: General graph of neighbors $\mathcal{G}_1(\mathcal{S})$.

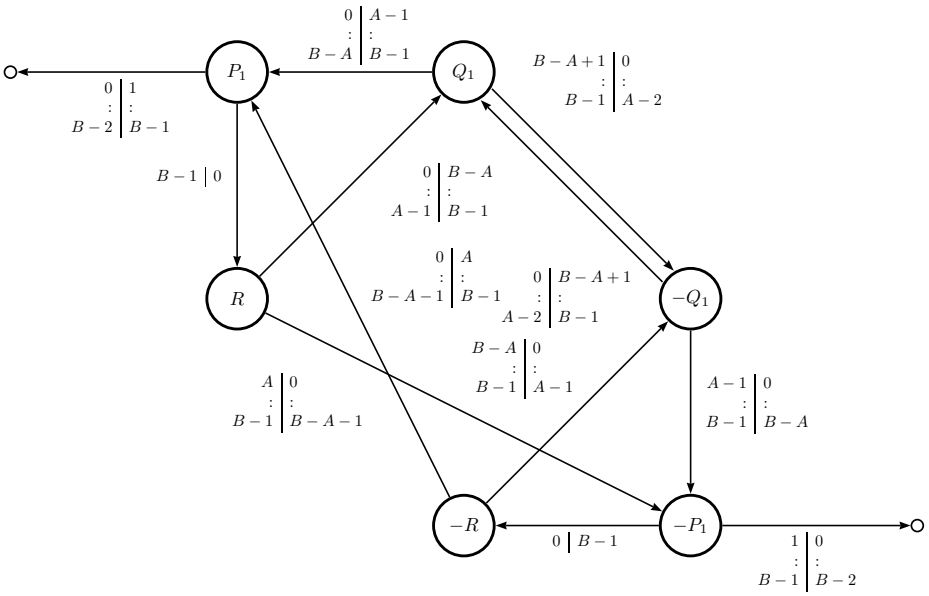

Figure 4.3: First level graph of neighbors.

1. *All states of W belong to level* 1.

2. *Going the walk W backwards from s_0, one comes to one of the cycles $\pm Q_n \leftarrow \mp Q_n \leftarrow \pm Q_n$, for some n with $2 \leq n \leq J$.*

We recall that the L-vertices of a tile are the points shared by the tile and other L distinct neighbors (see Definition 3.2.7). Characterization 3.2.10 of the last chapter indicated how to get the L-vertices of the crystile $\mathcal{T}$ using the neighborhood graph $\mathbf{G}(\mathcal{S})$. It is also possible to define L-folded powers of this graph and to read at once the L-vertices of the tile. We rather define the L-folded power of $\mathcal{G}_1(\mathcal{S})$.

Definition 4.1.12 (L-folded power of the graph of neighbors)**.** The *L-folded power* of the graph of neighbors, denoted by $\mathcal{G}_L(\mathcal{S})$, is constructed as follows.

- The states of $\mathcal{G}_L(\mathcal{S})$ are the $L-$subsets of $\mathcal{S}$.
- There exists an edge
$$\{s_{11}, \ldots, s_{1L}\} \xrightarrow{d} \{s_{21}, \ldots, s_{2L}\}$$
in $\mathcal{G}_L(\mathcal{S})$ if, after possible rearrangement of $s_{21}, \ldots, s_{2L}$, there exist the edges
$$s_{1l} \xrightarrow{d|d_l} s_{2l} \quad (1 \leq l \leq L)$$
in $\mathcal{G}_1(\mathcal{S})$ for some $d_1, \ldots, d_L \in \mathcal{D}$.
- The states that are not the endpoints of infinite walks are removed, together with the edges leading to them.

This leads to the following characterization of the L-vertices.

Characterization 4.1.13. *The following assertions are equivalent.*

1. *The point $x = \sum_{j\geq 1} \mathbf{A}^{-j} d_j$ belongs to $V_L(s_{01}, \ldots, s_{0L})$*
2. *In $\mathcal{G}_L(\mathcal{S})$, there is an infinite walk*
$$\{s_{01}, \ldots, s_{0L}\} \xleftarrow{d_1} \{s_{11}, \ldots, s_{1L}\} \xleftarrow{d_2} \{s_{21}, \ldots, s_{2L}\} \xleftarrow{d_3} \ldots$$

This follows as in Characterization 3.2.10 from the fact that a point x belonging to $\mathcal{T} \cap (\mathcal{T} + s)$ admits the two representations $x = \sum_{j\geq 1} \mathbf{A}^{-j} d_j = s + \sum_{j\geq 1} \mathbf{A}^{-j} d'_j$ if and only if there is an infinite walk
$$s \xleftarrow{d_1|d'_1} s_1 \xleftarrow{d_2|d'_2} s_2 \xleftarrow{d_3|d'_3} \ldots$$
in the graph $\mathcal{G}_1(\mathcal{S})$.

Remark 4.1.14.

- For $L = 2$ we come to the subgraph of level 1 depicted in Figure 4.4. Note that the edge from $\{Q_1, -Q_1\}$ to itself only exists for $2A \geq B + 3$.
- For $L = 3$, it is mentioned in [5, p.1478] that the subgraph of level 1 is empty. So there are no three infinite walks in level 1 of the graph $\mathcal{G}_1(\mathcal{S})$ with the same input digits that end in three different states of level 1. This can be checked here directly using the graphs of Figures 4.3 and 4.4.

This provides the tools for the next section.

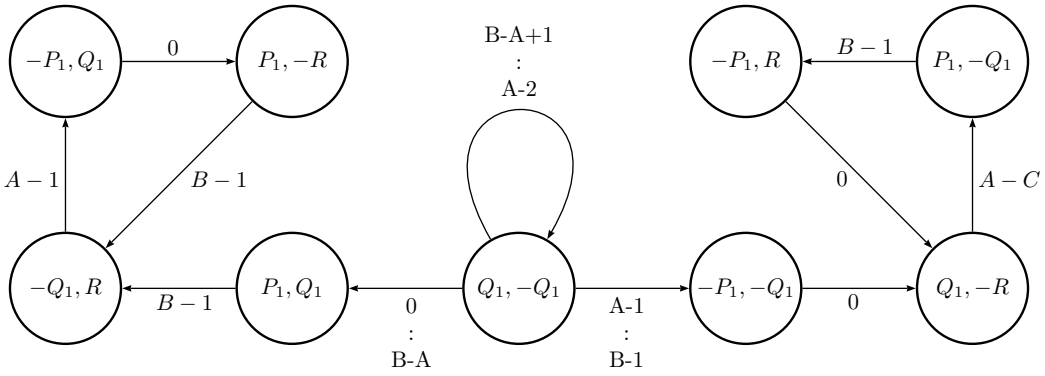

Figure 4.4: Graph $\mathcal{G}_2(\mathcal{S})$ (restriction to the states of level 1).

4.2 Fundamental group of CNS-tiles

The main result of this section will appear in [41]. Topological properties of quadratic CNS-tiles have been studied by Akiyama and Thuswaldner in [5]: depending on J, the tile is either homeomorphic to a disk ($J = 1$) or it has a disconnected interior ($J > 1$). This means that the fundamental group $\pi_1(\mathcal{T})$ of a quadratic CNS-tile $\mathcal{T}$ is trivial in the former case. A result by Luo and Thuswaldner [48] states that the fundamental group of such a tile is either trivial or uncountable. An overview of these results can be found in [4]. We will use the criterion given in [48] to prove the uncountability of $\pi_1(\mathcal{T})$ in the latter case ($J > 1$).

We recall the criterion for uncountability of the fundamental group of a tile given by Luo and Thuswaldner in [48].

Proposition 4.2.1. *Let $\mathcal{T}$ be a connected $\mathbb{Z}^2$-tile in $\mathbb{R}^2$. Furthermore, suppose that there exist $s_1, s_2 \in \mathcal{S}$ such that the following assertions hold.*

(1) $\#V_2(s_1, s_2) \geq 2$ and $V_2(s_1, s_2) \setminus V_3 \neq \emptyset$.

(2) For each $i \in \{0, 1, 2\}$, there exists a string w_i such that using w_i as input string in $\mathcal{G}_1(\mathcal{S} \cup \{0\})$ starting at $0, s_1, s_2$ yields the output strings c_0^i, c_1^i, c_2^i satisfying

$$\max\left\{|c_i^i|, |c_{i+1}^i|\right\} < |c_{i+2}^i| \quad (\textit{indices are written modulo } 3).$$

Then the fundamental group of $\mathcal{T}$ is uncountable.

A short explanation to this criterion reads as follows. Under the assumptions (1) and (2), the complement of the tile $\mathcal{T}$ in $\mathbb{R}^2$ is shown to be disconnected: two subpieces of $\mathcal{T}$ can be found whose union has a bounded complementary component that also intersects the complement of $\mathcal{T}$. Thus the complement of this tile is disconnected, it even has infinitely many components. Therefore the tile $\mathcal{T}$ cannot be locally simply connected, which is equivalent to the uncountability of its fundamental group by a result of Conner and Lamoreaux [12].

We can now state and prove the following theorem on the fundamental group of quadratic CNS-tiles.

Theorem 4.2.2. *Let $\mathcal{T}$ be the quadratic CNS-tile corresponding to the polynomial $x^2 + Ax + B$. Then the fundamental group of $\mathcal{T}$ is:*

- *trivial for $2A < B + 3$,*
- *uncountable for $2A \geq B + 3$.*

Proof. The first part has been proved in [5], we prove the second part by showing that both items of the above criterion are true. Let $s_1 = P_1$, $s_2 = -Q_1$.

1. *Claim.* The point
$$x \;=\; \sum_{j\geq 1} \mathbf{A}^{-j} d_j$$
with
$$d_{1+3k} \;=\; \begin{pmatrix} B-A \\ 0 \end{pmatrix},\;\; d_{2+3k} \;=\; \begin{pmatrix} 0 \\ 0 \end{pmatrix},\;\; d_{3+3k} \;=\; \begin{pmatrix} B-1 \\ 0 \end{pmatrix}$$
belongs to $V_2(P_1, -Q_1) \setminus V_3$.
Indeed, looking at the first level subgraph of $\mathcal{G}_2(\mathcal{S})$ (Figure 4.4), the infinite cycle
$$\{P_1, -Q_1\} \xleftarrow{B-A} \{Q_1, -R\} \xleftarrow{0} \{-P_1, R\} \xleftarrow{B-1} \{P_1, -Q_1\} \xleftarrow{B-A} \;...$$
provides a point of $V_2(P_1, -Q_1)$ because of Characterization 4.1.13.
Then, as seen in the second item of Remark 4.1.14, an infinite walk in $\mathcal{G}_1(\mathcal{S})$ with the same input digits as the cycle above and ending in $P \notin \{P_1, -Q_1\}$ could not have all states in level 1. Note that the levels would grow up going this infinite walk in $\mathcal{G}_1(\mathcal{S})$. Thus, one should come to a cycle in level $n \geq 2$ (see Proposition 4.1.11): $\pm Q_n \leftarrow \mp Q_n \leftarrow \pm Q_n$; this would imply the existence of the edge $-Q_n \xleftarrow{B-A} Q_n$ in the walk, which is not true (according to Table 4.1 page 81). This proves the claim.
The point
$$y = \mathbf{A}^{-1} \begin{pmatrix} B-A \\ 0 \end{pmatrix} + \mathbf{A}^{-3} \begin{pmatrix} A-1 \\ 0 \end{pmatrix} + \sum_{j\geq 4} \mathbf{A}^{-j} \begin{pmatrix} A-2 \\ 0 \end{pmatrix}$$
is distinct from x and also belongs to $V_2(P_1, -Q_1)$ (this set is even easily seen to contain infinitely many elements, using Characterization 4.1.13 and the graph of Figure 4.4).
Thus the first item of the criterion is proved.

2. The second part is obtained by looking at the graph in Figure 4.3.
With the input strings
$$\begin{aligned} w_0 &= (0,0,0,0), \\ w_1 &= (B-1, 0, B-1, A-1, 1, 0), \\ w_2 &= (B-1, B-1, 0, 0, 0, 0), \end{aligned}$$
one gets
$$\begin{aligned} \max\left\{|c_0^0|, |c_1^0|\right\} \;&=\; 1 \;<\; |c_2^0| \;=\; 3, \\ \max\left\{|c_1^1|, |c_2^1|\right\} \;&=\; 3 \;<\; |c_0^1| \;=\; 5, \\ \max\left\{|c_2^2|, |c_0^2|\right\} \;&=\; 2 \;<\; |c_1^2| \;=\; 5. \end{aligned}$$
Thus the second item of the criterion is fulfilled and Theorem 4.2.2 is proved.

□

An example of a CNS-tile with uncountable fundamental group can be seen in Figure 4.2. This tile $\mathcal{T}$ is associated to the quadratic polynomial $x^2 + 4x + 5$. It is a limit case in the sense of Theorem 4.2.2, since the quantity $2A-B$ is here exactly 3, the threshold value where the CNS-tiles "begin" to have uncountable fundamental group. The interior of $\mathcal{T}$ cannot be connected, because a self-affine plane tile with connected interior is already disk-like (see Proposition 3.3.4 and [47]). Ngai and Tang proved that the closure of the interior components of $\mathcal{T}$ are disks (see [54]). The purpose of the next section is mainly the computation of one of them.

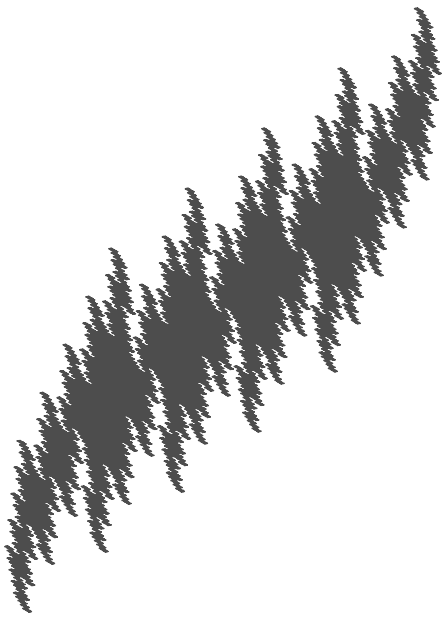

Figure 4.5: A CNS-tile with uncountable fundamental group (limit case, with $A = 4, B = 5$).

4.3 Interior component of a CNS-tile

Tis section is contained in the joint paper [45] written with Jörg Thuswaldner. $\mathcal{T}$ denotes here the tile of Figure 4.6, *i.e.*, the non disk-like tile already depicted at the end of the last section. The closure C_0 of the interior component containing the origin can be seen in the same figure. We want to describe it as a graph directed self-similar set. Indeed, the sequences $(d_i)_i \in \mathbb{N}$ of digits such that the point $\sum_{i=1}^{\infty} \mathbf{A}^{-i} d_i$ belongs to C_0 will be given. Because of the self-similar structure, common subsequences of digits appear in these sequences, such that the set of sequences characterizing C_0 can be read off from a finite graph. A byproduct is the computation of the Hausdorff dimension of the boundary of C_0 using the technique of Appendix B. Amazingly, it is be strictly less than the Hausdorff dimension of the whole boundary of $\mathcal{T}$.

The polynomial $P = x^2 + 4x + 5$ is irreducible. By Definition 4.1.1, the root $\alpha = -2 + \sqrt{-1}$ of the polynomial $x^2 + 4x + 5$ together with $\mathcal{N} := \{0, 1, 2, 3, 4\}$ forms a canonical number system $(\alpha, \mathcal{N})$, *i.e.*, each element $x \in \mathbb{Z}[\alpha]$ has a unique representation

$$x = \sum_{i=0}^{\ell(x)} a_i \alpha^i$$

for some non-negative integer $\ell(x)$ and $a_i \in \mathcal{N}$ with $a_{\ell(x)} \neq 0$ for $x \neq 0$. It is a special case of CNS in imaginary quadratic fields (see [20, 33]). We use a matrix $\mathbf{A}$ associated to the polynomial that is similar to the matrix introduced in Definition 4.1.3. Indeed, let us define the natural embedding

$$\begin{array}{rcl} \Phi : \mathbb{C} & \to & \mathbb{R}^2 \\ x & \mapsto & (\Re(x), \Im(x)). \end{array}$$

Then the multiplication by α can be represented by the 2×2 matrix

$$\mathbf{A} := \begin{pmatrix} -2 & -1 \\ 1 & -2 \end{pmatrix},$$

i.e., for every $x \in \mathbb{C}$,

$$\Phi(\alpha x) = \mathbf{A}\Phi(x).$$

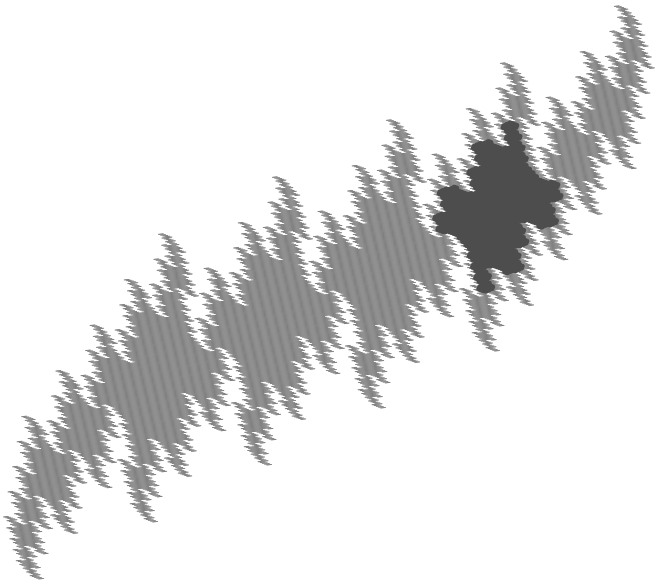

Figure 4.6: Tile associated to the base $-2+\sqrt{-1}$ with interior component containing 0.

$\mathcal{T}$, the set of points of integer part zero in the base α embedded into the plane is therefore

$$\mathcal{T} = \left\{ \sum_{i=1}^{\infty} \Phi(\alpha^{-i} a_i); (a_i)_{i\in\mathbb{N}} \in \mathcal{N}^{\mathbb{N}} \right\} = \left\{ \sum_{i=1}^{\infty} \mathbf{A}^{-i} \Phi(a_i); (a_i)_{i\in\mathbb{N}} \in \mathcal{N}^{\mathbb{N}} \right\}. \tag{4.3.1}$$

It is depicted in Figure 4.6. Thus each point of this set can be represented by an infinite string $w = (a_1, a_2, a_3, \ldots)$ with $a_i \in \mathcal{N}$. The set $\mathcal{T}$ satisfies the set equation

$$\mathcal{T} = \bigcup_{i=0}^{4} \psi_i(\mathcal{T}), \tag{4.3.2}$$

where ψ_i $(0 \le i \le 4)$ are contractions defined via the matrix $\mathbf{A}$ and the embedding Φ by

$$\psi_i(x) = \mathbf{A}^{-1}\left(x + \Phi(i)\right),\ x \in \mathbb{R}^2 \qquad (0 \le i \le 4). \tag{4.3.3}$$

Since $\mathcal{T}$ is a CNS-tile, it is a self-similar continuum with non-empty interior which induces a *tiling* of the plane by its translates (see Definition 4.1.3 and also [30]): the family of sets

$$\{\mathcal{T} + \Phi(\omega); \omega \in \mathbb{Z}[\alpha]\} \tag{4.3.4}$$

is a tiling of the plane.

Some research on the structure of the components of the interior of self-similar and self-affine tiles has already been done. Bailey *et al.* [6] investigate the interior of the Lévy dragon, which is a self-affine continuum with disconnected interior providing a tiling of the plane. They stated many conjectures concerning the geometrical shape of the connected components of its interior. Ngai and Nguyen [53] study the components of the Heighway dragon. Moreover, as mentionned in the introduction of this section, Ngai and Tang [54, 55] gave general results on components of the interior of self-affine tiles. As an example they consider our tile $\mathcal{T}$ in [54] and prove that it has no cut point, and that the closure of each component of its interior is homeomorphic to a closed disk.

In order to describe the closure C_0 of the connected component containing $\Phi(0)$ (or 0, for short), we need some notations.

Notation 4.3.1. For a finite string $w = (a_1, \ldots, a_n)$ we define the map ψ_w by

$$\psi_w(x) := \psi_{a_1} \cdots \psi_{a_n}(x) = \mathbf{A}^{-n}x + \sum_{i=1}^{n} \mathbf{A}^{-i}\Phi(a_i), \qquad x \in \mathbb{R}^2. \tag{4.3.5}$$

Following Definition 3.1.7, the set $\psi_w(\mathcal{T})$ is called an n-th level subpiece of $\mathcal{T}$. So by definition it contains all the points represented by an infinite string of the shape $(a_1, \ldots, a_n, d_1, d_2, \ldots)$ with $d_i \in \mathcal{N}$.

Note that iterating (4.3.2) we have for every $n \geq 1$ the subdivision principle

$$\mathcal{T} = \bigcup_{w,|w|=n} \psi_w(\mathcal{T}). \tag{4.3.6}$$

The description of C_0 will be in terms of n-th level subpieces with $n \geq 0$. Indeed, it will be shown that C_0 can be obtained as the closure of the union of such subpieces; the strings w involved in this union will be read off from a graph $\mathcal{G}$ presented in details in the next subsection and depicted on Figure 4.7. Consequently, the set C_0 will be viewed as the attractor of a graph-directed construction (see Definition 2.1.17). For the so-called accepting state $\circ$, there is by convention an edge $\circ \xrightarrow{a} \circ$ for every $a \in \mathcal{N}$.

4.3.1 Component graph $\mathcal{G}$

Let us introduce the graph $\mathcal{G}$ and explain how the set C_0 can be derived from it. We need some notations. The graph $\mathcal{G}$ is right resolving, *i.e.*, each walk of $\mathcal{G}$ is uniquely defined by its starting state together with its labeling.

Notation 4.3.2. We will write $w = (A; a_1, \ldots, a_n)$ for a walk w starting in A with labeling the string $(a_1, \ldots, a_n)$.

Notation 4.3.3. For subsets of the walks in $\mathcal{G}$ we adopt the following notations.

p	set of all walks in $\mathcal{G}$,
p_n	set of all walks in $\mathcal{G}$ having length n,
$p(A_1)$	set of walks in p starting at node A_1,
$p_n(A_1)$	set of walks in p_n starting at node A_1,
$p(A_1, A_2)$	set of walks in $p(A_1)$ ending at node A_2,
$p_n(A_1, A_2)$	set of walks in $p_n(A_1)$ ending at node A_2.

Notation 4.3.4. If w is a walk in $\mathcal{G}$ with labeling $(a_1, \ldots, a_n)$, then we denote the walk which corresponds to w in the transposed graph $\mathcal{G}^T$ by w^T (backwards walk). Its labeling is obviously $(a_n, \ldots, a_1)$. The terminal state of a walk w in $\mathcal{G}$ shall be denoted by $t(w)$. If w_1 and w_2 are two walks in $\mathcal{G}$ and w_2 starts at the terminal state of w_1 then we write $w_1 \& w_2$ for the concatenation of these two walks. If we emphasize on the labeling $(a_1, \ldots, a_n)$ of a walk w we will write $w = (a_1, \ldots, a_n)$.

So, for instance, by the above notation, if we concatenate $w_1 = (A_1; a_1, \ldots, a_n)$ and $w_2 = (A_2; b_1, \ldots, b_m)$ we will often write $(A_1, a_1, \ldots a_n)\&(b_1, \ldots, b_m)$ because the starting state of w_2 is defined via w_1.

Notation 4.3.5. For a walk w of length n and $k \leq n$ we denote by $w|_k$ the walk consisting of the first k edges of w, *i.e.*, $(a_1, \ldots, a_n)|_k = (a_1, \ldots, a_k)$. If $v = w|_k$ we write $v \prec w$.

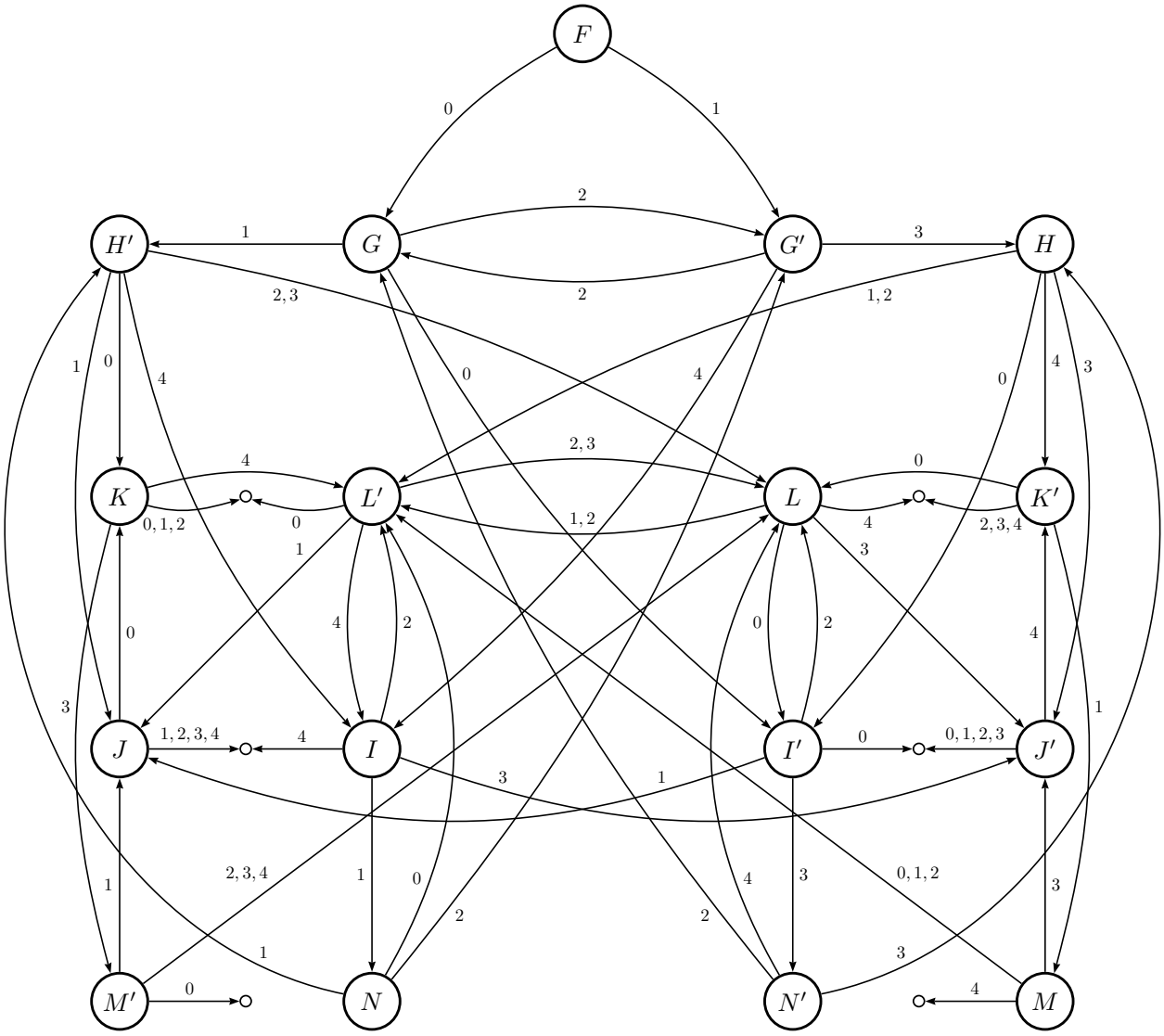

Figure 4.7: The graph $\mathcal{G}$ describing the closure of the interior component of $\mathcal{T}$ containing 0.

Notation 4.3.6. If A is a state of $\mathcal{G}$, we call A' its dual. By convention we set $F' = F$, $\circ = \circ'$ and $A'' = A$ for all the other states of $\mathcal{G}$.

Note that in $\mathcal{G}$ every edge $A_1 \xrightarrow{a} A_2$ has a dual edge $A_1' \xrightarrow{4-a} A_2'$.

By attaching the contraction ψ_a defined in (4.3.3) to each edge labelled by a in $\mathcal{G}$, the graph $\mathcal{G}$ leads to a system of graph directed sets. For each state A of $\mathcal{G}$ let

$$\mathbf{M}(A) := \left\{ x = \sum_{i \geq 1} \mathbf{A}^{-i} \Phi(a_i); w = (a_1, a_2, \ldots) \text{ infinite walk of } p(A) \right\}. \tag{4.3.7}$$

Then we have the following result.

Proposition 4.3.7. *The vector $\{\mathbf{M}(A); A \in \mathcal{G}\}$ together with the graph $\mathcal{G}$ defines a system of graph directed sets. It is even a system of self-similar graph directed sets.*

Proof. We have to verify the conditions in Definition 2.1.17 and Proposition 2.1.18. $\mathbf{M}(A)$ is obviously bounded. The fact that it is closed follows by a Cantor diagonal argument very similar to the one used in Kátai [29].

The family $\bigcup_B \{\psi_e(\mathbf{M}(B)); e \in E_{AB}\}$ is non-overlapping because $\mathbf{M}(B) \subset \mathcal{T}$ and $\mathcal{G}$ is right resolving (note that $(\alpha, \mathcal{N})$ admits unique representations). Furthermore, it is easy to see that $\{\mathbf{M}(A) \mid A \in \mathcal{G}\}$ fulfills (2.1.2). □

In particular,

$$\mathbf{M} := \mathbf{M}(F)$$

is a compact set and $\mathbf{M} \subset \mathcal{T}$. The aim is to show that $\mathbf{M} = C_0$. We state the main results of this section and postpone their proofs to the subsequent subsections, since they will require the several lemmata and propositions.

Theorem 4.3.8. *Let $(\alpha = -2 + \sqrt{-1},\ \mathcal{N} = \{0, 1, 2, 3, 4\})$ be the quadratic canonical number system related to the polynomial $x^2 + 4x + 5$. Let $\mathcal{T}$ be the fundamental domain associated to $(\alpha, \mathcal{N})$. Then $\mathrm{int}(\mathbf{M})$ is the component of $\mathrm{int}(\mathcal{T})$ containing 0. Moreover, $\mathbf{M}$ is the closure of its interior, hence $\mathbf{M} = C_0$, the closure of the component of $\mathrm{int}(\mathcal{T})$ containing 0.*

Remark 4.3.9. Note that the above mentioned result of Ngai and Tang [54] implies that C_0 is homeomorphic to a closed disk.

For the proof of this theorem we will consider approximations of the set $\mathbf{M}$ in terms of finite walks of the graph $\mathcal{G}$.

Notation 4.3.10. For some $n \in \mathbb{N}$ and some state A of $\mathcal{G}$ let $W \subset p_n(A)$ be a set of walks. Then we set

$$\mathcal{M}(W) := \bigcup_{w \in W} \psi_w(\mathcal{T}).$$

Here, according to (4.3.5), $\psi_w(\mathcal{T})$ is the subpiece associated to the labeling of w. The approximating sets are obtained by taking for W the sets

$$G_n := p_n(F, \circ) \qquad (n \geq 3). \tag{4.3.8}$$

It is easy to see that for every $n > 3$, $\mathcal{M}(G_{n-1}) \subset \mathcal{M}(G_n) \subset \mathbf{M}$. Note that there exists no walk in $p_n(F, \circ)$ if $n < 3$. This means that there are no subpieces $\psi_w(\mathcal{T})$ with $|w| < 3$ entirely contained in $\mathbf{M}$.

We will show that $\mathbf{M} = C_0$ in the following way. First we show that the interior of $\mathbf{M}$ is connected and contained in the interior of $\mathcal{T}$, hence $\mathrm{int}(\mathbf{M}) \subset \mathrm{int}(C_0)$. In a second step we show that its boundary lies on the boundary of $\mathcal{T}$, which implies that $C_0 \subset \mathbf{M}$. By proving that $\mathbf{M}$ is the closure of its interior, *i.e.*, $\overline{\mathrm{int}(\mathbf{M})} = \mathbf{M}$, this will finally yield $\mathbf{M} = C_0$.

The connectivity of $\mathrm{int}(\mathbf{M})$ will be obtained by considering the approximations $\mathcal{M}(G_n)$ for $n \geq 3$, since we will show that

$$\mathrm{int}(\mathbf{M}) \subset \bigcup_{n \geq 3} \mathcal{M}(G_n).$$

Using this fact, we will be able to connect a point from $\mathrm{int}(\mathbf{M})$ to 0 by a path going from subpiece to subpiece with increasing size (*i.e.*, over subpieces $\psi_w(\mathcal{T})$ with decreasing $|w|$) within $\mathrm{int}(\mathcal{T})$.

The second main result concerns the Hausdorff dimension of the boundary of the interior component containing zero. It reads as follows.

Theorem 4.3.11. *Let* $(\alpha = -2 + \sqrt{-1},\ \mathcal{N} = \{0, 1, 2, 3, 4\})$ *be the quadratic canonical number system related to the polynomial* $x^2 + 4x + 5$. *Let* $\mathcal{T}$ *be the fundamental domain associated to* $(\alpha, \mathcal{N})$ *and denote by* C_0 *the component of* $\mathrm{int}(\mathcal{T})$ *containing* 0. *Then*

$$\dim_H \partial C_0 = \frac{2 \log 3}{\log 5} = 1.36521\ldots.$$

Remark 4.3.12. Since the Hausdorff dimension of $\partial\mathcal{T}$ is given by

$$\dim_H \partial T = \frac{2 \log \beta}{\log 5} = 1.60858\ldots$$

where β is the dominant root of the polynomial $x^3 - 3x^2 - x + 5$ we have that

$$\dim_H \partial C_0 < \dim_H \partial T.$$

The computations of Theorem 4.3.11 and Remark 4.3.12 are essentially done by standard techniques from fractal geometry, see Proposition B.0.27 of the appendix.

The remaining part of this section is organized as follows. In Subsection 4.3.2 we present an automaton $\mathcal{B}_0$ which is helpful to determine whenever subpieces intersect each other. It is a subgraph of the graph of neighbors defined in Definition 4.1.7. This leads to the definition of an action of $\mathcal{B}_0$ on $\mathcal{G}$ in a way that is stated in this subsection too. Subsections 4.3.3 and 4.3.4 will be helpful for the proof of the connectivity of $\mathrm{int}(\mathbf{M})$. Subsection 4.3.5 shows that the boundary of $\mathbf{M}$ is contained in the boundary of $\mathcal{T}$. Subsection 4.3.6 is devoted to the construction of connected paths within the interior of $\mathcal{T}$ together with some of its neighbors, that will be also used to show the connectivity of $\mathrm{int}(\mathbf{M})$ inside $\mathrm{int}(\mathcal{T})$. Subsection 4.3.7 contains the proof of Theorem 4.3.8 and in Subsection 4.3.8 we prove Theorem 4.3.11.

4.3.2 Counting automaton $\mathcal{B}_0$ and its action on the graph $\mathcal{G}$

We define a counting automaton and an action of this automaton on the preceding graph $\mathcal{G}$.

Counting automaton $\mathcal{B}_0$.

We call *counting automaton* the first level graph of neighbors of Figure 4.3. It was given in [58] for bases of quadratic canonical number systems in general and it is reproduced in Figure 4.8 for $\alpha = -2 + \sqrt{-1}$. We denote the automaton on Figure 4.8 by $\mathcal{B}_0$. Note that it is only a subgraph of the graph of neighbors, since only six particular neighbors are considered among the ten (*cf.*

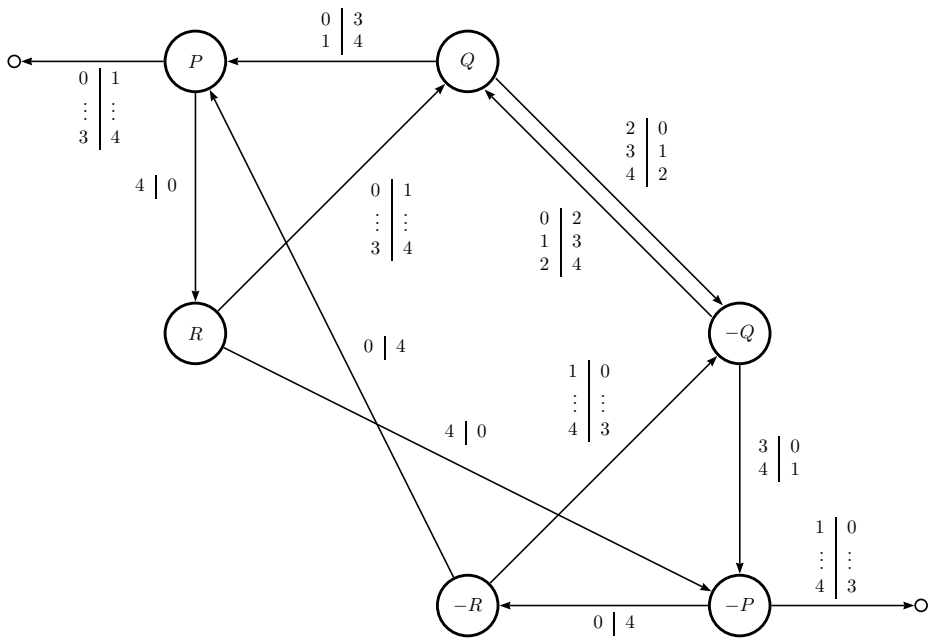

Figure 4.8: The counting automaton $\mathcal{B}_0$.

Definitions 4.1.6 and 4.1.7).

Its states are defined by

$$\pm P := \pm\Phi(1), \qquad \pm Q := \pm\Phi(3+\alpha), \qquad \pm R := \pm\Phi(-4-\alpha),$$

and $\circ$ denotes the accepting state 0 (compare with page 80).

The edges of $\mathcal{B}_0$ are defined as follows. There exists an edge from a state S to a state S' in $\mathcal{B}_0$ labelled by $a|a'$ with $a, a' \in \mathcal{N}$ if and only if

$$S + \Phi(a) = \mathbf{A}S' + \Phi(a').$$

In particular, since $\circ$ denotes 0, there is an edge $\circ \xrightarrow{a|a} \circ$ for each $a \in \mathcal{N}$ (these edges are not represented in Figure 4.8).

Remark 4.3.13. Note that $\mathcal{B}_0$ is right resolving: to any state S and any input digit $a \in \mathcal{N}$, there is exactly one state S' and one output digit a' such that the addition in the graph can be performed, *i.e.*, such that $S \xrightarrow{a|a'} S' \in \mathcal{B}_0$.

Thus the automaton $\mathcal{B}_0$ can also perform the addition of $S + \sum_{i=0}^{n-1} \mathbf{A}^i\Phi(a_{n-i})$ for $S \in \mathcal{B}_0$ and $a_i \in \mathcal{N}$, simply by feeding $\mathcal{B}_0$ with the input digit string $(a_n, \ldots, a_1)$ from left to right starting from S and collecting the output digit string $(a'_n, \ldots, a'_1)$ and the landing state S'. In particular, to

$$S \xrightarrow{a_n|a'_n} S_1 \xrightarrow{a_{n-1}|a'_{n-1}} \cdots \xrightarrow{a_1|a'_1} S' \tag{4.3.9}$$

corresponds the addition

$$S + \sum_{i=0}^{n-1} \mathbf{A}^i\Phi(a_{n-i}) = \sum_{i=0}^{n-1} \mathbf{A}^i\Phi(a'_{n-i}) + \mathbf{A}^n S'. \tag{4.3.10}$$

Note that for $S' = 0$, *i.e.*, for a walk leading from S to 0 in $\mathcal{B}_0$, the term $\mathbf{A}^n S'$ vanishes. In this case the automaton produces from the string $(a_n, \ldots, a_1)$ corresponding to the "$\mathbf{A}$-adic" expansion of $z = \sum_{i=0}^{n-1} \mathbf{A}^i \Phi(a_{n-i})$ the string $(a'_n, \ldots, a'_1)$ which is the string of the "$\mathbf{A}$-adic" expansion of $z+S$.

Remark 4.3.14. By Remark 4.3.13, the final state S' and the outputs $(a'_n, \ldots, a'_1)$ are uniquely defined by the starting state S and the inputs $(a_n, \ldots, a_1)$.

The automaton emerging from $\mathcal{B}_0$ by leaving away the accepting state is called $\mathcal{B}$. It is helpful in order to characterize the boundary of $\mathcal{T}$, as the following results show.

Proposition 4.3.15 (Scheicher and Thuswaldner [58])**.** *The following equation holds for the boundary $\partial\mathcal{T}$ of $\mathcal{T}$:*

$$\partial\mathcal{T} = \bigcup_{S \in \mathcal{B}} (\mathcal{T} \cap (\mathcal{T} + S)). \tag{4.3.11}$$

Thus, even if $\mathcal{T}$ has more neighbors than the six presented here (see [5]), these neighbors are sufficient to describe the whole boundary.

Proposition 4.3.16 (Müller *et al.* [52])**.** *For $S \in \{\pm P, \pm Q, \pm R\}$ let $B_S := \mathcal{T} \cap (\mathcal{T} + S)$. Then $B_S \neq \emptyset$. Furthermore, if there exists an infinite walk*

$$S \xleftarrow{a_1|a'_1} S_1 \xleftarrow{a_2|a'_2} \ldots$$

in $\mathcal{B}$ such that $x = \sum_{i \geq 1} \mathbf{A}^{-i} \Phi(a_i)$ then $x \in B_S$.

As a consequence of these propositions and of the definition of $\mathcal{B}_0$, we have the following way to characterize that two n-th level subpieces of $\mathcal{T}$ have common points.

Characterization 4.3.17. *Let $n \in \mathbb{N}$ and $w = (a_1, \ldots, a_n)$, $w' = (a'_1, \ldots, a'_n)$ be two strings of length n. If there is a walk*

$$S_n \xrightarrow{a_n|a'_n} S_{n-1} \xrightarrow{a_{n-1}|a'_{n-1}} \ldots \xrightarrow{a_1|a'_1} \circ$$

in $\mathcal{B}_0$, then

$$\psi_w(\mathcal{T}) \cap \psi_{w'}(\mathcal{T}) \neq \emptyset.$$

Graph action of $\mathcal{B}_0$ on $\mathcal{G}$.

The structure of $\mathbf{M}$ will be understood with the help of the following graph action of $\mathcal{B}_0$ on the graph $\mathcal{G}$.

Definition 4.3.18 (Graph action of the counting automaton)**.** Let S be a state in $\mathcal{B}_0$, A a state of $\mathcal{G}$ and let $w = (A; a_1, \ldots, a_n) \in p_n(A)$. Take $(a_n, \ldots, a_1)$ as the input string for the automaton $\mathcal{B}_0$ with starting state S and denote the output string by $(a'_n, \ldots, a'_1)$. Then we define $\Psi_S(w) := (A; a'_1, \ldots a'_n)$. Ψ_S is called the *addition of S*. If the automaton $\mathcal{B}_0$ rests in $\circ$ after reading $(a_n, \ldots, a_1)$ and if $\Psi_S(w) \in p_n(A)$ then we say that the addition of S is *admissible* for w. Note that for a walk $w = (A)$ of length zero only $\Psi_\circ(w) = w$ is admissible.

Remark 4.3.19. By Characterization 4.3.17, the admissible addition of S to a string w produces a string $w' := \Psi_S(w)$ such that $\psi_w(\mathcal{T}) \cap \psi_{w'}(\mathcal{T}) \neq \emptyset$.

Definition 4.3.20 (Equivalence of walks)**.** Fix $n \in \mathbb{N}$, a state $A \in \mathcal{G}$ and let $w_1, w_2 \in W \subset p_n(A)$. Let $\psi_{w_1}(\mathcal{T})$ and $\psi_{w_2}(\mathcal{T})$ be the corresponding subsets of $\mathcal{T}$. We say that w_1 and w_2 are *W-equivalent* to each other, if there exist finitely many states $S_1, \ldots, S_m$ of $\mathcal{B}$ such that the following conditions hold with admissible additions Ψ_{S_j}.

$$\begin{aligned} \Psi_{S_m} \circ \cdots \circ \Psi_{S_1}(w_1) &= w_2 \quad \text{and} \\ \Psi_{S_j} \circ \cdots \circ \Psi_{S_1}(w_1) &\in W \quad (1 \leq j \leq m). \end{aligned}$$

We denote this by $w_1 \sim w_2\,(W)$ or simply by $w_1 \sim w_2$ if the underlying set W is clear from the context. In this case we also call the corresponding sets $\psi_{w_1}(\mathcal{T})$ and $\psi_{w_2}(\mathcal{T})$ W-equivalent and use the same notation $\psi_{w_1}(\mathcal{T}) \sim \psi_{w_2}(\mathcal{T})$.

If $w_1 = \Psi_S(w_2)$ we also write in a slight abuse of notation $w_1 \sim_S w_2$ or $w_2 \ {}_S\sim w_1$.

It is easy to check that $\sim$ is an equivalence relation.

Remark 4.3.21. We want to give some comments on these definitions.

1. Let $w = (A; a_1, \ldots, a_n) \in p_n(A)$ be a walk and assume that Ψ_{S_n} with $S_n \in \mathcal{B}_0$ is an admissible addition for w. Then from Definition 4.3.18 it follows that there exists a walk

$$S_n \xrightarrow{a_n|a'_n} S_{n-1} \xrightarrow{a_{n-1}|a'_{n-1}} \ldots \xrightarrow{a_2|a'_2} S_1 \xrightarrow{a_1|a'_1} \circ$$

in $\mathcal{B}_0$ such that $w' = (A; a'_1, \ldots, a'_n) \in p_n(A)$. Furthermore, we can perform this addition "digit wise", *i.e.*,

$$\Psi_{S_n}(A; a_1, \ldots, a_n) = \Psi_{S_j}(A; a_1, \ldots, a_j)\&(a'_{j+1}, \ldots, a'_n) = (A; a'_1, \ldots, a'_n).$$

Note that from this we easily see that

$$\psi_{\Psi_{S_n}(w)}(\mathcal{T}) = \psi_w(\mathcal{T} + S_n).$$

We even have, if $S_n^{(1)}, \ldots, S_n^{(m)}$ are m states of $\mathcal{B}_0$ such that the additions $\Psi_{S_n^{(j)}} \circ \cdots \circ \Psi_{S_n^{(1)}}(w)$ are admissible for $1 \leq j \leq m$, that

$$\psi_{\Psi_{S_n^{(m)}} \circ \cdots \circ \Psi_{S_n^{(1)}}(w)}(\mathcal{T}) = \psi_w(\mathcal{T} + S_n^{(m)} + \ldots + S_n^{(1)}).$$

2. Let w_1, w_2 be W-equivalent for some $W \subset p_n(A)$. Then there exist $v_1, \ldots, v_m$ with $v_1 := w_1$ and $v_m := w_2$ such that

$$\psi_{v_j}(\mathcal{T}) \cap \psi_{v_{j+1}}(\mathcal{T}) \neq \emptyset \quad (1 \leq j \leq m-1).$$

This follows immediately from Remark 4.3.19 together with Definition 4.3.20.

3. Let $W \subset p_n(A)$ and let $k < n$ be integers. Let $w_1, w_2 \in W$ such that $w_1|_k = w_2|_k =: \sigma$. Then there exist

$$\tau_1, \tau_2 \in W_\sigma := \{\tau; \sigma\&\tau \in W\}$$

such that $w_i = \sigma\&\tau_i$ $(i = 1, 2)$. If τ_1 and τ_2 are equivalent in W_σ then w_1 and w_2 are equivalent in W. This follows from the following fact together with Definition 4.3.20. Let $\tau, \tau' \in W_\sigma$ and $S \in \mathcal{B}_0$. Then

$$\Psi_S(\tau) = \tau' \quad \Longrightarrow \quad \Psi_S(\sigma\&\tau) = \Psi_\circ(\sigma)\&\tau' = \sigma\&\tau'.$$

This implies that

$$\tau \sim \tau'(W_\sigma) \quad \Longrightarrow \quad \sigma\&\tau \sim \sigma\&\tau'(W),$$

and this means that in order to examine equivalences of walks it often suffices to examine equivalences of their tails.

Definition 4.3.22 (Transitivity of a set of strings)**.** Fix $n \in \mathbb{N}$ and let $W \subset p_n(A)$ be a set of strings. Then W and the set

$$\mathcal{M}(W) := \{\psi_w(\mathcal{T}); w \in W\}$$

are called *transitive* if we have $w_1 \sim w_2(W)$ for each two $w_1, w_2 \in W$.

Remark 4.3.23. Since the subpiece $\psi_w(\mathcal{T})$ is arcwise connected for every string w (remember that $\mathcal{T}$ is arcwise connected), by definition of the equivalence relation in W, a transitive set $W \subset p_n(F, \circ)$ yields an arcwise connected subset $\mathcal{M}(W)$ of $\mathbf{M}$.

We end this subsection with a last definition.

Definition 4.3.24 (Admissible graph action)**.** Let A be a node of $\mathcal{G}$ and S a state of $\mathcal{B}_0$. If Ψ_S is admissible for all walks in $p(F, A)$ then we call Ψ_S an *admissible graph action* for A on $\mathcal{G}$, or an *A-action*, for short.

If Ψ_S is an A-action then we call

$$F(\Psi_S, A) := \{t(w'); w' = \Psi_S(w) \text{ for a walk } w \in p(F, A)\}$$

the *ending set of* (Ψ_S, A).

Remark 4.3.25. Consider the assertion

$$\Psi_S \textit{ is an } A\textit{-action with ending set } F(\Psi_S, A),$$

then we define the dual assertion

$$\Psi_{-S} \textit{ is an } A'\textit{-action with ending set } \{Z'; Z \in F(\Psi_S, A)\}.$$

4.3.3 Admissibility of all the additions for a class of walks in $\mathcal{G}$

This subsection is devoted to the proof of the following result.

Proposition 4.3.26. *Let w be a finite walk in $p(F, \circ)$. Then for each state S of $\mathcal{B}$ the addition $\Psi_S(w)$ is admissible for w.*

Remark 4.3.27. By Remarks 4.3.19 and 4.3.21.1 , this implies that for $w \in p_n(F, \circ)$, all the sets $\psi_w(\mathcal{T} + S)$ with $S \in \mathcal{B}_0$ are subpieces of $\mathcal{T}$ that have non-empty intersection with $\psi_w(\mathcal{T})$.

Suppose that w is a finite walk in $p(F, \circ)$. Then w is of the shape

$$F \xrightarrow{a_1} A_1 \xrightarrow{a_2} \cdots \xrightarrow{a_k} A_k \xrightarrow{a_{k+1}} \circ \xrightarrow{a_{k+2}} \cdots \xrightarrow{a_n} \circ \qquad (A_k \neq \circ) \tag{4.3.12}$$

for some $2 \leq k < n$. Let $S_n := S$. Note that S_n together with the labels $(a_1, \ldots, a_n)$ defines uniquely the walk

$$S_n \xrightarrow{a_n|a'_n} S_{n-1} \xrightarrow{a_{n-1}|a'_{n-1}} \cdots \xrightarrow{a_{k+2}|a'_{k+2}} S_{k+1} \xrightarrow{a_{k+1}|a'_{k+1}} S_k \xrightarrow{a_k|a'_k} \cdots \xrightarrow{a_1|a'_1} S_0 \tag{4.3.13}$$

in $\mathcal{B}_0$ (recall that $\mathcal{B}_0$ is right resolving by Remark 4.3.13). By the definition of Ψ_S this walk yields the identities

$$\Psi_S(w) = \Psi_{S_j}(a_1, \ldots, a_j)\&(a'_{j+1}, \ldots, a'_n) = \Psi_{S_k}(a_1, \ldots, a_k)\&(a'_{k+1}, \ldots, a'_n). \tag{4.3.14}$$

We want to show that $\Psi_S(w)$ is a walk in $p(F)$ and that $S_0 = \circ$ for all states S of $\mathcal{B}$. We first need the following lemma.

Lemma 4.3.28. *Ψ_S is an A-action in the following cases:*

(L,-Q): Ψ_{-Q} is an L-action with $F(\Psi_{-Q}, L) \subset \{\circ, L', K'\}$.

(L,R): Ψ_R is an L-action with $F(\Psi_R, L) \subset \{\circ, I', J', L', M'\}$.

(L,P): Ψ_P is an L-action with $F(\Psi_P, L) \subset \{L, M, I, N'\}$.

(L,-P): Ψ_{-P} *is an* L*-action with* $F(\Psi_{-P}, L) \subset \{L, H, J\}$.

(M,-Q): Ψ_{-Q} *is an* M*-action with* $F(\Psi_{-Q}, M) \subset \{\circ, J'\}$.

(M,R): Ψ_R *is an* M*-action with* $F(\Psi_R, M) \subset \{\circ, L'\}$.

(M,P): Ψ_P *is an* M*-action with* $F(\Psi_P, M) \subset \{\circ\}$.

(M,-P): Ψ_{-P} *is an* M*-action with* $F(\Psi_{-P}, M) \subset \{L\}$.

(H,-Q): Ψ_{-Q} *is an* H*-action with* $F(\Psi_{-Q}, H) \subset \{I', K\}$.

(H,P): Ψ_P *is an* H*-action with* $F(\Psi_P, H) \subset \{I, L\}$.

(H,-P): Ψ_{-P} *is an* H*-action with* $F(\Psi_{-P}, H) \subset \{G\}$.

(I,-Q): Ψ_{-Q} *is an* I*-action with* $F(\Psi_{-Q}, I) \subset \{H', J\}$.

(I,R): Ψ_R *is an* I*-action with* $F(\Psi_R, I) \subset \{\circ, L', K, I'\}$.

(I,-P): Ψ_{-P} *is an* I*-action with* $F(\Psi_{-P}, I) \subset \{H, L\}$.

(J,Q): Ψ_Q *is an* J*-action with* $F(\Psi_Q, J) \subset \{I, K'\}$.

(J,-Q): Ψ_{-Q} *is an* J*-action with* $F(\Psi_{-Q}, J) \subset \{\circ, J', M'\}$.

(J,R): Ψ_R *is an* J*-action with* $F(\Psi_R, J) \subset \{\circ, L'\}$.

(J,P): Ψ_P *is an* J*-action with* $F(\Psi_P, J) \subset \{L\}$.

(J,-P): Ψ_{-P} *is an* J*-action with* $F(\Psi_{-P}, J) \subset \{\circ, K\}$.

(K,Q): Ψ_Q *is an* K*-action with* $F(\Psi_Q, J) \subset \{H, J'\}$.

(K,-Q): Ψ_{-Q} *is an* K*-action with* $F(\Psi_{-Q}, K) \subset \{\circ, L'\}$.

(K,-R): Ψ_{-R} *is an* K*-action with* $F(\Psi_{-R}, K) \subset \{\circ, I\}$.

(K,P): Ψ_P *is an* K*-action with* $F(\Psi_P, K) \subset \{\circ, J\}$.

Moreover, the duals of these assertions are also true, that is to say: if for some pair $S \in \mathcal{B}$ *and* $A \in \mathcal{G}$

$$\textit{(A,S):}\ \Psi_S \textit{ is an } A\textit{-action with } F(\Psi_S, A) \subset \{A_1, \ldots, A_k\}$$

holds then also the dual statement

$$\textit{(A',-S):}\ \Psi_{-S} \textit{ is an } A'\textit{-action with } F(\Psi_{-S}, A') \subset \{A'_1, \ldots, A'_k\}$$

holds.

Remark 4.3.29. Note that $\Psi_\circ$ is an A-action (with set of ending states $\{A\}$) for every $A \in \mathcal{G}$.

Proof. The statement will be proved by induction on the length of the walks $w \in p(F)$. The assertion $(A, S)_n$ stands for: *(A,S) holds for all walks up to length* n. If there is no walk in $p_k(F, A)$ for $k \leq n$, then $(A, S)_n$ is true.
For $n \leq 1$ the statements $(A, S)_n$ for the pairs (A, S) in the proposition are all true.
Suppose now that $(A, S)_{n-1}$ is true for all pairs (A, S) of the proposition and their duals. We show that all $(A, S)_n$'s and their duals are also true. We will show how to proceed for the case of $(L, -Q)_n$ and sum up the results for all the cases in a table.

$(A,S)_n$	a_n	A_{n-1} (A_{n-2})	a'_n (a'_{n-1})	S_{n-1} (S_{n-2})	end of $\Psi_{S_{n-i}}(w\|_{n-i})$	end of $\Psi_S(w)$
$(L,-Q)_n$	$0,1,2$	H'	4	Q	I,K'	$\circ$
		K'	2		$\circ,L$	$\circ,L'$
		I'	4		H,J'	K'
		L'	4		$\circ,L,K$	$\circ,L'$
		M'	4		$\circ,J$	$\circ$
	$3,4$	H'	0	$-P$	I',L'	$\circ$
		L'	0		I',L',M',N	$\circ,L'$
		M'	$0,1$		$\circ$	$\circ$
		N' (I')	1 (2)	$-P$ ($\circ$)	I'	L'
$(L,R)_n$	$0,1,2,3$	H'	$3,4$	Q	I,K'	$\circ,J'$
		K'	1		$\circ,L$	$\circ,L'$
		L'	$3,4$		$\circ,L,K$	$\circ,J',M',L'$
		I'	3		H,J'	$\circ,J'$
		M'	$3,4$		$\circ,J$	$\circ$
	4	M'	0	$-P$	$\circ$	$\circ$
		N'	0 (2)	$-P$ ($\circ$)	I'	I'
$(L,P)_n$	$0,1,2,3$	H'	$3,4$	$\circ$	H'	I,L
		K'	1		K'	M
		L'	$3,4$		L'	L,I
		I'	3		I'	N'
		M'	$3,4$		M'	L
	4	M' (K)	0 (4)	R (Q)	H,J'	L
		N' (I')	0 (4)		J',H	L
$(L,-P)_n$	$1,2,3,4$	H'	$1,2$	$\circ$	H'	J,L
		L'	$1,2$		L'	J,L
		I'	1		I'	J
		M'	$1,2,3$		M'	J,L
		N'	3		N'	H
	0	K' (J')	4 (3)	$-R$ ($-Q$)	I',K	L
$(M,-Q)_n$	1	K'	3	Q	$\circ,L$	$\circ,J'$
$(M,R)_n$	1	K'	2	Q	$\circ,L$	$\circ,L'$
$(M,P)_n$	1	K'	2	$\circ$	K'	$\circ$
$(M,-P)_n$	1	K'	0	$\circ$	K'	L
$(H,-Q)_n$	3	N' (I')	0 (2)	$-P$ ($\circ$)	I'	I'
		G' ($F;G,N$)	0 ($0;1$)	$-P$ ($\circ$)	F,G,N	I',K
$(H,P)_n$	3	N',G'	4	$\circ$	N',G'	L,I
$(H,-P)_n$	3	N',G'	2	$\circ$	N',G'	G
$(I,-Q)_n$	4	H'	1	$-P$	I',L'	J
		L'			I',M',L',N	J,H'
		G' ($F;G,N$)	1 ($0;1$)	$-P$ ($\circ$)	F,G,N	H',J
$(I,R)_n$	4	H'	0	$-P$	I',L'	$\circ,L'$
		L'			I',M',L',N	$\circ,L'$
		G' ($F;G,N$)	0 ($0;1$)	$-P$ ($\circ$)	F,G,N	I',K
$(I,-P)_n$	4	G',L',H'	3	$\circ$	G',L',H'	H,L
$(J,Q)_n$	1	H'	4	P	G'	I
		M'			L'	I
		I'			H',L'	I
		L'			H',L',J'	I,K'
$(J,-Q)_n$	1	H'	3	Q	K',I	$\circ,J'$
		M'			$\circ,J$	$\circ$
		I'			H,J'	$\circ,J'$
		L'			$\circ,L,K$	$\circ,J',M'$

Table 4.2: Proof of Lemma 4.3.28.

$(A,S)_n$	a_n	A_{n-1} (A_{n-2})	a'_n (a'_{n-1})	S_{n-1} (S_{n-2})	end of $\Psi_{S_{n-i}}(w\|_{n-i})$	end of $\Psi_S(w)$
$(J,R)_n$	1	H'	2	Q	K',I	$\circ, L'$
		M'			$\circ, J$	$\circ$
		I'			H, J'	$\circ, L'$
		L'			$\circ, L, K$	$\circ, L'$
$(J,P)_n$	1	H',M',I',L'	2	$\circ$	H',M',I',L'	L
$(J,-P)_n$	1	H',M',I',L'	0	$\circ$	H',M',I',L'	$\circ, K$
$(K,Q)_n$	0	H'	3	P	G'	H
		J			L	J'
$(K,-Q)_n$	0	H', J	2	Q	K',I	$\circ, L'$
$(K,-R)_n$	0	H'	4	P	G'	I
		J			L	$\circ$
$(K,P)_n$	0	H', J	1	$\circ$	H', J	$\circ, J$

Table 4.3: Proof of Lemma 4.3.28: end of the preceding table.

We have to show that Ψ_{-Q} is an L-action for all walks w of length at most n with ending set $F(\Psi_{-Q}, L) \subset \{\circ, L', K'\}$. Let $w = (a_1, \ldots, a_n)$ such that there is a walk

$$A \xrightarrow{a_1} A_1 \xrightarrow{a_2} \ldots \xrightarrow{a_{n-2}} A_{n-2} \xrightarrow{a_{n-1}} A_{n-1} \xrightarrow{a_n} L$$

in $\mathcal{G}$. Then by Remark 4.3.13 the input digits $(a_n, \ldots, a_1)$ define a unique walk in $\mathcal{B}_0$ starting from $-Q$:

$$-Q \xrightarrow{a_n|a'_n} S_{n-1} \xrightarrow{a_{n-1}|a'_{n-1}} S_{n-2} \xrightarrow{a_{n-2}|a'_{n-2}} \ldots \xrightarrow{a_1|a'_1} S_0.$$

First suppose that $a_n \in \{0,1,2\}$, *i.e.*, by $\mathcal{B}_0$, $S_{n-1} = Q$. Then

$$\Psi_{-Q}(w) = \Psi_Q(w|_{n-1})\&(a'_n).$$

According to $\mathcal{G}$, since w ends up in L and $a_n \in \{0,1,2\}$, $w|_{n-1}$ can end up in H', K', I', L' or M', *i.e.*, $A_{n-1} \in \{H', K', I', L', M'\}$. If $A_{n-1} = H'$, then $a_n = 2$, because the edge leading from H' to L in $\mathcal{G}$ has only the labels $\{2,3\}$, and we assumed $a_n \in \{0,1,2\}$. Thus $a'_n = 4$, as indicated by the edge $-Q \xrightarrow{2|4} Q$ of $\mathcal{B}_0$. Moreover, by $(H', Q)_{n-1}$, which is the dual of $(H, -Q)_{n-1}$, we have $Q \xrightarrow{w|_{n-1}^T} \circ$ in $\mathcal{B}_0$ and $\Psi_Q(w|_{n-1})$ ends up in $\{I, K'\}$. Thus $-Q \xrightarrow{w^T} \circ$, *i.e.*, $S_0 = \circ$, and $\Psi_{-Q}(w)$ ends up in $\{\circ\}$, because of the edges $I \xrightarrow{4} \circ$ and $K' \xrightarrow{4} \circ$ in $\mathcal{G}$. We can argue along the same lines if $A_{n-1} \in \{K', I', L', M'\}$. All these cases lead to walks $\Psi_{-Q}(w)$ ending in $\circ$, K' or L'.

Secondly, suppose that $a_n \in \{3,4\}$, *i.e.*, by $\mathcal{B}_0$, $S_{n-1} = -P$. Then

$$\Psi_{-Q}(w) = \Psi_{-P}(w|_{n-1})\&(a'_n).$$

According to $\mathcal{G}$, since w ends up in L and $a_n \in \{3,4\}$, $w|_{n-1}$ can only end up in H', L', M' or N', *i.e.*, $A_{n-1} \in \{H', L', M', N'\}$. The first three cases can be treated as above and lead to $\Psi_{-Q}(w)$ ending in $\circ$ or L', so let us assume that $A_{n-1} = N'$. Then, the only edge in $\mathcal{G}$ leading from N' to L being $N' \xrightarrow{4} L$, we have $a_n = 4$, and since there is only one edge landing in N' ($I' \xrightarrow{3} N'$), we even have $A_{n-2} = I'$ and $a_{n-1} = 3$. Thus, by the edges $-Q \xrightarrow{4|1} -P \xrightarrow{3|2} \circ$ of $\mathcal{B}_0$, we read $a'_n = 1$, $a'_{n-1} = 2$ and $S_{n-2} = \circ$. Consequently, we have $\circ \xrightarrow{w|_{n-2}^T} \circ$, and $\Psi_\circ(w|_{n-2}) = w|_{n-2}$ ends up in $\{I'\}$. Thus again $S_0 = \circ$ and

$$\Psi_{-Q}(w) = \Psi_\circ(w|_{n-2})\&(a'_{n-1}, a'_n) = w|_{n-2}\&(2,1)$$

ends up in $\{L'\}$, as it can be checked on $\mathcal{G}$ by considering the edges $I' \xrightarrow{2} L \xrightarrow{1} L'$.

Thus in all cases $\Psi_{-Q}(w)$ is a walk in $p(F)$ ending up in $\{\circ, L', K'\}$. Thus $(L, -Q)_n$ is true and we are done.

All the other assertions can be treated likewise. The occurring cases are summed up in Tables 4.2 and 4.3 from which the complete proof can be read off easily. In these tables, A_{n-2}, a'_{n-1} and S_{n-2} are given if they are needed, and in this case we use $i = 2$ in the 6-th column, otherwise $i = 1$. □

Proposition 4.3.26 will be proved inductively: let w be a finite walk in $p(F, \circ)$ and $j \geq k+1$, where k is defined by (4.3.12). We will show that for every $j \geq k+1$, the addition $\Psi_S(w|_j)$ is admissible for each state S of $\mathcal{B}$: taking for j the length n of w will yield the result. Lemma 4.3.30 will contain the induction start, Lemma 4.3.31 the induction step.

Lemma 4.3.30. *Suppose that w is a walk of the shape (4.3.12). Then the following assertions hold.*

(i) $\Psi_P(w|_{k+1})$ *ends in* $\{\circ, M', K', J\}$.

(ii) $\Psi_Q(w|_{k+1})$ *ends in* $\{\circ, J, K, L\}$.

(iii) $\Psi_R(w|_{k+1})$ *ends in* $\{\circ, L', J', I', K\}$.

(iv) $w|_{k+1}$ *ends in* $\{\circ\}$.

Their associated duals also hold ("$\Psi_S(w|_{k+1})$ ends in the set of states $\mathcal{A}$" has the dual "$\Psi_{-S}(w|_{k+1})$ ends in $\mathcal{A}'$ ").

In particular, $\Psi_S(w|_{k+1})$ is a walk in $p(F)$ for all $S \in \mathcal{B}_0$. Moreover, $S \xrightarrow{w|_{k+1}^T} \circ$ for all $S \in \mathcal{B}_0$. That is to say, $\Psi_S(w|_{k+1})$ is admissible for all $S \in \mathcal{B}_0$.

Proof. Let $S \in \mathcal{B}_0$. Note that the following edges exist:

$$\begin{array}{rl} A_k \xrightarrow{a_{k+1}} \circ & \text{in } \mathcal{G} \text{ by definition of } k \text{ and} \\ S \xrightarrow{a_{k+1}|a'_{k+1}} S' & \text{in } \mathcal{B} \text{ for some } S' \in \mathcal{B}_0 \end{array} \tag{4.3.15}$$

(the second edge is uniquely defined by S and a_{k+1}). We recall the identity:

$$\Psi_S(w|_{k+1}) = \Psi_{S'}(w|_k)\&(a'_{k+1}). \tag{4.3.16}$$

To (i): $S = P$. Depending on a_{k+1}, the edge $P \xrightarrow{a_{k+1}|a'_{k+1}} S'$ of (4.3.15) in $\mathcal{B}_0$ implies that $S' = \circ$ or R, which fix the range of a'_{k+1} ($a'_{k+1} = 0$ if $S' = R$ and $a'_{k+1} \in \{1, \ldots, 4\}$ if $S' = \circ$). The possible states A_k are also determined by a_{k+1} via the existence of the edge $A_k \xrightarrow{a_{k+1}} \circ$ in $\mathcal{G}$ (see (4.3.15)). Using the corresponding assertion (A_k, S') of Lemma 4.3.28 it is then easy to get the possible endings of $\Psi_{S'}(w|_k)$. Now if $Y \in \mathcal{G}$ is such an ending, then, by (4.3.16), with the range of a'_{k+1} one obtains the possible endings Z of $\Psi_S(w|_{k+1})$ by looking for all edges $Y \xrightarrow{a'_{k+1}} Z$ in $\mathcal{G}$. Let us consider an example: if $a_{k+1} = 4$, we are considering the edge $P \xrightarrow{4|0} R$ in B_0, thus $S' = R$ and $a'_{k+1} = 0$. Moreover, $A_k \in \{K', L, J, I, M\}$ because these states are the only starting states of edges in $\mathcal{G}$ labelled by 4 and leading to $\circ$. For $A_k = K'$, using (K', R) of Lemma 4.3.28 we get that $\Psi_R(w|_k)$ ends up in $\circ$ or I'. Consequently, since $a'_{k+1} = 0$, $\Psi_P(w|_{k+1})$ ends up in $\circ$: indeed, we have $\circ \xrightarrow{0} \circ$ and $I' \xrightarrow{0} \circ$ in $\mathcal{G}$. Note that (K', R) also implies $R \xrightarrow{w|_k^T} \circ$ in $\mathcal{B}_0$, thus $P \xrightarrow{w|_{k+1}^T} \circ$.
The results for the other values of a_{k+1} are given in Table 4.4.

The proof is the same for the other cases ($S = Q, S = R$) and their duals, it is summed up in Table 4.4 for $S = Q$ and $S = R$. Item (iv) is clear. □

S	a_{k+1}	S'	A_k	end of $\Psi_{S'}(w\|_k)$	a'_{k+1}	end of $\Psi_S(w\|_{k+1})$
P	$0,1,2,3$	$\circ$	L'	L'	1	J
			J	J	$2,3,4$	$\circ$
			J'	J'	$1,2,3,4$	$\circ, K'$
			K	K	$1,2,3$	$\circ, M'$
			K'	K'	$3,4$	$\circ$
			M'	M'	$3,4$	$\circ$
	4	R	J	$\circ, L'$		
			I	$\circ, I', K, L'$		
			L	$\circ, J', L', M', I'$	0	$\circ$
			K'	$\circ, I'$		
			M	$\circ, L'$		
Q	$0,1$	P	K	$\circ, J$	$3,4$	$\circ$
			L'	H', J', L'	3	$\circ, L$
			J	L	4	$\circ$
			M'	L'	3	L
			I'	$\circ, K'$	$3,4$	L
			J'	$\circ, K'$	$3,4$	$\circ$
	$2,3,4$	$-Q$	K'	H', J	$0,1,2$	$\circ, K, J, L$
			L	$\circ, L', K'$	2	$\circ, L$
			K	$\circ, L'$	0	$\circ$
			J'	K, I'	$0,1$	$\circ$
			I	H', J	2	$\circ, L$
			J	$\circ, M', J'$	$0,1,2$	$\circ, J, L$
			M	$\circ, J'$	2	$\circ$
R	$0,1,2,3$	Q	K	H, J'	$1,2,3$	$\circ, L'$
			K'	$\circ, L$	$3,4$	$\circ, J'$
			L'	$\circ, L, K$	1	$\circ, L'$
			J	I, K'	$2,3,4$	$\circ, L', J'$
			J'	$\circ, M, J$	$1,2,3,4$	$\circ, J', L'$
			I'	H, J'	1	$\circ, L'$
			M'	$\circ, J$	1	$\circ$
	4	$-P$	K'	$\circ, J'$		$\circ, L'$
			L	H, J, L		I', K
			J	$\circ, K$	0	$\circ$
			I	H, L		I'
			M	L		I'

Table 4.4: Proof of Lemma 4.3.30.

Again, let w be a finite walk in $p(F,\circ)$ and $j \geq k+1$, where k is defined by (4.3.12). We call (B_j) the assertion: *for all* $S \in \mathcal{B}_0, \Psi_S(w|_j)$ *is a walk in* $p(F)$ *with possible ending states given in Table 4.5. Moreover,* $S \xrightarrow{w|_j^T} S_0 = \circ$ *in* $\mathcal{B}_0$. In particular, (B_j) states that $\Psi_S(w|_j)$ is admissible for all $S \in \mathcal{B}_0$.
By Lemma 4.3.30, (B_{k+1}) already holds. The induction step is contained in the following lemma.

walk	possible ending states
$\Psi_\circ(w\|_j)$	$\{\circ\}$
$\Psi_P(w\|_j)$	$\{\circ, M', K', J\}$
$\Psi_{-P}(w\|_j)$	$\{\circ, M, K, J'\}$
$\Psi_Q(w\|_j)$	$\{\circ, J, K, L, M\}$
$\Psi_{-Q}(w\|_j)$	$\{\circ, J', K', L', M'\}$
$\Psi_R(w\|_j)$	$\{\circ, L', J', I', M', K\}$
$\Psi_{-R}(w\|_j)$	$\{\circ, L, J, I, M, K'\}$

Table 4.5: Table of statement (B_j).

Lemma 4.3.31. *If* (B_j) *holds for some* $j \geq k+1$*, then* (B_{j+1}) *holds too.*

Proof. First we deal with the case of $S = P$. Then there is an edge $P \xrightarrow{a_{j+1}|a'_{j+1}} S'$ in $\mathcal{B}_0$, thus $S' \in \{\circ, R\}$. Remember that $\Psi_P(w|_{j+1}) = \Psi_{S'}(w|_j)\&(a'_{j+1})$.

By assumption (B_j), $S' \xrightarrow{w|_j^T} \circ$, thus $P \xrightarrow{a_{j+1}|a'_{j+1}} S' \xrightarrow{w|j^T} \circ$, *i.e.*, $P \xrightarrow{w|j+1^T} \circ$ in $\mathcal{B}_0$.

Moreover, if $S' = \circ$, then $\Psi_P(w|_{j+1}) = w|_j\&(a'_{j+1})$ is a walk in $p(F)$ that ends at $\circ$: indeed, $w|_j$ is in $p(F)$ and $j \geq k+1$, so by (4.3.12) $w|_j$ already ends at $\circ$; its concatenation with (a'_{j+1}) remains in $p(F)$, because $\circ \xrightarrow{a'_{j+1}} \circ$.

If $S' = R$, then the edge $P \xrightarrow{a_{j+1}|a'_{j+1}} R$ in $\mathcal{B}_0$ indicates that $a'_{j+1} = 0$. Hence $\Psi_P(w_{j+1}) = \Psi_R(w|_j)\&(a'_{j+1})$, with $\Psi_R(w|_j)$ walk in $p(F)$ ending at $Y \in \{\circ, L', J', I', M', K\}$ by assumption (B_j) (see Table 4.5 for the endings). Now we can check on $\mathcal{G}$ that there is an edge starting from each $Y \in \{\circ, L', J', I', M', K\}$ and labelled by 0. They all lead to $\circ$.

The other cases $(S = Q, S = R)$ as well as their duals are treated in a similar way (see Table 4.6 for $S = Q, S = R$). □

Proof of Proposition 4.3.26. Let w be a walk in $p_n(F,\circ)$ of the shape (4.3.12) and the resulting walk in $\mathcal{B}_0$ given by (4.3.13). If $n = k+1$, then $w|_{k+1} = w$ and Lemma 4.3.30 gives the result

S_{j+1}	S_j	a'_{j+1}	end of $\Psi_{S_j}(w\|_j)$	end of $\Psi_{S_{j+1}}(w\|_{j+1})$
P	$\circ$	$1,2,3,4$	$\circ$	$\circ$
	R	0	$\circ, J', L', I', M', K$	$\circ$
Q	P	$3,4$	$\circ, J, K', M'$	$\circ, L$
	$-Q$	$0,1,2$	$\circ, L', K', J', M'$	$\circ, J, L, M$
R	Q	$1,2,3,4$	$\circ, L, K, J, M$	$\circ, L', J', M'$
	$-P$	0	$\circ, J', K, M$	$\circ, L'$

Table 4.6: Proof of Lemma 4.3.31.

immediately. Otherwise, starting from the same lemma and going on with Lemma 4.3.31 from $j = k + 1$ to $j = n$, we also obtain the statement of Proposition 4.3.26. □

4.3.4 Equivalences of paths

The main result of this subsection, Proposition 4.3.33, will be used in Subsection 4.3.7 to construct arcs inside int(**M**) from arbitrary points contained in a subpiece $\psi_w(\mathcal{T})$, where $w \in p(F, \circ)$, to the point 0 (contained in $\psi_{(0,0,0)}(\mathcal{T})$).
In the following, the equivalences of walks from the set G_k defined as in (4.3.8) for some $k \in \mathbb{N}$ will take place in G_k. First we note the following fact about the walks of length 3.

Remark 4.3.32. We have $G_3 = \{(F; 0, 0, 0), (F; 1, 4, 4)\}$ and these walks are equivalent in G_3. Namely, $(F; 1, 4, 4) = \Psi_{-P}((F; 0, 0, 0))$. In other words, G_3 is transitive.

Proposition 4.3.33. *Let $n \geq 4$ and $w \in G_n$. Then there is a walk $w' \in G_{n+1}$ such that $w'|_{n-1} \in G_{n-1}$ and $w\&d \sim w'$ for some $d \in \{0, \ldots, 4\}$.*

In view of Remark 4.3.21.2 this proposition says the following. Let w be a walk in G_n and let $\psi_w(\mathcal{T})$ be the associated subset of $\mathcal{T}$. Then $\psi_w(\mathcal{T})$ contains a subpiece $\psi_{w\&d}(\mathcal{T})$ with the following property. There exist walks $w\&d = v_1, v_2, \ldots, v_k = w'$ in G_{n+1} such that the associated subpieces satisfy

$$\psi_{v_j}(\mathcal{T}) \cap \psi_{v_{j+1}}(\mathcal{T}) \neq \emptyset \qquad (1 \leq j \leq k-1).$$

Since $w'' := w'|_{n-1} \in G_{n-1}$, this means that one can draw an arc from each piece $\psi_w(\mathcal{T})$ of $\mathcal{M}(G_n)$ to a piece $\psi_{w''}(\mathcal{T})$ of $\mathcal{M}(G_{n-1})$. By induction on n this will lead to a proof of the connectivity of **M** because it allows to draw arcs from each point of **M** to the connected set $\psi_{(F;0,0,0)}(\mathcal{T}) \subset \mathbf{M}$.

Remark 4.3.34.

1. If $w\&d \sim w'$ for $w \in G_n$ and $d \in \{0, \ldots, 4\}$, then by using $\Psi_{\pm P}$ we even have $w\&d \sim w'$ for every $d \in \{0, \ldots, 4\}$.

2. If two walks w and w' of G_n are equivalent, then there exist $d, d' \in \{0, \ldots, 4\}$ with $w\&d \sim w'\&d'$. This means that two intersecting pieces $\psi_w(\mathcal{T})$ and $\psi_{w'}(\mathcal{T})$ (*i.e.*, such that $\psi_w(\mathcal{T}) \cap \psi_{w'}(T) \neq \emptyset$) contain intersecting subpieces $\psi_{w\&d}(\mathcal{T})$ and $\psi_{w'\&d'}(\mathcal{T})$. In particular it is sufficient to find a walk $w' \in G_n$ with $w'|_{n-1} \in G_{n-1}$ and $w \sim w'$. In this case w will automatically fulfil Proposition 4.3.33.

3. For $p \in \mathbb{N}$, we introduce the notation $w \ {}_{S^p}\sim \ w'$: this means that w' is obtained after applying Ψ_S to w for p times.

Proposition 4.3.33 will be shown via the following lemmata. By Remark 4.3.21.3, we just have to concentrate on the tails of the walks. Moreover, the lemmata correspond to the following classes of walks:

$$E_n(A) := \{w \in G_n,\ w \text{ contains the edge } A \to \circ\ \} \qquad (a \in \mathcal{G} \setminus \{\circ\}).$$

Sloppily spoken the walks contained in $E_n(A)$ are those walks of G_n which reach the accepting state via the state A. Note that

$$G_n = \bigcup_{A \in \mathcal{G}} E_n(A). \tag{4.3.17}$$

Lemma 4.3.35. *Let $n \geq 4$ and $w \in E_n(K) \cup E_n(K')$. Then there is a walk $w' \in G_{n+1}$ such that $w'|_{n-1} \in G_{n-1}$ and $w\&d \sim w'$ for some $d \in \{0, \ldots, 4\}$.*

Proof. Let us consider $w \in E_n(K)$. If $w|_{n-1} \in E_{n-1}(K)$, we are ready. We suppose it is not the case. We have the following cases for the tails τ of $w = \sigma\&\tau$ (σ is fixed by w and τ).

(1) $\tau = (J; 0, a)$ with $a \in \{0, 1, 2\}$. Then

$$(J; 0, 2)\ {}_{-P}\sim (J; 0, 1)\ {}_{-P}\sim (J; 0, 0)\ {}_{Q}\sim (J; 1, 3) \prec (J; 1),$$

which ends at $\circ$. Thus $w \sim \sigma\&(J; 1, 3)$ with $\sigma\&(J; 1) \in G_{n-1}$, and we are ready by Remark 4.3.34.2.

(2) $\tau = (A; d, 1, 0, a)$ with $(A, d) \in \mathcal{C} := \{(F, 0), (G', 2), (N', 2), (I, 1)\}$ and $a \in \{0, 1, 2\}$. Then for all constellations $(A, d) \in \mathcal{C}$, we have

$$\begin{array}{rl} (A; d, 1, 0, 0)\ {}_P \sim & (A; d, 1, 0, 1)\ {}_P \sim (A; d, 1, 0, 2)\ {}_Q \sim (A; d+1, 4, 2, 0)\ {}_Q \sim (A; d+1, 4, 3, 3) \\ {}_{(-P)^3} \sim & (A; d+1, 4, 3, 0)\ {}_Q \sim (A; d+1, 4, 4, 3) \prec (A; d+1, 4, 4), \end{array}$$

which ends at $\circ$. Thus $w \sim \sigma\&(A; d+1, 4, 4, 3)$ with $\sigma\&(A; d+1, 4, 4) \in G_{n-1}$, and we are ready by Remark 4.3.34.2.

One can proceed identically for $w \in E_n(K')$ by considering the dual walks of the previous ones. Thus Lemma 4.3.35 is proved. □

Lemma 4.3.36. *Let $n \geq 4$ and $w \in E_n(J) \cup E_n(J')$. Then there is a walk $w' \in G_{n+1}$ such that $w'|_{n-1} \in G_{n-1}$ and $w\&d \sim w'$ for some $d \in \{0, \ldots, 4\}$.*

Proof. Let us consider $w \in E_n(J)$. If $w|_{n-1} \in E_{n-1}(J)$, we are ready. We suppose it is not the case. Then the tail τ of $w = \sigma\&\tau$ has the form $\tau = (A; 1, a)$ with $A \in \mathcal{A} := \{L', M', I', H'\}$ and $a \in \{1, 2, 3, 4\}$. We have the following equivalences for $A \in \mathcal{A}$:

$$(A; 1, 1)\ {}_P \sim (A; 1, 2)\ {}_P \sim (A; 1, 3)\ {}_P \sim (A; 1, 4)\ {}_{-Q} \sim (A; 0, 1).$$

For $A \in \{L', M', I'\}$, $\sim (A; 0, 1) \prec (A; 0)$, which ends at $\circ$. Thus $w \sim \sigma\&(A; 0, 1)$ with $\sigma\&(A; 0) \in G_{n-1}$, and we are ready by Remark 4.3.34.2.

For $A = H'$, we have $w = \sigma\&(H'; 0, 1)$ which is now a walk belonging to $E_n(K)$, thus we obtain the required result by using Lemma 4.3.35.

One can proceed identically for $w \in E_n(J')$, thus Lemma 4.3.36 is proved. □

Lemma 4.3.37. *Let $n \geq 4$ and $w \in E_n(L) \cup E_n(L')$. Then there is a walk $w' \in G_{n+1}$ such that $w'|_{n-1} \in G_{n-1}$ and $w\&d \sim w'$ for some $d \in \{0, \ldots, 4\}$.*

Proof. Let us consider $w \in E_n(L')$. If $w|_{n-1} \in E_{n-1}(L')$, we are ready. We suppose it is not the case. Then w belongs to one of the following classes of tails τ of $w = \sigma\&\tau$ (σ is fixed by w and τ).

(1.*i*) $\tau = (L; 2, 0)$. Then $(L; 2, 0)\ {}_Q \sim (L; 3, 3)$ which leads to a walk $\sigma\&(L; 3, 3)$ equivalent to w which belongs to $E_n(J')$, treated in Lemma 4.3.36.

(1.*ii*) $\tau = (L; 1, 0)$. We subdivide this class into the following smaller classes:
A. $(A; d, 1, 0)$ with $(A, d) \in \mathcal{C}_A := \{(K', 0), (H', a), (L', a), a \in \{2, 3\}\}$.
B. $(K; 3, d, 1, 0)$ with $d \in \{2, 3, 4\}$.
C. $(I'; 3, 4, 1, 0)$.
D. $(A; d, 0, (3, 4, 0)^p, 2, 1, 0)$ for some $p \in \mathbb{N}$ and

$$\begin{array}{rl} (A, d) \in \mathcal{C}_D := & \{(F, 0), (K', 0), (I', 2), (M', 4), \\ & (G', a), (N', a), (H'a), (L', a), (M', a), a \in \{2, 3\}\}. \end{array}$$

Here $(3, 4, 0)^p$ inside the walk means that the sequence of digits $(3, 4, 0)$ has to be read p times before going on to the digit 2. This corresponds to the cycle $I' \to N' \to L \to I'$ in the graph of Figure 4.7.

A. We have for $(A, d) \in \mathcal{C}_A$: $(A; d, 1, 0)\ {}_{-Q} \sim (A; d+1, 4, 2) \prec (A; d+1, 4)$, which ends at $\circ$.

B. We have for $d = 3, 4$ that $(K; 3, d, 1, 0)\ {}_{-P} \sim (K; 2, d-3, 0, 4) \prec (K; 2)$, which ends at $\circ$, and $(K; 3, 2, 1, 0)\ {}_{-Q} \sim (K; 3, 3, 4, 2) \prec (K; 3, 3, 4)$, which ends at $\circ$.

C. We have $(I';3,4,1,0)\ {}_{-P}\sim (I';2,1,0,4)\prec (I';2,1,0)$, which ends at $\circ$ too.

D. The following chain holds for every $(A,d)\in\mathcal{C}_D\setminus\{(M',4)\}$ and $p\geq 0$:

$$\begin{aligned}(A;d,0,(3,4,0)^p,2,1,0)\ {}_{-P}\sim\ & (A;d+1,(3,4,0)^p,3,4,0,4)\\ \succ\ & (A;d+1,(3,4,0)^p,3,4,0,4,4)\\ {}_{Q}\sim\ & (A;d+1,(3,4,0)^p,3,4,0,3,1)\\ {}_{P^2}\sim\ & (A;d+1,(3,4,0)^p,3,4,0,3,3)\\ {}_{-Q}\sim\ & (A;d+1,(3,4,0)^p,3,4,0,2,0)\\ {}_{(-Q)^3}\sim\ & (A;d,0,(3,4,0)^p,2,2,0,2)\\ \prec\ & (A;d,0,(3,4,0)^p,2,2,0),\end{aligned}$$

which is of type $(L;2,0)$ treated in Item $(1.i)$.

If (A,d) happens to be $(M',4)$, we go into smaller classes by considering the tails

$$(A';1,0,3,4,0,(3,4,0)^p,2,1,0)$$

with $A'\in\mathcal{A}:=\{G,N,H',M',L',I'\}$ and for $A'\in\mathcal{A}$ we get the chain

$$\begin{aligned}(A';1,0,3,4,0,(3,4,0)^p,2,1,0)\ {}_{-P}\sim\ & (A';2,3,4,0,(3,4,0)^p,3,4,0,4)\\ \succ\ & (A';2,3,4,0,(3,4,0)^p,3,4,0,4,4)\\ {}_{Q}\sim\ & (A';2,3,4,0,(3,4,0)^p,3,4,0,3,1)\\ {}_{P^2}\sim\ & (A';2,3,4,0,(3,4,0)^p,3,4,0,3,3)\\ {}_{-Q}\sim\ & (A';2,3,4,0,(3,4,0)^p,3,4,0,2,0)\\ {}_{(-Q}\sim\ & (A';1,0,3,4,0,(3,4,0)^p,2,2,0,2)\\ \prec\ & (A';1,0,3,4,0,(3,4,0)^p,2,2,0),\end{aligned}$$

which is again of type $(L;2,0)$ treated in Item $(1.i)$.

(2) $\tau\in\{(I,2),(M,0),(M,a),(H,a),a\in\{1,2\}\}$. Then

$$(A;2,0)\ {}_{Q}\sim(S;3,3)\in E_n(J')$$

for $A\in\{I,M,H\}$, and for the other cases one can consider the smaller classes:

- for $A\in\{G',N'\}$,
$$(A;3,1,0)\ {}_{Q}\sim(A;4,4,2)\prec(A;4,4),$$
which ends at $\circ$.
- for $d\in\{0,1\}$,
$$(K';1,d,0)\ {}_{-Q}\sim(K';2,d+3,2)\prec(K';2),$$
which ends at $\circ$.

(3) $\tau=(N;0,0)$. Then w must end in the form $(I;1,0,0)$, and the following chain holds.

$$\begin{aligned}(I;1,0,0)\succ\ & (I;1,0,0,0)\ {}_{Q}\sim(I;1,0,1,3)\ {}_{P}\sim(I;1,0,1,4)\\ {}_{Q}\sim\ & (I;2,3,3,2)\ {}_{(-P)^2}\sim(I;2,3,3,0)\\ {}_{Q}\sim\ & (I;2,3,4,3)\prec(I;2,3,4),\end{aligned}$$

which is of type $(L';3,4)$. Since this is the dual of the tail $(L;1,0)$, it can be treated as in Item $(1.ii)$.

(4) $\tau = (K; 4, 0)$. Then the walk w ends in the following way: $(A; d, 1, 0, (4, 1, 0)^p, 4, 0)$ for some $p \in \mathbb{N}$ and

$$\begin{aligned}(A, d) \in \mathcal{C} := \quad & \{(F, 0), (G', 2), (N', 2), (I, 1), \\ & (G, 1), (N, 1), (K, 3), (G, 0), (L, 0), (H, 0), \\ & (I, 2), (N, 0), (M, 0), (M, a), (L, a), (H, a), a \in \{1, 2\}\}.\end{aligned}$$

For $(A, d) \in \mathcal{C}$, the following chain holds:

$$\begin{aligned}(A; d, 1, 0, (4, 1, 0)^p, 4, 0) \succ \quad & (A; d, 1, 0, (4, 1, 0)^p, 4, 0, 0)\ {}_Q\!\sim (A; d, 1, 0, (4, 1, 0)^p, 4, 1, 3) \\ {}_P\!\sim \quad & (A; d, 1, 0, (4, 1, 0)^p, 4, 1, 4)\ {}_Q\!\sim (A; d + 1, (4, 1, 0)^p, 4, 2, 2, 3, 2) \\ {}_{(-P)^2}\!\sim \quad & (A; d + 1, (4, 1, 0)^p, 4, 2, 2, 3, 0) \\ {}_Q\!\sim \quad & (A; d + 1, (4, 1, 0)^p, 4, 2, 2, 4, 3).\end{aligned}$$

If now $p = 0$ and $(A, d) \in \{(G', 2), (N', 2), (I, 2), (M, 2), (L, 2), (H, 2)\}$, then we have

$$(A; d + 1, (4, 1, 0)^p, 4, 2, 2, 4, 3) \prec (A; d + 1, 4, 2),$$

which ends at $\circ$; otherwise

$$(A; d + 1, (4, 1, 0)^p, 4, 2, 2, 4, 3) \prec (A; d + 1, (4, 1, 0)^p, 4, 2, 2, 4),$$

which is of type $(L'; 3, 4)$, *i.e.*, of the dual of the tail $(L; 1, 0)$, that can be treated similarly as in Item $(1.ii)$.

Proceeding identically for $w \in E_n(L)$, we obtain Lemma 4.3.37. □

Lemma 4.3.38. *Let $n \geq 4$ and $w \in E_n(M) \cup E_n(M')$. Then there is a walk $w' \in G_{n+1}$ such that $w'|_{n-1} \in G_{n-1}$ and $w\&d \sim w'$ for some $d \in \{0, \ldots, 4\}$.*

Proof. Let us consider $w \in E_n(M')$. If $w|_{n-1} \in E_{n-1}(M')$, we are ready. We suppose it is not the case. Then w belongs to the following classes of tails τ of $w = \sigma\&\tau$: $(A; d, 1, 0, (4, 1, 0)^p), 3, 0)$ for some $p \in \mathbb{N}$ and

$$\begin{aligned}(A, d) \in \mathcal{C} := \quad & \{(F, 0), (G', 2), (N', 2), (I, 1), \\ & (G, 1), (N, 1), (K, 3), (G, 0), (L, 0), (H, 0), \\ & (I, 2), (N, 0), (M, 0), (M, a), (L, a), (H, a), a \in \{1, 2\}\}.\end{aligned}$$

For $(A, d) \in \mathcal{C}$, we have the equivalence

$$(A; d, 1, 0, (4, 1, 0)^p), 3, 0)\ {}_{-P}\!\sim (A; d + 1, (4, 1, 0)^p, 4, 2, 2, 4).$$

If now $p = 0$ and $(A, d) \in \{(G', 2), (N', 2), (I, 2), (M, 2), (L, 2), (H, 2)\}$, then we have

$$(A; d + 1, (4, 1, 0)^p, 4, 2, 2, 4) \prec (A; d + 1, 4, 2)$$

which ends at $\circ$, otherwise the tail of the equivalent walk is of type $(L; 4)$ which was treated in Lemma 4.3.37.

We can proceed similarly for the dual case, and Lemma 4.3.38 is proved. □

Lemma 4.3.39. *Let $n \geq 4$ and $w \in E_n(I) \cup E_n(I')$. Then there is a walk $w' \in G_{n+1}$ such that $w'|_{n-1} \in G_{n-1}$ and $w\&d \sim w'$ for some $d \in \{0, \ldots, 4\}$.*

Proof. Let us consider $w \in E_n(I)$. If $w|_{n-1} \in E_{n-1}(I)$, we are ready. We suppose it is not the case. Then w belongs to the following classes of tails τ of $w = \sigma\&\tau$: $(A; d, 4, (1, 0, 4)^p), 4)$ for some $p \in \mathbb{N}$ and

$$\begin{aligned}(A, d) \in \mathcal{C} := \quad & \{(G, 1), (N, 1), (F, 1), (G, 2), (N, 2) \\ & (I, 2), (K, 4), (M, 0), (M, a), (L, a), (H, a), a \in \{1, 2\}\}.\end{aligned}$$

For $(A,d) \in \mathcal{C} \setminus \{(M,0)\}$, we have the equivalence

$$(A; d, 4, (1,0,4)^p), 4)\ _P \sim (A; d-1, (1,0,4)^p, 0, 0).$$

We consider the following cases:

- for $p = 0$ and $(A,d) = (F,1)$, then $w = (F; 1, 4, 4) \in G_3$ has length $n = 3$;
- for $p = 0$ and $(A,d) \in \{(G,2),(N,2)\}$, $(A; d-1, 0, 0)$ is the tail of a walk belonging to $E_n(K)$, treated in Lemma 4.3.35;
- for $p = 0$ and $(A,d) = (I,2)$, $(I; 1, 0, 0)$ is the tail of a walk in $E_n(L')$, treated in Lemma 4.3.37;
- otherwise $(A; d-1, (1,0,4)^p, 0, 0) \prec (A; d-1, (1,0,4)^p, 0)$, which ends at $\circ$.

For $(A,d) = (M,0)$, we go into the smaller classes $(A'; 3, 4, 1, 0, 4, (1,0,4)^p, 4)$ with $p \geq 0$ and $A' \in \{G', X', I, M, L, H\}$. In these cases,

$$(A'; 3, 4, 1, 0, 4, (1,0,4)^p, 4)\ _P \sim (A'; 2, 1, 0, 4, (1,0,4)^p, 0, 0) \prec (A'; 2, 1, 0, 4, (1,0,4)^p, 0),$$

which ends at $\circ$.

Dealing with the walks of $E_n(I')$ in the same way, we obtain Lemma 4.3.39. □

Proposition 4.3.33 now follows from Lemmata 4.3.35 to 4.3.39 together with the equation (4.3.17).

4.3.5 Boundary of the graph directed set M

As will be seen later, the last two subsections assure the connectivity of the subset of $\mathbf{M}$ consisting of the union of the subpieces $\psi_w(\mathcal{T})$ where w is a walk of $\mathcal{G}$ starting at F and ending at the accepting state $\circ$. By definition, this subset is dense in $\mathbf{M}$. The present subsection now uses the walks of $p(F)$ that do not end at $\circ$ to prove that the boundary $\partial\mathbf{M}$ of $\mathbf{M}$ lies in the boundary of $\mathcal{T}$.

Proposition 4.3.40. *Let $w_0 := (a_1, \ldots, a_n)$ be a walk in $p(F)$ which does not end at $\circ$. Then*

$$\psi_{w_0}(\mathcal{T}) \cap \partial\mathcal{T} \neq \emptyset.$$

For w_0 as in the proposition, we will show that $w := (0,4)\&w_0$ satisfies $\psi_w(\mathcal{T}) \cap B_Q \neq \emptyset$. Note that then $\psi_w(\mathcal{T}) = \psi_0 \circ \psi_4 \circ \psi_{w_0}(\mathcal{T})$; we will see that this piece stays in contact with $\partial\mathcal{T}$ after application of the inverse of $\psi_0 \circ \psi_4$. We need the following lemma.

For A a state of $\mathcal{G}$, $\mathcal{S}$ a subset of $\mathcal{B}$ and $n \geq 3$, let (B_n) be the following assertion.

If w_0 is a walk of length $n-2$ in $p(F)$ ending at $A \neq \circ$, then $w^T := ((0,4)\&w_0)^T$ is the labelling of a walk in $\mathcal{B}$ starting at S and ending at Q for every $S \in \mathcal{S}$, where $(A, \mathcal{S})$ are given in the Table 4.7 (the duals have to be added, they associate A' to $-\mathcal{S}$).

Lemma 4.3.41. *The assertion (B_n) holds for every $n \geq 3$.*

Proof. For $n = 3$ we have $w = (0,4,0)$ and $A = G$, or $w = (0,4,1)$ and $A = G'$. It is easily seen on $\mathcal{B}_0$ that $S \xrightarrow{w^T} Q$ for all S in the corresponding $\mathcal{S}$.

Let us suppose (B_n) to be true for an $n \geq 3$. We show that (B_{n+1}) also holds. Let $w = (0, 4, a_3, \ldots, a_{n+1})$ with $(F; a_3, \ldots, a_{n+1}) =: w_0 \in p(F)$.

If w_0 ends up in $A = G$, then $u := (a_3, \ldots, a_n)$ ends up in G' or N' and $a_{n+1} = 2$, because $G' \xrightarrow{2} G$ and $N' \xrightarrow{2} G$ are the only edges of $\mathcal{G}$ leading to G (the case $F \xrightarrow{a_{n+1}} G$ is not possible, since there would be no edge labelled by a_n leading to F). If u ends up in G', then by assumption we

have $S \xrightarrow{w|_n^T} Q$ for all $S \in \{Q, -Q, R, -R\}$. Since $R \xrightarrow{2} S = Q$, $-Q \xrightarrow{2} S = Q$ and $-R \xrightarrow{2} S = -Q$, $Q \xrightarrow{2} S = -Q$ all exist in $\mathcal{B}$, we obtain for every $S' \in \{\pm Q, \pm R\}$: $S' \xrightarrow{2} S \xrightarrow{w|_n^T} Q$, *i.e.*, $S' \xrightarrow{w^T} Q$. If u ends up in N', then by assumption we have $S \xrightarrow{w|_n^T} Q$ for all $S \in \{Q, -Q, \}$. Thus one can use the preceding walks in $\mathcal{B}$: $R \xrightarrow{2} S = Q$, $-Q \xrightarrow{2} S = Q$ and $-R \xrightarrow{2} S = -Q$, $Q \xrightarrow{2} S = -Q$ all exist in $\mathcal{B}$, hence for every $S' \in \{\pm Q, \pm R\}$, $S' \xrightarrow{2} S \xrightarrow{w|_n^T} Q$, *i.e.*, $S' \xrightarrow{w^T} Q$.

The results for the other possible endings A of w_0 are summed up in Table 4.8 (the duals can be treated likewise). □

Proof of Proposition 4.3.40. Let $w := (0,4)\&w_0$ with w_0 a walk in $p(F)$ that does not end at $\circ$. Then

$$\psi_w(\mathcal{T}) \cap B_Q \neq \emptyset.$$

Indeed, by Proposition 4.3.16, it suffices to show that there exists a walk $Q \xleftarrow{w} S$ in $\mathcal{B}$. This is what Lemma 4.3.41 does. Now recall that $\psi_w(\mathcal{T}) = \psi_0 \circ \psi_4 \circ \psi_{w_0}(\mathcal{T})$. Thus again by Proposition 4.3.16 there exists an infinite walk $Q \xleftarrow{0} S \xleftarrow{4} S' \xleftarrow{w_0} \dots$ in $\mathcal{B}$. This implies that $S' \in \{P, Q, -R\}$, as can be checked on $\mathcal{B}_0$. Thus there is an infinite walk $S' \xleftarrow{w_0} \dots$ in B with $S' \in \mathcal{B}$, and therefore $\psi_{w_0}(\mathcal{T}) \cap \partial\mathcal{T} \neq \emptyset$, as assured by Proposition 4.3.16. □

In what follows we will use the following notations.

Notation 4.3.42. We fix a metric $\mathrm{dist}(\cdot,\cdot)$ on $\mathbb{R}^2$.

Proposition 4.3.43. *The boundary of* $\mathbf{M}$ *is contained in the boundary of* $\mathcal{T}$*.*

Proof. Let $x \in \partial\mathbf{M}$. We will show that for every $\varepsilon > 0$, we have $\mathrm{dist}(x, \partial\mathcal{T}) < \varepsilon$. This will imply that $x \in \partial\mathcal{T}$, since $\partial\mathcal{T}$ is a closed set. We consider two cases.

Case 1. For every $n \geq 3$, $x \notin \mathcal{M}(G_n)$ (see Definition 4.3.10). The element x belonging to $\mathbf{M}$, we can write $x = \sum_{i=1}^{\infty} \mathbf{A}^{-i}\Phi(a_i)$ with $w_n := (a_1, \dots, a_n) \in p_n(F)$. In our assumption, for every $n \geq 3$, we have $w_n \notin p_n(F, \circ)$. Let $\varepsilon > 0$ and n_0 such that for $n \geq n_0$, $\mathrm{diam}(\psi_w(\mathcal{T})) < \varepsilon$ for every w of length $|w| = n$. Then

$$x \in \psi_{w_{n_0}}(\mathcal{T}) \text{ with } \begin{cases} w_{n_0} \in p_{n_0}(F) \text{ (by definition),} \\ w_{n_0} \notin p_{n_0}(F, \circ) \text{ (by assumption).} \end{cases}$$

By Proposition 4.3.40, $\psi_{w_{n_0}}(\mathcal{T}) \cap \partial T \neq \emptyset$, thus $\mathrm{dist}(x, \partial T) < \varepsilon$ since $\mathrm{diam}(\psi_{w_{n_0}}(\mathcal{T})) < \varepsilon$.

Case 2. There is an $n_0 \geq 3$ with $x \in \mathcal{M}(G_{n_0})$. Because of Equation (4.3.2), we even have $x \in \mathcal{M}(G_n)$ for all $n \geq n_0$.

A	$\mathcal{S}$
G	$\{Q, -Q, R, -R\}$
H	$\{Q, R, -R\}$
I	$\{P, Q\}$
J	$\{-R\}$
K	$\{-P\}$
L	$\{Q, -R\}$
M	$\{Q\}$
N	$\{Q, -Q\}$

Table 4.7: Table for assertion (B_n).

A	end of $w\|_n$	a_{n+1}	$S' \xrightarrow{a_{n+1}} S$
G	G', N'	2	$R, -Q \to Q$ $-R, Q \to -Q$
H	G', N'	3	$R \to Q$ $-R, Q \to -Q$
I	H', G', L'	4	$P \to R$ $Q \to -Q$
J	H', M', I'	1	$-R \to -Q$
K	H', J	0	$-P \to -R$
L	H', L'	2, 3	$Q \to -Q$ $-R \to -Q$
	M'	2, 3, 4	$Q \to -Q$ $-R \to -Q$
	N'	4	$Q \to -Q$ $-R \to -Q$
	K'	0	$Q \to P$ $-R \to P$
M	K'	1	$Q \to P$
N	I	1	$Q \to P$ $-Q \to Q$

Table 4.8: Proof of Lemma 4.3.41.

We denote by $B_r(0)$ the open ball $\{y \in \mathbb{R}^2,\ \mathrm{dist}(0,y) < r\}$. By compactness of $\mathcal{T}$, it is possible to find $r_1 > 0$ such that

$$\mathcal{T} \subset B_{r_1}(0). \tag{4.3.18}$$

Since $\{P, Q\}$ is a basis of the lattice $\Phi(\mathbb{Z}[\alpha])$ by (4.3.4), there exist positive integers m_1, m_2 such that

$$B_{r_1}(0) \ \subset \bigcup_{\substack{n_1 \in \{-m_1, \dots, m_1\} \\ n_2 \in \{-m_2, \dots, m_2\}}} (\mathcal{T} + n_1 P + n_2 Q) \ \subset \ B_{r_2}(0). \tag{4.3.19}$$

The second inclusion follows again from the compactness of $\mathcal{T}$, $r_2 > 0$ is simply chosen large enough.
Let now $\varepsilon > 0$, $n \geq n_0$ such that $\mathrm{diam}(\psi_w(B_{r_2}(0))) < \varepsilon$ for every w of length $|w| = n$, and let $w \in p_n(F, \circ) = G_n$ such that $x \in \psi_w(\mathcal{T})$. Then using (4.3.18) and (4.3.19), the following inclusions hold:

$$x \in \psi_w(\mathcal{T}) \ \subset \ \psi_w(B_{r_1}(0)) \ \subset \ \underbrace{\psi_w\left(\bigcup_{\substack{n_1 \in \{-m_1, \dots, m_1\} \\ n_2 \in \{-m_2, \dots, m_2\}}} (\mathcal{T} + n_1 P + n_2 Q)\right)}_{= \bigcup_{\substack{n_1 \in \{-m_1, \dots, m_1\} \\ n_2 \in \{-m_2, \dots, m_2\}}} \psi_w(\mathcal{T} + n_1 P + n_2 Q)} \ \subset \ \psi_w(B_{r_2}(0)).$$

Our aim is to find a $y \in \partial\mathcal{T}$ in the union above. Since x and y will then both belong to $\psi_w(B_{r_2}(0))$, which has diameter less than ε, we will be done. Note that $\psi_w(B_{r_1}(0))$ is a neighborhood of x, a point of $\partial\mathbf{M}$, hence this neighborhood has nonempty intersection with the complement of $\mathbf{M}$ in $\mathbb{R}^2$.

Remember that w is a walk of $p_n(F,\circ)$. Now we make the following assumption.

- Each of the following additions is admissible,
- Each of the following additions yields a walk that is contained in $p(F,\circ)$.

$$\begin{aligned}
W_1 &:= \{\Phi_{n_1P}\circ\Phi_{n_2Q}(w)\,|\,0\le n_1\le m_1;\,0\le n_2\le m_2\},\\
W_2 &:= \{\Phi_{n_1(-P)}\circ\Phi_{n_2Q}(w)\,|\,0\le n_1\le m_1;\,0\le n_2\le m_2\},\\
W_3 &:= \{\Phi_{n_1P}\circ\Phi_{n_2(-Q)}(w)\,|\,0\le n_1\le m_1;\,0\le n_2\le m_2\},\\
W_4 &:= \{\Phi_{n_1(-P)}\circ\Phi_{n_2(-Q)}(w)\,|\,0\le n_1\le m_1;\,0\le n_2\le m_2\}.
\end{aligned}$$

Set $W := W_1\cup W_2\cup W_3\cup W_4$. With a slight abuse of notation we may write

$$W := \{\Phi_{n_1P}\circ\Phi_{n_2Q}(w)\,|\,-m_1\le n_1\le m_1;\,-m_2\le n_2\le m_2\}.$$

By assumption all walks of W are contained in $G_n = p_n(F,\circ)$. Thus

$$\begin{aligned}
\psi_w(B_{r_1}(0)) &\subset \bigcup_{n_1,n_2}\psi_w(\mathcal{T}+n_1P+n_2Q)\\
&= \bigcup_{n_1,n_2}\psi_{\Phi_{n_1P}\circ\Phi_{n_2Q}(w)}(\mathcal{T}) \qquad \text{(by Remark 4.3.21.1)}\\
&\subset \mathcal{M}(G_n)\\
&\subset \mathbf{M},
\end{aligned}$$

which contradicts the fact that $\psi_w(B_{r_1}(0))$ contains points of the complement $\mathbb{R}^2\setminus\mathbf{M}$. So our assumption is wrong.

Therefore one of the following alternatives must hold.

- at least one of the additions in W is not admissible or
- at least one element $w_0\in W$ does not belong to G_n.

In view of Proposition 4.3.26 we conclude that at least one $w_0\in W$ does not belong to $G_n = p_n(F,\circ)$. Proposition 4.3.26 also shows that all additions are admissible for each element of G_n, *i.e.*, starting from a word in G_n, each addition $\Psi_{\pm P},\Psi_{\pm Q}$ leads to a word in $p_n(F)$. Thus, starting at w, by a sequence of admissible additions we can reach a word $w_0\in W$ which belongs to $p_n(F)\setminus p_n(F,\circ)$. Let us write

$$w_0 = \Phi_{n_1P}\circ\Phi_{n_2Q}(w)\in p_n(F)\setminus p_n(F,\circ)$$

for some $n_1\in\{-m_1,\dots,m_1\}$, $n_2\in\{-m_2,\dots,m_2\}$. (Note that by Remark 4.3.21.1

$$\psi_w(\mathcal{T}+n_1P+n_2Q) = \psi_{w_0}(\mathcal{T})$$

because we have a sequence of admissible additions from w to w_0.) For this choice of w_0 we have

- $\psi_{w_0}(\mathcal{T})\subset\psi_w(B_{r_2}(0))$ by assumption,
- $\psi_{w_0}(\mathcal{T})\cap\partial\mathcal{T}\neq\emptyset$ by Proposition 4.3.40.

This implies that $\psi_w(B_{r_2}(0))$ contains x as well as some point of $\partial\mathcal{T}$, hence $\operatorname{dist}(x,\partial T)<\varepsilon$.

Consequently, in both cases for every $\varepsilon>0$, $\operatorname{dist}(x,\partial T)<\varepsilon$, thus $x\in\partial\mathcal{T}$, and this holds for every $x\in\partial\mathbf{M}$, hence, $\partial\mathbf{M}\subset\partial\mathcal{T}$. □

4.3.6 Generalized fundamental inequality and consequences

This subsection is devoted to a generalization of the fundamental inequality found in [5]. This will lead to the construction of an arcwise connected skeleton inside the interior of the tile $\mathcal{T}$ together with some of its neighbors. We denote by $\mathbf{S}$ the set of elements of $\mathbb{Q}[\alpha]$ with integer part zero with respect to the basis α and the digits $\mathcal{N} = \{0, 1, 2, 3, 4\}$:

$$\mathbf{S} := \left\{ \sum_{i=1}^{l} \Phi(\alpha^{-i} a_i); l \in \mathbb{N}, (a_i)_{1 \leq i \leq l} \in \mathcal{N}^l \right\}.$$

Consequently we have $\overline{\Phi(\mathbf{S})} = \mathcal{T}$.

Remark 4.3.44. We recall that the tile $\mathcal{T}$ is symmetric with respect to the point

$$\Phi(c) := \Phi\left(\frac{4}{2(\alpha - 1)}\right)$$

(see [5, Lemma 3.2]).

Proposition 4.3.45 (Generalized fundamental inequality)**.** *There is an $\varepsilon > 0$ such that for any $x \in \mathbf{S} + 2\alpha$ we have*

$$\Im(x) > \Im(c) + \varepsilon.$$

Proof. This follows from the minoration

$$\Im(\sum_{i=1}^{l} a_i \alpha^{-i}) \geq -\left| \sum_{i=1}^{l} a_i \alpha^{-i} \right| \geq -\frac{4}{|\alpha - 1|},$$

so that for $x \in \mathbf{S} + 2\alpha$ we have $\Im(x) > 0 > I(c) = -\frac{1}{5}$. □

Corollary 4.3.46. *Let $\gamma \in \mathbb{Z}[\alpha]$ and put $\gamma = u + v\alpha$ with u, v in $\mathbb{Z}$. Then there exists a constant $\varepsilon > 0$ such that for any $x \in \mathcal{S}$,*

$$\begin{cases} \Im(x) + \Im(\gamma) > \Im(c) + \varepsilon & \text{if } v \geq 2, \\ \Im(x) + \Im(\gamma) < \Im(c) - \varepsilon & \text{if } v \leq -2. \end{cases}$$

Proof. This is proved in the same way as in [5, Lemma 4.3]. □

We will now construct a generalized version of the skeleton constructed in [5] where the tiles were disk-like. To this matter set the backbone

$$\mathcal{L} := \{\Phi(c) + w\Phi(1); w \in [0, 4]\}.$$

Furthermore, let

$$V_0 := \bigcup_{S \in \mathcal{B}_0} (\mathcal{T} + S).$$

Then the following lemma holds.

Lemma 4.3.47. *We have $\mathcal{L} \subset \mathrm{int}(\mathbf{A}V_0)$.*

Proof. Note that

$$\begin{aligned}\mathrm{int}(\mathbf{A}(V_0)) &= \mathbb{R}^2 \setminus \bigcup_{x\in\mathbb{Z}^2\setminus\mathcal{B}_0} (\mathbf{A}(\mathcal{T}+x)) \\ &= \mathbb{R}^2 \setminus \Bigg(\bigcup_{u\in\mathbb{Z},\,|v|\geq 2} (\mathcal{T}+\Phi(u+v\alpha)) \cup \\ &\qquad \bigcup_{v=1,\,u\leq -1 \text{ or } u\geq 10} (\mathcal{T}+\Phi(u+v\alpha)) \cup \\ &\qquad \bigcup_{v=0,\,u\leq -6 \text{ or } u\geq 10} (\mathcal{T}+\Phi(u+v\alpha)) \cup \\ &\qquad \bigcup_{v=-1,\,u\leq -6 \text{ or } u\geq 5} (\mathcal{T}+\Phi(u+v\alpha)) \Bigg).\end{aligned}$$

Thus we have to show that $(\mathcal{T}+\Phi(u+v\alpha))\cap\mathcal{L}=\emptyset$ for all constellations (u,v) occurring in the above unions.
Let first $\gamma = u+v\alpha$ with $u\in\mathbb{Z}$ and $|v|\geq 2$. Then Corollary 4.3.46 and the fact that $\overline{\Phi(\mathbf{S})}=\mathcal{T}$ imply that $(\mathcal{T}+\Phi(\gamma))\cap\mathcal{L}=\emptyset$.
For the pairs of the shape $(u,0)$, $u\leq -6$ or $u\geq 10$ we see that $(\mathcal{T}+\Phi(\gamma))\cap\mathcal{L}=\emptyset$ in exactly the same way as in [5, Lemma 4.4].
If now $v=-1$, suppose first that $u\leq -6$. If $x\in\ \alpha^{-1}(\mathbf{S}-\alpha^2)+u$, then $\alpha x\in\ \mathbf{S}+5+(u+4)\alpha$. From $u+4\leq -2$ and by Corollary 4.3.46, we can write $\Im(\alpha x)<\Im(c)-\varepsilon$, and consequently:

$$\forall j\in\{0,\ldots,4\},\ \Im(\alpha x)=\Im(\alpha x+j)=\Im(\alpha(x+\alpha^{-1}j))<\Im(c)-\varepsilon,$$

thus

$$\forall j\in\{0,\ldots,4\},\ \forall x\in\ \alpha^{-1}(\mathbf{S}-\alpha^2+j)+u,\ \ \Im(\alpha x)<\Im(c)-\varepsilon.$$

From $\overline{\Phi(\mathbf{S})}=\mathcal{T}$, we conclude that this inequality also holds if we replace $\mathbf{S}$ by $\mathcal{T}$, and from the set equation of $\mathcal{T}$ we obtain, taking the union over $j\in\{0,\ldots,4\}$,

$$\forall\Phi(x)\in\mathcal{T}+\Phi(u-\alpha),\ \ \Im(\alpha x)\leq\Im(c)-\varepsilon.$$

On the other hand, for an element of $\mathcal{L}$, *i.e.*, $\Phi(x)=\Phi(c)+w\Phi(1), w\in[0,4]$, we have

$$\Im(\alpha x)=w+\Im(\alpha c)\geq\Im(\alpha c)=-1/5=\Im(c),$$

which implies that $(\mathcal{T}+\Phi(u-\alpha))\cap\mathcal{L}=\emptyset$ for all $u\leq -6$.
Suppose secondly that $u\geq 5$. If again $x\in\ \alpha^{-1}(\mathbf{S}-\alpha^2)+u$, then $\alpha x\in\ \mathbf{S}+5+(u+4)\alpha$. From $u\geq 5$ and by Corollary 4.3.46, we have $\Im(\alpha x)>\Im(c)+\varepsilon+4\Im(\alpha)$, and consequently, by a similar reasoning as above, we obtain

$$\forall\Phi(x)\in\mathcal{T}+\Phi(u-\alpha),\ \ \Im(\alpha x)\geq\Im(c)+\varepsilon+4.$$

On the other hand, for $\Phi(x)\in\mathcal{L}$, we have $\Im(\alpha x)\leq\Im(c)+4$, thus again $(\mathcal{T}+\Phi(u-\alpha))\cap\mathcal{L}=\emptyset$ for all $u\geq 5$.

The remaining case $v=1$ is treated likewise, thus the proof is complete. □

Composing small pieces of backbones, let us define the n-skeleton by

$$\mathcal{K}_n=\bigcup_{m=1}^{n}\left(\bigcup_{(a_1,a_2,\ldots a_m)}\sum_{i=1}^{m}A^{-i}\Phi(a_i)+\mathbf{A}^{-m-1}(\mathcal{L})\right).$$

Lemma 4.3.48. *$\mathcal{K}_n$ is arcwise connected and $\mathcal{K}_n \subset \mathrm{int}(V_0)$.*

Proof. The arcwise connectivity can be shown as in [5, Lemma 4.6].
For the second part, note that for every $(a_1, \ldots, a_m)$, by Lemma 4.3.47 we have for the small pieces

$$\sum_{i=1}^{m} \mathbf{A}^{-i}\Phi(a_i) + \mathbf{A}^{-1-m}\mathcal{L} \subset \sum_{i=1}^{m} \mathbf{A}^{-i}\Phi(a_i) + \mathrm{int}\left(\mathbf{A}^{-m}V_0\right).$$

Now remember that using the automaton $\mathcal{B}_0$ one can compute for $S \in \mathcal{B}_0$ that

$$\begin{array}{rcl} \sum_{i=1}^{m} \mathbf{A}^{-i}\Phi(a_i) + \mathbf{A}^{-m}S & = & \mathcal{A}^{-m}\left(S + \sum_{i=0}^{m-1} \mathbf{A}^{-i}\Phi(a_{m-i})\right) \\ & = & \mathbf{A}^{-m}\left(\mathbf{A}^{m}S' + \sum_{i=0}^{m-1} \mathbf{A}^{-i}\Phi(a'_{m-i})\right) \quad \text{(by (4.3.10))} \\ & = & \sum_{i=1}^{m} \mathbf{A}^{-i}\Phi(a'_i) + S' \end{array}$$

with $S' \in \mathcal{B}_0$ and $a'_i \in \mathcal{N}$. From this we can conclude that

$$\sum_{i=1}^{m} \mathbf{A}^{-i}\Phi(a_i) + \mathcal{A}^{-m}V_0 \subset V_0,$$

hence the union of the backbones remains in $\mathrm{int}(V_0)$. □

Remark 4.3.49. Note that the middle points $\sum_{i=1}^{m} \mathbf{A}^{-i}\Phi(a_i)$ of the union of all backbones are dense in $\mathcal{T}$.

4.3.7 The component of $\mathrm{int}(\mathcal{T})$ containing 0

We are now almost ready to prove Theorem 4.3.8 concerning the description of C_0. We will first construct an arc from an arbitrary point in $\mathrm{int}(\mathbf{M})$ to zero entirely contained in $\mathrm{int}(\mathbf{M})$.

Lemma 4.3.50. *If $x \in \mathrm{int}(\mathbf{M})$, then there is an $n \geq 3$ such that $x \in \mathcal{M}(G_n)$.*

Proof. Let $x = \sum_{j\geq 1} \Phi(\alpha^{-j}aj) \in \mathrm{int}(\mathbf{M})$. In particular, $w = (a_j)_{j\geq 1}$ is an infinite walk in $p(F)$. Suppose $x \notin \mathcal{M}(G_n)$ for any $n \geq 3$, *i.e.*, $w_n := (F; a_1, a_2, \ldots, a_n) \in p_n(F)$ does not end at $\circ$ for any $n \geq 3$. We show that $x \in \partial\mathcal{T}$, which is a contradiction, since $\mathbf{M} \subset \mathcal{T}$, hence $\mathrm{int}(\mathbf{M}) \subset \mathrm{int}(\mathcal{T})$. We have by definition that $x \in \psi_{w_n}(\mathcal{T})$ for every $n \geq 3$. Fix $\varepsilon > 0$, then for n large enough we also have that

$$\begin{cases} \mathrm{diam}(\psi_{w_n}(\mathcal{T})) < \varepsilon, \\ \psi_{w_n}(\mathcal{T}) \cap \partial\mathcal{T} \neq \emptyset \text{ (by Lemma 4.3.40).} \end{cases}$$

Thus for every $\varepsilon > 0$, $\mathrm{dist}(x, \partial\mathcal{T}) < \varepsilon$, hence $x \in \partial\mathcal{T}$, since $\partial\mathcal{T}$ is a closed set. □

Lemma 4.3.51. *Let $n \geq 3$, $S \in \mathcal{B}$ and $v_1, v_2 \in G_n$ such that $v_2 = \Psi_S(v_1)$. Then $\psi_{v_1}(\mathcal{T}) \cap \psi_{v_2}(\mathcal{T})$ contains points of $\mathrm{int}(\mathcal{T})$.*

Proof. Since both subpieces $\psi_{v_1}(\mathcal{T})$ and $\psi_{v_2}(\mathcal{T})$ are subsets of $\mathcal{T}$, points of their intersection that are not in $\mathrm{int}(\mathcal{T})$ must be in $\partial\mathcal{T}$. We show that there are at most countably many such points, whereas $\psi_{v_1}(\mathcal{T}) \cap \psi_{v_2}(\mathcal{T})$ is uncountable.

The uncountability of $\psi_{v_1}(\mathcal{T}) \cap \psi_{v_2}(\mathcal{T})$ follows from the fact that $v_2 = \Psi_S(v_1)$, hence $\psi_{v_2}(\mathcal{T}) = \psi_{v_1}(\mathcal{T} + S)$, with $S \in \mathcal{B}$ (see Remark 4.3.21.1). Since $\mathcal{T} \cap (\mathcal{T} + S)$ has uncountably many points for $S \in \mathcal{B}$ (see [5, Section 9]), this remains true after applying the homeomorphism ψ_{v_1}.

On the other side, a point x of $\psi_{v_1}(\mathcal{T}) \cap \psi_{v_2}(\mathcal{T})$ which lies on $\partial\mathcal{T}$ also belongs to a translate $\mathcal{T} + S'$ of $\mathcal{T}$ with $S' \in \mathcal{B}$, by the boundary equation (4.3.11). This translate is the union of the

subpieces $\psi_w(\mathcal{T}) + S'$ with $|w| = |v_1| =: n$. Let us write $v_1 =: (a_1, \dots, a_n)$ and $w =: (b_1, \dots, b_n)$. Then the point $\mathbf{A}^n x$ belongs to the triple intersection

$$\left(\mathcal{T} + \sum_{i=0}^{n-1} \mathbf{A}^i \Phi(a_{n-i})\right) \cap \left(\mathcal{T} + S + \sum_{i=0}^{n-1} \mathbf{A}^i \Phi(a_{n-i})\right) \cap \left(\mathcal{T} + \mathbf{A}^n S' + \sum_{i=0}^{n-1} \mathbf{A}^i \Phi(b_{n-i}) \right),$$

or, equivalently, the point $\mathbf{A}^n x - \sum_{i=0}^{n-1} \mathbf{A}^i a_{n-i}$ belongs to the triple intersection

$$\mathcal{T} \cap (S + \mathcal{T}) \cap (S'' + \mathcal{T}) =: V(S, S'')$$

with $S'' := \mathbf{A}^n S' + \sum_{i=0}^{n-1} \mathbf{A}^i \Phi(b_{n-i}) - \sum_{i=0}^{n-1} \mathbf{A}^i \Phi(a_{n-i})$. Note that $S'' \notin \{\circ, S\}$. Indeed, using (4.3.9), (4.3.10) and Remark 4.3.14, $S'' = \circ$ as well as $S'' = S$ would imply $S' = \circ$.
Thus to each point x of $\psi_{v_1}(\mathcal{T}) \cap \psi_{v_2}(\mathcal{T}) \cap \partial\mathcal{T}$ corresponds exactly one point of V_3, the set of all triple points of $\mathcal{T}$ (*i.e.*, where $\mathcal{T}$ meets with two other translates). Since V_3 is at most countable (see [5, Theorem 10.1]), there are at most countably many points in $\psi_{v_1}(\mathcal{T}) \cap \psi_{v_2}(\mathcal{T}) \cap \partial\mathcal{T}$. Together with the first part of this proof this means that $\psi_{v_1}(\mathcal{T}) \cap \psi_{v_2}(\mathcal{T}) \cap \mathrm{int}(\mathcal{T})$ is not empty. □

Proposition 4.3.52. *Let $x \in \mathrm{int}(\mathbf{M})$ and an $n \geq 3$ given by Lemma 4.3.50,* i.e., *such that $x \in \mathcal{M}(G_n)$. Then there is an arc p from x to an element y of $\mathrm{int}(\mathcal{M}(G_{n-1}))$ with $p \subset \mathrm{int}(\mathcal{T})$.*

Proof. In this proof we will often use the fact that $\mathcal{T}$ is the closure of its interior. This has been shown in a more general context in Wang [62]. Let $w \in G_n$ such that $x \in \psi_w(\mathcal{T})$. By Proposition 4.3.33 there exists a finite chain of walks $v_1, \dots, v_m \in G_{n+1}$ with the following properties:

$$\begin{aligned} v_1 &= w\&d \text{ for some } d \in \{0, \dots, 4\}, \\ \Psi_{S_i}(v_i) &= v_{i+1} \text{ for some } S_j \in \mathcal{B} \quad (1 \leq i \leq m-1), \\ v_m\,|_{n-1} &\in G_{n-1}. \end{aligned}$$

Now choose $x_i \in \mathrm{int}(\psi_{v_i}(\mathcal{T}))$ arbitrary and set $y := x_m$. Note that $\psi_{v_m}(\mathcal{T}) \subset \psi_{v_m|_{n-1}}(\mathcal{T}) \subset \mathcal{M}(G_{n-1})$, thus y has the required property. First we shall construct an arc $p_1 \subset \mathrm{int}(\mathcal{T})$ from x to x_1. Without loss of generality, one can suppose that $x \in \psi_{v_1}(\mathcal{T})$ (see Remark 4.3.34.1).

Since $x \in \mathrm{int}(\mathbf{M})$ there exists an $\varepsilon > 0$ such that $B_\varepsilon(x) \subset \mathrm{int}(\mathbf{M})$. Thus there is a $z_1 \in B_\varepsilon(x) \cap \mathrm{int}(\psi_{v_1}(\mathcal{T}))$. Connect x with z_1 by a straight line segment ℓ_1. Obviously, $\ell_1 \subset \mathrm{int}(\mathbf{M})$.

Now $x_1, z_1 \in \mathrm{int}(\psi_{v_1}(\mathcal{T}))$. Thus there exists $\varepsilon_2 > 0$ such that

$$\begin{aligned} B_{\varepsilon_2}(z_1) &\subset \mathrm{int}(\psi_{v_1}(\mathcal{T})), \\ B_{\varepsilon_2}(x_1) &\subset \mathrm{int}(\psi_{v_1}(\mathcal{T})). \end{aligned}$$

By Remark 4.3.49 at the end of the previous section there exists a $j \in \mathbb{N}$ such that $\psi_{v_1}(\mathcal{K}_j)$ contains points z_2, z_3 with

$$\begin{aligned} z_2 &\in B_{\varepsilon_2}(z_1), \\ z_3 &\in B_{\varepsilon_2}(x_1). \end{aligned}$$

Now connect z_1 with z_2 by the line segment ℓ_2 and connect z_3 with x_1 by the line segment ℓ_3. Both of these line segments are obviously contained in $\mathrm{int}(\mathcal{T})$. Since $\mathcal{K}_j$ is arcwise connected by Lemma 4.3.48 there exists an arc $q_1 \in \psi_{v_1}(\mathcal{K}_j)$ connecting z_2 with z_3. We have to show that $q_1 \subset \mathrm{int}(\mathcal{T})$.

What we know from Lemma 4.3.48 is that

$$q_1 \subset \mathrm{int}(\psi_{v_1}(V_0)) = \mathrm{int}\left(\bigcup_{S \in \mathcal{B}_0} \psi_{v_1}(\mathcal{T} + S)\right) = \mathrm{int}\left(\bigcup_{S \in \mathcal{B}_0} \psi_{\Psi_S(v_1)}(\mathcal{T})\right).$$

We used here Remark 4.3.21.1. Indeed, since $v_1 \in G_{n+1}$, all the additions $\Psi_S(v_1)$ with $S \in \mathcal{B}$ are admissible by Proposition 4.3.26. So for all $S \in \mathcal{B}_0$, $\psi_{v_1}(\mathcal{T}+S)$ is contained in $\mathcal{T}$, because it is a subpiece of level $n+1$ of $\mathcal{T}$. This implies that $\mathrm{int}(\psi_{v_1}(V_0)) \subset \mathrm{int}(\mathcal{T})$. Thus $q_1 \subset \mathrm{int}(\mathcal{T})$. Summing up we have constructed an arc $p_1 := \ell_1\ell_2q_1\ell_3$ from x to x_1 which is contained in $\mathrm{int}(\mathcal{T})$.

In the next step we construct an arc p_{i+1} from x_i to x_{i+1}, still inside $\mathrm{int}(\mathcal{T})$. Because $\Psi_{S_i}(v_i) = v_{i+1}$ for some $S_i \in \mathcal{B}$, Lemma 4.3.51 implies the existence of a $z_1 \in \psi_{v_i}(\mathcal{T}) \cap \psi_{v_{i+1}}(\mathcal{T})$ which is contained in $\mathrm{int}(\mathcal{T})$. Thus there exists an $\varepsilon_1 > 0$ with $B_{\varepsilon_1}(z_1) \subset \mathrm{int}(\mathcal{T})$. Furthermore,

$$\begin{aligned} z_1 \in \psi_{v_i}(\mathcal{T}) &\implies \exists z_2 \in B_{\varepsilon_1}(z_1) \cap \mathrm{int}(\psi_{v_i}(\mathcal{T})), \\ z_1 \in \psi_{v_{i+1}}(\mathcal{T}) &\implies \exists z_3 \in B_{\varepsilon_1}(z_1) \cap \mathrm{int}(\psi_{v_{i+1}}(\mathcal{T})). \end{aligned}$$

Now connect z_2 with z_1 by the line segment ℓ_1 and connect z_1 with z_3 by the line segment ℓ_2. Both of these line segments are obviously contained in $\mathrm{int}(\mathcal{T})$.

As above we can now construct using the n-skeletons an arc $q_1 \subset \mathrm{int}(\mathcal{T})$ connecting x_i with z_2 and an arc $q_2 \subset \mathrm{int}(\mathcal{T})$ connecting z_3 with x_{i+1}. The arc $p_{i+1} := q_1\ell_1\ell_2q_2 \subset \mathrm{int}(\mathcal{T})$ now connects x_i with x_{i+1}.

Setting $p := p_1 \dots p_m$ we have a path connecting x with y lying entirely in the interior of $\mathcal{T}$. □

Proposition 4.3.53. *Let x be a point of* $\mathrm{int}(\mathbf{M})$*. Then there is an arc connecting x to* 0*.*

Proof. By Lemma 4.3.50 there is an $n \geq 3$ such that $x \in \mathcal{M}(G_n)$. By applying Proposition 4.3.52 $n-3$ times we can construct an arc inside $\mathrm{int}(\mathcal{T})$ from x to some $y \in \mathrm{int}(\mathcal{M}(G_3))$. Since $\mathcal{M}(G_3) = \psi_{(0,0,0)}(\mathcal{T}) = \psi_{(1,4,4)}(\mathcal{T})$ with $(F;1,4,4) = \Psi_{-P}((F;0,0,0))$ (see Remark 4.3.32), an arc q'' from y to $0 \in \psi_{(0,0,0)}(\mathcal{T})$ inside $\mathrm{int}(\mathcal{T})$ can be constructed in the same way as the arcs p_i in the proof of Proposition 4.3.52, using the n-skeletons. Now $q = q'q''$ does the job. □

We obtain directly from the above proposition the following result.

Corollary 4.3.54. *The set* $\mathrm{int}(\mathbf{M})$ *is a subset of the interior component of $\mathcal{T}$ containing* 0*.*

The reverse inclusion is the purpose of the next proposition.

Proposition 4.3.55. *The component of* $\mathrm{int}(\mathcal{T})$ *containing* 0 *is a subset of* $\mathrm{int}(\mathbf{M})$*.*

Proof. Let y be a point in $\mathrm{int}(\mathcal{T})$ such that there is an arc $p : [0,1] \to \mathrm{int}(\mathcal{T})$ connecting 0 and y. Suppose that y does not belong to $\mathrm{int}(\mathbf{M})$. Since $\partial\mathbf{M} \subset \partial\mathcal{T}$ (see Proposition 4.3.43), y does not belong to $\mathbf{M}$. Let

$$t_0 := \inf\{t \in [0,1]; p(t) \notin \mathbf{M}\}.$$

Then $t_0 \in (0,1)$ and $p(t_0) \in \partial\mathbf{M}$, because every neighborhood of this point encounters $\mathbf{M}$ as well as its complement. Since again $\partial\mathbf{M} \subset \partial\mathcal{T}$, we obtain that $p(t_0) \in \partial\mathcal{T}$, a contradiction to the definition of p. □

Lemma 4.3.56. *The set* $\mathbf{M}$ *is the closure of its interior,* i.e., $\overline{\mathrm{int}(\mathbf{M})} = \mathbf{M}$*.*

Proof. Let $x \in \mathbf{M}$ and $\varepsilon > 0$ be arbitrary. Let $n \geq 3$ be large enough such that $\mathrm{diam}(\psi_w(\mathcal{T})) < \varepsilon$ for each $w \in p_n(F)$. There exists a walk $v \in p_n(F)$ such that $x \in \psi_v(\mathcal{T})$. It can easily be read off from the graph $\mathcal{G}$ that each $v \in p_n(F)$ can be extended to a walk $v' = v\&(b_1,b_2) \in G_{n+2} = p_{n+2}(F,\circ)$. Thus

$$\psi_{v'}(\mathcal{T}) \subset \mathbf{M} \Longrightarrow \mathrm{int}(\psi_{v'}(\mathcal{T})) \subset \mathrm{int}(\mathbf{M})$$

and

$$\psi_{v'}(\mathcal{T}) \subset \psi_v(\mathcal{T}).$$

Select $y \in \mathrm{int}(\psi_{v'}(\mathcal{T}))$. Then the above inclusions imply that $y \in \mathrm{int}(\mathbf{M})$ and $\mathrm{dist}(x,y) < \varepsilon$.

Since ε can be arbitrarily small we have that $x \in \overline{\mathrm{int}(\mathbf{M})}$. □

Proof of Theorem 4.3.8. The first part of this theorem follows from Corollary 4.3.54 and Proposition 4.3.55. The second part is given by Lemma 4.3.56. □

4.3.8 Dimension calculation

The present subsection is devoted to the proof of Theorem 4.3.11. Let $\mathcal{G}'$ be the graph that emerges from $\mathcal{G}$ by removing the states $\circ$ and all edges leading to them. Then $\mathcal{G}'$ defines system of graph directed sets $(\delta\mathbf{M}(A))_A$ where A runs through the states of $\mathcal{G}'$. Let $\delta\mathbf{M} := \delta\mathbf{M}(F)$ be the set corresponding to the state F. The following lemma shows that $\delta\mathbf{M}$ is very close to ∂C_0.

Lemma 4.3.57. *The symmetric difference*

$$\delta\mathbf{M} \triangle \partial C_0$$

is countable.

Proof. First note that Lemma 4.3.50 implies that $\delta\mathbf{M} \subset \partial C_0$.

Suppose now that $x \in \partial C_0 \setminus \delta\mathbf{M}$. Then the address of x corresponds to the labelling of a walk which is contained in $\mathcal{G}$ but not in $\mathcal{G}'$, *i.e.*, there exists a walk $w \in G_n$ for some n such that $x \in \psi_w(\mathcal{T})$ and, *a fortiori*, $x \in \partial\psi_w(\mathcal{T})$. Since $\partial C_0 \subset \partial\mathcal{T}$ holds by Proposition 4.3.43, $x \in \partial\mathcal{T}$. Thus, x has to lie in another tile of the tiling induced by $\mathcal{T}$. However, in view of Proposition 4.3.26 and the remark after it,

$$x \in \psi_w(\mathcal{T} + S)$$

where S is a neighbor of $\mathcal{T}$ not contained in $\mathcal{B}$. It is well known (see for instance [5, Chapters 9 to 11]) that there exist only countably many points in $\partial\psi_w(\mathcal{T})$ with this property. Since, moreover, there are only countably many paths contained in

$$\bigcup_{n\geq 3} G_n$$

we conclude that there exist only countably many points x in the set $\partial C_0 \setminus \delta\mathbf{M}$. □

Now from basic fractal geometry we get the following corollary.

Corollary 4.3.58.

$$\dim_H \partial C_0 = \dim_H \delta\mathbf{M}.$$

Thus calculating the Hausdorff dimension of ∂C_0 is reduced to calculating the Hausdorff dimension of the GIFS attractor $\delta\mathbf{M}$. However, calculating the Hausdorff dimension of a self similar GIFS satisfying the open set condition can be performed by standard methods from fractal geometry (*cf.* Appendix B or for instance [18, 50]). With that Theorem 4.3.11 is proved.

4.4 Comments and questions

We have shown in the last section how to obtain the closure $\mathbf{M}$ of the interior component of $\mathcal{T}$ that contains the origin $\Phi(0)$. This component was depicted in Figure 4.6. It is of natural interest to wonder how the closure of the interior component of $\mathcal{T}$ containing a given point x could be computed. For the other "big" components (see Figure 4.10), *i.e.*, the ones containing $\Phi(1), \Phi(2)$ and $\Phi(3)$, the description is similar: it suffices to replace the edges at the top of the graph $\mathcal{G}$ describing $\mathbf{M}$ in a way that can be seen in Figure 4.9.

Thus the closure of each of these components is simply the image of $\mathbf{M}$ by translations (see Figure 4.10).

For other "smaller components", we conjecture that there closure is similar to $\mathbf{M}$, the similitude may be given by a pre-graph that would be connected to $\mathcal{G}$ via the state F. One can also wonder if the computation of the graph $\mathcal{G}$ is also possible for other quadratic number systems. Eventually,

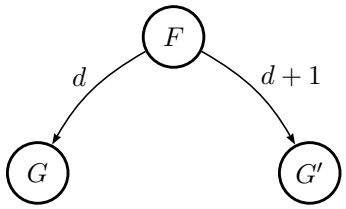

Figure 4.9: Top edges in $\mathcal{G}$ for the closure of the component containing $\Phi(d),\ d = 0, 1, 2, 3$.

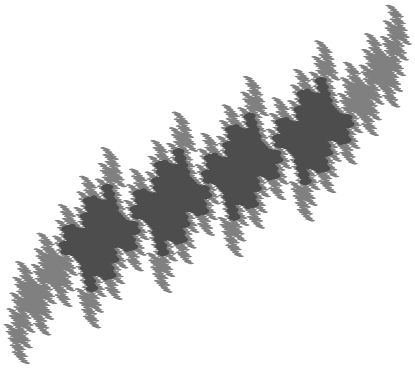

Figure 4.10: Tile associated to the base $-2 + \sqrt{-1}$ with "big" interior components.

other topological properties of lattice tiles associated to quadratic canonical number systems may be studied, like the existence of cut points in the case that the fundamental group is uncountable. The particular example of the last section was already proved to have no cut point (see [54]). What about the general case ?

Chapter 5

Conclusion

In this PhD thesis, topological properties of fractal tiles giving rise to tessellations of the plane were studied. The fractal structure induces some regularity that allows to establish algorithmic criteria to answer topological questions about the tiles. Even the description of a connected inner component ended up in a finite graph. Concerning the criteria of homeomorphy to a closed disk, they mainly relie on the Jordan curve theorem: showing that the boundary of a tile is a simple closed curve, one obtains its disk-likeness of the tiles. This is the reason why we were so much interested in the neighbor relations of the tiles. In higher dimensional spaces, statements analogous to Jordan curve theorem are not valid. The topology of 3 dimensional tiles for example would be much more complicated. But could we state simple criteria of homeomorphy to a closed ball? Rather than the first homotopy group, what could be said about the homology groups of the tiles?

Appendix A

Plane topology

The tiles are compact sets, and we restrict our topological study to plane connected tiles. The plane can be considered after one-point compactification as the Riemann sphere. This leads to many interesting results in the study of the topology of plane compact sets. We will be interested in the characterizations of homeomorphy to a closed disk.

Most of the definitions and facts given here can be found in Kuratowski's book *Topology II* [36].

Definition A.0.1 (Connectedness, local connectedness, arcwise connectedness, cut)**.** Given a set M in a topological space X, we say that M is

(i) *connected* iff it can not be partitioned into two non-empty disjoint relatively open subsets. Otherwise M is *disconnected*.

(ii) *locally connected at* x iff every neighborhood of x contains a connected relatively open neighborhood. M is *locally connected* if it is locally connected at each of its points.

(iii) *arcwise connected* if any two points of M are the end points of a homeomorphic image of $[0, 1]$ contained in M.

(iv) a *cut* of X or a *separation* of X if its complement $X \setminus M = M^c$ is disconnected.

If n points $x_1, \ldots, x_n, n \geq 2$, belong to pairwise distinct connected components of $X \setminus M$, we say that $x_1, \ldots, x_n$ are *separated by* M; if $n = 2$, we also say that M is a *cut between* x_1 *and* x_2, or that M *cuts between* x_1 *and* x_2 *in* X.

Definition A.0.2 (Continuum)**.** A *continuum* is a connected compact Hausdorff space.

Notation A.0.3. The diameter of a compact set M in a metric space is the maximal distance between two points of M and is denoted by $\mathrm{diam}(M)$.

Close to the local connectedness is the following *property* (S).

Definition A.0.4. A set M in a metric space has *property* (S) provided that for every $\varepsilon > 0$, M is the union of finitely many connected sets of diameter less than ε.

Proposition A.0.5 (*cf.* [63, §XV])**.** *A set having property* (S) *is locally connected.*

Proposition A.0.6 (*cf.* [63, §XX])**.** *Every locally connected continuum is arcwise connected.*

Definition A.0.7 (Connected component, quasi component)**.** In a topological space X, the *connected components* of M are the maximal (with respect to the inclusion relation) connected subsets. Equivalently, the connected component at the point $p \in X$ is the intersection of all connected subsets of X containing p. The *quasi-component* at the point $p \in X$ is the intersection of all closed-open (or *clopen*) sets of X containing p.

Lemma A.0.8 (*cf.* [36, §47, II, p.169, Theorem 2])**.** *In compact spaces, the quasi-components are connected and coincide therefore with the components.*

Definition A.0.9 (Janiszewski space)**.** A locally connected continuum X is a *Janiszewski space* ([36, §61, I, p.505]) provided that the union $M \cup N$ of two continua $M, N \subset X$ is a cut of X whenever their intersection $M \cap N$ is not connected.

Lemma A.0.10 (*cf.* [36, §61, I, Theorem 7])**.** *Let B, C be two closed or two open sets of a Janiszewski space X. If none of these sets is a cut between p and q and if $B \cap C$ is connected, then $B \cup C$ is not a cut between p and q either.*

Since the 2-dimensional sphere $\mathbb{S}^2$ is a Janiszewski space [36, §61, I, Theorem 2], we can infer two separation theorems for the plane $\mathbb{R}^2$ as follows.

Lemma A.0.11. *If the common part of two continua M, N in the plane is disconnected, then there exist two points p_0, p_1 separated by $M \cup N$ but not by either M or N.*

Lemma A.0.12. *Let M, N be compact sets in the plane and suppose that there exist $n(\geq 2)$ points separated by $M \cup N$ but not by either M or N. Then the common part $M \cap N$ has at least n components.*

Definition A.0.13 (Chain, circular chain)**.** Suppose that $M_1, M_2, \ldots, M_n, n \geq 3$, are compact sets in the plane. If $\#(M_i \cap M_{i+1}) = 1$ for $1 \leq i \leq n-1$ and $M_i \cap M_j = \emptyset$ for $|i-j| \geq 2$, we say that $M_1, M_2, \ldots, M_n$ form a *chain*. If $\#(M_i \cap M_{i+1}) = 1$ for $1 \leq i \leq n-1$, $\#(M_n \cap M_1) = 1$ and $M_i \cap M_j = \emptyset$ for $2 \leq |i-j| \leq n-2$, we say that $M_1, M_2, \ldots, M_n$ form a *circular chain*.

By Lemmata A.0.10 to A.0.12, we have the following two corollaries which will be used in the proof of Theorems 3.3.1 and 3.3.9.

Corollary A.0.14. *If $M_1, \ldots, M_n (n \geq 3)$ are compact sets in the plane which form a chain, then every two points separated by $\bigcup_j M_j$ are separated by a single M_j.*

Corollary A.0.15. *If the continua $M_1, \ldots, M_n (n \geq 3)$ in the plane form a circular chain and each of them does not separate the plane, then $\mathbb{R}^2 \setminus \left(\bigcup_j M_j\right)$ is the union of two regions.*

Definition A.0.16 (Deformation, see [36, §54, IV])**.** Let $X \subset Y$ and $f : X \to Y$ be a continuous function. If there exists a continuous function $h : X \times [0,1] \to Y$ such that $h(x,0) = x$ and $h(x,1) = f(x)$, the set $f(X)$ is said to be obtained from X by a *deformation* in Y.

Lemma A.0.17 (*cf.* [36, § 59, IV, Theorem 2])**.** *If a compact set $F \subset \mathbb{R}^2$ separates between two points p and q, then every set obtained from F by a deformation in $\mathbb{R}^2 \setminus \{p, q\}$ separates between p and q.*

Lemma A.0.18 (*cf.* [36, § 61, II, Theorem 5])**.** *Every locally connected continuum which separates the plane between two continua A and B contains a simple closed curve which separates the plane between A and B.*

We also recall a theorem of Torhorst.

Lemma A.0.19 (*cf.* [36, §61, II, Theorem 4])**.** *Let $M \subset \mathbb{S}^2$ be a locally connected continuum having no cutpoint and R a component of M^c. Then $\overline{R}$ is homeomorphic to a disk.*

Dealing with disk-like tiles in crystallographic tilings, we also need the following considerations. For a closed disk D, distinct points of the boundary are *accessible* (see [36, §47, III]) from any given point of the interior of D by disjoint simple open arcs within D^o. More precisely, for distinct $a_1, \ldots, a_n \in \partial D$, $n \in \mathbb{N}$ and $p \in D^o$, there are pairwise disjoint simple open arcs $A_1, \ldots, A_n \subset D^o$ leading from p to $a_1, \ldots, a_n$, respectively. This fact is needed in order to prove the following lemma.

Lemma A.0.20. *Let D_1, D_2 be two closed disks with disjoint interiors such that there exists a bounded connected component Z of $(D_1 \cup D_2)^c$. Then $\overline{Z} \cap D_1 \cap D_2$ consists of two points a, b. Furthermore, $\overline{Z} \cap D_i$, $i = 1, 2$, are simple arcs meeting in their end points a and b, and there are $C_1 \subset D_1^o$, $C_2 \subset D_2^o$ simple open arcs from a to b such that $Z = \text{Interior}\,(C_1 \cup C_2 \cup \{a, b\}) \cap (D_1 \cup D_2)^c$.*
(Here the interior $\text{Interior}(C)$ *of the simple closed curve C is defined as the bounded component of the complement of C.)*

Proof. Note that $D_1 \cup D_2$, union of disks with disjoint interiors, is a locally connected continuum with no cut points because its complement has a bounded component, so by Lemma A.0.19 $\overline{Z}$ is disk-like, thus its boundary $\partial Z = \overline{Z} \cap (D_1 \cup D_2)$ is a simple closed curve and $Z = \text{Interior}(\partial Z)$.
The intersection $\overline{Z} \cap D_1 \cap D_2$ has at least two points because ∂Z is connected and has no cut point. Let us suppose that it contains three distinct points a, b, c. Then, choosing $p_i \in D_i^o$, $i = 1, 2$, and disjoint simple open arcs C_α^i from p_i to α within D_i^o for $i = 1, 2$ and $\alpha = a, b, c$, we obtain three disjoint simple open arcs from p_1 to p_2, namely $C_\alpha := \{\alpha\} \cup C_\alpha^1 \cup \left(-C_\alpha^2\right)$ for $\alpha = a, b, c$, ($-C_\alpha^2$ stands for the arc C_α^2 travelled in the reverse way) with the property that $C_\alpha \subset D_1^o \cup D_2^o \cup \{\alpha\}$. Thus $\theta := \{p_1, p_2\} \cup \bigcup_\alpha C_\alpha$ is a theta-curve. Since $Z \subset \theta^c$ is connected, it must be entirely included in one open disk-like region B of θ^c. This implies that a, b, c are all on $\overline{B}$, contradicting the fact that these points lie on the distinct arcs of θ.
Thus $\overline{Z} \cap D_1 \cap D_2$ consists of exactly two points a, b, and the remaining assertions follow: $A_i := \overline{Z} \cap D_i$ for $i = 1, 2$ is a continuum and each point of A_i different from a, b is a cut point of A_i, so A_i is a simple arc on ∂Z (see [36, §49, IV, Theorem 4]). Every two simple open arcs C_1, C_2 from a to b within D_1^o, D_2^o are homotopic to A_1, A_2 within D_1, D_2 and have the required property. □

Appendix B

Boundary of tiles and fractal dimension

By definition, the tiles have positive Lebesgue measure. Nevertheless, if they fulfill a replicating property, their boundary happens to contain the irregular structure, hence the fractality. We give here the important results about the connectedness of the boundary of tiles and about the fractal dimension of the boundary of reptiles.

We recall some results on the boundary connectedness and arcwise connectedness of attractors and tiles.

Lemma B.0.21 (see [2, Theorem 1.1])**.** *Let $f_1, \dots, f_k$ be injective contractions on $\mathbb{R}^n$ ($n \geq 2$) satisfying the open set condition, and let E be the attractor. Then the boundary ∂E of E is connected whenever E is.*

Tai-Man Tang proved also the following.

Proposition B.0.22 (*cf.* [61])**.** *Let $f_1, \dots, f_k$ are injective contractions on $\mathbb{R}^n$, $n \geq 2$ satisfying the open set condition, and let E be the attractor. Suppose that E is connected. Then ∂E is arcwise connected.*

Remember that a compact set in $\mathbb{R}^n$ which coincides with the closure of its interior is a tile, and it is said to tile $\mathbb{R}^n$ by $\mathbb{Z}^n$ if the translates of this set by the vectors of $\mathbb{Z}^n$ form a tiling of $\mathbb{R}^n$ (Remark 2.2.12).

Lemma B.0.23 (see [2, Theorem 3.1])**.** *Let T be an arcwise connected compact set that tiles $\mathbb{R}^n$ by $\mathbb{Z}^n$, then its boundary ∂T is connected.*

Luo Jun [46] noticed that a quick proof exists for the following stronger result.

Lemma B.0.24. *Let $(T_i)_{i\in I}$ be a family of connected compact sets that provide a tiling of $\mathbb{R}^n$. Then the boundary of T_i is connected for each $i \in I$.*

Proof. This follows from the unicoherence of Euclidean spaces (see Definition B.0.25 and [63]). Indeed, writing $\mathbb{R}^n = T_i \cup \bigcup_{j\neq i,\ j\in I} T_j$, we obtain that $\partial T_i = T_i \cap \bigcup_{j\neq i,\ j\in I} T_j$ is connected. □

Definition B.0.25 (Unicoherent space)**.** A connected space is *unicoherent* if, representing it as any union of two closed connected sets, the intersection of these sets is connected.

Equation (3.2.3) on page 21 shows that the boundary of a crystile may be related to some graph directed construction. If the maps $g^{-1}\delta$ in this equation are similarity contractions, it is then possible to compute the Hausdorff dimension of the boundary of the crystile. We shortly recall the definition of the Hausdorff dimension and state a result on its value for self-similar systems of graph directed sets (see Definition 2.1.19 in Chapter 2).

Definition B.0.26 (Hausdorff dimension)**.** If F is a subset of the Euclidean space $\mathbb{R}^n$ and $s \geq 0$, one defines for $\delta > 0$

$$\mathcal{H}^s_\delta(F) = \inf\{\sum_{i=0}^{\infty} \operatorname{diam}(U_i)^s\},$$

where the infimum is taken over all at most countable covers $(U_i)_i$ of F for which $0 \leq \operatorname{diam}(U_i) \leq \delta$ holds for every i. The number

$$\mathcal{H}^s(F) = \lim_{\delta \to 0} \mathcal{H}^s_\delta(F)$$

is well defined for all $s > 0$, and there is a unique value of s for which $\mathcal{H}^s(F)$ jumps from ∞ to 0. This value is called the *Hausdorff dimension* (or *Hausdorff-Besicovitch dimension* sometimes) of F and denote it by $\dim_H F$.

We refer to [17] for more details on this subject.

Proposition B.0.27 ([18, 50])**.** *Let $(K_1, \dots K_q)$ be a system of graph directed sets with respect to the contractions T_e ($e \in E$). Let r_e be the contraction ratio of T_e for each $e \in E$ and let $E_{i,j}$ be the set of edges from the vertex i to the vertex j for all $i, j = 1, \dots, q$. For $s \geq 0$, denote by $A^{(s)}$ the matrix whose (i,j)-th entry is*

$$A^{(s)}_{i,j} = \sum_{e \in E_{i,j}} r_e^s.$$

If $\rho(A^{(s)})$ stands for the spectral radius of the matrix $A^{(s)}$, then there is exactly one value s_0 of s for which

$$\rho(A^{(s_0)}) = 1.$$

Moreover, $0 < \mathcal{H}^{s_0}(K_i) < \infty$, thus s_0 is the Hausdorff dimension of K_i for all $i = 1, \dots, q$.

We note that for self-affine systems of graph directed sets, only the box-counting dimension can be computed exactly (see [13]). The Hausdorff dimension is known in particular cases, for example the boundary of tiles associated to canonical number systems (see [58]).

Index

Notations

$\mathcal{K}(X)$	set of non-empty compact subsets of X	$p.10$
$\text{int}(M)$, M°	set of inner points of M	$p.13$
$\text{Isom}(\mathbb{R}^n)$	group of all isometries of $\mathbb{R}^n$	$p.13$
id	identity mapping	$p.13$
$m_1 \circ m_2$, $m_1 m_2$	mapping composition $x \mapsto m_1(m_2(x))$	$p.15$
$\mathcal{S}$	set of neighbors of the central tile	$p.15$
$\mathcal{A}$	set of adjacent neighbors of the central tile	$p.15$
B_γ	intersection set $T \cap \gamma(T)$ (T central tile)	$p.16$
A_γ, t_γ	linear and translation part of an isometry γ	$p.17$
$\text{diam}(K)$	maximal distance between two points of a compact set K	$p.19$
$V_L(\gamma_1, \ldots, \gamma_L)$	set of points belonging to T,$\gamma_1(T)$,... and $\gamma_L(T)$	$p.22$
V_L	set of L-vertices	$p.22$
$\text{Interior}(C)$	bounded component of the complement of a simple closed curve C	$p.29$
$\text{Exterior}(C)$	unbounded component of the complement of a simple closed curve C	$p.29$
$B_r(x)$	closed ball of radius r around x	$p.47$
J	for a quadratic polynomial $x^2 + Ax + B$, $J = \max\left\{1, \left\lfloor \frac{B-1}{B-A+1} \right\rfloor\right\}$	$pp.78$-79
$\circ$	the state $(0,0)$	$p.80$
Ψ_w	for a sequence of digits $w = (a_1, \ldots, a_n)$, $\Psi_w = \Psi_{a_1} \circ \ldots \circ \Psi_{a_n}$	$p.88$
$\dim_H F$	Hausdorff dimension of the set F	$p.122$

Bibliography

[1] Colin Adams, Frank Morgan, and John M. Sullivan. When soap bubbles collide. *Amer. Math. Monthly*, 114(4):329–337, 2007.

[2] Shigeki Akiyama, Jun Luo, and Jörg Thuswaldner. On boundary connectedness of connected tiles. *Math. Proc. Camb. Soc.*, 137:397–410, 2004.

[3] Shigeki Akiyama and Hui Rao. New criteria for canonical number systems. *Acta Arith.*, 111:5–25, 2004.

[4] Shigeki Akiyama and Jörg Thuswaldner. A survey on topological properties of tiles related to number systems. *Geom. Dedicata*, 109:89–105, 2004.

[5] Shigeki Akiyama and Jörg Thuswaldner. The topological structure of fractal tilings generated by quadratic number systems. *Comput. and Math. with Appl.*, 49:1439–1485, 2005.

[6] Scott Bailey, Theodore Kim, and Robert S. Strichartz. Inside the Lévy dragon. *Amer. Math. Monthly*, 109:689–703, 2002.

[7] Christoph Bandt and Yang Wang. Disk-like self-affine tiles in $\mathbb{R}^2$. *Discrete Comput. Geom.*, 26:591–601, 2001.

[8] Michael F. Barnsley, John H. Elton, and Douglas P. Hardin. Recurrent iterated function systems. *Constr. Approx.*, 5:3–31, 1989.

[9] Frank S. Beckmann and Donald A. Quarles. On isometries of euclidean spaces. *Proc. Amer. Math. Soc.*, 4:810–815, 1953.

[10] Horst Brunotte. Characterization of CNS trinomials. *Acta Sci. Math. (Szeged)*, 68:673–679, 2003.

[11] Johann J. Burckhardt. *Die Bewegungsgruppen der Kristallographie*. Birkhäuser, Basel, 1947.

[12] Greg R. Conner and Jack W. Lamoreaux. On the existence of universal covering spaces for metric spaces and subsets of the euclidean plane. *preprint*.

[13] Anca Deliu, Jeff Geronimo, Ronald W. Schonkwiler, and Douglas P. Hardin. Dimensions associated with recurrent self-similar sets. *Math. Proc. Cambridge Philos. Soc.*, 110(2):327–336, 1991.

[14] Da-Wen Deng and Sze-Man Ngai. Vertices of self-similar tiles. *Illinois J. Math.*, 49(3):857–872, 2005.

[15] Reinhard Diestel. *Graph Theory*. Electronic version. Springer-Verlag, New York-Heidelberg, 2005.

[16] Ryszard Engelking. *Dimension Theory*. PWN-Polish Scientific Publishers, Warszawa, 1978.

[17] Kenneth J. Falconer. *Fractal Geometry*. John Wiley and Sons, Chichester, 1990.

[18] Kenneth J. Falconer. *Techniques in Fractal Geometry*. John Wiley and Sons, Chichester, New York, Weinheim, Brisbane, Singapore, Toronto, 1997.

[19] Götz Gelbrich. Crystallographic reptiles. *Geom. Dedicata*, 51(3):235–256, 1994.

[20] William J. Gilbert. Radix representations of quadratic fields. *J. Math. Anal. Appl.*, 83:264–274, 1981.

[21] Karlheinz Gröchenig and Andrew Haas. Self-similar lattice tilings. *J. Fourier Anal. Appl.*, 1:131–170, 1994.

[22] Branko Grünbaum and Geoffrey C. Shephard. *Tilings and patterns*. Freeman, New York, 1987.

[23] Masayoshi Hata. On the structure of self-similar sets. *Japan J. Appl. Math.*, 2:381–414, 1985.

[24] Allen Hatcher. *Algebraic topology*. Cambridge University Press, 2002.

[25] David Hilbert. Über die stetige Abbildung einer Linie auf ein Flächenstück. *Math. Ann.*, 38:459–460, 1891.

[26] W Hurewicz and H. Wallman. *Dimension Theory*. Princeton University Press, Princeton, 1941.

[27] John E. Hutchinson. Fractals and self-similarity. *Indiana Univ. Math. J.*, 30:713–747, 1981.

[28] Shunji Ito. On the fractal curves induced from the complex radix expansion. *Tokyo J. Math.*, 12(2):299–320, 1989.

[29] Imre Kátai. Number systems and fractal geometry. *Janus Pannonius University Pecs*, 1995.

[30] Imre Kátai and I. Kőrnyei. On number systems in algebraic number fields. *Publ. Math. Debrecen*, 41(3–4):289–294, 1992.

[31] Imre Kátai and Bela Kovács. Kanonische Zahlensysteme in der Theorie der Quadratischen Zahlen. *Acta Sci. Math. (Szeged)*, 42:99–107, 1980.

[32] Imre Kátai and Bela Kovács. Canonical number systems in imaginary quadratic fields. *Acta Math. Hungar.*, 37:159–164, 1981.

[33] Imre Kátai and János Szabó. Canonical number systems for complex integers. *Acta Sci. Math. (Szeged)*, 37(3-4):255–260, 1975.

[34] Ibrahim Kirat and Ka-Sing Lau. On the connectedness of self-affine tiles. *J. London Math. Soc.*, 62:291–304, 2000.

[35] Donald E. Knuth. *The Art of Computer Programming, Vol 2: Seminumerical Algorithms*. Addison Wesley, London, 3rd edition, 1998.

[36] Kazimierz Kuratowski. *Topology. Vol. II*. New edition, revised and augmented. Translated from the French by A. Kirkor. Academic Press, New York, 1968.

[37] Jeffrey C. Lagarias and Yang Wang. Integral self-affine tiles in $\mathbb{R}^n$ I. standard and nonstandard digit sets. *J. London Math. Soc.*, 54(2):161–179, 1996.

[38] Jeffrey C. Lagarias and Yang Wang. Self-affine tiles in $\mathbb{R}^n$. *Adv. Math.*, 121:21–49, 1996.

[39] Jeffrey C. Lagarias and Yang Wang. Integral self-affine tiles in $\mathbb{R}^n$ II. lattice tilings. *J. Fourier Anal. Appl.*, 3:83–102, 1997.

[40] Douglas Lind. Dynamical properties of quasihyperbolic toral automorphisms. *Ergodic Dynamical systems*, 2:49–68, 1982.

[41] Benoît Loridant. Fundamental group of tiles associated to quadratic canonical number systems. *Math. Slovaca*, to appear.

[42] Benoît Loridant and Jun Luo. On a thoerem of bandt and wang and its extension to $p2$-tiles. *Discrete Comput. Geom.*, submitted.

[43] Benoît Loridant, Jun Luo, and Jörg Thuswaldner. A new criterion for disk-like crystallographic reptiles. In *Topology Proc.*, to appear.

[44] Benoît Loridant, Jun Luo, and Jörg Thuswaldner. Topology of crystallographic tiles. *Geom. Dedicata*, to appear.

[45] Benoît Loridant and Jörg Thuswaldner. Interior components of a tile associated to a quadratic canonical number system. *Topology Appl.*, to appear.

[46] Jun Luo. private communication. 2007.

[47] Jun Luo, Hui Rao, and Bo Tan. Topological structure of self-similar sets. *Fractals*, 10:223–227, 2002.

[48] Jun Luo and Jörg Thuswaldner. On the fundamental group of self-affine plane tiles. *Ann. Inst. Fourier (Grenoble)*, 56(7):2493–2524, 2006.

[49] Benoît Mandelbrot. *Les objets fractals : forme, hasard et dimension.* Flammarion, 1975.

[50] R. Daniel Mauldin and Stanley C. Williams. Hausdorff dimension in graph directed constructions. *Trans. Amer. Math. Soc.*, 309:811–829, 1988.

[51] Edwin E. Moise. *Geometric Topology in Dimensions* 2 *and* 3. Graduate Texts in Mathematics. Springer-Verlag, New York-Heidelberg, 1977.

[52] Wolfgang Müller, Jörg Thuswaldner, and Robert F. Tichy. Fractal properties of number systems. *Periodica Math. Hungar.*, 42:51–68, 2001.

[53] Sze-Man Ngai and N. Nguyen. The heyweigh dragon revisited. *Discrete Comp. Geometry*, 29:603–623, 2003.

[54] Sze-Man Ngai and Tai-Man Tang. A technique in the topology of connected self-similar tiles. *Fractals*, 12(4):389–403, 2004.

[55] Sze-Man Ngai and Tai-Man Tang. Topology of connected self-similar tiles in the plane with disconnected interior. *Topology Appl.*, 150:139–155, 2005.

[56] Giuseppe Peano. Sur une courbe, qui remplit toute une aire plane. *Math. Ann.*, 36:157–160, 1890.

[57] Attila Pethö. On a polynomial transformation and its application to the construction of a public key cryptosystem. In *Computational number theory (Debrecen 1989)*, pages 31–43. de Gruyter, Berlin, 1991.

[58] Klaus Scheicher and Jörg Thuswaldner. Canonical number systems, counting automata and fractals. *Math. Proc. Cambridge Philos. Soc.*, 133:163–182, 2002.

[59] Klaus Scheicher and Jörg Thuswaldner. Neighbours of self-affine tiles in lattice tilings. In Peter (ed.) et al. Grabner, editor, *Fractals in Graz 2001. Analysis, dynamics, geometry, stochastics. Proceedings of the conference, Graz, Austria, June 2001*, pages 241–262. Birkhäuser, 2003.

[60] Klaus Scheicher and Jörg Thuswaldner. On the characterization of canonical number systems. *Osaka J. Math.*, 41:327–351, 2004.

[61] Tai-Man Tang. Arcwise connectedness of the boundaries of connected self-similar sets. *Acta Math. Hungar.*, 109(4):295–303, 2005.

[62] Yang Wang. Self-affine tiles. In K. S. Lau, editor, *Advances in Wavelet*, pages 261–285. Springer, 1998.

[63] Gordon T. Whyburn and Edwin Duda. *Dynamic Topology*. Undergraduate Texts in Mathematics. Springer-Verlag, New York Inc., 1979.